BETA-CELL FATE: FROM GENE CIRCUITS TO DISEASE MECHANISMS

EDITED BY: Simona Chera, Kenichiro Furuyama, Hanne Scholz, Shane T. Grey and Luiza Ghila

PUBLISHED IN: Frontiers in Endocrinology and Frontiers in Genetics

frontiers Research Topics

frontiers

ISSN 1664-8714
ISBN 978-2-88974-712-2
DOI 10.3389/978-2-88974-712-2

About Frontiers

Frontiers is more than just an open-access publisher of scholarly articles: it is a pioneering approach to the world of academia, radically improving the way scholarly research is managed. The grand vision of Frontiers is a world where all people have an equal opportunity to seek, share and generate knowledge. Frontiers provides immediate and permanent online open access to all its publications, but this alone is not enough to realize our grand goals.

Frontiers Journal Series

The Frontiers Journal Series is a multi-tier and interdisciplinary set of open-access, online journals, promising a paradigm shift from the current review, selection and dissemination processes in academic publishing. All Frontiers journals are driven by researchers for researchers; therefore, they constitute a service to the scholarly community. At the same time, the Frontiers Journal Series operates on a revolutionary invention, the tiered publishing system, initially addressing specific communities of scholars, and gradually climbing up to broader public understanding, thus serving the interests of the lay society, too.

Dedication to Quality

Each Frontiers article is a landmark of the highest quality, thanks to genuinely collaborative interactions between authors and review editors, who include some of the world's best academicians. Research must be certified by peers before entering a stream of knowledge that may eventually reach the public - and shape society; therefore, Frontiers only applies the most rigorous and unbiased reviews.
Frontiers revolutionizes research publishing by freely delivering the most outstanding research, evaluated with no bias from both the academic and social point of view. By applying the most advanced information technologies, Frontiers is catapulting scholarly publishing into a new generation.

What are Frontiers Research Topics?

Frontiers Research Topics are very popular trademarks of the Frontiers Journals Series: they are collections of at least ten articles, all centered on a particular subject. With their unique mix of varied contributions from Original Research to Review Articles, Frontiers Research Topics unify the most influential researchers, the latest key findings and historical advances in a hot research area! Find out more on how to host your own Frontiers Research Topic or contribute to one as an author by contacting the Frontiers Editorial Office: frontiersin.org/about/contact

BETA-CELL FATE: FROM GENE CIRCUITS TO DISEASE MECHANISMS

Topic Editors:
Simona Chera, University of Bergen, Norway
Kenichiro Furuyama, Kyoto University, Japan
Hanne Scholz, Oslo University Hospital, Norway
Shane T. Grey, Garvan Institute of Medical Research, Australia
Luiza Ghila, University of Bergen, Norway

Citation: Chera, S., Furuyama, K., Scholz, H., Grey, S. T., Ghila, L., eds. (2022). Beta-Cell Fate: From Gene Circuits to Disease Mechanisms. Lausanne: Frontiers Media SA. doi: 10.3389/978-2-88974-712-2

Table of Contents

frontiers in Genetics

EDITORIAL
published: 25 February 2022
doi: 10.3389/fgene.2022.822440

Editorial: Beta-Cell Fate: From Gene Circuits to Disease Mechanisms

Luiza Ghila[1], Kenichiro Furuyama[2], Shane T. Grey[3,4], Hanne Scholz[5,6] and Simona Chera[1]**

[1]Center for Diabetes Research, Department of Clinical Science, Faculty of Medicine, University of Bergen, Bergen, Norway, [2]Center for iPS Cell Research and Application (CiRA), Kyoto University, Kyoto, Japan, [3]Immunology Department, Garvan Institute of Medical Research, Darlinghurst, NSW, Australia, [4]Faculty of Medicine, St Vincent's Clinical School, University of New South Wales Sydney, Sydney, NSW, Australia, [5]Hybrid Technology Hub-Centre of Excellence, Faculty of Medicine, University of Oslo, Oslo, Norway, [6]Department of Transplant Medicine and Institute for Surgical Research, Oslo University Hospital, Oslo, Norway

Keywords: MODY (mature onset diabetes of the young), T1D (type 1 diabetes), T2D (type 2 diabetes), mRNA processing, UPR stress, islet heterogeneity, cell reprogramming

Editorial on the Research Topic

Beta-Cell Fate: From Gene Circuits to Disease Mechanisms

Diabetes represents a group of energy metabolism pathologies where the most common forms of the disease exhibit a polygenic and multifactorial aetiology (American Diabetes Association, 2005). Diabetes has truly reached worldwide epidemic proportions with 537 million people living with diabetes worldwide (International Diabetes Federation, 2021). While diabetes can be managed, for many people the onset of life-threatening complications including blindness, kidney failure, heart attacks, stroke, and lower limb amputation further exacerbates the impact on mortality and morbidity (6.7 million deaths related to diabetes complications were reported in 2021). The major difficulty is distinguishing from the plethora of modulations the ones directly responsible for disease initiation. To date it remains largely unknown what are the external factors and cellular signals leading to insulin-producing β-cells decay or dysfunction are and what molecular mechanisms and cellular processes characterize this transition. Identifying the mechanisms governing the onset and progression of these complex conditions is exceedingly challenging, due to their multifactorial environmental component and the intricate genetic susceptibility interaction. Nevertheless, the past decade registered important advances towards understanding these issues. Moreover, the role of the other pancreatic cell populations in the onset, progression, and treatment of diabetes started to be revealed (Chera and Herrera, 2016). These advances contribute towards a more comprehensive demultiplexing of the large diversity of diabetes mechanisms, which is expected to critically contribute to an unambiguous diabetes reclassification.

The aim of this Research Topic was to provide a snapshot of current studies focused on molecular circuits and cellular processes involved in the development, function, and dysfunction of β-cells, touching multiple aspects of islet niche and disease progression.

MOLECULAR LEVEL/NOVEL MOLECULAR PLAYERS

Both T1D and T2D have a complex polygenic and multifactorial aetiology, hence providing a highly variable cellular and molecular readout, even between genetically related individuals. Due to this intrinsic high level of complexity, caused by the overlap between environment and intricate genetic susceptibility, there are still not clearly defined molecular and cellular mechanisms of disease onset and progression. Conversely, monogenic disorders are caused by single gene defects occurring in all cells of the organism. Therefore, the characterization of the causative genes and their associated

OPEN ACCESS

Edited and reviewed by:
Jordi Pérez-Tur,
Spanish National Research Council (CSIC), Spain

****Correspondence:***
Luiza Ghila
luiza.ghila@uib.no
Simona Chera
simona.chera@uib.no

Specialty section:
This article was submitted to Genetics of Common and Rare Diseases, a section of the journal Frontiers in Genetics

Received: *25 November 2021*
Accepted: *04 February 2022*
Published: *25 February 2022*

Citation:
Ghila L, Furuyama K, Grey ST, Scholz H and Chera S (2022) Editorial: Beta-Cell Fate: From Gene Circuits to Disease Mechanisms. Front. Genet. 13:822440. doi: 10.3389/fgene.2022.822440

molecular mechanisms involved in monogenic diabetes onset contribute to understanding the complex non-inherited T1D or T2D disorders.

To date, the genetic predisposition for monogenic diabetes was mostly studied in populations from western countries. To bridge this gap, Zhong et al. analyzed the clinical and genetic characteristics of 200 diabetic patients from Northern China to map the monogenic diabetes prevalence and identify putative novel mutations responsible for MODY. The study pinpointed a heterozygous missense mutation in the coding region of FOXM1 (rs535471991) as a potentially pathogenic variant, most likely affecting the risk of MODY. In the same line, Lin et al. described a case of ABCC8-MODY, previously unreported in China.

Furthermore, by analyzing 160 Egyptian patients, Kassem et al. investigated the correlation between two SERPINB1 SNPs and type 2 diabetes risk. They revealed that SERPINB1 SNP rs152826 can potentially predict glycemic control in diabetic patients while suggesting that the AA genotype of this SNP can be associated with an overall better glycemic regulation. In contrast, the G allele might be a "risk allele" for poor glycemic control.

Although numerous human participants were recruited for genome-wide association studies (GWAS), the genome and environmental factors (lifestyle) variability usually confound datasets, especially when studying a complex trait like blood glucose homeostasis. Hence, meticulous animal model studies are still a critical tool in diabetes research allowing accurate manipulation of both environment and genetic variance. In an original research article, Aga, Hallahan et al. crossed normoglycemic lean inbred DBA mouse with the diabetes-prone New Zealand obese (NZO) strain to identify novel potential T2D genes by using positional cloning. Focused on the most prominent diabetes quantitative trait loci (QTL) Nidd/DBA on chromosome 4, this study identified Kti12, Osbpl9, Ttc39a, and Calr4 as potential T2D candidates.

Interestingly, the associated loci for T1D and T2D seem to be almost completely separated, despite a partially shared phenotype. However, some genes from the risk loci for T1D and T2D might actually interact in common networks in order to mutually regulate crucial pancreatic islet functions. In order to investigate this avenue, Kaur et al. used a dual systems genetics approach by analyzing 57 T1D and 243 T2D established GWAS loci. This study identified a number of novel plausible common candidate genes and pathways for T1D and T2D: nine genes in common T1D and T2D loci that harbor islet eQTLs in linkage disequilibrium with disease-associated variants (GSDMB, CARD9, DNLZ, ERAP1, PPIP5K2, TMEM69, SDCCAG3, PLEKHA1, and HEMK1), and four genes in common T1D and T2D loci mutually regulated by palmitate and cytokines (ASCC2, HIBADH, RASGRP1, and SRGAP2).

Prolonged chronic hyperglycemia is a leading risk factor for developing micro- and macrovascular complications. Interestingly, some individuals do not develop these complications, despite long disease duration suggesting the involvement of protective mechanisms in these patients or, alternatively, the presence of risk factors in the patients that do progress to complications. Keindl et al. studied a panel of inflammatory markers in the plasma of long-term T1D patients with and without vascular complications and found that increased plasma level of a cytokine, soluble interleukin-2 receptor alpha (sIL-2R), was positively associated with the presence of vascular complications.

CELLULAR LEVEL/NOVEL CELLULAR PROCESSES

As also seen above, numerous alleles and mutations associated with increased risk of developing T1D or T2D diabetes (Fuchsberger et al., 2016) were identified in recent years, however cellular fate determination, identity, and function are also regulated at other levels, i.e. mRNA processing or protein folding, packing and sorting. Moss and Sussel summarise in a review the current knowledge on RNA-binding proteins, alternative-splicing events, and transcriptome-wide changes in RNA methylation landscape influencing specific functions of insulin-producing β-cells. As islet cells are mainly secretory cells handling a high amount of hormone production, there is strong pressure on the endoplasmic reticulum (ER) intrinsic folding capacity. This might lead to, for example, misfolded pro-insulin in β-cells triggering a physiological upregulation of the unfolded protein response (UPR) to restore homeostasis. Lenghel et al. discussed recent data addressing the role of UPR on the dedifferentiation or proliferation of β-cells, as well as in triggering inflammation at the islet level, and proposed possible therapies by using UPR for restoring β-cells homeostasis according to their stress level.

ISLET LEVEL/REGENERATIVE STRATEGIES

An increasing amount of recent studies suggest that diabetes is not only a β-cell disease, and several other islet cell types could also contribute to its physiopathology (Chakravarthy et al., 2017; Holst et al., 2017; Traub et al., 2017; Brissova et al., 2018; Cigliola et al., 2018; Rorsman and Huising, 2018; Furuyama et al., 2019; Cigliola et al., 2020; Nair et al., 2020). In a mini-review Bru-Tari et al. discussed recent work on islet cell heterogeneity and how this knowledge can be used to restore islet function and therefore to improve current β-cell replacement therapies. An alternative therapeutic strategy could be aimed at increasing the replication rate of insulin-producing β-cells (Nir et al., 2007), which is at very low levels in homeostatic islets. Along these lines, Jiang et al. studied the role of SNAPIN, a protein that interacts with SNARE complexes, in mediating β-cell proliferation. One potential approved drug with β-cell regenerative potential might be liraglutide, an analogue of glucagon-like peptide-1. Villalba et al. investigated the role of liraglutide on the restoration of β-cell mass in regards to neogenesis and transdifferentiation, although additional lineage-tracing studies will be required to clarify the origin of the cells involved in these processes.

PERSPECTIVES

A major goal of diabetes research is mapping the diverse specific cellular and molecular mechanisms leading to disease onset and progression. Advances in this area will lead to an improved diabetes classification and a more targeted management of the different diabetes subtypes. The need for this fine-tuned reclassification is clearly illustrated by the current high incidence of diabetes-related complications resulting from insufficient disease models supporting appropriate clinical decision-making. Better disease knowledge and, consequently, its improved management will help avoid unnecessary treatments, improve the patients' quality of living, reduce costs and ultimately bend the mortality curve.

Thus, in our view, demultiplexing the pathophysiological mechanisms characterising diabetes will remain a key goal of diabetes research, which can be achieved by further *1*) mapping associated genetic factors, including the mechanistic characterization and pathogenicity assessment of relevant genetic variants in different ethnic groups; *2*) identifying key regulators controlling the cellular processes and molecular landscape leading to disease onset and complications; 3) developing top-notch cell and animal models for studying islet cell function, dysfunction, and extra-pancreatic confounding effects.

AUTHOR CONTRIBUTIONS

LG and SC drafted the editorial. KF, SG, and HS each contributed by revising and editing. LG, SG, HS, and SC handled the received manuscripts. All authors listed have made a substantial, direct, and intellectual contribution to the work, and approved it for publication.

FUNDING

This work was supported by funds from the Research Council of Norway (NFR 247577 (SC), 251041 (SC) and 314397 (SC); CoE 262613 (HS)); Novo Nordic Foundation (NNF15OC0015054 and NNF21OC0067325) to SC; Diabetesforbundets forskningsfond to LG, SC, and HS.

ACKNOWLEDGMENTS

We are grateful to the editors, authors, and reviewers for their contribution emphasizing new research avenues in this rapidly changing and challenging field.

REFERENCES

American Diabetes Association (2005). Diagnosis and Classification of Diabetes Mellitus. *Diabetes Care* 28 Suppl 1, S37–S42. doi:10.2337/diacare.28.suppl_1.s37

Brissova, M., Haliyur, R., Saunders, D., Shrestha, S., Dai, C., Blodgett, D. M., et al. (2018). α Cell Function and Gene Expression Are Compromised in Type 1 Diabetes. *Cel Rep.* 22 (10), 2667–2676. doi:10.1016/j.celrep.2018.02.032

Chakravarthy, H., Gu, X., Enge, M., Dai, X., Wang, Y., Damond, N., et al. (2017). Converting Adult Pancreatic Islet α Cells into β Cells by Targeting Both Dnmt1 and Arx. *Cel Metab.* 25 (3), 622–634. doi:10.1016/j.cmet.2017.01.009

Chera, S., and Herrera, P. L. (2016). Regeneration of Pancreatic Insulin-Producing Cells by *In Situ* Adaptive Cell Conversion. *Curr. Opin. Genet. Dev.* 40, 1–10. doi:10.1016/j.gde.2016.05.010

Cigliola, V., Ghila, L., Thorel, F., van Gurp, L., Baronnier, D., Oropeza, D., et al. (2018). Pancreatic Islet-Autonomous Insulin and Smoothened-Mediated Signalling Modulate Identity Changes of Glucagon$^+$ α-cells. *Nat. Cel Biol.* 20 (11), 1267–1277. doi:10.1038/s41556-018-0216-y

Cigliola, V., Ghila, L., Chera, S., and Herrera, P. L. (2020). Tissue Repair Brakes: A Common Paradigm in the Biology of Regeneration. *Stem Cells* 38 (3), 330–339. doi:10.1002/stem.3118

Fuchsberger, C., Flannick, J., Teslovich, T. M., Mahajan, A., Agarwala, V., Gaulton, K. J., et al. (2016). The Genetic Architecture of Type 2 Diabetes. *Nature* 536 (7614), 41–47. doi:10.1038/nature18642

Furuyama, K., Chera, S., van Gurp, L., Oropeza, D., Ghila, L., Damond, N., et al. (2019). Diabetes Relief in Mice by Glucose-Sensing Insulin-Secreting Human α-cells. *Nature* 567 (7746), 43–48. doi:10.1038/s41586-019-0942-8

Holst, J. J., Holland, W., Gromada, J., Lee, Y., Unger, R. H., Yan, H., et al. (2017). Insulin and Glucagon: Partners for Life. *Endocrinology* 158 (4), 696–701. doi:10.1210/en.2016-1748

International Diabetes Federation (2021). *IDF Diabetes Atlas*. 10th Edn. Brussels, Belgium: International Diabetes Federation.

Nair, G. G., Tzanakakis, E. S., and Hebrok, M. (2020). Emerging Routes to the Generation of Functional β-cells for Diabetes Mellitus Cell Therapy. *Nat. Rev. Endocrinol.* 16 (9), 506–518. doi:10.1038/s41574-020-0375-3

Nir, T., Melton, D. A., and Dor, Y. (2007). Recovery from Diabetes in Mice by β Cell Regeneration. *J. Clin. Invest.* 117 (9), 2553–2561. doi:10.1172/JCI32959

Rorsman, P., and Huising, M. O. (2018). The Somatostatin-Secreting Pancreatic δ-Cell in Health and Disease. *Nat. Rev. Endocrinol.* 14 (7), 404–414. doi:10.1038/s41574-018-0020-6

Traub, S., Meier, D. T., Schulze, F., Dror, E., Nordmann, T. M., Goetz, N., et al. (2017). Pancreatic α Cell-Derived Glucagon-Related Peptides Are Required for β Cell Adaptation and Glucose Homeostasis. *Cel. Rep.* 18 (13), 3192–3203. doi:10.1016/j.celrep.2017.03.005

Conflict of Interest: The authors declare that the research was conducted in the absence of any commercial or financial relationships that could be construed as a potential conflict of interest.

Publisher's Note: All claims expressed in this article are solely those of the authors and do not necessarily represent those of their affiliated organizations, or those of the publisher, the editors and the reviewers. Any product that may be evaluated in this article, or claim that may be made by its manufacturer, is not guaranteed or endorsed by the publisher.

frontiers in Endocrinology

ORIGINAL RESEARCH
published: 13 May 2020
doi: 10.3389/fendo.2020.00258

Repurposed Analog of GLP-1 Ameliorates Hyperglycemia in Type 1 Diabetic Mice Through Pancreatic Cell Reprogramming

Adrian Villalba[1], Silvia Rodriguez-Fernandez[1], David Perna-Barrull[1], Rosa-Maria Ampudia[1], Laia Gomez-Muñoz[1], Irma Pujol-Autonell[1], Eva Aguilera[2], Mireia Coma[3], Mary Cano-Sarabia[4], Federico Vázquez[2], Joan Verdaguer[5,6] and Marta Vives-Pi[1,6†]*

[1] Immunology Section, Germans Trias i Pujol Research Institute, Autonomous University of Barcelona, Badalona, Spain, [2] Endocrinology Section, Germans Trias i Pujol Research Institute, Autonomous University of Barcelona, Badalona, Spain, [3] Anaxomics Biotech SL, Barcelona, Spain, [4] Catalan Institute of Nanoscience and Nanotechnology, CSIC and The Barcelona Institute of Science and Technology, Bellaterra, Spain, [5] Immunology Unit, Department of Experimental Medicine, Faculty of Medicine, IRBLleida, University of Lleida, Lleida, Spain, [6] CIBER of Diabetes and Associated Metabolic Disease (CIBERDEM), ISCIII, Madrid, Spain

OPEN ACCESS

Edited by:
Simona Chera,
University of Bergen, Norway

Reviewed by:
Quan Zhang,
University of Oxford, United Kingdom
Anabel Rojas,
Andalusian Center of Molecular Biology and Regenerative Medicine (CABIMER), Spain

***Correspondence:**
Marta Vives-Pi
mvives@igtp.cat

†ORCID:
Marta Vives-Pi
http://orcid.org/0000-0003-3735-0779

Specialty section:
This article was submitted to Cellular Endocrinology, a section of the journal Frontiers in Endocrinology

Received: 13 January 2020
Accepted: 07 April 2020
Published: 13 May 2020

Citation:
Villalba A, Rodriguez-Fernandez S, Perna-Barrull D, Ampudia R-M, Gomez-Muñoz L, Pujol-Autonell I, Aguilera E, Coma M, Cano-Sarabia M, Vázquez F, Verdaguer J and Vives-Pi M (2020) Repurposed Analog of GLP-1 Ameliorates Hyperglycemia in Type 1 Diabetic Mice Through Pancreatic Cell Reprogramming. Front. Endocrinol. 11:258. doi: 10.3389/fendo.2020.00258

Type 1 diabetes is an autoimmune disease caused by the destruction of the insulin-producing β-cells. An ideal immunotherapy should combine the blockade of the autoimmune response with the recovery of functional target cell mass. With the aim to develop new therapies for type 1 diabetes that could contribute to β-cell mass restoration, a drug repositioning analysis based on systems biology was performed to identify the β-cell regenerative potential of commercially available compounds. Drug repositioning is a strategy used for identifying new uses for approved drugs that are outside the scope of the medical indication. A list of 28 non-synonymous repurposed drug candidates was obtained, and 16 were selected as diabetes mellitus type 1 treatment candidates regarding pancreatic β-cell regeneration. Drugs with poor safety profile were further filtered out. Lastly, we selected liraglutide for its predictive efficacy values for neogenesis, transdifferentiation of α-cells, and/or replication of pre-existing β-cells. Liraglutide is an analog of glucagon-like peptide-1, a drug used in patients with type 2 diabetes. Liraglutide was tested in immunodeficient NOD-*Scid IL2rg*$^{-/-}$ (NSG) mice with type 1 diabetes. Liraglutide significantly improved the blood glucose levels in diabetic NSG mice. During the treatment, a significant increase in β-cell mass was observed due to a boost in β-cell number. Both parameters were reduced after withdrawal. Interestingly, islet bihormonal glucagon^{+}insulin^{+} cells and insulin^{+} ductal cells arose during treatment. *In vitro* experiments showed an increase of insulin and glucagon gene expression in islets cultured with liraglutide in normoglycemia conditions. These results point to β-cell replacement, including transdifferentiation and neogenesis, as aiding factors and support the role of liraglutide in β-cell mass restoration in type 1 diabetes. Understanding the mechanism of action of this drug could have potential clinical relevance in this autoimmune disease.

Keywords: beta cell regeneration, neogenesis, transdifferentiation, liraglutide, drug repositioning

INTRODUCTION

An essential requirement to cure type 1 diabetes is the recovery of β-cells lost after the autoimmune destruction. The pancreas can restore β-cells from different sources, after injury (1) or drug administration (2, 3) in mice, and upon pathophysiological conditions in humans (4). With the aim to develop new therapies for β-cell replacement, a repositioning analysis based on systems biology was performed to identify the regenerative potential of commercially available compounds.

Drug repositioning is a strategy for identifying new uses for approved drugs that are outside the scope of the medical indication. This approach uses a bioinformatics tool, based on networks of drugs, proteins, and diseases, which screens approved compounds that can be repurposed for other diseases (5). This has resulted in successful drug discovery for diseases (6) such as cancer (7) and Alzheimer's disease (8). Given that, we aimed to look for drugs that can induce β-cell replacement through α-cell to β-cell transdifferentiation (9), neogenesis from multipotent ductal progenitors (1), and/or replication of pre-existing β-cells (10). This resulted in the identification of liraglutide—an analog of glucagon-like peptide-1 (aGLP-1), a drug used in patients with type 2 diabetes (11), especially those with obesity (12).

GLP-1 is produced in the gut after food intake and acts by increasing insulin release. Liraglutide ameliorates insulin resistance in type 2 diabetes models (13, 14). Recently, GLP-1 has been shown to promote transdifferentiation from α-cells to β-cells (15, 16).

We report here that liraglutide ameliorates hyperglycemia in mice with type 1 diabetes by inducing insulin$^+$glucagon$^+$ cells and insulin-producing cells from the pancreatic ducts. This is the first description of an approved drug—identified by a repositioning—that promotes the generation of insulin-expressing cells from pancreatic ducts and ameliorates hyperglycemia in experimental type 1 diabetes.

MATERIALS AND METHODS

Systems Biology Analysis for Drug Discovery and Repositioning Analysis

The therapeutic performance mapping system is a top-down systems biology approach based on artificial intelligence and pattern recognition that integrates all available pharmacological knowledge to create mathematical models that simulate human pathophysiology *in silico*. The methodology employed has been previously described (17) and applied elsewhere (18, 19).

A manually curated list of proteins known to be involved in the mechanisms of β-cell regeneration—α-cell to β-cell transdifferentiation, neogenesis from ductal precursors, and β-cell replication—was obtained (**Supplementary Table 1**) and used for focusing the analysis toward β-cell regeneration in a human biological network context.

The human biological network created incorporated the available relationships (edges or links) between proteins (nodes) from a regularly updated in-house database drawn from public sources: KEGG (20, 21), REACTOME (22), INTACT (23), BIOGRID (24), HPRD (25), and TRRUST (26). All information of the key proteins defined during the molecular and the biological characterization and stored in relevant databases (drug targets, other diseases effectors, biomarkers…) was incorporated into the biological networks (27).

Artificial neural networks (ANNs) are supervised algorithms that identify relations between proteins (e.g., drug targets) and clinical elements of the network (18, 19) by inferring the probability of the existence of a specific relationship between two or more protein sets. This is based on a validation of the predictive capacity of the model toward the truth table, a selected collection of known input (drug targets)–output (indications) relationships defined through specific scientific literature search and hand-curated assignment of proteins to the conditions included in the biological effector database (17). The learning methodology used consisted of an architecture of stratified ensembles of neural networks as a model, trained with a gradient descent algorithm to approximate the values of the given truth table. The neural network model used was a multilayer perceptron (MLP) neural network classifier. The MLP gradient descent training depends on randomization initialization and, to avoid random errors, 1,000 MLPs are trained with the training subset and the best 100 MLPs are used. In order to correctly predict the effect of a drug independently of the number of targets, different ensembles of neural networks are trained for different subsets of drugs according to their number of targets (drugs with one target, two targets, three targets…). Then, the predictions for a query drug are calculated by all the ensembles and pondered according to the number of targets of the query drug (the difference between the number of targets of the query and the number of targets of the drugs used to calculate each ensemble is used to ponder the result of each ensemble). A cross-validation with the truth table information showed that the accuracy of the described ANNs to reproduce the indications compiled in DrugBank (28, 29) is 81.23% for those drugs with all targets in the human biological network. ANNs were used to screen the predicted relationship of 6,605 different drugs toward the β-cell regeneration molecular definition. The repurposed drug candidates were sorted and selected by its relationship with β-cell regeneration mechanisms.

Mice and Diabetes Induction

NOD mice, immunodeficient NOD.SCID-IL2Rγ$^{-/-}$ (NSG) mice, and C3HeB/FeJ mice were bred in our own facility. The NOD and NSG mice were kept under specific pathogen-free conditions. The NSG model was selected for its lack of an adaptive immune system, resulting in the absence of autoimmunity, and allowing to determine the raw effect of the drug. Type 1 diabetes was induced in NSG mice at 8–14 weeks of age by a single i.p. injection of streptozotocin (STZ, 150 mg/kg)

Abbreviations: ANN, artificial neural network; AUC, area under the curve; aGLP-1, analog glucagon-like peptide-1; NSG, immunodeficient NOD.SCID-IL2Rγ$^{-/-}$ mice; IPGTT, intraperitoneal glucose tolerance test; ITT, insulin tolerance test; STZ, streptozotocin.

(Sigma-Aldrich). Type 1 diabetes was confirmed at 48–72 h post-STZ injection, after either two successive 2-h fasting blood glucose levels higher than 250 mg/dl or with one higher than 300 mg/dl. The mice were euthanized by cervical dislocation. All animal studies were approved by the institutional animal ethics committee.

Treatment With aGLP-1

Immediately after type 1 diabetes diagnosis, the NSG mice (n = 12 mice/group) were treated with liraglutide (Victoza®, Novo Nordisk A/S), injected (s.c.) daily up to 30 days, following the dosage of 0.3 mg/kg at day 1, 0.6 mg/kg at day 2, and 1 mg/kg from day 3 onwards as described (30). After the withdrawal of the liraglutide treatment, the mice were maintained for 5 days. The control group (n = 6 mice) received phosphate-buffered saline (PBS). Blood glucose was determined twice weekly, after 2 h of fasting, throughout the study.

Intraperitoneal Glucose Tolerance Test and Insulin Tolerance Test

Intraperitoneal glucose tolerance test (IPGTT) was performed in fasting conditions in the three groups: (1) diabetic NSG mice responding to liraglutide after 15 days of treatment (Lira, n = 3), (2) untreated diabetic and hyperglycemic NSG mice (T1D, n = 3), and (3) healthy and normoglycemic NSG mice (sham, n = 3). At point 0, basal glucose level was determined. The mice were subsequently given an i.p. injection of 2 mg of glucose (Sigma-Aldrich) per gram of body weight and glycemia was measured after 15, 30, 60, 120, and 210 min. Insulin tolerance test (ITT) was performed in fasting conditions in 8-week-old and normoglycemic NOD mice and C3HeB/FeJ mice injected s.c. with insulin (0.5 U/kg, n = 3) or liraglutide (1 mg/kg, n = 3). Glycemia was determined after 15, 30, and 60 min.

Immunofluorescence Staining and Histometric Analysis

Immunofluorescence staining was performed to identify pancreatic insulin-producing cells in a minimum of three mice per condition. Briefly, the pancreas were harvested and snap-frozen in an isopentane/cold acetone bath. A minimum of eight cryostat sections (5 μm) from every organ were sequentially stained by indirect immunofluorescence with antibodies to insulin, glucagon, CK19 (Sigma-Aldrich), or Pdx1 (Abcam) and FITC- or TRITC-labeled secondary antibodies (Sigma-Aldrich) as described (31). The nuclei were stained with Hoechst (Invitrogen). The samples were observed in a fluorescence microscope and analyzed (ImageJ Software) (32). For histometric analysis, six mice per group were used. To determine the β-cell counts, one section every 150 μm of tissue was sampled as described (33), resulting in 12–16 sections per pancreas. The β-cell mass was calculated by multiplying the relative insulin$^+$ area per total pancreas weight, and the β-cell number as well as the insulin$^+$ aggregates were calculated by manually counting the nuclei within the insulin$^+$ area and extrapolating to the whole organ as previously described (34). The β-cell size was assessed by dividing the insulin$^+$ area per total nuclei (34). The intensity of fluorescence was measured in arbitrary units using Fiji (32).

To determine the insulin$^+$glucagon$^+$ cells, pancreas from three mice from each group were analyzed (T1D, Lira 48 h, Lira, post-Lira, and sham). Briefly, 12 non-overlapping pancreatic cryostat sections from each mouse were stained for insulin and glucagon. A minimum of 72 islets per mouse was considered and the percentage of islets that contained bihormonal cells was determined. To assess ductal insulin$^+$ cells, pancreas from four mice from each group were analyzed (T1D, sham, and Lira). Briefly, four non-overlapping pancreatic cryostat sections from each mouse were stained for CK19 and insulin. A minimum of 23 ductal areas *per section* was considered and the percentage of ducts that contained insulin$^+$ cells was determined. To prove the colocalization of insulin and glucagon in islet cells and insulin and CK19 in ductal cells, confocal microscopy was performed using an Axiobserver Z1 (Zeiss) and by analyzing 1-μm sections.

In vivo Tracking of Liraglutide

Liraglutide was conjugated to AlexaFluor750 (AF750, Invitrogen) using a standard method (Thiol-Reactive Probes, Invitrogen). *In vivo* and *ex vivo* near-infrared fluorescence imaging was performed (Pearl Impulse imaging system, LI-COR) in NOD mice anesthetized with ketamine (50 mg/kg) and xylazine (5 mg/kg) at 15 and 60 min after the s.c. administration of 1 mg/kg of AF750-liraglutide in 50 μl of PBS. At the end of each checkpoint, spleen, stomach, fat, heart, liver, pancreas, lungs, kidney, salivary glands, thymus, and bladder were imaged *ex vivo*. Fluorescent signal intensity was semi-quantitatively assessed: the levels were normalized by subtracting the background and represented as a relative index of fluorescence in each organ per gram of tissue.

Islets and β-Cell Line

Islets from young non-diabetic NOD mice (n = 7) were obtained from pancreas digested with collagenaseP (2.5 mg/ml in PBS; Sigma-Aldrich), after having been injected through the common bile duct, resected, and incubated at 37°C for 30 min. The pancreas was dissociated and the islets were hand-picked. Groups of 50 islets were cultured in a medium of high (10 mM, RPMI-1640, Biowest) or normal glucose concentration (6.1 mM, Ham F-10, Gibco) as described (35), both in basal conditions—culture media—and by adding liraglutide at 1,000 nM for 48 h.

The β-cell line NIT-1 (ATCC) (36) was cultured (35) with liraglutide at 10, 100, and 1,000 nM for 12, 24, and 48 h. Viability was assessed with annexin V (AnnV) PE (Immunotools) and 7-amino-actinomycin D (7aad) labeling (BD Pharmingen) and analyzed with FACS Canto II (BD Biosciences).

Gene Expression Analysis

To determine the effects of liraglutide on gene expression, quantitative RT-PCR was performed. Briefly, RNA was isolated from islets using RNeasy Micro Kit (Qiagen) and reverse-transcribed with a cDNA Reverse-Transcription Kit (ThermoFisher Scientific). cDNA synthesis was performed using random hexamers (0.5 mg/ml, BioTools) and reverse

transcriptase Moloney–murine–leukemia–virus (200 U/ml, Promega). Targeted cDNA was pre-amplified with TaqMan PreAmp MasterMix (ThermoFisher Scientific). Quantitative RT-PCR assays were performed with TaqMan universal assay (ThermoFisher Scientific) on a LightCycler®480 (Roche) using the following TaqMan assays: *Ins2* (Mm00731595_gH), *Gcg* (Mm00801714_m1), *Ki67* (Mm01278617_m1), and *Il17a* (Mm00439618_m1). The expression for each gene of interest was normalized to that of the housekeeping gene *Gapdh* (Mm99999915_g1), as described in the $2^{-\Delta Ct}$ method (37). Values from islets were normalized using their respective basal controls and represented as a ratio (relative gene expression).

Effect of Liraglutide on NIT-1 Cell Line

NIT-1 cells were stained with anti-CD44 BV786 (BD Biosciences), anti-class I major histocompatibility complex (MHC) eFluor-450 (eBioscience), anti-CD14 PE, and anti-CD49b FITC (Immunotools). Viability was assessed with AnnV PE (Immunotools) and 7aad (BD Biosciences) as detailed above. Median fluorescence intensity and viability were determined using flow cytometry (LSR Fortessa, BD Biosciences). Corresponding fluorescence minus one staining was used as control. The data were analyzed using FlowJo (Tree Star Inc).

Statistical Analysis

Prism 7.0 (GraphPad Software Inc.) was used to perform the statistical analyses. For comparisons of unpaired data, a non-parametric Mann–Whitney test was used. The statistical tests applied to each data set are specified in each figure legend.

RESULTS

Liraglutide Is a Repurposed Candidate for β-Cell Regeneration

A total of 28 non-synonymous repurposed drug candidates showed a $p < 0.05$ (predicted value $\geq$76.075%), and 16 were selected as type 1 diabetes treatment candidates in the context of pancreatic β-cell regeneration. Drugs with poor safety profile were further filtered out. Lastly, we selected liraglutide (predicted value of 96.88%) that fulfilled all the criteria and had a novel, potentially beneficial mechanism toward β-cell regeneration.

Liraglutide Improves Hyperglycemia in Diabetic Mice

We determined the effect of liraglutide in immunodeficient NSG mice because of their absence of autoimmunity and low phenotypic heterogeneity. Type 1 diabetes was induced in NSG mice by a single STZ injection. All mice showed disease symptoms at 48–72 h after administration. A total of 50% (six of 12) of the treated NSG mice were responders to liraglutide according to the improvement of blood glucose levels during treatment. The remaining six mice did not have decreased blood glucose levels in any way. No differences in terms of initial fasting glycemia (mg/dl) were found between the responder (346.8 ± 72.5, mean ± SD) and the non-responder (397.7 ± 57.71) mice. The NSG mice with diabetes partially recovered normoglycemia during liraglutide administration until day 30 (Lira responders) when compared to the non-treated mice (T1D) (**Figure 1A**). After treatment withdrawal, all mice became hyperglycemic. A statistical difference between the treated and the control groups was observed when analyzing the area under the curve (AUC) after 15 days of treatment (**Figure 1B**). The response of the NSG mice to liraglutide after an acute increase in blood glucose levels showed that the treated diabetic mice (Lira) recovered normoglycemia at 210 min after glucose injection similarly to the non-diabetic group, whereas the diabetic non-treated mice remained hyperglycemic (>400 mg/dl, T1D) (**Figure 1C**). Significant differences found between the treated and the non-treated mice demonstrate that insulin production and secretion improve by the effect of this aGLP-1. The analysis of AUC showed an intermediate response to glucose stimulation in the liraglutide-treated group (**Figure 1D**). To elucidate whether liraglutide acts in a similar manner as insulin administration, an ITT was performed in normoglycemic NOD mice. The group treated with insulin displayed a reduction in glycemia after 30 min that was maintained until 60 min. By contrast, the liraglutide-treated group displayed an increase in glycemia until 30 min, which was normalized at 60 min similarly to the insulin-treated animals (**Figure 1E**). Despite that no significant differences were observed, the opposite tendency between both groups observed in the AUC (**Figure 1F**) revealed that liraglutide and insulin do not act similarly. To determine the effect of the genetic background, the acute effect of liraglutide was also determined on the C3HeB/FeJ strain. The results showed an insulinotropic effect of liraglutide in this strain of mice (**Supplementary Figure 1**) with a tendency to differ at the endpoint (60 min) in comparison to insulin.

Liraglutide Transiently Increases the β-Cell Mass

The β-cell mass of the NSG mice after 7–15 days of treatment with liraglutide significantly increased when compared to that of the diabetic non-treated mice, although they did not reach normal levels (**Figure 2A**). This effect was lost 5 days after withdrawal. In this sense, an increase in β-cell number was detected during the treatment in comparison to T1D and post-treatment groups (**Figure 2B**). These alterations were maintained even with normalized values to body weight or pancreatic tissue (**Supplementary Table 2**). Similarly, the percentage of islets emerging from ducts was increased both during treatment and after therapy removal (**Figure 2C**). These alterations were not related to changes in either β-cell size (**Figure 2D**) or insulin fluorescence intensity (33) (**Figure 2E**).

Liraglutide Induces Endocrine Cell Rearrangement in the Pancreas

The histological analysis revealed the presence of bihormonal cells ($insulin^+glucagon^+$) in the islets of NSG mice at the beginning of the treatment with liraglutide but not after 7–15 days or withdrawal (**Figure 3**). A total of 48.14 ± 1.53% of islets contained bihormonal cells, and the

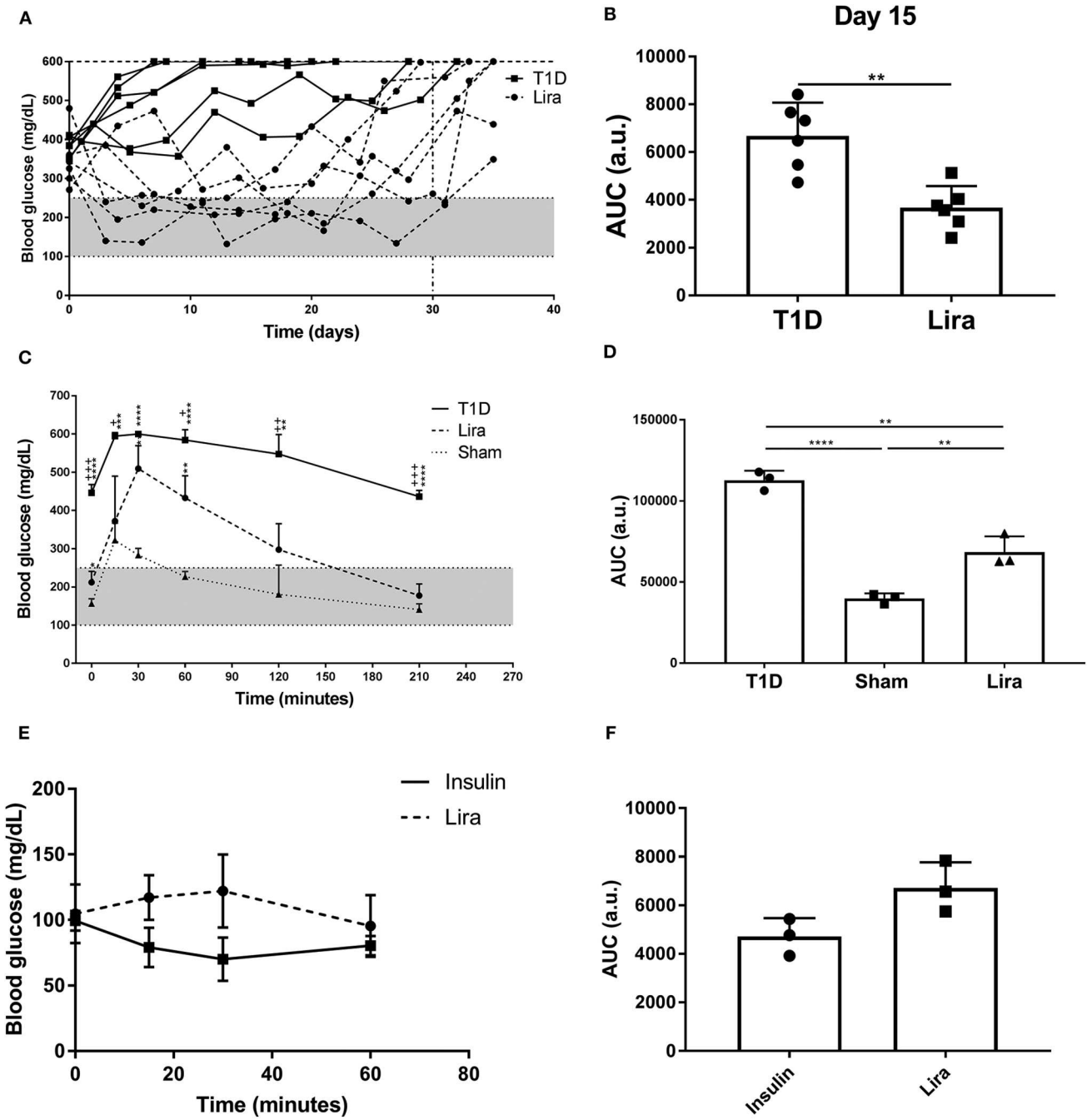

FIGURE 1 | Effect of liraglutide in diabetic immunodeficient NOD.SCID-IL2Rγ$^{-/-}$ (NSG) mice. **(A)** Two-hour fasting blood glucose levels (mg/dl) in mice rendered diabetic by a single dose of streptozotocin (150 mg/kg) and then treated with daily s.c. injections of liraglutide (Lira responders, circles) and phosphate-buffered saline (T1D, squares) from day 0 to 30 (dashed line). The filled area corresponds to normoglycemia levels in mice. **(B)** Area under the curve (AUC) of the graph in **(A)** at day 15, when all animals remain alive. Results are mean ± SD, and differences were found between groups (**$p < 0.01$, Mann–Whitney test). **(C)** Intraperitoneal glucose tolerance test in diabetic NSG mice treated with daily s.c. liraglutide for 15 days (Lira, dashed line), non-treated diabetic animals (T1D, continuous line), and normoglycemic mice (sham, dotted line). Statistical differences were found between Lira and T1D groups (+$p < 0.05$, ++$p < 0.01$, + + +$p < 0.001$, Mann–Whitney test) and in both groups when compared to sham (dotted line) (*$p < 0.05$, **$p < 0.01$, ***$p < 0.001$, ****$p < 0.0001$, Mann–Whitney test). The filled area corresponds to normoglycemia levels in mice. **(D)** AUC of the graph in **(C)**. The results are mean ± SD, and differences were found between groups (**$p < 0.01$, ****$p < 0.0001$, Mann–Whitney test). **(E)** Insulin tolerance test performed in normoglycemic mice injected with Lira (1 mg/kg, dashed line) or insulin (0.5 U/kg, continuous line). **(F)** AUC of the graph in **(E)**. The results are mean ± SD; no statistical differences were found between groups.

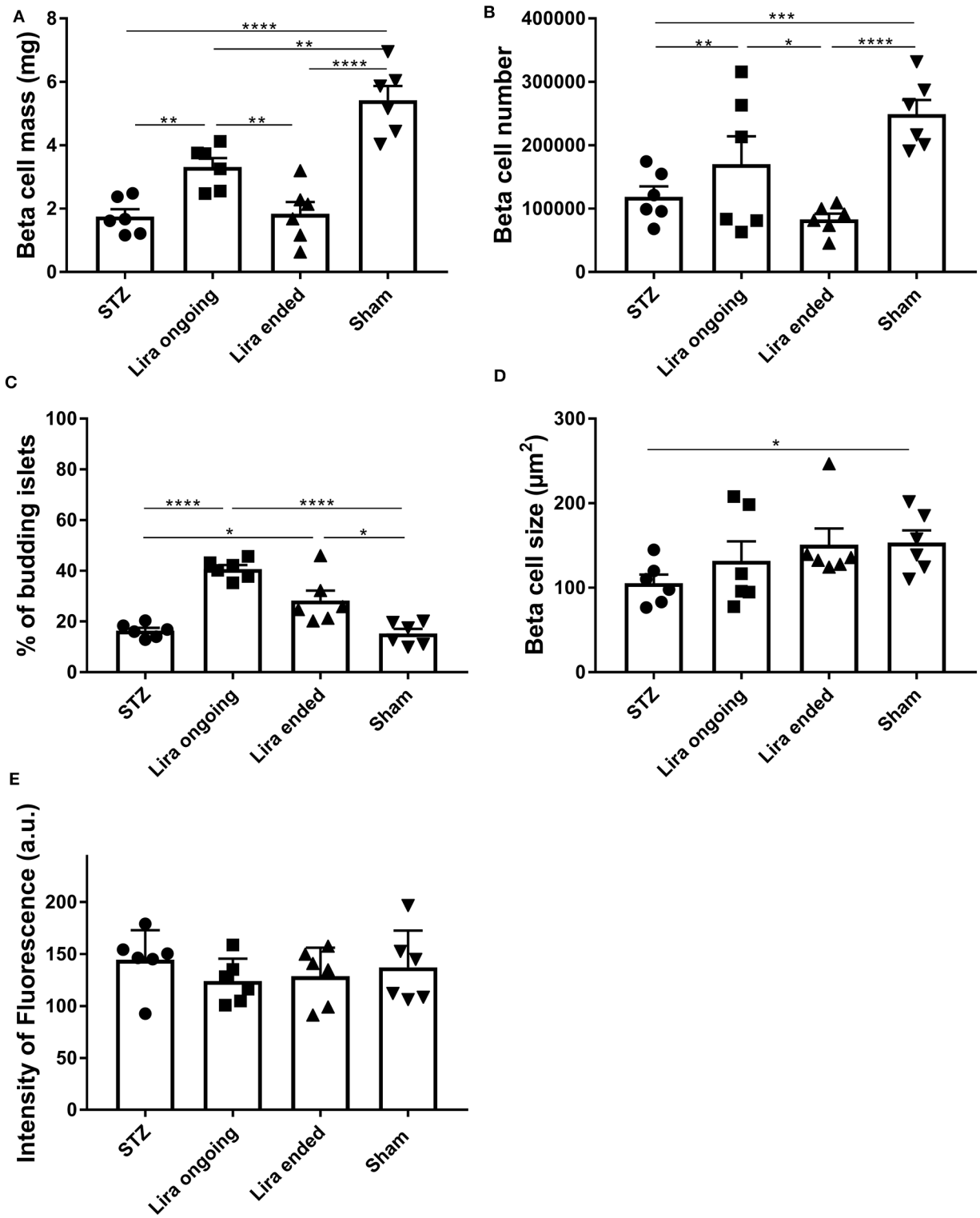

FIGURE 2 | Effect of liraglutide in the endocrine pancreas of diabetic immunodeficient NOD.SCID-IL2R$\gamma^{-/-}$ (NSG) mice. **(A)** β-cell mass (mg), **(B)** β-cell number, **(C)** percentage of budding islets (arising from ducts), and **(D)** β-cell size (μm^2) from NSG mice rendered diabetic by streptozotocin and treated with phosphate-buffered saline (T1D), with daily s.c. injections of liraglutide during 7–15 days (Lira), 5 days after the withdrawal of the liraglutide treatment (post-Lira) and normoglycemic mice (sham). The results are mean ± SD, and differences were found between groups (*$p < 0.05$, **$p < 0.01$, ***$p < 0.001$, ****$p < 0.0001$, Mann–Whitney test).

(Continued)

FIGURE 2 | (E) Intensity of fluorescence of insulin staining in 5-μm cryostat pancreatic sections of NSG mice. The intensity was measured for all the islets analyzed per animal, and the mean of the intensities of all the islets is represented as a symbol. The results are mean ± SD, and no statistical differences were found between groups (Mann–Whitney test).

percentage of insulin$^+$glucagon$^+$ cells in relation to the total number of beta cells in the islets was 11.38 ± 2.97%. No bihormonal cells were detected in the other groups. Confocal microscopy images prove the colocalization of insulin and glucagon in the same cell (bihormonal cells) (**Supplementary Figure 2**).

Moreover, the pancreatic sections of the NSG mice treated for 7–15 days and after withdrawal revealed the existence of insulin$^+$ bodies emerging from ducts and without resembling the classical islet shape (**Figure 4A**). Between 23 and 47 ducts (CK19+) were analyzed in every pancreatic section. The percentage of ducts that contained insulin$^+$ cells was 50.83 ± 7.31% in mice treated with liraglutide (Lira group), whereas no ducts with insulin$^+$ cells were detected in normoglycemic mice (sham group, 0%) or untreated T1D mice (T1D, 0%). The ducts that contained insulin$^+$ cells were analyzed and, in these ductal areas, 82.85 ± 4.37% of doble-positive CK19$^+$ insulin$^+$ cells were found. Interestingly, the ductal areas positive for insulin in mice treated with liraglutide were detected from 48 h to the end of the treatment and even 5 days after the withdrawal (**Figure 4B**, white arrows). Confocal microscopy images prove the colocalization of insulin and CK19 in the same cell (**Supplementary Figure 3**). These insulin$^+$CK19$^+$ cells were glucagon-negative (**Figure 4C**). Moreover, we assessed the expression of the β-cell marker Pdx1 in ductal cells, identifying a subpopulation of Pdx1$^+$ cells in pancreatic ducts from treated animals (white arrow, **Figure 4D**).

To determine if liraglutide effects could be due to the accumulation in the pancreas, its biodistribution was assessed. The *in vivo* tracking of AF750-liraglutide showed an affinity for several organs including the pancreas that was higher at 15 min (**Figure 5A**) than at 60 min (**Figure 5B**), revealing an acute effect.

To further investigate the short-term effects of liraglutide, the expression of specific genes was assessed in islets from healthy NOD mice (three to four per group) cultured with or without liraglutide for 48 h in normal and high glucose concentrations. Previously, and in order to discard autoreactive insulitis in the islets, the expression of *Il17a* was assessed and found negative (data not shown). After exposure to liraglutide, a trend to upregulate *Gcg* and to downregulate *Ki67* was observed both at doses of 6.1 mM glucose (**Figure 5C**) and 10 mM glucose (**Figure 5D**). Finally, after exposure to liraglutide, the insulin gene (*Ins2*) appeared upregulated in normal glucose concentration conditions and slightly downregulated in high glucose concentration conditions.

Liraglutide Alters Membrane Molecule Expression in NIT-1 Cell Line

NIT-1 cell viability remained unaffected by liraglutide (10, 100, and 1,000 nM) at both 12 and 48 h (**Figure 6A**) but showed a deleterious effect on the NIT-1 cell line at 100 and 1,000 nM during 24 h (**Figure 6A**). Interestingly, liraglutide increased the expression of adhesion molecules such as CD49b, CD44 (**Figure 6B**), and CD14, a receptor of the innate immunity, and reduced the expression of MHC class I.

DISCUSSION

Drug repositioning is an attractive strategy for identifying new uses for approved drugs. The algorithm of this method was fed with target proteins known to be involved in β-cell restoration processes—(i) α-cell to β-cell transdifferentiation (9), (ii) neogenesis from multipotent ductal progenitors (1), and (iii) self-replication of pre-existing β-cells (10)—and resulted in the identification of liraglutide as a repurposed drug. As mentioned, liraglutide is an aGLP-1 used to treat type 2 diabetes (11, 12). A recent clinical trial demonstrates that liraglutide reduced HbA1c and insulin requirements in patients with long-standing type 1 diabetes (38). Moreover, it has been described that liraglutide improves β-cell function in alloxan-induced diabetic mice (39).

Our data show that liraglutide improves hyperglycemia, even reaching normoglycemia, in NSG mice. This model was selected for its lack of an adaptive immune system, resulting in immunodeficiency, and absence of autoimmunity. This fact allows us to determine the effect of the drug without autoimmunity interferences and reduced heterogeneity. The amelioration of hyperglycemia was also observed upon glucose stimuli (IPGTT) in diabetic mice treated with liraglutide, whereas diabetic non-treated mice remained hyperglycemic. By contrast, the administration of liraglutide to normoglycemic NOD mice resulted in a weak and transient increase of glycemia levels, as opposed to the effects of insulin administration. Taken together, these results indicate that liraglutide ameliorates hyperglycemia both in fasting and fed conditions but acting differently to insulin. The acute effect of liraglutide on a different mouse strain was insulinotropic as expected. These differences between NOD and C3 mice could be due, at least in part, to genetic differences in the structure and the size of the endocrine pancreas in both strains, specifically in the α- and β-cell mass (40). Another influencing factor should be the islet leukocyte infiltration, a feature of the NOD model, which promotes an inflammatory microenvironment, thus affecting insulin metabolism. The acute effect of liraglutide on a different mouse strain—C3 mice were normoglycemic and free of insulitis—was insulinotropic as expected. The NOD mice are also normoglycemic, but they display islet leukocyte infiltration despite no signs of overt diabetes having been observed at 8 weeks of age. The observation of spontaneous insulitis is restricted to mice with a diabetogenic genetic background, specifically NOD and NOR strains, and CD-1 outbred mice (31). The C3 mice display non-diabetogenic genetic background, do not develop spontaneously

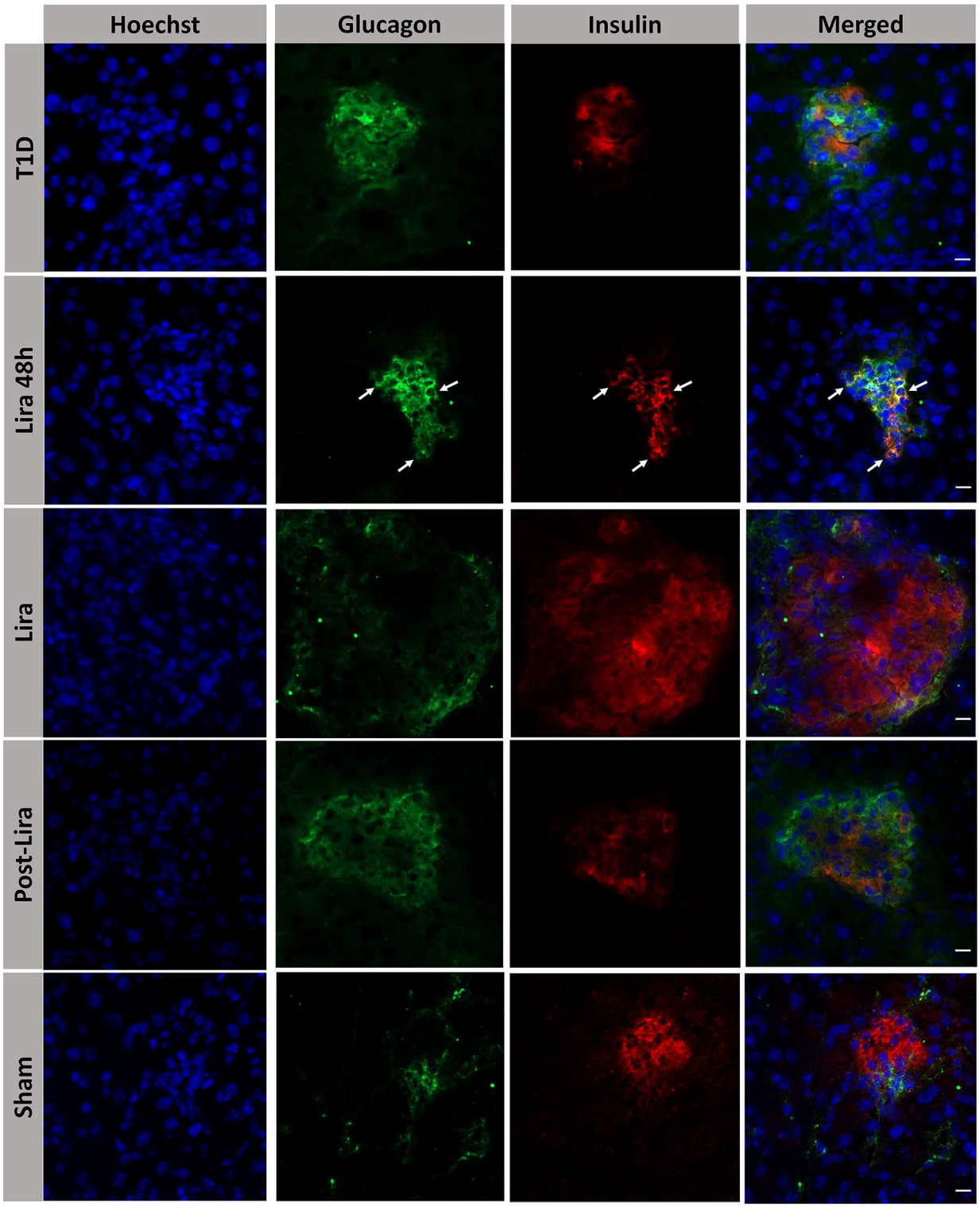

FIGURE 3 | Assessment of the effect of liraglutide in the induction of bihormonal insulin^{+} glucagon^{+} cells. Triple immunofluorescence staining of 5-μm cryostat pancreatic sections for α-cells (glucagon, green) and β-cells (insulin, red) in immunodeficient NOD.SCID-IL2Rγ$^{-/-}$ mice rendered diabetic by streptozotocin and treated with phosphate-buffered saline (T1D), or with liraglutide for 48 h (Lira 48 h), for 7–15 days (Lira) and after withdrawal of liraglutide at day 30 (post-Lira). Normoglycemic mice were included as control (sham). The white arrows in Lira 48 h staining depict bihormonal cells. The nuclei in all pictures were stained with Hoechst (blue). The scale bar indicates 5 μm.

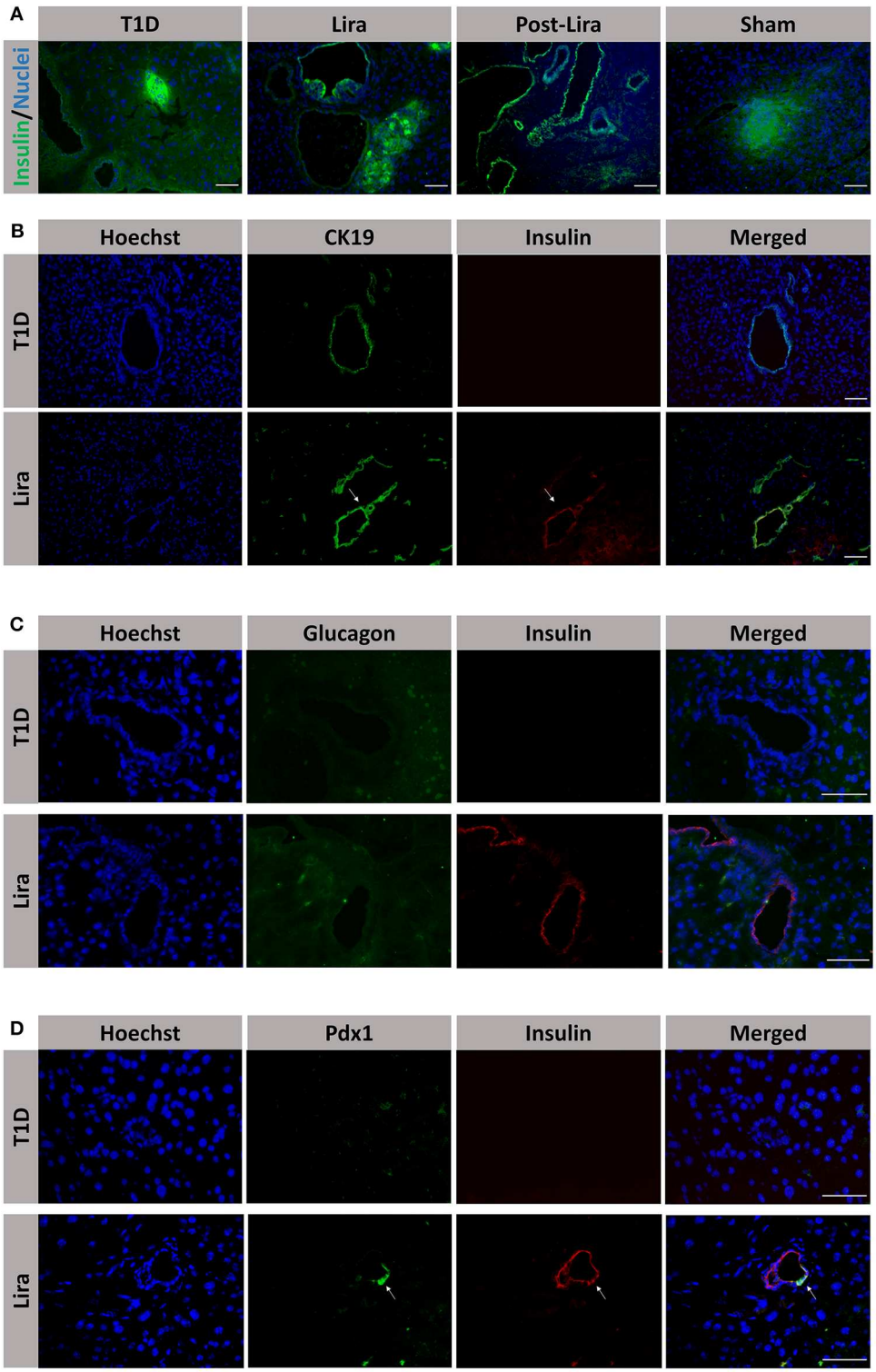

FIGURE 4 | Assessment of the effect of liraglutide in the induction of insulin-expressing ducts. **(A)** Staining for β-cells in the pancreas of immunodeficient NOD.SCID-IL2Rγ$^{-/-}$ (NSG) mice rendered diabetic by streptozotocin and treated with phosphate-buffered saline (PBS; T1D), or with liraglutide for 48 h (Lira 48 h), for 7–15 days (Lira) and after the withdrawal of liraglutide at day 30 (post-Lira). The Lira and post-Lira groups show the presence of neo-islets emerging from the ducts. Normoglycemic mice were included as control (sham). **(B)** Staining for ductal cells (CK19, green) and β-cells (insulin, red) in the same groups than in **(A)**. The white arrow depicts a CK19^{+} duct that is positive for insulin expression. **(C)** Staining for glucagon (green) and insulin (red) in ductal cells of animals treated with

(Continued)

FIGURE 4 | liraglutide for 7–15 days (Lira). **(D)** Staining for Pdx1 (green) and insulin (red) in the ductal part of diabetic NSG mice treated with PBS (T1D) or liraglutide for 7–15 days (Lira). The white arrows depict positivity for both Pdx1 and insulin in the ducts. The nuclei in all pictures are stained with Hoechst (blue). The scale bar in all pictures indicates 50 μm.

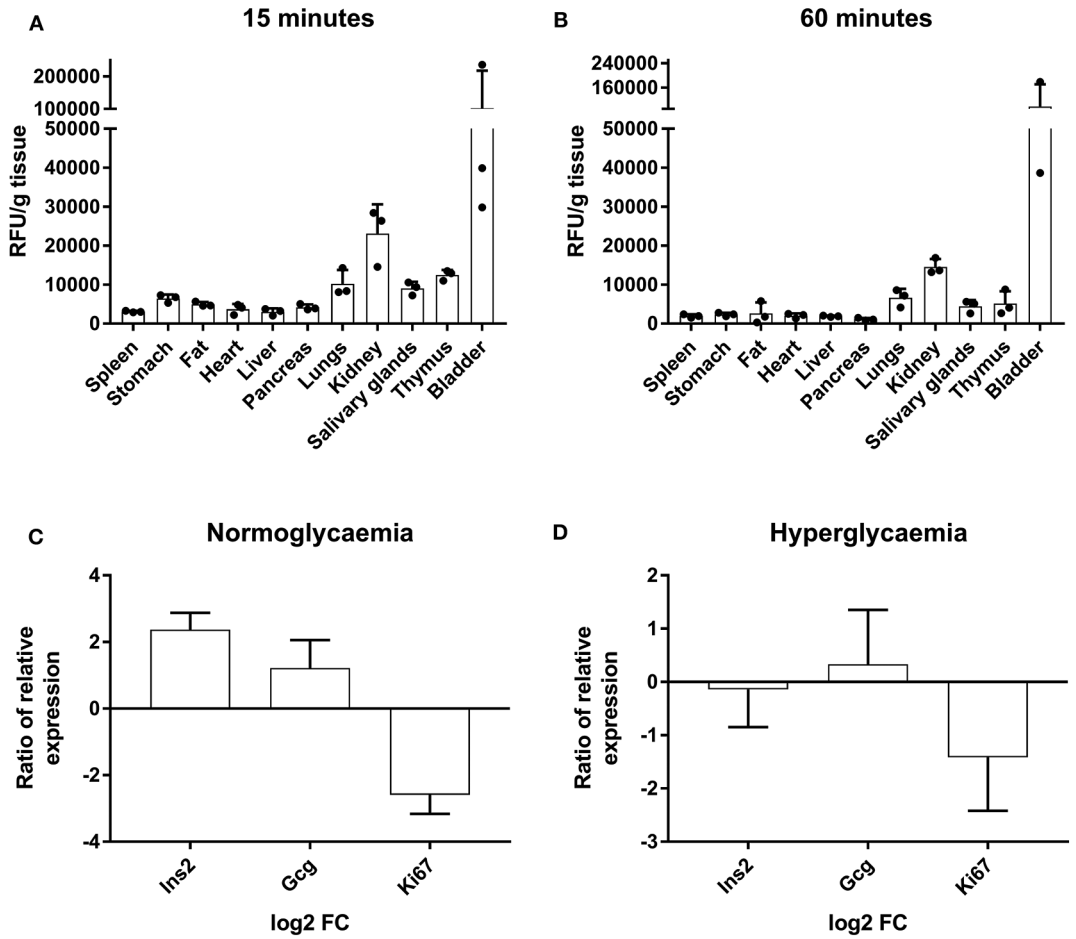

FIGURE 5 | Tracking of AF750-labeled liraglutide in prediabetic NOD mice and determination of gene expression in islets of Langerhans. **(A)** Histogram of *ex vivo* fluorescent signal relative to the grams of tissue of several organs from NOD mice at 15 min and **(B)** at 60 min after a s.c. injection of AF750-labeled liraglutide. The results are mean ± SEM of three independent experiments. **(C,D)** Ratio of relative gene expression of the selected genes in isolated islets of Langerhans after 48 h of 1,000-nM liraglutide treatment ($n \geq 3$) in relation to basal conditions analyzed by qRT-PCR in conditions of normoglycemia and hyperglycemia. Gene expression was normalized to *Gapdh*. The bars show the mean ± SD of the log2 of fold change using basal transcription as standard value.

autoimmune diabetes, and may have diabetes that can be induced by STZ treatment (41). In NOD mice, insulitis promotes an inflammatory microenvironment, thus causing β-cell stress and metabolic abnormalities (42, 43). Liraglutide administered to NOD mice may also impair insulin secretion at this stage because of the inflammatory environment in this strain.

Intriguingly, the effect was transient as previously described (30). This effect correlated with the transitory increase in the β-cell mass, confirming that insulin secretion induced by liraglutide (11) is not the only event that contributes to the restoration of normoglycemia. This increase is not due to β-cell hyperplasia but by an increase in the number of insulin^{+} cells and the formation of neo-islets emerging from ducts. Thus, it is reasonable to speculate that the continuous presence of liraglutide is required for the maintenance of islet β-cell mass by promoting the main mechanism responsible for the improvement of blood glucose levels in treated mice, at least during the first 30 days of treatment stages. Elucidating the mechanisms of action of liraglutide in diabetic mice with diabetogenic background will contribute to the design of β-cell regenerative strategies.

To further explore the regeneration mechanism, we then searched for processes described in any of the pathways that liraglutide was predicted to act on. Suggesting transdifferentiation, transient bihormonal cells were found within the islets, a feature of α-cell to β-cell conversion detected after β-cell loss (44). Because glycemia normalization occurs

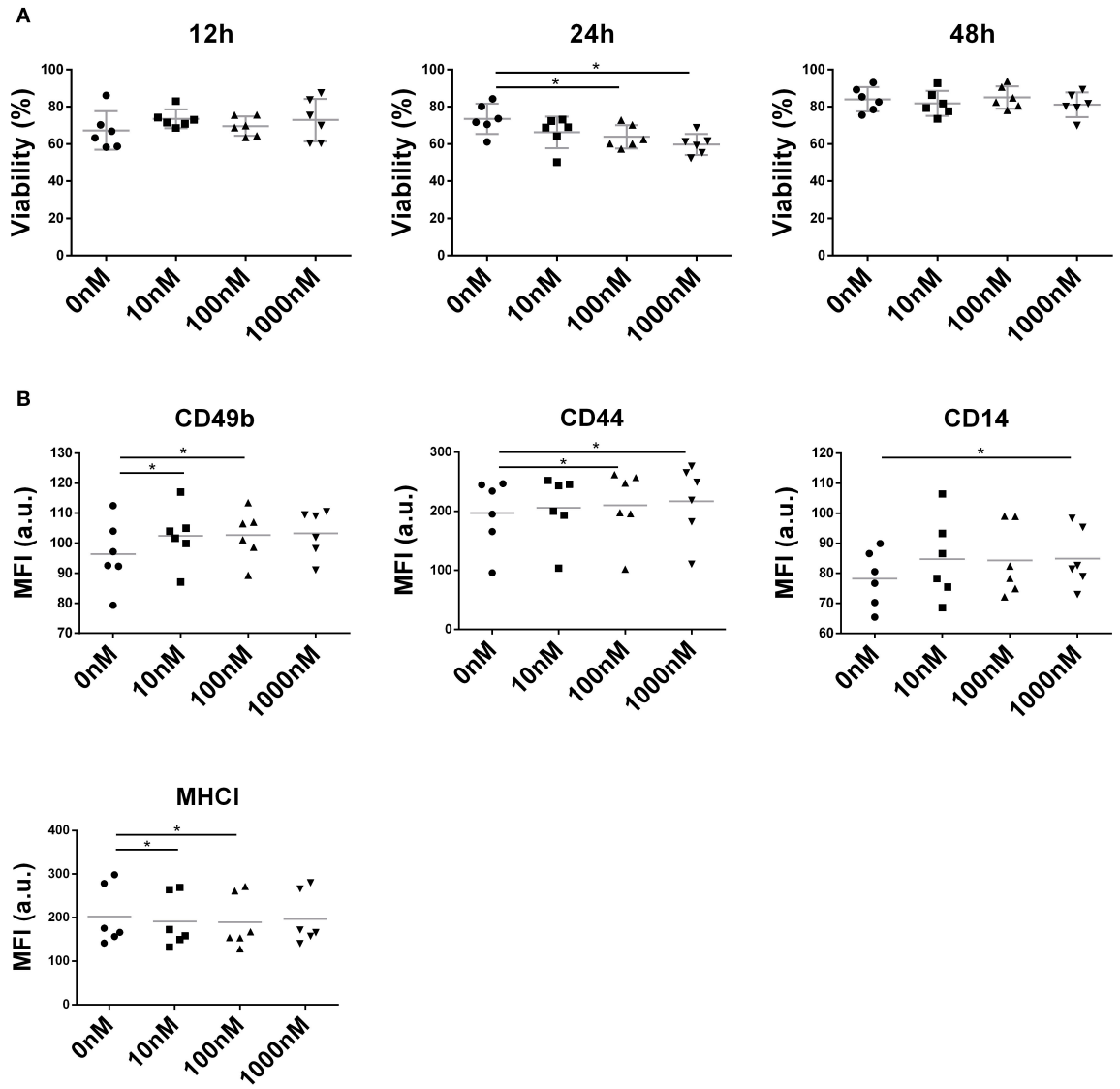

FIGURE 6 | Effect of liraglutide in the NIT-1 β-cell line. **(A)** Percentage of viable NIT-1 cells (annexin V PE^{-}, $7aad^{-}$) after 12, 24, and 48 h of co-culture with increasing liraglutide concentrations (10, 100, and 1,000 nM) and control condition (*$p < 0.05$, Mann–Whitney test). **(B)** Median of fluorescence intensity for CD49b, CD44, CD14, and MHC class I surface expression (*$p < 0.05$, Mann–Whitney test).

almost immediately after the first injections, newly formed $insulin^{+}$ cells with an α-cell origin could contribute to glucose homeostasis. Our results fit well with the recent demonstration that exendin-4, another aGLP-1, also induces bihormonal cells as a consequence of transdifferentiation (16). Other drugs that induce this type of transdifferentiation also cause extreme islet hyperplasia during the early stages of administration (3), but this fact has not been observed with liraglutide, thus suggesting that liraglutide might act through different pathways. Bihormonal cells detected at 48 h after administration agreed with an increase in both insulin and glucagon transcripts in islets treated *in vitro* with liraglutide. Although hormone colocalization *per se* is not a demonstration of a real conversion from α-cell to β-cell, it is logical to speculate that these cells correspond to emergent β-cells. In mice, α-cells can become insulin-expressing cells after β-cell ablation, thus promoting diabetes recovery. Recent results confirm that human α-cells are able to secrete insulin and reverse diabetes, but surprisingly, these cells express α-cell markers (45). Nevertheless, to prove that liraglutide induces a real conversion from glucagon-producing cells into insulin-producing β-cells—as reported with GLP-1 peptide (16), it would be of interest to perform lineage tracing experiments with transgenic models.

Furthermore, during the treatment and even after removal of liraglutide, $insulin^{+}$ bodies were found to be emerging from $CK19^{+}$ ductal cells that expressed insulin. Whether

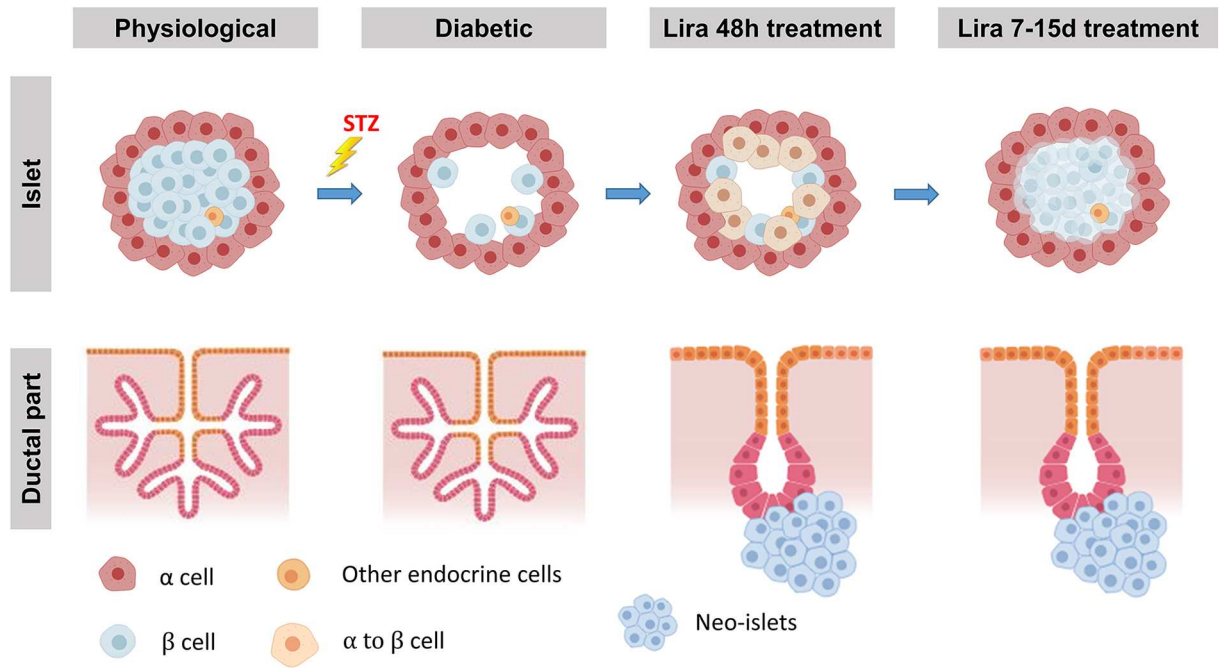

FIGURE 7 | Proposed model of Lira-induced β-cell regeneration. The islets displaying their physiological conditions are depleted from most β-cells when treated with streptozotocin, while the ductal part of the pancreas remains unaffected. We propose that liraglutide can induce a regeneration process in two steps. The first one, triggered at least 48 h after the treatment, consists in the transdifferentiation from mature α-cells into new insulin-expressing β-like cells. During the second step, while β-cell mass seems to be partially recovered, neo-islets formed by insulin-expressing β-like cells from CK19$^+$ cells in the ductal part of the pancreas arise from the ducts.

these neo-islets emerged from specific multipotent progenitors remains to be explored, but it has been proposed that early transdifferentiation promotes later neogenesis from ducts (3, 46). Further experiments are required in order to confirm this, given that the cell population identified in the ductal part are Neurogenin3$^+$ progenitors that underwent epithelial-to-mesenchymal transition to differentiate into β-like cells (9, 47). Neo-islets have also been reported in human pancreas (48), including those from patients with type 1 diabetes (49), but this is the first demonstration of insulin$^+$ cells with a ductal origin caused by liraglutide. Pdx1, a mature β-cell and endocrine progenitor marker, also depicted a ductal population. Because GLP-1 receptor is also expressed in ductal cells (50), insulin expression could be induced by liraglutide in these cells. These results suggest that the role of this drug in ameliorating hyperglycemia follows a mechanism that is non-exclusive to β-cells and has other players involved, such as islet insulin$^+$glucagon$^+$ cells and ductal insulin-expressing cells. The herein reported findings go beyond the previously reported beneficial effect of liraglutide in β-cell function, both *in vivo* (39) and *in vitro* in terms of insulin secretion (51). However, neogenesis from ducts was not reported in a previous study due to differences in dosage, disease induction, and especially lineage tracing issues (39). It is difficult to assess which insulin-producing cell types are quantitatively contributing to the improvement of hyperglycemia. First, despite the fact that the percentage of bihormonal cells at 48 h is almost 11% of total insulin$^+$ cells, these data reflect a specific stage, and it is still unknown how many insulin$^+$ cells are arising from transdifferentiation throughout the treatment. Indeed it is reasonable to speculate that ductal insulin$^+$ cells are participating in insulin secretion, but it remains to be investigated if they are glucose responsive. Finally, both a decrease in the percentage of budding islets and the fact that liraglutide is an insulinotropic agent may explain the transient effect in the glycemia after withdrawal.

Taking these observations together, we propose a two-step simultaneous mechanism of β-cell regeneration (**Figure 7**): first, an early, acute, and transient transdifferentiation mechanism from α-cell to β-cell (3, 38) and, second, an early and permanent neogenic process of insulin$^+$ cells from the ducts. After withdrawal, the first mechanism seems to be suppressed—probably after the loss of insulin$^+$ cell identity—while the second one persists.

In conclusion, liraglutide, a repurposed compound, ameliorates hyperglycemia in experimental type 1 diabetes. Our results point to β-cell replacement, including transdifferentiation and neogenesis, as aiding factor. Liraglutide could be a candidate to restore β-cell mass in combined therapies, together with an immunomodulatory strategy to arrest autoimmunity.

DATA AVAILABILITY STATEMENT

All datasets generated for this study are included in the article/ **Supplementary Material**.

ETHICS STATEMENT

This study was carried out in strict accordance with the recommendations in the Guide for the Care and Use of Laboratory Animals of the Generalitat de Catalunya, Catalan Government. The protocol was approved by the Committee on the Ethics of Animal Experiments of the Germans Trias i Pujol Research Institute (Permit DAAM 9521) and has followed the principles outlined in the Declaration of Helsinki for animal experimental investigation.

AUTHOR CONTRIBUTIONS

AV, FV, IP-A, and MV-P designed the experiments. MC conducted the drug reposition analysis. AV, DP-B, SR-F, and R-MA performed the experiments in mice. AV, DP-B, SR-F, and LG-M carried out the *in vitro* experiments. MC-S bound the drug to the fluorochrome. JV contributed to islet isolation. AV and MV-P wrote the manuscript. SR-F, IP-A, EA, and JV contributed to the discussion. All the authors revised the manuscript and gave final approval of the version to be published.

FUNDING

This work has been funded by Fundació La Marató de TV3 (project 201632_10). CIBER of Diabetes and Associated Metabolic Diseases (CIBERDEM) is an initiative from Instituto de Salud Carlos III, Spanish Ministry of Science and Innovation. SR-F was supported by the Generalitat de Catalunya (AGAUR grant).

ACKNOWLEDGMENTS

We are grateful to Mr. M. Fernandez and Mr. G. Requena for their support in flow cytometry. We acknowledge Dr. M. P. Armengol, from the Histopathology and Electron Microscopy Facility, for her help. Special thanks to Ms. Deborah Culell-Young for English grammar assistance.

SUPPLEMENTARY MATERIAL

The Supplementary Material for this article can be found online at: https://www.frontiersin.org/articles/10.3389/fendo.2020.00258/full#supplementary-material

REFERENCES

1. Xu X, D'Hoker J, Stangé G, Bonné S, De Leu N, Xiao X, et al. β cells can be generated from endogenous progenitors in injured adult mouse pancreas. *Cell*. (2008) 132:197–207. doi: 10.1016/j.cell.2007.12.015
2. Li J, Casteels T, Frogne T, Ingvorsen c, Honoré C, et al. Artemisinins target GABA A receptor signaling and impair α cell identity. *Cell*. (2017) 168:86–100. doi: 10.1016/j.cell.2016.11.010
3. Ben-othman N, Vieira A, Courtney M, Record F, Gjernes E, et al. Long-term GABA administration induces alpha cell-mediated βeta like cell neogenesis. *Cell*. (2017) 168:73–85. doi: 10.1016/j.cell.2016.11.002
4. Dadheech N, Garrel D, Buteau J. Evidence of unrestrained beta-cell proliferation and neogenesis in a patient with hyperinsulinemic hypoglycaemia after gastric bypass surgery. *Islets*. (2018) 10:213–20. doi: 10.1080/19382014.2018.1513748
5. Lotfi Shahreza M, Ghadiri N, Mousavi SR, Varshosaz J, Green JR. A review of network-based approaches to drug repositioning. *Brief Bioinform*. (2018) 19:878–92. doi: 10.1093/bib/bbx017
6. Pushpakom S, Iorio F, Eyers PA, Escott KJ, Hopper S, Wells A, et al. Drug repurposing: progress, challenges and recommendations. *Nat Rev Drug Discov*. (2018) 18:41–58. doi: 10.1038/nrd.2018.168
7. Sleire L, Førde HE, Netland IA, Leiss L, Skeie BS, Enger PØ. Drug repurposing in cancer. *Pharmacol Res*. (2017) 124:74–91. doi: 10.1016/j.phrs.2017.07.013
8. Kumar S, Chowdhury S, Kumar S. *In silico* repurposing of antipsychotic drugs for Alzheimer's disease. *BMC Neurosci*. (2017) 18:76. doi: 10.1186/s12868-017-0394-8
9. Al-Hasani K, Pfeifer A, Courtney M, Ben-Othman N, Gjernes E, Vieira A, et al. Adult duct-lining cells can reprogram into β-like cells able to counter repeated cycles of toxin-induced diabetes. *Dev Cell*. (2013) 26:86–100. doi: 10.1016/j.devcel.2013.05.018
10. Dor Y, Brown J, Martinez OI, Melton DA. Adult pancreatic beta-cells are formed by self-duplication rather than stem-cell differentiation. *Nature*. (2004) 429:41–6. doi: 10.1038/nature02520
11. Jacobsen L V., Flint A, Olsen AK, Ingwersen SH. Liraglutide in type 2 diabetes mellitus: clinical pharmacokinetics and pharmacodynamics. *Clin Pharmacokinet*. (2016) 55:657–72. doi: 10.1007/s40262-015-0343-6
12. Iepsen EW, Torekov SS, Holst JJ. Liraglutide for type 2 diabetes and obesity: a 2015 update. *Expert Rev Cardiovasc Ther*. (2015) 13:753–67. doi: 10.1586/14779072.2015.1054810
13. Anholm C, Kumarathurai P, Pedersen LR, Nielsen OW, Kristiansen OP, Fenger M, et al. Liraglutide effects on beta-cell, insulin sensitivity and glucose effectiveness in patients with stable coronary artery disease and newly diagnosed type 2 diabetes. *DiabetesObes Metab*. (2017) 19:850–7. doi: 10.1111/dom.12891
14. Jinnouchi H, Sugiyama S, Yoshida A, Hieshima K, Kurinami N, Suzuki T, et al. Liraglutide, a glucagon-like peptide-1 analog, increased insulin sensitivity assessed by hyperinsulinemic-euglycemic clamp examination in patients with uncontrolled type 2 diabetes mellitus. *J Diabetes Res*. (2015) 2015:706416. doi: 10.1155/2015/706416
15. Zhang Z, Hu Y, Xu N, Zhou W, Yang L, Chen R, et al. A New Way for Beta Cell Neogenesis: Transdifferentiation from Alpha Cells Induced by Glucagon-Like Peptide 1. *J Diabetes Res*. (2019) 2019:2583047. doi: 10.1155/2019/2583047
16. Lee Y-S, Lee C, Choung J-S, Jung H-S, Jun H-S. Glucagon-like peptide 1 increases β-cell regeneration by promoting α- to β-cell transdifferentiation. *Diabetes*. (2018) 67:2601–14. doi: 10.2337/db18-0155
17. Jorba G, Aguirre-Plans J, Junet V, Segú-Vergés C, Ruiz JL, Pujol A, et al. *In-silico* simulated prototype-patients using TPMS technology to study a potential adverse effect of sacubitril and valsartan. *PLoS ONE*. (2020) 15:e0228926. doi: 10.1371/journal.pone.0228926
18. Romeo-Guitart D, Forés J, Herrando-Grabulosa M, Valls R, Leiva-Rodríguez T, Galea E, et al. Neuroprotective drug for nerve trauma revealed using artificial intelligence. *Sci Rep*. (2018) 8:1879. doi: 10.1038/s41598-018-19767-3
19. Herrando-Grabulosa M, Mulet R, Pujol A, Mas JM, Navarro X, Aloy P, et al. Novel neuroprotective multicomponent therapy for amyotrophic lateral

sclerosis designed by networked systems. *PLoS ONE*. (2016) 11:e0147626. doi: 10.1371/journal.pone.0147626
20. Kanehisa M, Goto S. KEGG: kyoto encyclopedia of genes and genomes. *Nucleic Acids Res*. (2000) 28:27–30. doi: 10.1093/nar/28.1.27
21. Kanehisa M, Furumichi M, Tanabe M, Sato Y, Morishima K. KEGG: new perspectives on genomes, pathways, diseases and drugs. *Nucleic Acids Res*. (2017) 45:D353–61. doi: 10.1093/nar/gkw1092
22. Croft D, Mundo AF, Haw R, Milacic M, Weiser J, Wu G, et al. The reactome pathway knowledgebase. *Nucleic Acids Res*. (2014) 42:D472–7. doi: 10.1093/nar/gkt1102
23. Orchard S, Ammari M, Aranda B, et al. The MIntAct project–IntAct as a common curation platform for 11 molecular interaction databases. *Nucleic Acids Res*. (2014) 42:D358–63. doi: 10.1093/nar/gkt1115
24. Salwinski L, Miller CS, Smith AJ, Pettit FK, Bowie JU, Eisenberg D. The database of interacting proteins: 2004 update. *Nucleic Acids Res*. (2004) 32:D449–51. doi: 10.1093/nar/gkh086
25. Keshava Prasad TS, Goel R, Kandasamy K, Keerthikumar S, Kumar S, Mathivanan S, et al. Human protein reference database - 2009 update. *Nucleic Acids Res*. (2009) 37(Suppl. 1):767–72. doi: 10.1093/nar/gkn892
26. Han H, Shim H, Shin D, Shim JE, Ko Y, Shin J, et al. TRRUST: a reference database of human transcriptional regulatory interactions. *Sci Rep*. (2015) 5:11432. doi: 10.1038/srep11432
27. Pache RA, Aloy P. Incorporating high-throughput proteomics experiments into structural biology pipelines: identification of the low-hanging fruits. *Proteomics*. (2008) 8:1959–64. doi: 10.1002/pmic.200700966
28. Wishart DS, Knox C, Guo AC, Cheng D, Shrivastava S, Tzur D, et al. DrugBank: a knowledgebase for drugs, drug actions and drug targets. *Nucleic Acids Res*. (2008) 36:D901–6. doi: 10.1093/nar/gkm958
29. Wishart DS, Feunang YD, Guo AC, Lo EJ, Marcu A, Grant JR, et al. DrugBank 5.0: a major update to the DrugBank database for 2018. *Nucleic Acids Res*. (2018) 46:D1074–82. doi: 10.1093/nar/gkx1037
30. Rydén AK, Perdue NR, Pagni PP, Gibson CB, Ratliff SS, Kirk RK, et al. Anti-IL-21 monoclonal antibody combined with liraglutide effectively reverses established hyperglycaemia in mouse models of type 1 diabetes. *J Autoimmun*. (2017) 84:65–74. doi: 10.1016/j.jaut.2017.07.006
31. Alba A, Puertas MC, Carrillo J, Planas R, Ampudia R, Pastor X, et al. IFN beta accelerates autoimmune type 1 diabetes in nonobese diabetic mice and breaks the tolerance to beta cells in nondiabetes-prone mice. *J Immunol*. (2004) 173:6667–75. doi: 10.4049/jimmunol.173.11.6667
32. Schindelin J, Arganda-Carreras I, Frise E, Kaynig V, Longair M, Pietzsch T, et al. Fiji: an open-source platform for biological-image analysis. *Nat Methods*. (2012) 9:676–82. doi: 10.1038/nmeth.2019
33. Chintinne M, Stangé G, Denys B, In 't Veld P, Hellemans K, Pipeleers-Marichal M, et al. Contribution of postnatally formed small beta cell aggregates to functional beta cell mass in adult rat pancreas. *Diabetologia*. (2010) 53:2380–8. doi: 10.1007/s00125-010-1851-4
34. Chintinne M, Stange G, Denys B, Ling Z, In P, Pipeleers D. Beta cell count instead of beta cell mass to assess and localize growth in beta cell population following pancreatic duct ligation in mice. *PLoS ONE*. (2012) 7:e43959. doi: 10.1371/journal.pone.0043959
35. Perna-Barrull D, Rodriguez-Fernandez S, Pujol-Autonell I, Gieras A, Ampudia-Carrasco RM, Villalba A, et al. Prenatal betamethasone interferes with immune system development and alters target cells in autoimmune diabetes. *Sci Rep*. (2019) 9:1235. doi: 10.1038/s41598-018-37878-9
36. Hamaguchi K, Gaskins HR, Leiter EH. NIT-1, a pancreatic beta-cell line established from a transgenic NOD/Lt mouse. *Diabetes*. (1991) 40:842–9. doi: 10.2337/diabetes.40.7.842
37. Livak KJ, Schmittgen TD. Analysis of relative gene expression data using real-time quantitative PCR and the 2[-Delta Delta C(T)]. Method*Methods*. (2001) 25:402–8. doi: 10.1006/meth.2001.1262
38. Ahren B, Hirsch IB, Pieber TR, Mathieu C, Gomez-Peralta F, Hansen TK, et al. Efficacy and safety of liraglutide added to capped insulin treatment in subjects with type 1 diabetes: the adjunct two randomized trial. *Diabetes Care*. (2016) 39:1693–701. doi: 10.2337/dc16-0690
39. Tamura K, Minami K, Kudo M, Iemoto K, Takahashi H. Liraglutide improves pancreatic beta cell mass and function in alloxan-induced diabetic mice. *PLoS ONE*. (2015) 1:e0126003. doi: 10.1371/journal.pone.0126003
40. Bock T, Pakkenberg B, Buschard K. Genetic background determines the size and structure of the endocrine pancreas. *Diabetes*. (2005) 54:133–7. doi: 10.2337/diabetes.54.1.133
41. Leiter EH Schile A. Genetic and pharmacologic models for type 1 diabetes. *Curr Protoc Mouse Biol*. (2013) 3:9–19. doi: 10.1002/9780470942390.mo120154
42. Strandell E, Sandler S, Boitard C Eizirik DL. Role of infiltrating T cells for impaired glucose metabolism in pancreatic islets isolated from non-obese diabetic mice. *Diabetologia*. (1992) 35:924–31. doi: 10.1007/BF00401420
43. Eizirik DL, Colli ML Ortis F. The role of inflammation in insulitis and beta-cell loss in type 1 diabetes. *Nat Rev Endocrinol*. (2009) 5:219–26. doi: 10.1038/nrendo.2009.21
44. Thorel F, Népote V, Avril I, Kohno K, Desgraz R, Chera S, et al. Conversion of adult pancreatic α-cells to β-cells after extreme β-cell loss. *Nature*. (2010) 464:1149–54. doi: 10.1038/nature08894
45. Furuyama K, Chera S, van Gurp L, Oropeza D, Ghila L, Damond N, et al. Diabetes relief in mice by glucose-sensing insulin-secreting human α-cells. *Nature*. (2019) 567:43–8. doi: 10.1038/s41586-019-0942-8
46. Druelle N, Vieira A, Shabro A, Courtney M, Mondin M, Rekima S, et al. Ectopic expression of Pax4 in pancreatic δ cells results in β -like cell neogenesis. *J Cell Biol*. (2017) 216:449–462. doi: 10.1083/jcb.201704044
47. Bru-Tari E, Cobo-Vuilleumier N, Alonso-Magdalena P, Dos Santos RS, Marroqui L, Nadal A, et al. Pancreatic alpha-cell mass in the early-onset and advanced stage of a mouse model of experimental autoimmune diabetes. *Sci Rep*. (2019) 9:9515. doi: 10.1038/s41598-019-45853-1
48. Bogdani M, Lefebvre V, Buelens N, Bock T, Veld PI, Pipeleers D. Formation of insulin-positive cells in implants of human pancreatic duct cell preparations from young donors. *Diabetologia*. (2003) 46:830–8. doi: 10.1007/s00125-003-1118-4
49. Somoza N, Vargas F, Roura-Mir C, Vives-Pi M, Fernández-Figueras MT, Ariza A, et al. Pancreas in recent onset insulin-dependent diabetes mellitus. *J Immunol*. (1994) 153:1360–77.
50. Xu G, Stoffers DA, Habener JF, Bonner-Weir S. Exendin-4 stimulates both beta-cell replication and neogenesis, resulting in increased beta-cell mass and improved glucose tolerance in diabetic rats. *Diabetes*. (1999) 48:2270–6. doi: 10.2337/diabetes.48.12.2270
51. Xu X, Chen J, Hu L, Liang M, Wang X, Feng S, et al. Liraglutide regulates the viability of pancreatic α-cells and pancreatic β-cells through cAMP-PKA signal pathway. *Life Sci*. (2018) 195:87–94. doi: 10.1016/j.lfs.2017.12.012

Conflict of Interest: MC-S and MV-P are co-founders of Ahead Therapeutics SL, which aims at the clinical translation of immunotherapies for the treatment of autoimmune diseases. MC was employed by the company Anaxomics Biotech SL.

The remaining authors declare that the research was conducted in the absence of any commercial or financial relationships that could be construed as a potential conflict of interest.

frontiers in Endocrinology

ORIGINAL RESEARCH
published: 30 July 2020
doi: 10.3389/fendo.2020.00450

A Novel *SERPINB1* Single-Nucleotide Polymorphism Associated With Glycemic Control and β-Cell Function in Egyptian Type 2 Diabetic Patients

Dina H. Kassem[1], *Aya Adel*[2,3], *Ghada H. Sayed*[4] *and Mohamed M. Kamal*[1,2,3]*

[1] Department of Biochemistry, Faculty of Pharmacy, Ain Shams University, Cairo, Egypt, [2] Pharmacology and Biochemistry Department, Faculty of Pharmacy, The British University in Egypt, Cairo, Egypt, [3] The Center for Drug Research and Development (CDRD), Faculty of Pharmacy, The British University in Egypt, Cairo, Egypt, [4] Department of Clinical and Chemical Pathology, National Institute of Diabetes & Endocrinology, Cairo, Egypt

Aims: Serine protease inhibitor B1 (SerpinB1) is a neutrophil elastase inhibitor that has been proved to be associated with type 2 diabetes mellitus and pancreatic β-cell proliferation. In this study, we investigated 2 *SERPINB1* SNPs, rs114597282 and rs15286, regarding their association with diabetes risk and various anthropometric and biochemical parameters in Egyptian type 2 diabetic patients.

Materials and Methods: A total of 160 subjects (62 control and 98 type 2 diabetic patients) participated in this study. Various anthropometric and biochemical parameters were assessed. Genotyping assay for the two SNPs was done using TaqMan genotyping assays. The association of rs15286 variants with risk of diabetes, various biochemical parameters, and glycemic control in diabetic patients was assessed.

Results: All genotyped subjects were found to be homozygous TT for *SERPINB1* rs114597282. All genotype variants of *SERPINB1* rs15286 were found in our Egyptian subjects with A being the minor allele. The SNP rs15286 was not found to be associated with risk of diabetes. The AA genotype was found to be associated with lower fasting plasma glucose, lower HbA_{1c}%, and better β-cell function and glycemic control in diabetic patients. The G allele was associated with poor glycemic control.

Conclusions: The genotypes AA, AG, and GG of *SERPINB1* gene SNP rs15286 are all represented in the studied sample; however, it is not associated with risk of diabetes. Genotype AA of SNP rs15286 is associated with better glycemic control and better β-cell function in diabetic patients, while the G allele potentially represents the "risk allele" of poor glycemic control.

Keywords: serpinB1, type 2 diabetes mellitus, β-cell dysfunction, insulin resistance, hepatokines, gene polymorphism

OPEN ACCESS

Edited by:
Simona Chera,
University of Bergen, Norway

Reviewed by:
Bente Berg Johansson,
University of Bergen, Norway
Dario F. De Jesus,
Joslin Diabetes Center and Harvard Medical School, United States

***Correspondence:**
Mohamed M. Kamal
mohamed.kamal@bue.edu.eg

Specialty section:
This article was submitted to Diabetes: Molecular Mechanisms, a section of the journal Frontiers in Endocrinology

Received: *06 May 2020*
Accepted: *08 June 2020*
Published: *30 July 2020*

Citation:
Kassem DH, Adel A, Sayed GH and Kamal MM (2020) A Novel SERPINB1 Single-Nucleotide Polymorphism Associated With Glycemic Control and β-Cell Function in Egyptian Type 2 Diabetic Patients. Front. Endocrinol. 11:450. doi: 10.3389/fendo.2020.00450

INTRODUCTION

Diabetes mellitus (DM) is a complex multifaceted metabolic disorder. Unfortunately, its global prevalence is growing at an alarming rate especially in middle- and low-income countries (1). The number of people suffering DM globally has risen from about 108 million in 1980 to nearly 422 million in 2014 (2), with a further expected increase to about 630 million people worldwide

by the year 2045 (1). Type 2 DM is the most common type of DM, and genetic-predisposition accounts for nearly 60–90% of the susceptibility to its development (3). During the natural course of the disease, insulin resistance and β-cell loss or dysfunction are potential drivers for the various metabolic abnormalities associated with type 2 DM (3, 4). When the functional insulin-secreting β-cell mass is compromised, the normal physiological glucose homeostasis is disrupted and type 2 DM manifests (5).

Accordingly, vigorous efforts have been exerted over the past years to develop strategies which would help to compensate and/or expand functional β-cells. Among those approaches was the identification of factors/mediators capable of inducing proliferation and expansion of preexisting functional β-cells (5, 6). That approach attracted much interest especially that β-cell expansion and compensation capabilities have been reported in various conditions associated with insulin resistance such as obesity (7, 8) or pregnancy (9). Interestingly, in this regard, *El-Ouaamari and coworkers* highlighted the integrative cross talk between the liver and pancreatic β-cells via the secretion of hepatocyte-derived factor(s) in response to insulin resistance which induces β-cell proliferation (10).

Among these hepatocyte-derived factors, serine protease inhibitor B1 (serpinB1; serpin family B member 1) has been identified to play an important role in that process of β-cell compensation in response to insulin resistance (11). Interestingly, serpinB1 was also previously reported to act as a neutrophil elastase inhibitor (12), and improving glucose tolerance and insulin sensitivity was found to be associated with such inhibition (13). Additionally, a recent report sheds light on the possible association of serpinB1 with insulin sensitivity in healthy adults (14). It is noteworthy that serpinB1 is not the only serpin which could be associated with insulin sensitivity. Long before, the visceral adipose tissue-derived serpin—Vaspin—was also identified as an interesting insulin-sensitizing adipokine (15), with a putative interplay with other mediators in compensatory mechanisms for insulin resistance in type 2 DM (16).

Nevertheless, genetic variants of the *SERPINB1* gene and their possible implication into β-cell dysfunction and reduced β-cell compensation in diabetic patients have not been investigated (17). Just one family has been identified with a possibly damaging *SERPINB1* variant associated with diabetes (11). Thus, knowing that genome-wide association studies have revealed several genetic variants related to compromised β-cell function to be associated with type 2 DM (18, 19), as well as the extra layer of complexity in different ethnic populations (20), this inspired us to investigate if genetic variants of *SERPINB1* are associated with diabetes risk, glycemic control, and β-cell dysfunction in Egyptian type 2 diabetic patients. According to our knowledge, this is the first report investigating the association of *SERPINB1* genetic variants with type 2 DM.

MATERIALS AND METHODS

Study Population and Anthropometric Measurements

This study was approved by the ethical committee of the National Institute of Diabetes and Endocrinology—General Organization for Teaching Hospitals and Institutes (NIDE—GOTHI) under number IDE00203, and informed consent was obtained from every enrolled subject. The study was carried out in accordance with the Declaration of Helsinki recommendations and regulations (21). A total of 160 subjects were enrolled in the study; 62 non-diabetic healthy control subjects and 98 patients with type 2 DM. The definition of a non-diabetic was a subject who has a fasting plasma glucose (FPG) level lower than 110 mg/dl and has no family history of type 2 DM. All the control subjects were not receiving any dietary supplements or medications and were not suffering any health problems. The 98 patients with type 2 DM were recruited from the outpatient clinic of the National Institute of Diabetes and Endocrinology (NIDE). These 98 patients were further classified into diabetics with good glycemic control (HbA1c $\leq$ 7%) and diabetics with poor glycemic control (HbA1c $>$ 7%) as described previously (22) for odds ratio calculations. The characteristics of all the study subjects are summarized in **Table 1**. The exclusion criteria included renal or hepatic disease, thyroid dysfunction, acute or chronic inflammatory disease, type 1 DM, ischemic cardiovascular disease, cancer, acute or chronic infections, alcohol or drug abuse, and any hematological disorder. Subjects taking hormonal therapy were also excluded.

All the study subjects underwent physical examination and detailed history and laboratory investigations. Anthropometric measures included waist-to-hip ratio (WHR) and body mass index (BMI); body weight and standing height were measured in light clothing without shoes. The BMI was calculated as weight divided by squared height (kg/m^2). Waist circumference was measured to the nearest 0.1 cm at the narrowest point between the lowest rib and the uppermost lateral border of the iliac crest, while the hip was measured at its widest point.

Blood Sampling

All the blood samples were drawn after overnight fasting, and the samples were divided into four aliquots. The first aliquot of blood was collected on plain vacutainer tubes for serum preparation used for the assay of the lipid profile, as well as C-peptide levels. The second aliquot of blood was collected on vacutainer tubes containing sodium fluoride for measuring fasting plasma glucose (FPG). The third and fourth aliquots of blood were collected on vacutainer tubes containing sodium EDTA for measuring glycated hemoglobin (HbA_{1C}%), and for subsequent DNA extraction from whole blood. Afterward, serum samples were divided into aliquots and stored at −80°C for subsequent assays.

Laboratory Analyses

FPG and serum biochemical parameters including triglycerides (TG), total cholesterol (TC), and high-density lipoprotein-cholesterol (HDL-C) were measured using Spectrum Diagnostics kits (Egypt). Low-density lipoprotein cholesterol (LDL-C) levels were calculated by Friedewald's equation (23). HbA_{1C}% was determined using ion-exchange high-performance liquid chromatography (HPLC) by the Bio-Rad D-10 system (Bio-Rad Laboratories, Hercules, CA, USA).

Afterward, serum C-peptide levels were determined using the human C-peptide ELISA kit (DRG, USA). The homeostasis

TABLE 1 | Clinical and laboratory characteristics of the studied groups.

Factor	Controls	Type 2 DM	*p*-value	*p*-value¶
N (F/M)	62 (42/20)	98 (46/52)	***……***	***……***
Age (year)	38.2 ± 1.1	49.1 ± 1.1	***<0.001[a]***	***……..***
Diabetes duration (year)	…….	8.39 ± 0.74	***……***	***…….***
BMI (kg/m^2)	28.8 ± 0.62	31.5 ± 0.53	***0.001[a]***	***0.002***
WHR[c]	0.92 ± 0.08	0.95 ± 0.013	*0.085[b]*	*0.845*
FPG (mg/dl)[c]	86.5 ± 1.6	209.6 ± 7.4	***<0.001[b]***	***<0.001***
HbA_{1C} (%)	5.4 ± 0.07	8.4 ± 0.22	***<0.001[a]***	***<0.001***
TC (mg/dl)	150.6 ± 5.0	209.0 ± 5.2	***<0.001[a]***	***<0.001***
LDL-C (mg/dl)	88.2 ± 5.02	127.4 ± 4.4	***<0.001[b]***	***<0.001***
HDL-C (mg/dl)[c]	47.1 ± 0.74	44.7 ± 1.41	***0.014[b]***	*0.165*
TG (mg/dl)[c]	80.2 ± 4.8	177.9 ± 9.6	***<0.001[b]***	***<0.001***
LDL-C/HDL-C[c]	1.96 ± 0.13	3.22 ± 0.19	***<0.001[b]***	***<0.001***
TC/HDL-C[c]	3.3 ± 0.15	5.11 ± 0.22	***<0.001[a]***	***<0.001***
C-peptide (ng/ml)[c]	3.81 ± 0.26	0.84 ± 0.054	***<0.001[b]***	***<0.001***
HOMA2-β%[c]	213.6 ± 11.3	17.9 ± 1.2	***<0.001[b]***	***<0.001***
HOMA2-IR[c]	2.73 ± 0.19	0.94 ± 0.07	***<0.001[b]***	***<0.001***
Type of treatment (OHA/OHA + insulin/insulin)	…….	35/3/60	***…….***	***…….***

Results are expressed as mean ± S.E.M. DM, diabetes mellitus; BMI, body mass index; WHR, waist to hip ratio; FPG, fasting plasma glucose; TC, total cholesterol; LDL-C, low-density lipoprotein cholesterol; HDL-C, high-density lipoprotein cholesterol; TG, triglycerides; HbA_{1C}%, glycosylated hemoglobin; HOMA2-β%, homeostasis model assessment-β-cell function; HOMA2-IR, homeostasis model assessment-insulin resistance; OHA, oral hypoglycemic agent.

[a]Independent-sample T-test, two-tailed, p-value >0.05 non-significant. [b]Mann–Whitney U test, two-tailed, p-value >0.05 non-significant. [c]Log transformed for performing GLM. ¶P-value after adjustment for age, gender, and BMI by GLM. All significant p-values are written in bold and italics.

model assessment of β-cell function (HOMA2-β%) and insulin resistance (HOMA2-IR) was calculated from FPG (mg/dl) and fasting C-peptide (ng/ml) levels using an online HOMA2 calculator/algorithm (24). HOMA2 models were calculated using C-peptide to avoid interference of insulin in patients treated by insulin. All ELISA procedures were done according to the manufacturer's instructions using the ChroMate microplate reader (Awareness Technology, USA).

DNA Extraction and Genotyping Assay

The extraction of DNA from 150 μL whole blood (collected on EDTA anticoagulant) was done using the commercially available Quick DNA Miniprep Kit (Zymo Research, USA) according to the manufacturer's instructions, then the extracted DNA was quantified using a Quawell micro-volume spectrophotometer (USA).

Genotyping was done for 2 *SERPINB1* polymorphism, namely, *SERPINB1* rs114597282, which is a missense mutation with a C/T substitution (previously determined as a possibly damaging variant for *SERPINB1* gene) (11). The other SNP was *SERPINB1* rs15286, which is a transition A/G SNP (in the 3′UTR region of *SERPINB1*). Genotyping was done using TaqMan® SNP Genotyping assays with the following IDs: C_151309206_10 for rs114597282 and C____950920_1 for rs15286 using the TaqMan Universal Master Mix No UNG (Thermo Fisher Scientific, USA). Genotyping was done using a StepOnePlus thermal cycler (Applied Biosystems, USA). 20 ng of genomic DNA for each sample was genotyped using 10 μL (2×) TaqMan® Universal Master Mix, 0.5 μL (40×) TaqMan® SNP genotyping assay, and DNAse/RNAse-Free water (Gibco, Life Technologies, USA) to a total volume of 20 μL reaction using default genotyping settings with appropriate negative control.

Statistical Analysis

All results were expressed as mean ± standard error of mean (S.E.M). The Kolmogorov–Smirnov test was done to evaluate the distribution of various variables. The independent-sample *t*-test and Mann–Whitney *U*-test were used appropriately according to the data distribution for comparison between non-diabetic control and type 2 DM groups. The genotype distribution was validated to follow the Hardy–Weinberg equilibrium (HWE) using an online calculator (25), and the chi-square ($\chi 2$) test was used to compare allele frequency distributions of various genotypes in the studied groups. Finally, binary logistic regression analysis was used to calculate the odds ratios (ORs) and 95% confidence intervals (CIs) to investigate the possible association of rs15286 variants with type 2 DM or with glycemic control status. Kruskal–Wallis or one-way ANOVA tests were used appropriately according to the distribution of data for comparison between the levels of various parameters in various genotypes (3 groups) followed by Dunn's test for Kruskal–Wallis as multiple-comparison *post hoc* tests. General linear modeling (GLM), followed by Bonferroni *post hoc* test for multiple comparisons, was used to control for covariates such as age, gender, and BMI, and *p-values* were calculated after correction for these covariates. Any non-normally distributed data was logarithmically transformed before performing GLM. All statistical analyses were performed using Windows-based SPSS statistical package (SPSS version 17.0, SPSS Inc, Chicago, IL). *P*-values $\leq 0{\cdot}05$ were considered significant.

RESULTS

Clinical Laboratory Data of the Study Subjects

As shown in **Table 1**, this study included 160 subjects; 62 subjects (42 females and 20 males) who were apparently healthy volunteers served as the control group. The type 2 DM group consisted of 98 patients (46 females and 52 males). The mean age of the control group was 38.2 ± 1.1 years, while that of the type 2 DM group was 49.1 ± 1.1 years. The duration of diabetes was 8.39 ± 0.74 years. The body mass index was significantly elevated in the type 2 DM group as compared to the control group. However, the waist–hip ratio (WHR) was almost equal in both groups. In addition, FPG, HbA_{1C}%, and lipid profile including TG, TC, LDL-C, and even LDL-C/HDL-C and TC/HDL-C were all significantly elevated in type 2 DM as compared to the control group.

As for β-cell function indices, C-peptide was significantly decreased in type 2 DM patients as compared to control subjects (0.84 ± 0.054 ng/ml and 3.81 ± 0.26 ng/ml, respectively, $p <$

TABLE 2 | Association of *SERPINB1* rs15286 variants with risk of type 2 DM.

Serpin B1 rs15286 genotypes	Controls $n = 62$	Diabetic $n = 98$	χ^2	*p*-value	OR (95% CI)	*p*-value
	n (%)	*n* (%)				
AA	3 (4.8%)	6 (6.1%)				
AG	22 (35.5%)	26 (26.5%)	1.473	0.479	0.707 (0.392–1.274)	0.249
GG	37 (59.7%)	66 (67.4%)			0.655 (0.322–1.332)	0.242¶
AG/AA vs. GG	25 (40.3%) vs. 37 (59.7%)	32 (33.6%) vs. 66 (66.4%)	0.974	0.324	0.718 (0.371–1.388)	0.324
					0.741 (0.338–1.623)	0.454¶
AG/GG vs. AA	59 (95.2%) vs. 3 (4.8%)	92 (93.9%) vs. 6 (6.1%)	0.118	0.731	0.780 (0.188–3.238)	0.732
					0.799 (0.14–4.54)	0.800¶
Total	62 (100%)	98 (100%)				

A $\chi 2$ test was done for various genotypes, A allele and G allele, and diabetes status. The odds ratio (OR) was calculated using binary logistic regression using diabetes status as the dependent variable and genotype as the covariate, in addition to adjustment for age, gender and BMI as additional covariates.
¶Adjusted for the effect of covariates: age, gender, and BMI.

0.001). Moreover, HOMA2-β% was also severely diminished in type 2 diabetic patients as compared to the control group (17.9 ± 1.2% and 213.6 ± 11.3%, respectively, $p < 0.001$) (**Table 1**).

Association of *SERPINB1* rs15286 Variants With Type 2 DM Risk

As for the *SERPINB1* SNP rs114597282, 100% of the subjects either control or type 2 DM were found to have a homozygous TT genotype, which unfortunately hindered further processing or studying of any association of such SNP.

The distribution and the alleles' frequencies of the rs15286 SNP of *SERPINB1* are shown in **Table 2**. The observed distribution frequency of various alleles followed the Hardy–Weinberg equilibrium. The AA genotype represents the minor genotype in both control and type 2 DM groups with 4.8 and 6.1%, respectively, with a total of 5.625% of all subjects. On the other hand, GG was the major genotype in the genotyped subjects (60% in control and 67% in type 2 DM patients) with a total of 64.375% of all subjects. As for the AG genotype, it represented 35.5% in the control group and 26% in the diabetic group with an overall 30% of the subjects. In addition, the A allele represents the minor allele with 40% in control and 33.6% in the diabetic subjects, with a total of 35.625% of the studied subjects. The 2 groups did not differ significantly regarding the distribution of various genotypes (p-value = 0.479) and the frequency of A allele (p-value = 0.324) or G allele (p-value = 0.731). Moreover, the various genotypes, A allele or G allele, were not found to be associated with the risk of DM (OR = 0.655, CI = 0.322–1.332, p-value = 0.242; OR = 0.741, CI = 0.338–1.623, p-value = 0.454; OR = 0.799, CI = 0.14–4.54, p-value = 0.800, respectively). All ORs (95% CI) were adjusted for age, gender, and BM.

Anthropometric and Biochemical Parameters' Levels in Various Genotypes of *SERPINB1* rs15286 SNP

In order to study the levels of various parameters in the genotyped samples, we compared the levels of various anthropometric and biochemical parameters among the genotype variants in both control and type 2 DM groups. As shown in **Table 3**, all parameters failed to reach a significant difference among AA, AG, and GG genotypes in the control group. On the other hand, in the diabetic group, these genotypes showed a significant difference for FPG, HbA_{1C}%, and HOMA2-β% (p-values = 0.008, 0.006, and 0.004, respectively).

In order to gain further insight into the difference of these parameters' levels among various genotypes of diabetic patients, we compared the levels among these parameters pair-wise. **Figure 1A** showed that genotype AA is significantly associated with lower FPG as compared to both AG and GG genotypes (FPG AA: 141 ± 7.5 mg%, AG: 224.8 ± 13.8 mg%, and GG: 209.8 ± 9.1 mg%, p-value = 0.008). Similarly, HbA_{1C}% was significantly lower in the AA genotype than both AG and GG genotypes but failed to reach a significant increase in GG (HbA_{1C}%: AA: 6.6 ± 0.3%, AG: 8.97 ± 0.3%, and GG: 8.4 ± 0.3%, p-value = 0.006) as shown in **Figure 1B**. Interestingly, HOMA2-β% showed significant elevation in the AA genotype as compared to both AG and GG genotypes (HOMA2-β% AA: 32.8 ± 4.7%, AG: 14.4 ± 1.7, and GG: 18 ± 1.5, p-value = 0.004) as shown in **Figure 1C**. It is noteworthy that even after adjustment for age, gender, and BMI, genotype AA subjects remained relatively significantly different from the AG genotype regarding FPG, HbA_{1C}%, and HOMA2-β% levels (adjusted p-values were 0.014, 0.057, and 0.003, respectively) and also from the GG genotype (adjusted p-values were 0.035, 0.23, and 0.011, respectively).

Moreover, we studied the association of the various genotypes with the glycemic control status in the genotyped diabetic patients. We found that there is a significant difference in the distribution of the various genotypes (AA, AG, and GG) between the good and the poor glycemic control of diabetic patients (p-value = 0.002). On the other hand, there was no significant association between good glycemic control and the AA or AG genotype, i.e., the A allele (OR = 0.627; CI = 0.233–1.691; p-value = 0.357). Interestingly, there was a significant association between the AA genotype and prediction of good glycemic control (OR = 10.324, CI = 1.088–97.965; p-value = 0.042). Actually, these last OR and CI are the same for the AG or GG genotype, i.e., the G allele and the poor glycemic control in diabetic patients. All ORs and CIs are shown before and after adjustment for age, gender, and BMI in **Table 4**.

TABLE 3 | Association of *SERPINB1* rs15286 variants with various anthropometric and clinical characteristics of the studied subjects.

Parameter	SerpinB1 rs15286 genotypes									
	Control					Type 2 DM				
	AA	AG	GG	*p*-value	*p*-value¶	AA	AG	GG	*p*-value	*p*-value¶
N (F/M)	3 (3/0)	22 (15/7)	37 (24/13)	—-	—-	6 (4/2)	26 (13/13)	66 (29/37)	—-	—-
Age (year)	29.7 ± 3.8	40.4 ± 2.1	37.6 ± 1.3	*0.116*[a]	—-	54.7 ± 4.5	47.2 ± 2	49.3 ± 1.3	*0.271*[a]	—-
BMI (kg/m^2)	30.1 ± 5.2	28.3 ± 1.2	29.1 ± 0.7	*0.778*[a]	—-	31.7 ± 1.6	31.8 ± 0.9	31.4 ± 0.7	*0.934*[a]	—-
WHR[c]	0.89 ± 0.02	0.92 ± 0.01	0.93 ± 0.01	*0.469*[b]	*0.772*	0.97 ± 0.02	0.95 ± 0.03	0.95 ± 0.02	*0.522*[b]	*0.670*
FPG (mg/dl)[c]	81 ± 7.2	90.8 ± 2.3	84.5 ± 2.2	*0.11*[b]	*0.17*	141 ± 7.5	224.8 ± 13.8	209.8 ± 9.1	***0.008***[b,**]	***0.018*** *
HbA_{1C}(%)[c]	5.38 ± 0.02	5.6 ± 0.1	5.3 ± 0.1	*0.083*[b]	*0.109*	6.6 ± 0.3	8.97 ± 0.3	8.4 ± 0.3	***0.006***[b,**]	***0.055***
TG (mg/dl)[c]	78.7 ± 24	78.9 ± 8.9	81.1 ± 6	*0.733*[b]	*0.872*	248.3 ± 44.5	172.9 ± 16.9	173.5 ± 11.8	*0.258*[b]	*0.439*
TC (mg/dl)	162.7 ± 18.8	155.1 ± 5.1	147 ± 7.7	*0.65*[a]	*0.529*	212.7 ± 21.3	212.7 ± 9.1	207.3 ± 6.6	*0.889*[a]	*0.892*
LDL-C (mg/dl)	104.7 ± 16.3	92.3 ± 5.9	84.5 ± 7.5	*0.587*[a]	*0.484*	115.7 ± 12.8	128.3 ± 8.6	128.1 ± 5.5	*0.797*[a]	*0.633*
HDL-C (mg/dl)[c]	42 ± 4.6	47.1 ± 1.2	47.5 ± 0.9	*0.385*[b]	*0.128*	47 ± 3.8	45.8 ± 2.7	44.1 ± 1.8	*0.601*[b]	*0.750*
LDL-C/HDL-C[c]	2.5 ± 0.4	2 ± 0.17	1.9 ± 0.2	*0.164*[b]	*0.147*	2.5 ± 0.29	3.2 ± 0.37	3.3 ± 0.24	*0.561*[b]	*0.716*
TC/HDL-C[c]	3.9 ± 0.5	3.4 ± 0.19	3.2 ± 0.2	*0.22*[b]	*0.208*	4.6 ± 0.37	5.1 ± 0.4	5.2 ± 0.27	*0.881*[b]	*0.878*
C-peptide (ng/ml)[c]	4.4 ± 0.8	4.1 ± 0.4	3.6 ± 0.36	*0.239*[b]	*0.386*	0.98 ± 0.2	0.75 ± 0.04	0.87 ± 0.08	*0.2*[b]	*0.247*
HOMA2-β%[c]	280 ± 75.6	202.2 ± 15.8	215 ± 15.5	*0.571*[b]	*0.413*	32.8 ± 4.7	14.4 ± 1.7	18 ± 1.5	***0.004***[b,**]	***0.004*** **
HOMA2-IR[c]	3 ± 0.49	3 ± 0.29	2.5 ± 0.26	*0.127*[b]	*0.30*	0.83 ± 0.16	0.86 ± 0.07	0.98 ± 0.1	*0.781*[b]	*0.963*

Results are expressed as mean ± S.E.M. p-values are shown for ANOVA or Kruskal–Wallis test, before and also after adjustment for age, gender, and BMI by GLM. DM, diabetes mellitus; BMI, body mass index; WHR, waist to hip ratio; FPG, fasting plasma glucose; TC, total cholesterol; LDL-C, low-density lipoprotein cholesterol; HDL-C, high-density lipoprotein cholesterol; TG, triglycerides; HbA_{1C}%, glycosylated hemoglobin; HOMA2-β%, homeostasis model assessment-β cell function; HOMA2-IR, insulin resistance.

*[a]ANOVA, two-tailed, p-value >0.05 non-significant. [b]Kruskal–Wallis, two-tailed, p-value >0.05 non-significant. [c]Log transformed for performing GLM. ¶P-value after adjustment for age, gender and BMI by GLM. *Significant at $p < 0.05$ level. **Significant at $p < 0.01$ level. All significant p-values are written in bold and italics.*

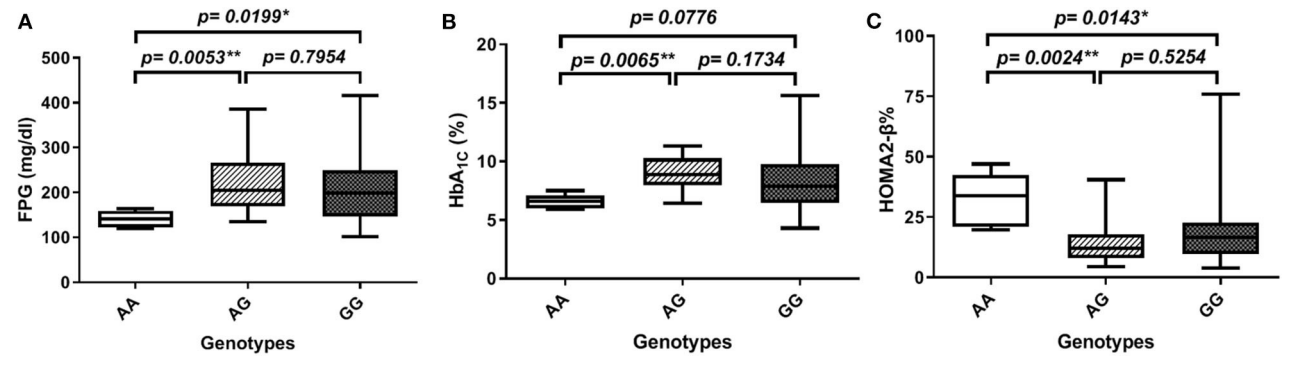

FIGURE 1 | Association of *SERPINB1* rs15286 variants with various parameters in type 2 DM. **(A)** FPG, **(B)** HbA_{1C}%, and **(C)** HOMA2-β%. The top and bottom whiskers represent the minimum and maximum values, while the band inside the box represents the median. *Significantly different from genotype AA at $p < 0.05$. **Significantly different from genotype AA at $p < 0.01$, assessed by the Kruskal–Wallis test followed by Dunn's *post hoc* test.

DISCUSSION

In this study, we assessed two *SERPINB1* gene SNPs in control and type 2 DM patients and investigated their association with the risk of diabetes and other anthropometric and biochemical parameters. The first SNP was *SERPINB1* rs114597282, which is a missense mutation with a C/T substitution. The other one was *SERPINB1* rs15286 which is a transition A/G SNP in the 3′UTR region of the *SERPINB1* gene. For SNP rs114597282, all our subjects, either control or diabetic patients, were of TT genotype, which did not allow any further analyses for this SNP. As for the other SNP rs15286, various genotypes, namely, AA, AG, and GG, were expressed in both control and diabetic subjects with AA being the minor genotype, while GG was the major genotype in both studied groups. However, we failed to find an association with the distribution of these genotypes with the risk of diabetes. Interestingly, we found that diabetic subjects having a rs15286 AA genotype showed lower levels of FPG and HbA_{1C}%, as well as higher HOMA2-β% compared to other genotypes. Moreover, there exists a significant association of genotype AA with the prediction of good glycemic control in diabetic patients, an association not found with the A allele alone. Meanwhile, our results showed a positive association between the G allele and the prediction of poor glycemic control. This indicates that type

TABLE 4 | Association of *SERPINB1* rs15286 variants with the glycemic control status of type 2 DM.

Serpin B1 rs15286 genotypes	Good glycemic control ($HbA_{1C} \leq 7\%$) $n = 31$	Poor glycemic control ($HbA_{1C} > 7\%$) $n = 67$	χ^2	*p*-value	OR (95% CI)	*p*-value
	n (%)	*n* (%)				
AA	5 (16.1%)	1 (1.5%)				
AG	3 (9.7%)	23(34.3%)	12.586	***0.002*****	0.188 (0.064–0.551)	***0.002*****
GG	23 (74.2%)	43 (64.2%)			0.212 (0.071–0.635)	***0.006***¶,**
AG/AA vs. GG	8 (25.8%) vs. 23 (74.2%)	24 (35.8%) vs. 43 (64.2%)	0.967	*0.326*	0.623 (0.242–1.606)	*0.328*
					0.627 (0.233–1.691)	*0.357*¶
AA vs. AG/GG	5 (16.1%) vs. 26 (83.9%)	1 (1.5%) vs. 66 (98.5%)	7.899	***0.005****	12.692 (1.414–113.917)	***0.023****
					10.324 (1.088–97.965)	***0.042***¶,*
Total	31 (100%)	67 (100%)				

A $\chi 2$ test was done for various genotypes, A allele and G allele, and glycemic control status of diabetic patients. The odds ratio (OR) was calculated using binary logistic regression using glycemic control status as the dependent variable and genotype as the covariate, in addition to adjustment for age, gender, and BMI as additional covariates.

¶Adjusted for the effect of covariates: age, gender, and BMI.

**Significant at $p < 0.05$. **Significant at $p < 0.01$. All significant p-values are written in bold and italics.*

2 diabetic patients' carriers of the AA genotype may potentially have better control over their blood glucose levels and better β-cell function than other genotypes of this *SERPINB1* SNP. On the other hand, those who are carriers of a G allele are at risk of poor glycemic control.

SerpinB1, also known as a monocyte neutrophil elastase inhibitor, is a protease inhibitor that regulates several inflammatory responses (26). Lately, serpinB1 has been associated with insulin signaling in 2 ways. First, neutrophil elastase was found to be associated with hepatic and adipose tissue insulin resistance and its deletion may improve insulin sensitivity (13). Second, *EL-Ouaamari and coworkers* could prove serpinB1 as a novel liver-derived secretory protein that promotes proliferation of human and mouse β-cells (11). Since then, a couple of reports tried to study the possible association of serpinB1 with insulin sensitivity or with type 2 DM (14, 27). However, still the genetic variants of the *SERPINB1* gene and their association with diabetes have not been studied.

Accordingly, we decided to study two *SERPINB1* SNPs and their association with various anthropometric and biochemical parameters in type 2 DM in comparison to control subjects. One of these SNPs was introduced by EL Ouaamari et al., namely, rs114597282, as a possibly damaging variant (11). However, we failed to find the various variants in our genotyped subjects as 100% of our subjects were homozygous TT. This comes in accordance with a previous reported frequency of 1.7% among African Americans and 0.01% among Europeans according to the 1,000 Genomes database. This may well explain that we failed to get any other variants from our 160 total subjects. Accordingly, further investigations are warranted on a larger sample size and in different populations to study this SNP in association with diabetes or even other diseases.

As for the other SNP rs15286, to our knowledge, this is the first report concerning this SNP for *SERPINB1* especially in DM. Our genotyped samples showed the 3 genotypes with AA being the minor genotype representing 5.6% of total subjects, AG representing 30% of the total subjects, and GG being the major one with 64.4% of total subjects. These results approached genotype frequencies from the 1,000 Genomes database, where the overall distribution of the genotypes in all populations were AA 7% (was 5.6% in our study), AG 37% (was 30% in our study), and GG 56% (was 64.4% in our study). The A allele represents the minor allele with 36.25% in the studied groups as compared to the minor allele frequency (MAF) of 25% and the G allele of 75% from the 1,000 Genomes phase 3 database. This is the first report about the frequency of this genotype in the Egyptian population which approaches the distribution of several other populations. This SNP requires further association studies on other populations and in other diseases.

In fact, the distribution and frequency of these genotypes failed to be associated with the risk of diabetes. However, we found that the AA genotype was significantly associated with lower FPG and HbA_{1C}% in diabetic patients. This finding implies that although this SNP genotype is not predictive of developing diabetes, individuals with AA genotypes are potentially less hyperglycemic and exhibit easier control on their diabetes, This was further confirmed with the positive association of the AA genotype and the good glycemic control in diabetic patients, while carriers of one G allele are under risk of poor glycemic control. We also observed that the presence of one A allele is not enough to reach a significant association with such good glycemic control. These findings may prove important in several ways. First, further studies should be conducted to explore if the patients with the AA genotype are less prone or, alternatively, patients with the G allele are more prone to diabetic complications which are mostly caused by hyperglycemia and associated glucotoxicity (28). Second, the AA patients may require lower doses of oral hypoglycemic or even insulin treatment to avoid possible hypoglycemia associated with excessive insulin or OHA dosing. Third, although more population-based studies are required, for *SERPINB1* SNP rs15286 so far, we can consider the G allele as the "bad allele" or the "risk allele." Diabetic patients who are carriers of the G allele are under risk of poor glycemic control and should be closely

monitored for their hyperglycemia. However, clinical trials are warranted to test these hypotheses.

Another interesting finding in this study is the higher HOMA2-β% associated with the AA genotypes in comparison to other genotypes. SerpinB1 has been portrayed as a β-cell-protective hepatokine. Whether the AA genotype may provide enhanced/better protection than other genotypes is a question that warrants further investigations especially in prediabetic patients. It is noteworthy that this is the first study that explores the association of a *SERPINB1* SNP variant with β-cell function in diabetic patients.

Nevertheless, this study faced several limitations that we have been aware of. First, further studies with larger samples representable of the different ethnic populations are warranted. Second, our failure to find various variants of the SNP rs114597282 constrained our capability to further study this SNP. In fact, although this study was limited by its relatively small sample size, our results demonstrate the interplay of *SERPINB1* SNP rs15826 with glycemic control in diabetic patients and shed light on the possible implication of *SERPINB1* gene polymorphism in diabetes pathogenesis, as well as the risk for developing diabetic complications.

In conclusion, to the best of our knowledge, this is the first report to show that the *SERPINB1* gene has the SNP rs15286 variant of all genotypes expressed in the Egyptian population, with the A allele as the minor allele of about 35% of the population. However, these genotypes are not associated with risk to diabetes. The AA genotype of this SNP is associated with an overall better glycemic control and better β-cell function in diabetic patients. The G allele can be considered as the "risk allele" for poor glycemic control in diabetic patients. Conclusively, *SERPINB1* SNP rs15826 can potentially predict glycemic control in diabetic patients and can enhance better treatment options for these patients based on their genotypes. In addition, this study opens the door for further studies to investigate the possible association between other *SERPINB1* gene variants and susceptibility for diabetes and/or diabetic complications in different ethnic populations. Furthermore, further research is required to study the effect of these SNPs on the serum levels of serpinB1, which may explain the better glycemic control associated with various genotypes. Finally, further studies are warranted to further elucidate the clinical impact of rs15286 variants on diabetic patients' treatment regimen in Egyptian as well as other populations.

DATA AVAILABILITY STATEMENT

The raw data supporting the conclusions of this article will be made available by the authors, without undue reservation, to any qualified researcher.

ETHICS STATEMENT

The studies involving human participants were reviewed and approved by National institute of Diabetes and Endocrinology—General Organization for Teaching Hospitals and Institutes (NIDE – GOTHI). The patients/participants provided their written informed consent to participate in this study.

AUTHOR CONTRIBUTIONS

MK and DK conceived and designed the experiments, analyzed the data, and wrote the manuscript. MK, DK, and AA performed the experiments. GH and AA provided and processed the samples. All the authors reviewed and approved the manuscript. All authors contributed to the article and approved the submitted version.

ACKNOWLEDGMENTS

Some experiments were done with partial funding from the Center of Drug Research and Development (CDRD), Faculty of Pharmacy, and The British University in Egypt (BUE). Additionally, we would like to express our appreciation to the members of the National Institute of Diabetes and Endocrinology (NIDE) for their kind help and support during samples collection.

REFERENCES

1. IDF. *International Diabetes Federation. IDF Diabetes Atlas*. 8th ed. (2017). Available online at: http://www.idf.org/diabetesatlas (accessed October 1, 2019).
2. WHO. *World Health Organization Media Center; Fact sheet for Diabetes* (2018). Available online at: http://www.who.int/mediacentre/factsheets/fs312/en/ (accessed October 1, 2019).
3. Kalin MF, Goncalves M, John-Kalarickal J, Fonseca V. Pathogenesis of Type 2 Diabetes Mellitus. In: Poretsky L, editor. *Principles of Diabetes Mellitus*. Cham: Springer International Publishing (2017). p. 1–11
4. Mezza T, Cinti F, Cefalo CMA, Pontecorvi A, Kulkarni RN, Giaccari A. β-cell fate in human insulin resistance and type 2 diabetes: a perspective on islet plasticity. *Diabetes.* (2019) 68:1121–9. doi: 10.2337/db18-0856
5. Basile G, Kulkarni RN, Morgan NG. How, when, and where do human β-cells regenerate? *Curr Diab Rep.* (2019) 19:48. doi: 10.1007/s11892-019-1176-8
6. Tanabe K, Amo-Shiinoki K, Hatanaka M, Tanizawa Y. Interorgan crosstalk contributing to β-Cell Dysfunction. *J Diab Res.* (2017) 2017:8. doi: 10.1155/2017/3605178
7. Saisho Y, Butler AE, Manesso E, Elashoff D, Rizza RA, Butler PC. β-cell mass and turnover in humans. *Effects Obes Aging.* (2013) 36:111–7. doi: 10.2337/dc12-0421
8. Montanya E. Insulin resistance compensation: not just a matter of β-cells? *Diabetes.* (2014) 63:832–4. doi: 10.2337/db13-1843
9. Butler AE, Cao-Minh L, Galasso R, Rizza RA, Corradin A, Cobelli C, et al. Adaptive changes in pancreatic beta cell fractional area and beta cell turnover in human pregnancy. *Diabetologia.* (2010) 53:2167–76. doi: 10.1007/s00125-010-1809-6
10. El Ouaamari A, Kawamori D, Dirice E, Liew CW, Shadrach JL, Hu J, et al. Liver-derived systemic factors drive β cell hyperplasia in insulin-resistant states. *Cell Rep.* (2013) 3:401–10. doi: 10.1016/j.celrep.2013.01.007
11. El Ouaamari A, Dirice E, Gedeon N, Hu J, Zhou J-Y, Shirakawa J, et al. SerpinB1 promotes pancreatic β-cell proliferation. *Cell Metab.* (2016) 23:194–205. doi: 10.1016/j.cmet.2015.12.001

12. Cooley J, Takayama TK, Shapiro SD, Schechter NM, Remold-O'Donnell E. The serpin MNEI inhibits elastase-like and chymotrypsin-like serine proteases through efficient reactions at two active sites. *Biochemistry*. (2001) 40:15762–70. doi: 10.1021/bi0113925
13. Talukdar S, Oh DY, Bandyopadhyay G, Li D, Xu J, McNelis J, et al. Neutrophils mediate insulin resistance in mice fed a high-fat diet through secreted elastase. *Nat Med*. (2012) 18:1407–12. doi: 10.1038/nm.2885
14. Glicksman M, Asthana A, Abel BS, Walter MF, Skarulis MC, Muniyappa R. Plasma serpinB1 is related to insulin sensitivity but not pancreatic β-Cell function in non-diabetic adults. *Physiol Rep*. (2017) 5:e13193. doi: 10.14814/phy2.13193
15. Hida K, Wada J, Eguchi J, Zhang H, Baba M, Seida A, et al. Visceral adipose tissue-derived serine protease inhibitor: a unique insulin-sensitizing adipocytokine in obesity. *Proc Natl Acad Sci USA*. (2005) 102:10610–5. doi: 10.1073/pnas.0504703102
16. El-Mesallamy HO, Kassem DH, El-Demerdash E, Amin AI. Vaspin and visfatin/Nampt are interesting interrelated adipokines playing a role in the pathogenesis of type 2 diabetes mellitus. *Metab Clin Exp*. (2011) 60:63–70. doi: 10.1016/j.metabol.2010.04.008
17. Tarasov AI, Rorsman P. Dramatis personae in β-cell mass regulation: enter serpinB1. *Cell Metab*. (2016) 23:8–10. doi: 10.1016/j.cmet.2015.12.011
18. Meroufel DN, Ouhaibi-Djellouli H, Mediene-Benchekor S, Hermant X, Grenier-Boley B, Lardjam-Hetraf SA, et al. Examination of the brain natriuretic peptide rs198389 single-nucleotide polymorphism on type 2 diabetes mellitus and related phenotypes in an Algerian population. *Gene*. (2015) 567:159–63. doi: 10.1016/j.gene.2015.04.073
19. Xue A, Wu Y, Zhu Z, Zhang F, Kemper KE, Zheng Z, et al. Genome-wide association analyses identify 143 risk variants and putative regulatory mechanisms for type 2 diabetes. *Nat Commun*. (2018) 9:2941. doi: 10.1038/s41467-018-04951-w
20. Shirakawa J, De Jesus DF, Kulkarni RN. Exploring inter-organ crosstalk to uncover mechanisms that regulate beta-cell function and mass. *Eur J Clin Nutr*. (2017) 71:896–903. doi: 10.1038/ejcn.2017.13
21. WMA. World medical association declaration of helsinki: ethical principles for medical research involving human subjects. *JAMA*. (2013) 310:2191–4. doi: 10.1001/jama.2013.281053
22. Kassaian SE, Goodarzynejad H, Boroumand MA, Salarifar M, Masoudkabir F, Mohajeri-Tehrani MR, et al. Glycosylated hemoglobin (HbA1c) levels and clinical outcomes in diabetic patients following coronary artery stenting. *Cardiovasc Diabetol*. (2012) 11:82. doi: 10.1186/1475-2840-11-82
23. Friedewald WT, Levy RI, Fredrickson DS. Estimation of the concentration of low-density lipoprotein cholesterol in plasma, without use of the preparative ultracentrifuge. *Clin Chem*. (1972) 18:499–502.
24. Wallace TM, Levy JC, Matthews DR. Use and Abuse of HOMA modeling. *Diabetes Care*. (2004) 27:1487–95. doi: 10.2337/diacare.27.6.1487
25. Rodriguez S, Gaunt TR, Day INM. Hardy-Weinberg equilibrium testing of biological ascertainment for Mendelian randomization studies. *Am J Epidemiol*. (2009) 169:505–14. doi: 10.1093/aje/kwn359
26. Silverman GA, Bird PI, Carrell RW, Church FC, Coughlin PB, Gettins PGW, et al. The Serpins are an expanding superfamily of structurally similar but functionally diverse proteins: evolution, mechanism of inhibition, novel functions, and a revised nomenclature. *J Biol Chem*. (2001) 276:33293–6. doi: 10.1074/jbc.R100016200
27. Takebayashi K, Hara K, Terasawa T, Naruse R, Suetsugu M, Tsuchiya T, et al. Circulating SerpinB1 levels and clinical features in patients with type 2 diabetes. *BMJ Open Diab Res Care*. (2016) 4:1–7. doi: 10.1136/bmjdrc-2016-000274
28. Campos C. Chronic hyperglycemia and glucose toxicity: pathology and clinical sequelae. *Postgrad Med*. (2012) 124:90–7. doi: 10.3810/pgm.2012.11.2615

Conflict of Interest: The authors declare that the research was conducted in the absence of any commercial or financial relationships that could be construed as a potential conflict of interest.

frontiers in Genetics

REVIEW
published: 01 September 2020
doi: 10.3389/fgene.2020.00983

mRNA Processing: An Emerging Frontier in the Regulation of Pancreatic β Cell Function

*Nicole D. Moss and Lori Sussel**

Cell, Stem Cells, and Development Graduate Program, Department of Pediatrics, Barbara Davis Center, University of Colorado Denver Anschutz Medical Campus, Aurora, CO, United States

Robust endocrine cell function, particularly β cell function, is required to maintain blood glucose homeostasis. Diabetes can result from the loss or dysfunction of β cells. Despite decades of clinical and basic research, the precise regulation of β cell function and pathogenesis in diabetes remains incompletely understood. In this review, we highlight RNA processing of mRNAs as a rapidly emerging mechanism regulating β cell function and survival. RNA-binding proteins (RBPs) and RNA modifications are primed to be the next frontier to explain many of the poorly understood molecular processes that regulate β cell formation and function, and provide an exciting potential for the development of novel therapeutics. Here we outline the current understanding of β cell specific functions of several characterized RBPs, alternative splicing events, and transcriptome wide changes in RNA methylation. We also highlight several RBPs that are dysregulated in both Type 1 and Type 2 diabetes, and discuss remaining knowledge gaps in the field.

Keywords: pancreatic islet, beta cells, diabetes, RNA processing, RNA binding proteins

OPEN ACCESS

Edited by:
Simona Chera,
University of Bergen, Norway

Reviewed by:
Ildem Akerman,
University of Birmingham, United Kingdom
Jonathan Lou S. Esguerra,
Lund University, Sweden

***Correspondence:**
Lori Sussel
lori.sussel@cuanschutz.edu

Specialty section:
This article was submitted to Genetics of Common and Rare Diseases, a section of the journal Frontiers in Genetics

Received: *03 July 2020*
Accepted: *03 August 2020*
Published: *01 September 2020*

Citation:
Moss ND and Sussel L (2020) mRNA Processing: An Emerging Frontier in the Regulation of Pancreatic β Cell Function. Front. Genet. 11:983. doi: 10.3389/fgene.2020.00983

INTRODUCTION

The highly specialized insulin-producing β cell population is located within the pancreatic islet of Langerhans (**Figure 1**). In humans and other vertebrates, β cells respond to changes in circulating blood glucose levels by secreting insulin. Coupled with the function of the other islet endocrine cell types, β cells help to maintain blood glucose homeostasis; loss or dysfunction of the β cell population results in diabetes. Over the last several decades, substantial research efforts have been directed toward understanding the gene regulatory networks required for the formation and function of the islet cell populations. This has included developmental studies in model organisms that have identified the key transcription factors required to make and maintain functional β cell populations. In addition, translational research approaches in human subjects, including Genome Wide Association Studies (GWAS) and other large sequencing efforts, have identified numerous alleles and mutations associated with increased risk of developing either Type 1 (T1D) or Type 2 (T2D) diabetes, many of which cause β cell dysfunction. Despite these efforts, there remain many gaps in our understanding of the mechanisms that regulate β cells and the pathways that contribute to their pathogenesis in diabetes.

Although much of the research to date has been focused on transcriptional regulation, β cell identity and function are also regulated at the level of mRNA, similar to many other cell types and organ systems. Throughout their life cycle, mRNA molecules undergo extensive processing events to transition from a pre-mRNA molecule to a mature mRNA. These events not only include

addition of a 5′-cap and 3′-poly-A tail, but also splicing of introns, nucleotide modification, stability, and subcellular localization (Licatalosi and Darnell, 2010; **Figure 1**). RNA-binding proteins (RBPs) are responsible for coordinating the events in the lifecycle of an mRNA. Over the past few years, several groups have begun to probe the function of specific RBPs in organogenesis and disease. Many studies have focused on the mis-regulation of mRNAs and RBP function in the context of diabetic complications (adipose, liver, muscle, retina, etc.), rather than specific changes in the β cells (Nutter and Kuyumcu-Martinez, 2018). In the pancreas, only a few groups have delved into the world of RNA regulation, often focusing on a single splicing target or RBP. In this review, we will highlight these studies describing RBP functions, transcriptome wide changes in RBP expression, alternative splicing, and RNA methylation, with a specific focus on regulation of mRNAs in the pancreatic islet population. This is a rapidly emerging field that will undoubtedly provide a unique perspective on a complex disease and will ultimately push the boundaries of therapeutic treatments for diabetes.

RNA-Binding Proteins in the β Cell

Several hundred RBPs have been identified (Hentze et al., 2018), each with the potential of having hundreds of targets within a cell (Keene, 2007; Hogan et al., 2008; Lukong et al., 2008; Blanchette et al., 2009; Li et al., 2014). Some RBPs have ubiquitous expression, while others are transiently expressed during development or restricted to a specific cell type (Gerstberger et al., 2014). Like many other proteins, RBPs are categorized by several modular domains. RBPs recognize RNA targets through a binding domain, in the form of an RNA recognition motif (RRM), K-homology (KH) domain, and RNA-binding zinc-finger (ZnF) domains, or can bind independent of sequence through a double-stranded RNA module (dsRBD) (Lunde et al., 2007). Additionally, RBPs have a variety of enzymatic and/or signaling domains that allow for functional activity (Lunde et al., 2007).

The role of RBPs in the formation and function of pancreatic endocrine cells is only beginning to be appreciated. Only a small number of known RBPs have been studied in the β cell, but as new transcriptomics data becomes available from both healthy and diseased islets, their role in β cell biology will become more apparent. Recently, several studies have identified RBPs that are enriched in pancreatic islet cells and become dysregulated under stress (Juan-Mateu et al., 2017; Jeffery et al., 2019; Ramos-Rodriguez et al., 2019). Stressors including chronic hyperglycemia (Puri and Hebrok, 2012; Brereton et al., 2014), exposure to pro-inflammatory cytokines (Ortis et al., 2010), and palmitate (saturated fatty acid) (Cnop et al., 2014) can result in changes in cellular and molecular identity. In a model of human β cells (EndoC-βH1), treatment with cell stressors (including cytokines, hypoxia, altered lipids, and high and low levels of glucose) also induced dysregulation of many RBPs (Jeffery et al., 2019).

Islet endocrine cells have a specific assemblage of RBPs that perform a variety of functions. Re-analysis of whole transcriptomic RNA-Sequencing (RNA-Seq) data from several human tissues (Eizirik et al., 2012) revealed that human islets share a notable number of RBPs with the brain, and β cells in particular are enriched for many "neuron specific" RBPs (Juan-Mateu et al., 2017; Alvelos et al., 2018). This is not surprising since, despite their disparate developmental origins, neurons and β cells share a large number of transcriptional networks (van Arensbergen et al., 2010). While it is clear that there are a whole host of RBPs expressed in mature insulin-secreting β cells (summarized in **Table 1**), there remains poor understanding about the role of RBP regulation in the developing pancreas (Baralle and Giudice, 2017). Additionally, the majority of these studies to date are limited to *in vitro* analysis of RBP requirements and molecular function. RBPs regulate several classes of RNAs, including both coding (mRNA) and non-coding (ncRNA) RNAs. A recent comprehensive review has discussed the critical role of RBPs Dicer and Argonaut in the regulation of miRNAs for β cell function and in T2D (Eliasson and Esguerra, 2020). Here we will provide a brief survey of the expression and function of several prominent RBP families that regulate mRNAs in pancreatic β cells.

Hu and Embryonic Lethal Abnormal Vision-Like Protein Family (HuD/ELAVL4)

The Hu/ELAV family of RBPs bind to AU-rich elements (AREs) in the 3′UTR of mRNAs and can modulate transcript stability and translation (Hinman and Lou, 2008). Hu/ELAV proteins bind to the AREs through three RRMs (Okano and Darnell, 1997). HuR/ELAVL1 is ubiquitously expressed, while the other three family members (HuB/ELAVL2, HuC/ELAVL3, HuD/ELAVL4) are most highly expressed in neurons (Hinman and Lou, 2008). However, a few recent studies have identified roles for one of these family members, HuD/ELAVL4, in the β cell (Lee et al., 2012; Kim et al., 2014; Hong et al., 2020). Normally, HuD expression is (1) glucose dependent; (2) regulated through insulin receptor (INSR) signaling; and (3) acts as a feedback mechanism that regulates translation of the *Preproinsulin2* (*Ins2)* mRNA (Lee et al., 2012). Rodents encode two *prepronsulin* (*Ins*) genes; however, interaction between HuD and the *preproinsulin1* (*Ins1*) transcript was not reported. Insulin is secreted from β cells in response to high levels of glucose. Circulating insulin can then bind the insulin receptor (INSR) on the surface of β cells and, through the PI3K/AKT pathway, the transcriptional repressor FOXO1 is phosphorylated. Phosphorylation of FOXO1 de-represses transcription of HuD. The HuD protein then binds the 5′UTR of *Ins2* mRNA and decreases *Ins2* translation, maintaining plasma insulin homeostasis. Consistently, $HuD^{-/-}$ mice displayed higher insulin levels and improved glucose tolerance, whereas transgenic mice overexpressing HuD had lower insulin levels and were glucose intolerant, reportedly due to less readily releasable insulin pools (Kim et al., 2014). It has also been demonstrated that nuclear HuD is increased under ER stress resulting in decreased intracellular insulin biosynthesis and decreased plasma insulin homeostasis (Yoo, 2013). In addition to regulating *Ins2* translation, HuD also regulates the translation of two genes encoding proteins important for β cell survival in stress conditions. Autophagy-related Gene 5 (ATG5) is a protein that can mediate stress induced β cell death (Fujimoto et al.,

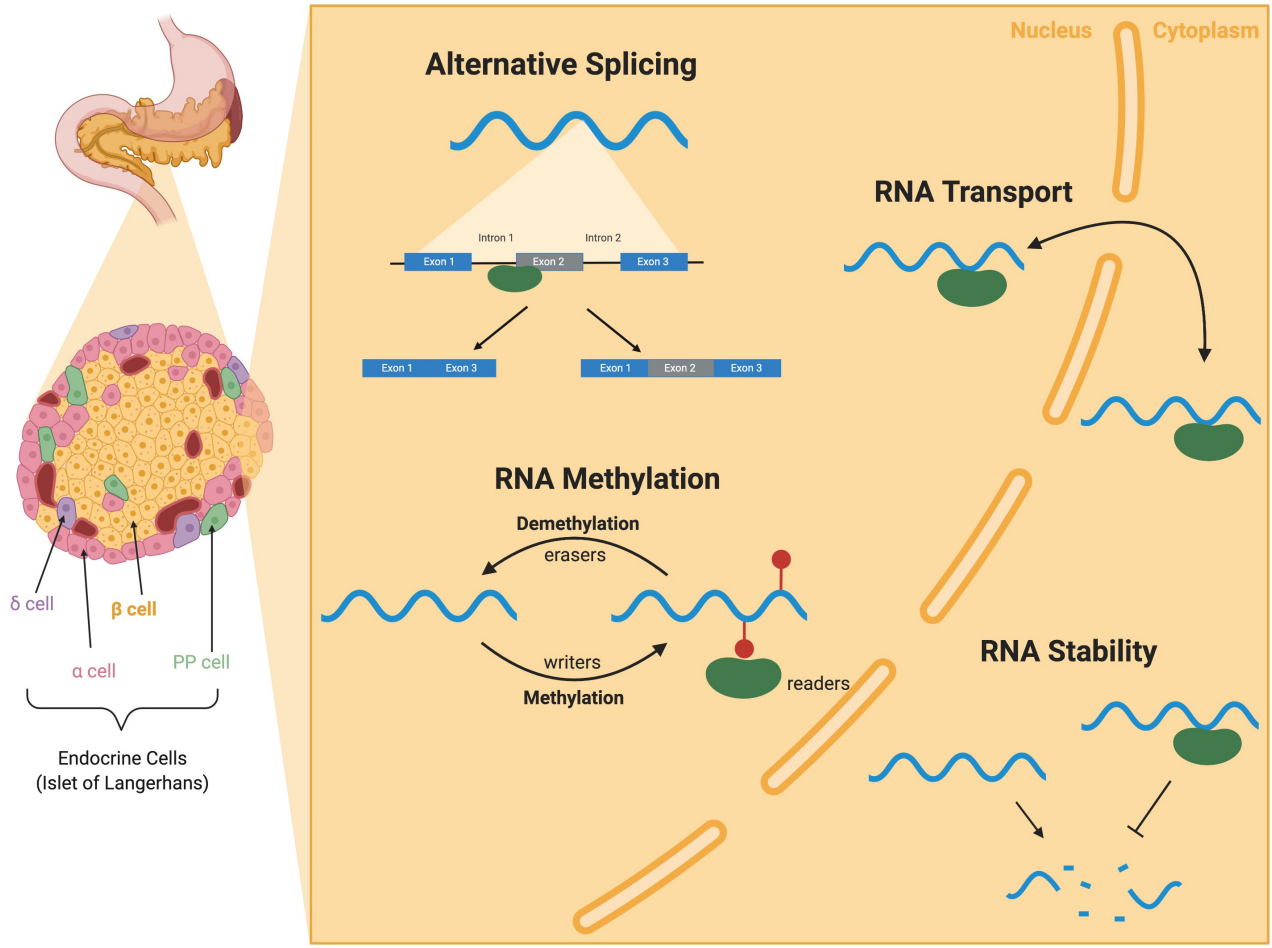

FIGURE 1 | *RNA-binding protein (RBP) mediated RNA regulation in the pancreatic β cell.* Insulin-secreting β cells reside in the islets of the pancreas along with several other endocrine cell types (α, δ, and PP cells). RBPs (green) are present in both the nucleus and the cytoplasm of cells and bind to RNA (blue) to perform a variety of functions. RBPs binding to introns and exons of pre-mRNAs contribute to *alternative splicing*. RBPs can also write, read, and erase methylation modification on mRNAs in *RNA methylation.* RBPs can also facilitate the *transport* of RNAs between the nucleus and cytoplasm and throughout the cell. RBP binding to the UTRs can alter mRNA stability and translation. Illustration created with BioRender.

2009). HuD binds to AREs in the 3′UTR of *Atg5* and enhances the assembly of polysomes to increase ATG5 protein levels. HuD also modulates β cell function through mitochondrial dynamics and stabilizing the mitochondrial gene *Mitofusin2* (*Mfn2*), which encodes a protein which mediates mitochondrial fusion and metabolism, and is an inhibitor of apoptosis in β cells (Baltrusch, 2016; Hong et al., 2020). Taken together, it is clear that RNA regulation by HuD is required for proper function and survival of pancreatic β cells through multiple mechanisms and pathways.

Polypyrimidine-Tract-Binding Protein (hnRNP1/PTB/PTBP1)

The polypyrimidine-tract-binding proteins (PTBs) are a group of RBPs that function through binding-mediated modifications in target mRNA (Wollerton et al., 2001; Mitchell et al., 2003; Auweter et al., 2007) to either recruit or block other trans-acting factors. PTB has four RRM domains each with specific consensus binding sequences that all bind stretches of pyrimidines (Sawicka et al., 2008). Additionally, PTBs can shuttle between the nucleus and the cytoplasm (Perez et al., 1997; Kamath et al., 2001; Li and Yen, 2002). PTB proteins have been implicated in the regulation of several RNA metabolism events including alternative splicing (Garcia-Blanco et al., 1989), polyadenylation (Lou et al., 1999; Castelo-Branco et al., 2004), mRNA stability (Wollerton et al., 2004), and translation (Jang and Wimmer, 1990). In the pancreas, PTB proteins have been shown to regulate insulin mRNA (human *INS* and rodent *Ins1* and *Ins2*) (Tillmar et al., 2002; Tillmar and Welsh, 2002; Fred et al., 2010, 2011, 2016) and insulin secretory granule biogenesis (Knoch et al., 2004, 2006). Specifically, the binding of PTB to *INS/Ins* mRNA increases in response to increased glucose and hypoxia (Tillmar et al., 2002; Tillmar and Welsh, 2002; Fred et al., 2011). Mutations in the *INS/Ins* 3′UTR or decreases in PTB expression by RNAi both result in decreased insulin and reporter expression respectively (Tillmar et al., 2002; Fred et al., 2016). Furthermore, binding of PTB to the 5′UTR of *INS* mRNA correspond to cap-independent

TABLE 1 | RNA-Binding Proteins (RBPs) in the Pancreatic β Cell.

RBP	Dysregulated condition	β cell specific function	References
AKAP17A	Dysregulated under cytokine treatment	*NA*	Jeffery et al., 2019
AUF1 (hnRNP-D)	Cytokine treatment reduces nuclear AUF1 without decreases in total AUF1	Increased AUF1 promotes apoptosis	Roggli et al., 2012; Vanzela and Cardozo, 2012; Magro and Solimena, 2013
CELF1/CUGBP1	Increased expression in diabetic models	Decreased GSIS by stabilizing PDE3B mRNA which mediates cAMP hydrolysis	Zhai et al., 2016; Nutter and Kuyumcu-Martinez, 2018; Good and Stoffers, 2020
DDX1	Decreased function under lipotoxicity	Regulates alternative splicing of voltage gaited Ca^{2+} channels and increases insulin translation through interactions translation initiation factors	Li et al., 2018; Zhong et al., 2018; Good and Stoffers, 2020
FTO	Decreased expression in T2D islets	Controversial regulation of insulin secretion	Kirkpatrick et al., 2010; Russell and Morgan, 2011; Dayeh et al., 2014; Fan et al., 2015; Taneera et al., 2015, 2018
hnRNPA2B1	Dysregulated under both high and low glucose conditions, hypoxia, and cytokine treatment	*NA*	Jeffery et al., 2019
hnRNPK/DDX3X	hnRNPK is phosphorylated and activated under metabolic stress	Binds to JUND 3′UTR to regulate translation	Good et al., 2019; Good and Stoffers, 2020
HuD (ELAVL4)	ER stress increases expression, HuD expression is glucose responsive and reduced in diabetes	Increased nuclear HuD results in decreased insulin biosynthesis, binds the 5′UTR of *Ins2* mRNA and decreases *Ins2* translation, regulates ATG5 translation and Mnf2 stability	Lee et al., 2012; Magro and Solimena, 2013; Yoo, 2013; Kim et al., 2014; Juan-Mateu et al., 2017; Hong et al., 2020
IMP	IMP3 dysregulated under lipotoxicity, IMP2 SNPs associated with moderately increased risk of T2D	*NA*	Christiansen et al., 2009; Nutter and Kuyumcu-Martinez, 2018; Jeffery et al., 2019
LSM14A	Dysregulated expression under low glucose and cytokine treatment	*NA*	Jeffery et al., 2019
Mushashi 1/2	ER stress increases expression of *Msi1* and *Msi2* and lipotoxicity increases expression of *Msi2*	Musashi 1 regulates ββ cell proliferation and both Musashi 1 and 2 decrease insulin gene expression	Szabat et al., 2011; Magro and Solimena, 2013
Nova 1/2	Decreased expression in cytokine treated cells	Loss of NOVA1 results in decreased insulin secretion and loss of either NOVA1 or NOVA2 results in decreased apoptosis	Villate et al., 2014; Juan-Mateu et al., 2017
PDI/PABP	*NA*	PDI binds the 5′UTR of insulin mRNA to promote insulin biosynthesis through interactions with PABP, PDI/PABP associate with insulin, PC1/3, and PC2 5′UTR to regulate translation, PABP can also interact with HuD to suppress insulin translation	Kulkarni et al., 2011; Magro and Solimena, 2013; Sarwade et al., 2020
PNISR	Dysregulated expression under low glucose, hypoxia, and cytokine treatment	*NA*	Jeffery et al., 2019
PTBP1 (hnRNP1/PTB)	hypoxia and prolonged high glucose leads to decreased PTB1 expression	PTB binds both insulin mRNA and insulin granule proteins to regulate stability and translation	Tillmar et al., 2002; Tillmar and Welsh, 2002; Knoch et al., 2004; Knoch et al., 2006; Fred et al., 2010, 2011, 2016; Magro and Solimena, 2013
Rbfox	*NA*	Rbfox1 and Rbfox2 modulate insulin secretion by regulating actin modifying proteins	Juan-Mateu et al., 2017; Good and Stoffers, 2020
RBM4	*NA*	Regulates alternative splicing of key β cell transcription factors (*Isl1, Pax4, Pax6, Glut2)*	Lin et al., 2013; Magro and Solimena, 2013
SRSF 1/2/3/6	SRSF1/3/6 are dysregulated under low glucose, SRSF3/6 are dysregulated under hypoxia, SRSF1/2/3 dysregulated in response to cytokine treatment	NA	Jeffery et al., 2019

translation of insulin mRNA (Fred et al., 2011). In addition to changes in PTB binding, T-cell restricted intracellular antigen 1-related protein (TIAR) also increases binding to *INS* mRNA during glucose stimulation (Fred et al., 2010). These proteins cooperate to regulate *INS* mRNA stability and biosynthesis (Fred et al., 2010). While cap-independent *INS* mRNA translation only accounts for a small portion of total translation, it can contribute 40–100% of insulin biosynthesis during stress conditions (Fred et al., 2011). In healthy β cells, transient increase in glucose levels increases PTB binding to 3′UTR promoting mRNA stability and 5′UTR promoting modest levels of cap-independent translation. However, prolonged high glucose exposure results in decreased PTB protein and ultimately decreased insulin biosynthesis (Fred et al., 2010). This is in part due to increased levels of miR-133a which targets PTB mRNA and could explain the mechanism for hyperglycemia-induced β cell dysfunction (Fred et al., 2010).

In addition to binding *INS/Ins* mRNA directly, PTB has been shown to bind and regulate components of the insulin secretory granules in response to changes in blood glucose levels. During glucose stimulated insulin secretion (GSIS), newly synthesized insulin granules preferentially undergo exocytosis (Gold et al., 1982; Halban, 1982) and this 2010process is impaired in T2D. New secretory granules are synthesized in response to glucose stimulation in the β cell, partially through regulation of PTB. Upon β cell stimulation (glucose or GLP-1), PTB is translocated from the nucleus to the cytoplasm (Knoch et al., 2004, 2006), where this process not only promotes stability of insulin mRNA (as described above), but also increases the stability of several insulin secretory granule proteins (Knoch et al., 2004). PTB translocation results from phosphorylation by PKA downstream of GLP-1 receptor and is cAMP-dependent (Knoch et al., 2006). The activated and cytosolic PTB is then able to bind and stabilize mRNAs that code for secretory granule proteins with putative PTB binding sites in the 3′UTR. Furthermore, knockdown of PTB by RNAi results in decreased expression of target mRNAs and secretory granules (Knoch et al., 2004). Taken together, glucose/GPL-1 dependent stimulation of β cells results in cytoplasmic translocation of PTB where it can act to stabilize insulin mRNA and components of the insulin secretory granule. In light of these findings, it is evident that PTB expression and activation represents a critical component in regulating GSIS.

Neuro-Oncological Ventral Antigens (NOVA1, NOVA2)

The Neuro-oncological ventral antigens (NOVA) are a family of two RBPs (NOVA1 and NOVA2) that account for approximately 700 alternative splicing events in neurons (Ule et al., 2005, 2006; Licatalosi et al., 2008; Zhang et al., 2010) and have been implicated in regulating alternative polyadenylation (Licatalosi et al., 2008). Both NOVA proteins bind to YCAY consensus sequences in target mRNAs through three hnRNPK-homology (KH)-type RNA binding motifs (Buckanovich and Darnell, 1997; Yang et al., 1998; Jensen et al., 2000). The positions of NOVA binding relative to the alternative splice site determines exon inclusion versus exclusion; exon inclusion is correlated with NOVA downstream binding (Ule et al., 2006; Zhang et al., 2010). Both *NOVA1 and NOVA2* are expressed in the pancreatic β cell (Villate et al., 2014; Juan-Mateu et al., 2017) and *in vitro* studies suggest they contribute to alternative splicing (Eizirik et al., 2012; Villate et al., 2014; Juan-Mateu et al., 2017). Knockdown of *Nova1* by RNAi in FACS-purified rat β cells resulted in changes in alternative splicing of 4961 isoforms and impaired GSIS (Villate et al., 2014). In INS-1E cells and MIN6 cells, knockdown of *Nova1* disrupts insulin secretion through changes in alternative splicing of key exocytosis factors *PLCβ1* and *Snap25,* and decreases in voltage-dependent Ca^{2+} current (Villate et al., 2014). NOVA1 has also been shown to regulate alternative splicing of the insulin receptor (INSR), suggesting that NOVA1 is required to promote exon 11 inclusion and expression of the INSR-B form of the receptor (Villate et al., 2014). Additionally, NOVA1 has been implicated in T1D and cytokine-induced apoptosis (Eizirik et al., 2012; Villate et al., 2014). In both cytokine-treated β cells and *Nova1* knockdown β cells, apoptosis increases through the upregulation of pro-apoptotic protein, Bim (Barthson et al., 2011; Villate et al., 2014). Similarly, *Nova1* is decreased in β cells treated with cytokines (Villate et al., 2014). *Bim* is regulated by FOXO3a, however phosphorylation of FOXO3a inhibits it's function (Sunters et al., 2003; Zhang et al., 2011). In *Nova1* knockdown β cells, *FoxO3a* expression is increased but phosphorylation is decreased, allowing for the subsequent upregulation of *Bim*. Similarly, NOVA2 has been shown to regulate β cell survival. *NOVA2/Nova2* knockdown in INS-1E, EndoC-βH1, and sorted rat β cells resulted in increased apoptosis (Juan-Mateu et al., 2017). Together these studies have identified several roles for NOVA RBPs in the function and survival of pancreatic β cells.

RNA Binding FOX Homologue (RBFOX1, RBFOX2, RBFOX3)

The RBFOX family of RBPs contains three highly conserved members – RBFOX1, RBFOX2, and RBFOX3. RBFOX RBPs all contain an RRM that recognizes the specific (U)GCAUG sequence in target mRNAs to promote alterative splicing and other RNA metabolic functions (Jin et al., 2003; Ponthier et al., 2006). *Rbfox2* is nearly ubiquitously expressed across cell types and throughout development, whereas *Rbfox1* and *Rbfox3* are considerably more cell type specific or only transiently expressed. The functions of the RBFOX proteins have been studied primarily in neurons and muscle tissue, and their activity is often required for development and maturation of these cell types (Gehman et al., 2012; Wei et al., 2015; Jacko et al., 2018). During pancreas development, scRNA-Seq reveals that *Rbfox2* is detectable throughout the embryonic (E15.5 and E18.5) mouse pancreas and hESC-derived pancreatic endocrine cells (Krentz et al., 2018). This dataset also shows that *Rbfox3* appears to be transiently expressed specifically within the $Neurog3^{+}$ endocrine progenitor population at E15.5 (Krentz et al., 2018). *Rbfox1* is not detectable in embryonic E15.5 or E18.5 mouse pancreas or within the hESC-derived endocrine cells (Krentz et al., 2018). Similarly in the adult pancreas, RNA-Seq on intact islets revealed high expression of *Rbfox2*; whereas *Rbfox1* and *Rbfox3* were barely detectable. Further analysis of the individual sorted mouse endocrine cells determined that *Rbfox2* is expressed in α, β, and δ cells; with its highest expression in the β cell population (DiGruccio et al., 2016). Within this dataset, Rbfox1

is undetectable in any of the endocrine populations, whereas Rbfox3 expression can be found in δ cells. Consistently, scRNA-Seq in adult islets show that the majority of endocrine cells express *Rbfox2,* whereas *Rbfox3* is predominantly restricted to δ cells and Rbfox1 is undetectable (DiGruccio et al., 2016; The Tabula Muris Consortium et al., 2018). Consistent with the mouse studies, bulk sequencing of human islets and other human tissues identified expression of both *RBFOX2* and *RBFOX3*, but not *RBFOX1* in whole islets (Juan-Mateu et al., 2017). Paradoxically, this group proceeded to knockdown *Rbfox2* and *Rbfox1* in rat INS1-E cells and suggested that both proteins regulate insulin content and insulin secretion through the alternative splicing of genes involved in actin regulation (Juan-Mateu et al., 2017). It is possible that there will be redundant functions of the highly conserved Rbfox family of RBPs in endocrine cells; however, it remains to be determined how their coordinated, transient and/or compensatory expression impacts endocrine cell development and function in disease states.

Serine/Arginine (SR)-Rich Proteins (SRSF1, SRSF3, SRSF6)

The serine/arginine (SR)-rich proteins are a large family of RBPs characterized by their serine/arginine rich domain and an RRM (Shepard and Hertel, 2009). SR proteins are involved in several aspects of RNA metabolism including both constitutive and alternative splicing events (Zhou and Fu, 2013). SR proteins can interact with core components of the spliceosome (U1 and U2 snRNPs) to promote or inhibit splice site usage. Additionally, SR proteins function in regulating mRNA transport and translation (Zhong et al., 2009). While the function of SR proteins in other cell types and systems have been reviewed extensively (Shepard and Hertel, 2009; Zhong et al., 2009; Zhou and Fu, 2013), relatively little is known about their role in β cells.

Nearly all members of the SR protein family are expressed in the mouse pancreas (The Tabula Muris Consortium et al., 2018) and several of these SR proteins become dysregulated in diabetes (Jeffery et al., 2019). In pancreatic endocrine cells, several SRSF proteins interact with the long non-coding RNA *Paupar* to influence the alternative splicing of *Pax6* to confer differential genomic binding of the PAX6 transcription factor (Kiselev et al., 2012; Singer et al., 2019). β cells express a higher ratio of the shorter PAX6 isoform lacking the 5a exon while α cells predominantly express the longer PAX6 5a isoform (Singer et al., 2019). Together, the differential expression in healthy vs. diabetic endocrine cells and function of SR proteins in mediating transcription factor function make SR proteins an interesting candidate for evaluating the role of RBPs in the onset of diabetes. Of note, the only functional studies of this family of RBPs have been on SRSF3 and many of the SR proteins themselves undergo cell type specific and stress induced alternative splicing, leaving extensive opportunity to evaluate their β cell specific functions in healthy and diabetic states.

Changes in RNA Regulation During Diabetes

Until recently, attempts to identify the genetic causes of T1D and T2D have predominantly relied on GWAS to identify single nucleotide polymorphisms (SNPs) and associated gene expression changes that could contribute to disease. Although these approaches have successfully identified a number of causative candidate alleles, they overlook altered splicing events that may affect gene function rather than expression levels. Furthermore, it is now apparent that differences in co- and posttranscriptional processing such as alternative splicing and N6-methyladenosine (m6A) modifications, can more effectively differentiate between T2D β cells than transcriptomics alone (De Jesus et al., 2019).

Alternative Splicing

Messenger RNA splicing occurs co-transcriptionally to remove introns from the pre-mRNA. This process is carried out by the spliceosome and is coordinated by a series of RBPs. In addition to removing introns, splicing machinery can also vary mRNAs through alternative exon and splice site usage, referred to as alternative splicing. Over 90% of human genes undergo alternative splicing, which more than quadruples the number of potential gene products (Fairbrother et al., 2002; Johnson et al., 2003). Recent work comparing transcriptomes of T2D diabetic and healthy donors identified dysregulation of 26% of alternative splicing events (Jeffery et al., 2019). The highest proportion of alternatively spliced genes in this study function in gene regulation. For example, the authors observed dysregulation of the alternative splicing regulators such as SRSF RBPs, which could each regulate hundreds of splicing events within the β cell. Stress induction of the EndoC-βH1 β cell line supported findings from human diabetic islets, showing a decrease in splicing regulators. Moreover, removal of the stress restored splicing factor expression and changes in transcriptome wide splicing events. Additionally, in a model of T1D, cytokine exposure of FAC sorted rat β cells resulted in differential expression of more than 20 RBPs involved in alternative splicing and changes in alternative splicing of cytokine regulated genes (Ortis et al., 2010). These groups all suggest that changes in the splicing landscape as well as changes in β cell differentiation markers, may be a mechanism of stress response to avoid apoptosis during the onset of diabetes, making the study of alternative splicing regulation in the β cell critical for not only understanding the pathogenesis of the disease but also in designing innovative treatment plans.

The onset of T2D and accelerated dysfunction of β cells has also been attributed to many environmental factors, including the disruption of circadian sleep/wake cycles (Gale et al., 2011). Although the disruption of circadian sleep/wake cycles has traditionally been associated with mRNA oscillations, a recent study implicates the RBP Thyroid Hormone Receptor-Associated Protein3 (THRAP3) as a regulator of alternative-splicing. This study demonstrated that THRAP3 regulated circadian clock-dependent alternative splicing by binding to and regulating alternative splicing of key exocytosis factors (Marcheva et al., 2020).

In addition to transcriptome wide changes in alternative splicing, several groups have explored the alternative splicing of specific genes involved in β cell development, function, and survival. Of note, several Maturity Diabetes of the Youth (MODY) and T2D associated genes such as *HNF-1α, GCK,* and

TCF7L2 have splicing variants (Prokunina-Olsson et al., 2009). While *TCF7L2* isoforms are not significantly altered in T2D (Prokunina-Olsson et al., 2009), both *HNF-1α* and *GCK* diabetes associated alleles result in alternative splicing variation (Cappelli et al., 2009; Lorini and D'Annunzio, 2009), and isoforms of HNF-1α are associated with differential efficiency in insulin gene regulation (Harries et al., 2006; Cappelli et al., 2009). T2D associated alterations in alternative splicing of *HNF-1α* and several other β cell genes are also reviewed by Dlamini et al. (2017). Based on recent findings in large transcriptomic analyses, this field is likely to grow dramatically.

m6A RNA Methylation

N6-methyladenosine (m6A) methylation is one of the most prevalent post-transcriptional RNA modifications and is regulated by a set of RNA-binding proteins – writers, readers, and erasers (**Figure 1**; Zhang et al., 2019). These modifications are introduced by a group of specialized methyltransferases ("writers") including METTL3 and METTL14. The m6A modifications can confer differential stability, changes in alternative splicing, subcellular localization, and translation efficiency (Zhang et al., 2019). The m6A modifications are often bound by a group of RBPs called readers to perform these differential functions. Finally, a third group of RBPs, including FTO (Fat Mass and Obesity-associated gene), are referred to as erasers and can remove m6A marks. A recent review by Zhang et al. (2019) details the current knowledge on mechanism and function of m6A methylation.

With respect to the β cell, a recent publication by De Jesus et al. (2019) describes the differential m6A methylation observed in T2D. RNA-Seq analysis and fluorescent labeling of human T2D islets compared to healthy controls revealed differential expression of key m6A modulators (METTL3, METTL14, ALKBH5, and YTHDF1). This finding was supported by an independent study showing decreased Mettl3/14 expression in diabetic db/db mice and type 2 diabetes patients (Wang et al., 2020). The decreased expression of m6A writers (METTL3 and METTL14) resulted in differential methylation of 6,078 sites in 4,155 genes (FDR < 0.05). The hypomethylation of genes in the T2D islets are associated with cell-cycle progression, insulin secretion, and the insulin/IGF-AKT-PDX1 pathway. This study also replicated T2D phenotypes and the m6A methylome in METTL3 or METTL14 deficient EndoC-βH1 cells and Mettl14 β-cell-specific knockout mice. Another group generated a similar β cell specific knockout of *Mettl14* in mice and observed that these mice display glucose intolerance, decreased GSIS and decreased β cell mass due to β cell death under normal conditions (Liu et al., 2019). These phenotypes are exaggerated in mice fed a high fat diet (Liu et al., 2019). Together these studies indicate a role for METTL14 and m6A modifications in the function and survival of β cells.

In the context of pancreas development, m6A writers (METTL3/14) are critical for β cell expansion and maturation but appear to be dispensable for the differentiation and maturation of other endocrine cell types (Wang et al., 2020). Wang et al. (2020) also showed that in the developing pancreas loss of *Mettl3* or *Mettl14* from endocrine progenitors independently results in hyperglycemia around weaning, but that loss of both methyltransferases results in significant hyperglycemia and hypo-insulinemia by 2-weeks of age. This functional defect is in part due to decreased proliferation and increased cell death, similar to what had been observed in the previously described β cell specific knockout mice. Additionally, using RNA-Seq and m6A Me-RIP-Seq, the authors concluded that *Mettl3/14* directly regulates the β cell maturation factor, MAFA, to promote stability. Other groups have also studied the effects of m6A modifications, particularly in adipogenesis, that could contribute to the pathogenesis of T2D (Gerken et al., 2007; Chu et al., 2008; Ben-Haim et al., 2015; Shen et al., 2015; Wood et al., 2016).

As a counterpoint to the m6A writers METTL3/14, FTO is an m6A eraser. FTO is expressed in a variety of cell and tissue types including endocrine cells (Taneera et al., 2015; DiGruccio et al., 2016; The Tabula Muris Consortium et al., 2018). Whole body knockouts and nervous system specific knockouts of *Fto* in mice result in postnatal growth deficiencies (Gao et al., 2010), however, its specific function in β cells is debated. In T2D human islets, FTO expression is reduced (Kirkpatrick et al., 2010; Taneera et al., 2018) and the FTO gene has decreased DNA methylation (Dayeh et al., 2014). Several groups have investigated the functional role of FTO in pancreatic islets using different experimental models. Overexpression of FTO in rat INS-1 cells appeared to affect first wave insulin secretion (Russell and Morgan, 2011), whereas overexpression in mouse MIN6 cells resulted in the inhibition of GSIS without changes in insulin gene expression (Fan et al., 2015). Given the discrepant results of these studies, in addition to the caveats associated with overexpression studies, perhaps the more relevant functional assessment was the use of siRNA knockdown to deplete FTO in an engineered human insulin secretion reporter rat β cell line (GRINCH) (Taneera et al., 2018). In these experiments, depletion of FTO resulted in decreased insulin mRNA expression and insulin secretion (Taneera et al., 2018).

While these emerging studies are beginning to highlight the relevance of m6A RNA methylation in β cell function, and the potential contribution of alterations in this RNA modification to the onset of diabetes, the underlying mechanism and direct targets of m6A methylation and demethylation that contribute to the observed functional changes have yet to be determined. Future studies of the islet cell-specific changes in RNA modifications that result from defects in the m6A pathway will provide critical new information about the regulation of islet function in normal and disease conditions.

DISCUSSION

Traditionally, endocrine cells have been molecularly defined by their cell-specific transcriptomes. Furthermore, validation of human diabetes GWAS studies have relied primarily on gene expression changes associated with disease. More recently, however, large scale high-throughput sequencing efforts have revealed the previously unappreciated importance of co- and post-transcriptional RNA regulation in the specification and function of differentiated cells. These high-resolution sequencing technologies have not only identified changes in expression

levels, they have unveiled numerous RNA modifications and alternative splicing events within each of the islet endocrine cell populations and in individual β cells. This discovery has prompted investigation into the many RBPs that are expressed in the pancreatic islet and those that become dysregulated in β cells undergoing stress conditions that mimic diabetes (**Table 1**). Each of these RBPs can have hundreds of targets and affect multiple pathways within a cell in both physiological and pathophysiological conditions (Keene, 2007; Hogan et al., 2008; Lukong et al., 2008; Blanchette et al., 2009; Li et al., 2014), making their potential impact on cellular identity and function pervasive. This also implies that there are many more layers of regulation in the β cell, particularly mediated by RBPs, that have yet to be explored. The knowledge gained from understanding regulation of β cell development and function at the level of mRNA modifications could be immensely useful to optimize protocols to generate insulin-secreting β-like cells from human stem cells (Hrvatin et al., 2014), which is currently a promising method of replacing β cell loss in T1D. Furthermore, characterization of dysregulated splicing events could open therapeutic opportunities to correct specific mRNAs using antisense oligonucleotide (ASO) technologies. ASOs are small synthetic nucleotide sequences that can target specific mRNA transcripts to target and eliminate anomalous splice variants (Schoch and Miller, 2017). Treatment with ASOs has become increasingly promising for treating neurodegenerative diseases (Schoch and Miller, 2017) and could be an innovative mechanism to correct aberrant splicing defects occurring in T2D β cells. Overall, the study of RBPs and RNA modifications are primed to be the next frontier of mechanisms that regulate β cell formation, function, and in the development of novel therapeutics.

AUTHOR CONTRIBUTIONS

NM researched the literature and wrote the manuscript. LS researched the literature and edited the manuscript. Both authors contributed to the article and approved the submitted version.

FUNDING

Funding to LS was provided from the NIH R01 DK111405, R01 DK082590, and P30DK116073 (DRC). Support was also provided from the University of Colorado RNA Biosciences Initiative (RBI).

ACKNOWLEDGMENTS

We would like to thank members of the Sussel lab for critical reading of the manuscript and useful discussions.

REFERENCES

Alvelos, M. I., Juan-Mateu, J., Colli, M. L., Turatsinze, J. V., and Eizirik, D. L. (2018). When one becomes many-alternative splicing in beta-cell function and failure. *Diabetes Obes. Metab.* 20(Suppl. 2), 77–87. doi: 10.1111/dom.13388

Auweter, S. D., Oberstrass, F. C., and Allain, F. H. (2007). Solving the structure of PTB in complex with pyrimidine tracts: an NMR study of protein-RNA complexes of weak affinities. *J. Mol. Biol.* 367, 174–186. doi: 10.1016/j.jmb.2006.12.053

Baltrusch, S. (2016). Mitochondrial network regulation and its potential interference with inflammatory signals in pancreatic beta cells. *Diabetologia* 59, 683–687. doi: 10.1007/s00125-016-3891-x

Baralle, F. E., and Giudice, J. (2017). Alternative splicing as a regulator of development and tissue identity. *Nat. Rev. Mol. Cell Biol.* 18, 437–451. doi: 10.1038/nrm.2017.27

Barthson, J., Germano, C. M., Moore, F., Maida, A., Drucker, D. J., Marchetti, P., et al. (2011). Cytokines tumor necrosis factor-alpha and interferon-gamma induce pancreatic beta-cell apoptosis through STAT1-mediated Bim protein activation. *J. Biol. Chem.* 286, 39632–39643. doi: 10.1074/jbc.m111.253591

Ben-Haim, M. S., Moshitch-Moshkovitz, S., and Rechavi, G. (2015). FTO: linking m6A demethylation to adipogenesis. *Cell Res.* 25, 3–4. doi: 10.1038/cr.2014.162

Blanchette, M., Green, R. E., MacArthur, S., Brooks, A. N., Brenner, S. E., Eisen, M. B., et al. (2009). Genome-wide analysis of alternative pre-mRNA splicing and RNA-binding specificities of the *Drosophila* hnRNP A/B family members. *Mol. Cell.* 33, 438–449. doi: 10.1016/j.molcel.2009.01.022

Brereton, M. F., Iberl, M., Shimomura, K., Zhang, Q., Adriaenssens, A. E., Proks, P., et al. (2014). Reversible changes in pancreatic islet structure and function produced by elevated blood glucose. *Nat Commun.* 5:4639.

Buckanovich, R. J., and Darnell, R. B. (1997). The neuronal RNA binding protein Nova-1 recognizes specific RNA targets in vitro and in vivo. *Mol. Cell. Biol.* 17, 3194–3201. doi: 10.1128/mcb.17.6.3194

Cappelli, A., Tumini, S., Consoli, A., Carinci, S., Piersanti, C., Ruggiero, G., et al. (2009). Novel mutations in GCK and HNF1A genes in Italian families with MODY phenotype. *Diabetes Res. Clin. Pract.* 83, e72–e74. doi: 10.1016/j.diabres.2008.12.007

Castelo-Branco, P., Furger, A., Wollerton, M., Smith, C., Moreira, A., and Proudfoot, N. (2004). Polypyrimidine tract binding protein modulates efficiency of polyadenylation. *Mol. Cell. Biol.* 24, 4174–4183. doi: 10.1128/mcb.24.10.4174-4183.2004

Christiansen, J., Kolte, A. M., Hansen, T., and Nielsen, F. C. (2009). IGF2 mRNA-binding protein 2: biological function and putative role in type 2 diabetes. *J. Mol. Endocrinol.* 43, 187–195. doi: 10.1677/jme-09-0016

Chu, X., Erdman, R., Susek, M., Gerst, H., Derr, K., Al-Agha, M., et al. (2008). Association of morbid obesity with FTO and INSIG2 allelic variants. *Arch. Surg.* 143, 235–240;discussion 241.

Cnop, M., Abdulkarim, B., Bottu, G., Cunha, D. A., Igoillo-Esteve, M., Masini, M., et al. (2014). RNA sequencing identifies dysregulation of the human pancreatic islet transcriptome by the saturated fatty acid palmitate. *Diabetes Metab. Res. Rev.* 63, 1978–1993. doi: 10.2337/db13-1383

Dayeh, T., Volkov, P., Salo, S., Hall, E., Nilsson, E., Olsson, A. H., et al. (2014). Genome-wide DNA methylation analysis of human pancreatic islets from type 2 diabetic and non-diabetic donors identifies candidate genes that influence insulin secretion. *PLoS Genet.* 10:e1004160. doi: 10.1371/journal.pgen.1004160

De Jesus, D. F., Zhang, Z., Kahraman, S., Brown, N. K., Chen, M., Hu, J., et al. (2019). m(6)A mRNA methylation regulates human beta-cell biology in physiological states and in type 2 diabetes. *Nat. Metab.* 1, 765–774. doi: 10.1038/s42255-019-0089-9

DiGruccio, M. R., Mawla, A. M., Donaldson, C. J., Noguchi, G. M., Vaughan, J., Cowing-Zitron, C., et al. (2016). Comprehensive alpha, beta and delta cell transcriptomes reveal that ghrelin selectively activates delta cells and promotes somatostatin release from pancreatic islets. *Mol. Metab.* 5, 449–458. doi: 10.1016/j.molmet.2016.04.007

Dlamini, Z., Mokoena, F., and Hull, R. (2017). Abnormalities in alternative splicing in diabetes: therapeutic targets. *J. Mol. Endocrinol.* 59, R93–R107.

Eizirik, D. L., Sammeth, M., Bouckenooghe, T., Bottu, G., Sisino, G., Igoillo-Esteve, M., et al. (2012). The human pancreatic islet transcriptome: expression

of candidate genes for type 1 diabetes and the impact of pro-inflammatory cytokines. *PLoS Genet.* 8:e1002552. doi: 10.1371/journal.pgen.1002552

Eliasson, L., and Esguerra, J. L. S. (2020). MicroRNA networks in pancreatic islet cells: normal function and type 2 diabetes. *Diabetes Metab. Res. Rev.* 69, 804–812. doi: 10.2337/dbi19-0016

Fairbrother, W. G., Yeh, R., Sharp, P. A., and Burge, C. B. (2002). Predictive Identification of Exonic Splicing Enhancers in Human Genes. *Science* 297, 1007–1013. doi: 10.1126/science.1073774

Fan, H. Q., He, W., Xu, K. F., Wang, Z. X., Xu, X. Y., and Chen, H. (2015). FTO inhibits insulin secretion and promotes NF-kappaB activation through positively regulating ROS production in pancreatic beta cells. *PLoS One* 10:e0127705. doi: 10.1371/journal.pone.0127705

Fred, R. G., Bang-Berthelsen, C. H., Mandrup-Poulsen, T., Grunnet, L. G., and Welsh, N. (2010). High glucose suppresses human islet insulin biosynthesis by inducing miR-133a leading to decreased polypyrimidine tract binding protein-expression. *PLoS One* 5:e10843. doi: 10.1371/journal.pone.0010843

Fred, R. G., Mehrabi, S., Adams, C. M., and Welsh, N. (2016). PTB and TIAR binding to insulin mRNA 3′- and 5′UTRs; implications for insulin biosynthesis and messenger stability. *Heliyon* 2:e00159. doi: 10.1016/j.heliyon.2016.e00159

Fred, R. G., Sandberg, M., Pelletier, J., and Welsh, N. (2011). The human insulin mRNA is partly translated via a cap- and eIF4A-independent mechanism. *Biochem. Biophys. Res. Commun.* 412, 693–698. doi: 10.1016/j.bbrc.2011.08.030

Fujimoto, K., Hanson, P. T., Tran, H., Ford, E. L., Han, Z., Johnson, J. D., et al. (2009). Autophagy regulates pancreatic beta cell death in response to Pdx1 deficiency and nutrient deprivation. *J. Biol. Chem.* 284, 27664–27673. doi: 10.1074/jbc.m109.041616

Gale, J. E., Cox, H. I., Qian, J., Block, G. D., Colwell, C. S., and Matveyenko, A. V. (2011). Disruption of circadian rhythms accelerates development of diabetes through pancreatic beta-cell loss and dysfunction. *J. Biol. Rhythms* 26, 423–433. doi: 10.1177/0748730411416341

Gao, X., Shin, Y. H., Li, M., Wang, F., Tong, Q., and Zhang, P. (2010). The fat mass and obesity associated gene FTO functions in the brain to regulate postnatal growth in mice. *PLoS One* 5:e14005. doi: 10.1371/journal.pone.0014005

Garcia-Blanco, M. A., Jamison, S. F., and Sharp, P. A. (1989). Identification and purification of a 62,000-dalton protein that binds specifically to the polypyrimidine tract of introns. *Genes Dev.* 3, 1874–1886. doi: 10.1101/gad.3.12a.1874

Gehman, L. T., Meera, P., Stoilov, P., Shiue, L., O'Brien, J. E., Meisler, M. H., et al. (2012). The splicing regulator Rbfox2 is required for both cerebellar development and mature motor function. *Genes Dev.* 26, 445–460. doi: 10.1101/gad.182477.111

Gerken, T., Girard, C. A., Tung, Y. C., Webby, C. J., Saudek, V., Hewitson, K. S., et al. (2007). The obesity-associated FTO gene encodes a 2-oxoglutarate-dependent nucleic acid demethylase. *Science* 318, 1469–1472. doi: 10.1126/science.1151710

Gerstberger, S., Hafner, M., and Tuschl, T. (2014). A census of human RNA-binding proteins. *Nat. Rev. Genet.* 15, 829–845. doi: 10.1038/nrg3813

Gold, G., Gishizky, M. L., and Grodsky, G. M. (1982). Evidence that glucose "marks" beta cells resulting in preferential release of newly synthesized insulin. *Science* 218, 56–58. doi: 10.1126/science.6181562

Good, A. L., Haemmerle, M. W., Oguh, A. U., Doliba, N. M., and Stoffers, D. A. (2019). Metabolic stress activates an ERK/hnRNPK/DDX3X pathway in pancreatic beta cells. *Mol. Metab.* 26, 45–56. doi: 10.1016/j.molmet.2019.05.009

Good, A. L., and Stoffers, D. A. (2020). Stress-induced translational regulation mediated by RNA binding proteins: key links to beta-cell failure in diabetes. *Diabetes Metab. Res. Rev.* 69, 499–507. doi: 10.2337/dbi18-0068

Halban, P. A. (1982). Differential rates of release of newly synthesized and of stored insulin from pancreatic islets. *Endocrinology* 110, 1183–1188. doi: 10.1210/endo-110-4-1183

Harries, L. W., Ellard, S., Stride, A., Morgan, N. G., and Hattersley, A. T. (2006). Isomers of the TCF1 gene encoding hepatocyte nuclear factor-1 alpha show differential expression in the pancreas and define the relationship between mutation position and clinical phenotype in monogenic diabetes. *Hum. Mol. Genet.* 15, 2216–2224. doi: 10.1093/hmg/ddl147

Hentze, M. W., Castello, A., Schwarzl, T., and Preiss, T. (2018). A brave new world of RNA-binding proteins. *Nat. Rev. Mol. Cell Biol.* 19, 327–341. doi: 10.1038/nrm.2017.130

Hinman, M. N., and Lou, H. (2008). Diverse molecular functions of Hu proteins. *Cell Mol. Life. Sci.* 65, 3168–3181. doi: 10.1007/s00018-008-8252-6

Hogan, D. J., Riordan, D. P., Gerber, A. P., Herschlag, D., and Brown, P. O. (2008). Diverse RNA-binding proteins interact with functionally related sets of RNAs, suggesting an extensive regulatory system. *PLoS Biol.* 6:e255. doi: 10.1371/journal.pbio.0060255

Hong, Y., Tak, H., Kim, C., Kang, H., Ji, E., Ahn, S., et al. (2020). RNA binding protein HuD contributes to beta-cell dysfunction by impairing mitochondria dynamics. *Cell Death Differ.* 27, 1633–1643. doi: 10.1038/s41418-019-0447-x

Hrvatin, S., O'Donnell, C. W., Deng, F., Millman, J. R., Pagliuca, F. W., DiIorio, P., et al. (2014). Differentiated human stem cells resemble fetal, not adult, beta cells. *Proc. Natl. Acad. Sci. U.S.A.* 111, 3038–3043. doi: 10.1073/pnas.1400709111

Jacko, M., Weyn-Vanhentenryck, S. M., Smerdon, J. W., Yan, R., Feng, H., Williams, D. J., et al. (2018). Rbfox splicing factors promote neuronal maturation and axon initial segment assembly. *Neuron* 97, 853–868.e6. doi: 10.1016/j.neuron.2018.01.020

Jang, S. K., and Wimmer, E. (1990). Cap-independent translation of encephalomyocarditis virus RNA: structural elements of the internal ribosomal entry site and involvement of a cellular 57-kD RNA-binding protein. *Genes Dev.* 4, 1560–1572. doi: 10.1101/gad.4.9.1560

Jeffery, N., Richardson, S., Chambers, D., Morgan, N. G., and Harries, L. W. (2019). Cellular stressors may alter islet hormone cell proportions by moderation of alternative splicing patterns. *Hum. Mol. Genet.* 28, 2763–2774. doi: 10.1093/hmg/ddz094

Jensen, K. B., Dredge, B. K., Stefani, G., Zhong, R., Buckanovich, R. J., Okano, H. J., et al. (2000). Nova-1 regulates neuron-specific alternative splicing and is essential for neuronal viability. *Neuron* 25, 359–371. doi: 10.1016/s0896-6273(00)80900-9

Jin, Y., Suzuki, H., Maegawa, S., Endo, H., Sugano, S., Hashimoto, K., et al. (2003). A vertebrate RNA-binding protein Fox-1 regulates tissue-specific splicing via the pentanucleotide GCAUG. *EMBO J.* 22, 905–912. doi: 10.1093/emboj/cdg089

Johnson, J. M., Castle, J., Garrett-Engele, P., Kan, Z., Loerch, P. M., Armour, C. D., et al. (2003). Genome-wide survey of human alternative pre-mRNA splicing with exon junction microarrays. *Science* 302, 2141–2144. doi: 10.1126/science.1090100

Juan-Mateu, J., Rech, T. H., Villate, O., Lizarraga-Mollinedo, E., Wendt, A., Turatsinze, J. V., et al. (2017). Neuron-enriched RNA-binding proteins regulate pancreatic beta cell function and survival. *J. Biol. Chem.* 292, 3466–3480. doi: 10.1074/jbc.m116.748335

Kamath, R. V., Leary, D. J., and Huang, S. (2001). Nucleocytoplasmic shuttling of polypyrimidine tract-binding protein is uncoupled from RNA export. *Mol. Biol. Cell* 12, 3808–3820. doi: 10.1091/mbc.12.12.3808

Keene, J. D. (2007). RNA regulons: coordination of post-transcriptional events. *Nat. Rev. Genet.* 8, 533–543. doi: 10.1038/nrg2111

Kim, C., Kim, W., Lee, H., Ji, E., Choe, Y. J., Martindale, J. L., et al. (2014). The RNA-binding protein HuD regulates autophagosome formation in pancreatic beta cells by promoting autophagy-related gene 5 expression. *J. Biol. Chem.* 289, 112–121. doi: 10.1074/jbc.m113.474700

Kirkpatrick, C. L., Marchetti, P., Purrello, F., Piro, S., Bugliani, M., Bosco, D., et al. (2010). Type 2 diabetes susceptibility gene expression in normal or diabetic sorted human alpha and beta cells: correlations with age or BMI of islet donors. *PLoS One* 5:e11053. doi: 10.1371/journal.pone.0011053

Kiselev, Y., Eriksen, T. E., Forsdahl, S., Nguyen, L. H., and Mikkola, I. (2012). 3T3 cell lines stably expressing Pax6 or Pax6(5a)–a new tool used for identification of common and isoform specific target genes. *PLoS One* 7:e31915. doi: 10.1371/journal.pone.0031915

Knoch, K. P., Bergert, H., Borgonovo, B., Saeger, H. D., Altkruger, A., Verkade, P., et al. (2004). Polypyrimidine tract-binding protein promotes insulin secretory granule biogenesis. *Nat. Cell Biol.* 6, 207–214. doi: 10.1038/ncb1099

Knoch, K. P., Meisterfeld, R., Kersting, S., Bergert, H., Altkruger, A., Wegbrod, C., et al. (2006). cAMP-dependent phosphorylation of PTB1 promotes the expression of insulin secretory granule proteins in beta cells. *Cell Metab.* 3, 123–134. doi: 10.1016/j.cmet.2005.12.008

Krentz, N. A. J., Lee, M. Y. Y., Xu, E. E., Sproul, S. L. J., Maslova, A., Sasaki, S., et al. (2018). Single-cell transcriptome profiling of mouse and hESC-derived pancreatic progenitors. *Stem Cell Rep.* 11, 1551–1564. doi: 10.1016/j.stemcr.2018.11.008

Kulkarni, S. D., Muralidharan, B., Panda, A. C., Bakthavachalu, B., Vindu, A., and Seshadri, V. (2011). Glucose-stimulated translation regulation of insulin by the 5′ UTR-binding proteins. *J. Biol. Chem.* 286, 14146–14156. doi: 10.1074/jbc.m110.190553

Lee, E. K., Kim, W., Tominaga, K., Martindale, J. L., Yang, X., Subaran, S. S., et al. (2012). RNA-binding protein HuD controls insulin translation. *Mol. Cell* 45, 826–835. doi: 10.1016/j.molcel.2012.01.016

Li, B., and Yen, T. S. (2002). Characterization of the nuclear export signal of polypyrimidine tract-binding protein. *J. Biol. Chem.* 277, 10306–10314. doi: 10.1074/jbc.m109686200

Li, X., Kazan, H., Lipshitz, H. D., and Morris, Q. D. (2014). Finding the target sites of RNA-binding proteins. *Wiley Interdiscip. Rev. RNA* 5, 111–130. doi: 10.1002/wrna.1201

Li, Z., Zhou, M., Cai, Z., Liu, H., Zhong, W., Hao, Q., et al. (2018). RNA-binding protein DDX1 is responsible for fatty acid-mediated repression of insulin translation. *Nucleic Acids Res.* 46, 12052–12066. doi: 10.1093/nar/gky867

Licatalosi, D. D., and Darnell, R. B. (2010). RNA processing and its regulation: global insights into biological networks. *Nat. Rev. Genet.* 11, 75–87. doi: 10.1038/nrg2673

Licatalosi, D. D., Mele, A., Fak, J. J., Ule, J., Kayikci, M., Chi, S. W., et al. (2008). HITS-CLIP yields genome-wide insights into brain alternative RNA processing. *Nature* 456, 464–469. doi: 10.1038/nature07488

Lin, J. C., Yan, Y. T., Hsieh, W. K., Peng, P. J., Su, C. H., and Tarn, W. Y. (2013). RBM4 promotes pancreas cell differentiation and insulin expression. *Mol. Cell. Biol.* 33, 319–327. doi: 10.1128/mcb.01266-12

Liu, J., Luo, G., Sun, J., Men, L., Ye, H., He, C., et al. (2019). METTL14 is essential for beta-cell survival and insulin secretion. *Biochim Biophys Acta Mol Basis Dis* 1865, 2138–2148. doi: 10.1016/j.bbadis.2019.04.011

Lorini, R., and D'Annunzio, G. (2009). The importance of the environmental factors in the outbreak of diabetes mellitus in the pediatric age. *Minerva Pediatr.* 61, 681–684.

Lou, H., Helfman, D. M., Gagel, R. F., and Berget, S. M. (1999). Polypyrimidine tract-binding protein positively regulates inclusion of an alternative 3′-terminal exon. *Mol. Cell. Biol.* 19, 78–85. doi: 10.1128/mcb.19.1.78

Lukong, K. E., Chang, K. W., Khandjian, E. W., and Richard, S. (2008). RNA-binding proteins in human genetic disease. *Trends Genet.* 24, 416–425. doi: 10.1016/j.tig.2008.05.004

Lunde, B. M., Moore, C., and Varani, G. (2007). RNA-binding proteins: modular design for efficient function. *Nat. Rev. Mol. Cell Biol.* 8, 479–490. doi: 10.1038/nrm2178

Magro, M. G., and Solimena, M. (2013). Regulation of beta-cell function by RNA-binding proteins. *Mol. Metab.* 2, 348–355. doi: 10.1016/j.molmet.2013.09.003

Marcheva, B., Perelis, M., Weidemann, B. J., Taguchi, A., Lin, H., Omura, C., et al. (2020). A role for alternative splicing in circadian control of exocytosis and glucose homeostasis. *Genes Dev.* 34, 1–17. doi: 10.1101/gad.338178.120

Mitchell, S. A., Spriggs, K. A., Coldwell, M. J., Jackson, R. J., and Willis, A. E. (2003). The Apaf-1 internal ribosome entry segment attains the correct structural conformation for function via interactions with PTB and unr. *Mol. Cell.* 11, 757–771. doi: 10.1016/s1097-2765(03)00093-5

Nutter, C. A., and Kuyumcu-Martinez, M. N. (2018). Emerging roles of RNA-binding proteins in diabetes and their therapeutic potential in diabetic complications. *Wiley Interdiscip. Rev. RNA* 9:e1459. doi: 10.1002/wrna.1459

Okano, H. J., and Darnell, R. B. (1997). A hierarchy of Hu RNA binding proteins in developing and adult neurons. *J. Neurosci.* 17, 3024–3037. doi: 10.1523/jneurosci.17-09-03024.1997

Ortis, F., Naamane, N., Flamez, D., Ladriere, L., Moore, F., Cunha, D. A., et al. (2010). Cytokines interleukin-1beta and tumor necrosis factor-alpha regulate different transcriptional and alternative splicing networks in primary beta-cells. *Diabetes Metab. Res. Rev.* 59, 358–374. doi: 10.2337/db09-1159

Perez, I., McAfee, J. G., and Patton, J. G. (1997). Multiple RRMs contribute to RNA binding specificity and affinity for polypyrimidine tract binding protein. *Biochemistry* 36, 11881–11890. doi: 10.1021/bi9711745

Ponthier, J. L., Schluepen, C., Chen, W., Lersch, R. A., Gee, S. L., Hou, V. C., et al. (2006). Fox-2 splicing factor binds to a conserved intron motif to promote inclusion of protein 4.1R alternative exon 16. *J. Biol. Chem.* 281, 12468–12474. doi: 10.1074/jbc.m511556200

Prokunina-Olsson, L., Welch, C., Hansson, O., Adhikari, N., Scott, L. J., Usher, N., et al. (2009). Tissue-specific alternative splicing of TCF7L2. *Hum. Mol. Genet.* 18, 3795–3804.

Puri, S., and Hebrok, M. (2012). Diabetic beta cells: to be or not to be? *Cell* 150, 1103–1104.

Ramos-Rodriguez, M., Raurell-Vila, H., Colli, M. L., Alvelos, M. I., Subirana-Granes, M., Juan-Mateu, J., et al. (2019). The impact of proinflammatory cytokines on the beta-cell regulatory landscape provides insights into the genetics of type 1 diabetes. *Nat. Genet.* 51, 1588–1595. doi: 10.1038/s41588-019-0524-6

Roggli, E., Gattesco, S., Pautz, A., and Regazzi, R. (2012). Involvement of the RNA-binding protein ARE/poly(U)-binding factor 1 (AUF1) in the cytotoxic effects of proinflammatory cytokines on pancreatic beta cells. *Diabetologia* 55, 1699–1708. doi: 10.1007/s00125-011-2399-7

Russell, M. A., and Morgan, N. G. (2011). Conditional expression of the FTO gene product in rat INS-1 cells reveals its rapid turnover and a role in the profile of glucose-induced insulin secretion. *Clin. Sci.* 120, 403–413. doi: 10.1042/cs20100416

Sarwade, R. D., Khalique, A., Kulkarni, S. D., Pandey, P. R., Gaikwad, N., and Seshadri, V. (2020). Translation of insulin granule proteins are regulated by PDI and PABP. *Biochem. Biophys. Res. Commun.* 526, 618–625. doi: 10.1016/j.bbrc.2020.03.106

Sawicka, K., Bushell, M., Spriggs, K. A., and Willis, A. E. (2008). Polypyrimidine-tract-binding protein: a multifunctional RNA-binding protein. *Biochem. Soc. Trans.* 36, 641–647. doi: 10.1042/bst0360641

Schoch, K. M., and Miller, T. M. (2017). Antisense oligonucleotides: translation from mouse models to human neurodegenerative diseases. *Neuron* 94, 1056–1070. doi: 10.1016/j.neuron.2017.04.010

Shen, F., Huang, W., Huang, J. T., Xiong, J., Yang, Y., Wu, K., et al. (2015). Decreased N(6)-methyladenosine in peripheral blood RNA from diabetic patients is associated with FTO expression rather than ALKBH5. *J. Clin. Endocrinol. Metab.* 100, E148–E154.

Shepard, P. J., and Hertel, K. J. (2009). The SR protein family. *Genome Biol.* 10:242. doi: 10.1186/gb-2009-10-10-242

Singer, R. A., Arnes, L., Cui, Y., Wang, J., Gao, Y., Guney, M. A., et al. (2019). The long noncoding RNA paupar modulates PAX6 regulatory activities to promote alpha cell development and function. *Cell Metab.* 30:e1098.

Sunters, A., Fernandez de Mattos, S., Stahl, M., Brosens, J. J., Zoumpoulidou, G., Saunders, C. A., et al. (2003). FoxO3a transcriptional regulation of Bim controls apoptosis in paclitaxel-treated breast cancer cell lines. *J. Biol. Chem.* 278, 49795–49805. doi: 10.1074/jbc.m309523200

Szabat, M., Kalynyak, T. B., Lim, G. E., Chu, K. Y., Yang, Y. H., Asadi, A., et al. (2011). Musashi expression in beta-cells coordinates insulin expression, apoptosis and proliferation in response to endoplasmic reticulum stress in diabetes. *Cell Death Dis.* 2, e232. doi: 10.1038/cddis.2011.119

Taneera, J., Fadista, J., Ahlqvist, E., Atac, D., Ottosson-Laakso, E., Wollheim, C. B., et al. (2015). Identification of novel genes for glucose metabolism based upon expression pattern in human islets and effect on insulin secretion and glycemia. *Hum. Mol. Genet.* 24, 1945–1955. doi: 10.1093/hmg/ddu610

Taneera, J., Prasad, R. B., Dhaiban, S., Mohammed, A. K., Haataja, L., Arvan, P., et al. (2018). Silencing of the FTO gene inhibits insulin secretion: an in vitro study using GRINCH cells. *Mol. Cell. Endocrinol.* 472, 10–17. doi: 10.1016/j.mce.2018.06.003

The Tabula Muris Consortium, Overall coordination, Logistical coordination, Organ collection and processing, Library preparation and sequencing, Computational data analysis et al. (2018). Single-cell transcriptomics of 20 mouse organs creates a Tabula Muris. *Nature* 562, 367–372. doi: 10.1038/s41586-018-0590-4

Tillmar, L., Carlsson, C., and Welsh, N. (2002). Control of insulin mRNA stability in rat pancreatic islets. Regulatory role of a 3′-untranslated region pyrimidine-rich sequence. *J. Biol. Chem.* 277, 1099–1106. doi: 10.1074/jbc.m108340200

Tillmar, L., and Welsh, N. (2002). Hypoxia may increase rat insulin mRNA levels by promoting binding of the polypyrimidine tract-binding protein (PTB) to the pyrimidine-rich insulin mRNA 3′-untranslated region. *Mol. Med.* 8, 263–272. doi: 10.1007/bf03402152

Ule, J., Stefani, G., Mele, A., Ruggiu, M., Wang, X., Taneri, B., et al. (2006). An RNA map predicting Nova-dependent splicing regulation. *Nature* 444, 580–586. doi: 10.1038/nature05304

Ule, J., Ule, A., Spencer, J., Williams, A., Hu, J. S., Cline, M., et al. (2005). Nova regulates brain-specific splicing to shape the synapse. *Nat. Genet.* 37, 844–852. doi: 10.1038/ng1610

van Arensbergen, J., Garcia-Hurtado, J., Moran, I., Maestro, M. A., Xu, X., Van de Casteele, M., et al. (2010). Derepression of polycomb targets during pancreatic organogenesis allows insulin-producing beta-cells to adopt a neural gene activity program. *Genome Res.* 20, 722–732. doi: 10.1101/gr.101709.109

Vanzela, E. C., and Cardozo, A. K. (2012). Is ARE/poly(U)-binding factor 1 (AUF1) a new player in cytokine-mediated beta cell apoptosis? *Diabetologia* 55, 1572–1576. doi: 10.1007/s00125-012-2552-y

Villate, O., Turatsinze, J. V., Mascali, L. G., Grieco, F. A., Nogueira, T. C., Cunha, D. A., et al. (2014). Nova1 is a master regulator of alternative splicing in pancreatic beta cells. *Nucleic Acids Res.* 42, 11818–11830. doi: 10.1093/nar/gku861

Wang, Y., Sun, J., Lin, Z., Zhang, W., Wang, S., Wang, W., et al. (2020). m(6)A mRNA methylation controls functional maturation in neonatal murine beta cells. *Diabetes* 69, 1708–1722. doi: 10.2337/db19-0906

Wei, C., Qiu, J., Zhou, Y., Xue, Y., Hu, J., Ouyang, K., et al. (2015). Repression of the central splicing regulator RBFox2 is functionally linked to pressure overload-induced heart failure. *Cell Rep.* 10, 1521–1533. doi: 10.1016/j.celrep.2015.02.013

Wollerton, M. C., Gooding, C., Robinson, F., Brown, E. C., Jackson, R. J., and Smith, C. W. (2001). Differential alternative splicing activity of isoforms of polypyrimidine tract binding protein (PTB). *RNA* 7, 819–832. doi: 10.1017/s1355838201010214

Wollerton, M. C., Gooding, C., Wagner, E. J., Garcia-Blanco, M. A., and Smith, C. W. (2004). Autoregulation of polypyrimidine tract binding protein by alternative splicing leading to nonsense-mediated decay. *Mol. Cell.* 13, 91–100. doi: 10.1016/s1097-2765(03)00502-1

Wood, A. R., Tyrrell, J., Beaumont, R., Jones, S. E., Tuke, M. A., Ruth, K. S., et al. (2016). Variants in the FTO and CDKAL1 loci have recessive effects on risk of obesity and type 2 diabetes, respectively. *Diabetologia* 59, 1214–1221. doi: 10.1007/s00125-016-3908-5

Yang, Y. Y., Yin, G. L., and Darnell, R. B. (1998). The neuronal RNA-binding protein Nova-2 is implicated as the autoantigen targeted in POMA patients with dementia. *Proc. Natl. Acad. Sci. U.S.A.* 95, 13254–13259. doi: 10.1073/pnas.95.22.13254

Yoo, Y. M. (2013). Melatonin-mediated insulin synthesis during endoplasmic reticulum stress involves HuD expression in rat insulinoma INS-1E cells. *J. Pineal Res.* 55, 207–220. doi: 10.1111/jpi.12064

Zhai, K., Gu, L., Yang, Z., Mao, Y., Jin, M., Chang, Y., et al. (2016). RNA-binding protein CUGBP1 regulates insulin secretion via activation of phosphodiesterase 3B in mice. *Diabetologia* 59, 1959–1967. doi: 10.1007/s00125-016-4005-5

Zhang, C., Frias, M. A., Mele, A., Ruggiu, M., Eom, T., Marney, C. B., et al. (2010). Integrative modeling defines the Nova splicing-regulatory network and its combinatorial controls. *Science* 329, 439–443. doi: 10.1126/science.1191150

Zhang, C., Fu, J., and Zhou, Y. (2019). A review in research progress concerning m6A methylation and immunoregulation. *Front. Immunol.* 10:922. doi: 10.3389/fimmu.2019.00922

Zhang, X., Tang, N., Hadden, T. J., and Rishi, A. K. (2011). Akt, FoxO and regulation of apoptosis. *Biochim. Biophys. Acta* 1813, 1978–1986. doi: 10.1016/j.bbamcr.2011.03.010

Zhong, W., Li, Z., Zhou, M., Xu, T., and Wang, Y. (2018). DDX1 regulates alternative splicing and insulin secretion in pancreatic beta cells. *Biochem. Biophys. Res. Commun.* 500, 751–757. doi: 10.1016/j.bbrc.2018.04.147

Zhong, X. Y., Wang, P., Han, J., Rosenfeld, M. G., and Fu, X. D. (2009). SR proteins in vertical integration of gene expression from transcription to RNA processing to translation. *Mol. Cell.* 35, 1–10. doi: 10.1016/j.molcel.2009.06.016

Zhou, Z., and Fu, X. D. (2013). Regulation of splicing by SR proteins and SR protein-specific kinases. *Chromosoma* 122, 191–207. doi: 10.1007/s00412-013-0407-z

Conflict of Interest: The authors declare that the research was conducted in the absence of any commercial or financial relationships that could be construed as a potential conflict of interest.

frontiers in Endocrinology

CASE REPORT
published: 11 September 2020
doi: 10.3389/fendo.2020.00645

ABCC8-Related Maturity-Onset Diabetes of the Young (MODY12): A Report of a Chinese Family

*Leweihua Lin, Huibiao Quan, Kaining Chen, Daoxiong Chen, Danhong Lin and Tuanyu Fang**

Department of Endocrinology, Hainan General Hospital, Hainan Affiliated Hospital of Hainan Medical University, Haikou, China

Maturity-onset diabetes mellitus of the young (MODY) is a monogenic diabetes characterized by autosomal dominant inheritance. Its atypical clinical features make diagnosis difficult and it can be misdiagnosed as type 1 or type 2 diabetes. Fourteen subtypes of MODY have been diagnosed so far, of which MODY12 is caused by mutation of the *ABCC8* (ATP Binding Cassette Subfamily C Member 8) gene, which is rarely reported in China. This paper reports a Chinese family of MODY12 caused by a rare missense mutation on the *ABCC8* gene, which has not been reported to be associated with MODY in China or in other countries, with the aim of increasing clinicians' awareness and attention to the disease.

Keywords: *ABCC8* gene, missense mutation, MODY, diabetes, metformin

OPEN ACCESS

Edited by:
Luiza Ghila,
University of Bergen, Norway

Reviewed by:
Pei-Chun Chen,
National Cheng Kung University, Taiwan
Tianhua Niu,
Tulane University, United States

****Correspondence:***
Tuanyu Fang
fangtuanyu_2010@163.com

Specialty section:
This article was submitted to Clinical Diabetes, a section of the journal Frontiers in Endocrinology

Received: *01 February 2020*
Accepted: *07 August 2020*
Published: *11 September 2020*

Citation:
Lin L, Quan H, Chen K, Chen D, Lin D and Fang T (2020) ABCC8-Related Maturity-Onset Diabetes of the Young (MODY12): A Report of a Chinese Family. Front. Endocrinol. 11:645. doi: 10.3389/fendo.2020.00645

INTRODUCTION

Monogenic diabetes refers to a specific type of diabetes resulting from monogenic mutation, of which the most common type is maturity-onset diabetes of the young (MODY). MODY is an autosomal dominant hereditary disease leading to dysfunction of the pancreatic β-cells. Since its discovery, mutations have been identified for at least these 14 genes (*HNF4A, GCK, HNF1A, PDX1, HNF1B, NEUROD1, KLF11, CEL, PAX4, INS, BLK, ABCC8* [ATP Binding Cassette Subfamily C Member 8], *KCNJ11, and APPL1*) for MODY (1–3). A very high prevalence of family members carry the mutated gene, and patients in the same family have similar clinical manifestations. About 80% of MODY is previously misdiagnosed as type 1 or type 2 diabetes (4–6) because it is a relatively rare condition and there is low awareness of the clinical phenotype and availability of testing. Its atypical clinical features are the main cause of its misdiagnosis, and the diagnosis relies more on genetic testing, which is expensive for the average wage-earner and is not covered by all medical insurance institutions at present. Correct diagnosis of MODY is essential for optimizing treatment, prognosis, and genetic counseling. At present, related research on MODY is relatively scarce in China. Here, we report a family of MODY12, which is caused by a rare missense mutation.

FAMILY

The 1999 World Health Organization diagnostic criteria were used to diagnose diabetes mellitus (DM) or impaired glucose tolerance (IGT) (7). The family has a family history of three generations of diabetes (**Figure 1**). A total of nine people have been diagnosed with diabetes or impaired glucose

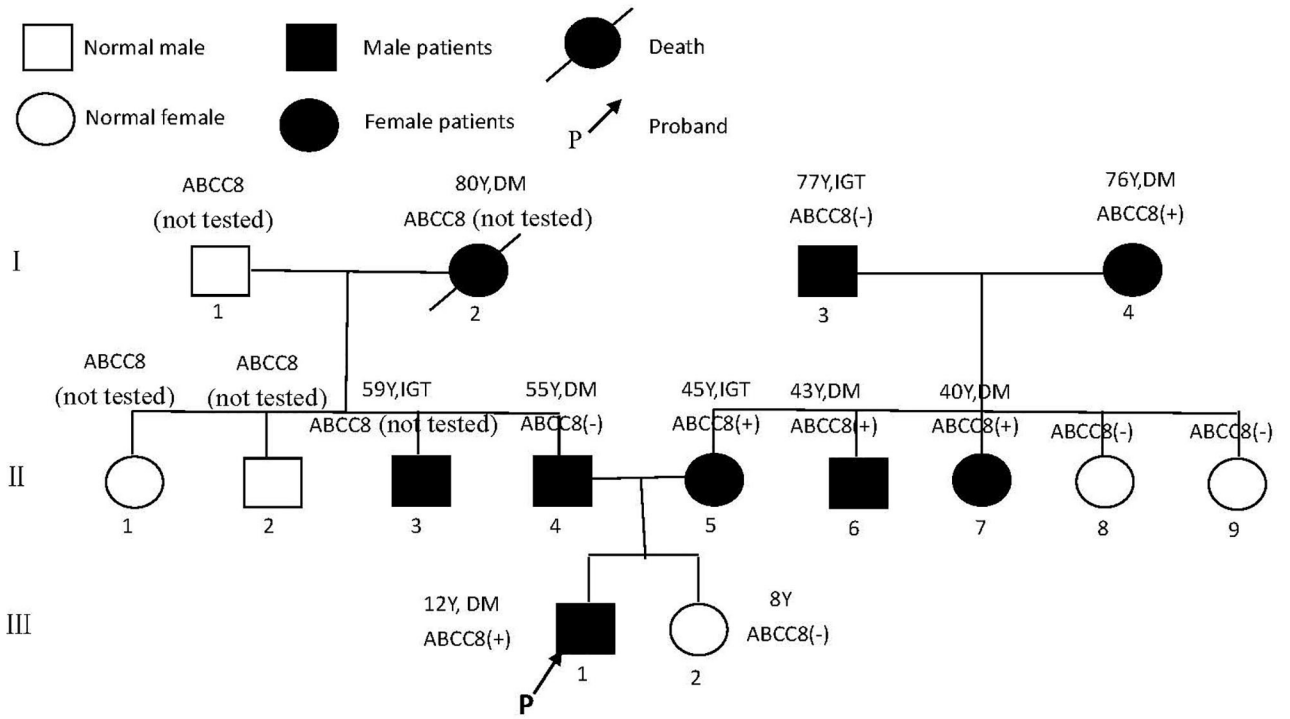

FIGURE 1 | Pedigree of family with diabetes.

tolerance, of whom three had been diagnosed before the age of 45 years, and the earliest diagnosed age is 12 years old.

The Proband (III1)

Male, 12 years old, Han ethnicity. He was admitted to hospital on January 4, 2019, because of polyuria, polydipsia, polyphagia, weight loss for half a year, binocular photophobia, and lacrimation for 2 weeks. There were no obvious causes for the above symptoms, and he had accompanying weight loss of 11 kg for half a year, but had ignored it. Two weeks ago, because of binocular photophobia, tearing, pain, and blurred vision, he visited a local hospital. There, it was found that his fasting blood glucose was 17.1 mmol/L and that he was positive for urine ketone bodies, which was considered type 1 diabetes viral keratitis. He was transferred to our hospital for further treatment.

Personal History

He was the first child of a 25-year-old woman with spontaneous term delivery at week 34 of an uneventful pregnancy; his birth weight was 2,700 g. When he was 3 months old, he received hyperbaric oxygen therapy for 4 months because of motor system developmental delay. At 1 year old, his growth and development were satisfactory as children of the same age. His intelligence is normal.

Family History

His grandmother was hospitalized when she was 80 years old for pancreatic cancer, where it was found that her blood sugar was elevated, but she eventually died from respiratory failure caused by infection.

Physical Examination

Height, 173 cm; weight, 70 kg; body mass index (BMI), 23.39 kg/m^2, regular pulse (86 beats per min), blood pressure (BP), 125/79 mmHg; waist circumference, 83 cm. He had binocular conjunctival hyperemia and edema. He had no buffalo hump, moon face, skin purple striae, or centripetal obesity. Cardiopulmonary examination showed no abnormality. Biochemical analysis revealed normal liver and kidney function, triglyceride (TG) of 1.16 mmol/L, total cholesterol (CHOL) of 5.82 mmol/L, and low-density lipoprotein cholesterol (LDL-C) of 4.04 mmol/L. His glycated hemoglobin A1c (HbA1c) level was 13.0%. C-peptide (0 min) was 0.438 nmol/L (chemiluminescent; reference range, 0.37–1.47 nmol/L), and C-peptide (120 min) was 1.440 nmol/L. He was negative for anti-glutamic acid decarboxylase (GAD) and anti-insulin autoantibodies. Urine microalbumin was 8.0 mg/L (reference range, 0–30 mg/L). Color ultrasound revealed left popliteal artery intimal–medial thickness and atherosclerotic plaque formation at the proximal part of the right subclavian artery. The optic fundi revealed no hemorrhages or exudates, and the fundal vessels were unremarkable. Neuroelectromyography was normal. He was put on combination therapy with basal (glargine) insulin and recombinant human insulin (RI) to control blood sugar; antiviral eyedrops and other treatments improved his condition. After 1 week, his glycemic control had improved remarkably,

with the vast majority of both fasting (4.2–6.1 mmol/L) and postprandial (6.2–10.0 mmol/L) glucose values within the target range. He had no hypoglycemia reaction, and his review for urine ketone bodies was negative. For better compliance, we changed the insulin combination therapy to mixed recombinant human insulin lispro injection (50R) (12 U daily) after discharge. After 4 months, his body weight gradually increased by about 8 kg (height, 176 cm). On May 16, 2019, we reviewed blood sugar (BS, 0–60–120 min) (no hypoglycemic drugs): 6.10–9.60–11.0 mmol/L, and C-peptide (0–60–120 min): 1.530–3.080–3.130 nmol/L. Biochemical analysis revealed growth hormone of 3.490 ng/ml (reference range, 0.077–10.8 ng/ml). Therefore, we attempted to discontinue insulin therapy and started treatment with 1.0 g/days metformin combined with diet and exercise therapy because of overweight. His glucose fluctuations were within the 6–10 mmol/L range. Reviewing his medical history and adolescent onset, his ketosis had a predisposing factor of viral keratitis, his blood sugar was easily controlled, he had good islet β-cell function, and he was negative for anti-GAD and anti-insulin autoantibodies. Based on the above, MODY was highly suspected. Accordingly, we conducted further investigations on his family.

The Proband's Father (II4)

He is 55 years old; Han ethnicity. BMI, 28.03 kg/m^2; waist circumference, 96 cm. BP, 135/82 mmHg. Oral glucose tolerance test (OGTT, 0–120 min): BS, 6.1–11.8 mmol/L; C-peptide, 1.010–4.200 nmol/L. HbA1c, 6.3%. TG, 2.20 mmol/L; CHOL, 5.51 mmol/L; LDL-C, 1.30 mmol/L; liver and kidney function, normal. At present, he is on diet and exercise treatments; his blood sugar is well-controlled.

The Proband's Mother (II5)

She is 45 years old; Han ethnicity. BMI, 23.18 kg/m^2; waist circumference, 78 cm. BP, 115/75 mmHg. OGTT (0–120 min): BS, 4.3–10.6 mmol/L; C-peptide, 1.000–4.150 nmol/L. HbA1c, 5.4%. At present, her diabetes is treated with diet and exercise; her blood sugar is well-controlled.

The Proband's Grandmother (I2)

Deceased; Han ethnicity. When she was 80 years old, she was found to have high blood sugar due to duodenal tubulopapillary adenocarcinoma (late stage). She was not examined further, and was not treated with anti-diabetic therapy. She subsequently died from obstructive jaundice, metabolic encephalopathy, and multiple organ failure.

The Proband's Uncle (II3)

He is 59 years old; Han ethnicity. BMI, 29.75 kg/m^2; waist circumference, 98 cm. BP, 135/82 mmHg. OGTT (0–120 min): BS, 5.2–8.6 mmol/L; C-peptide, 1.020–4.760 nmol/L. HbA1c, 6.2%. At present, his diabetes is treated with diet and exercise; his blood sugar is well-controlled.

The Proband's Uncle (II6)

He is 48 years old; Han ethnicity. He was diagnosed with diabetes 5 years ago, and his diabetes is treated irregularly with glipizide; his blood sugar is generally under control, with no spontaneous ketosis tendency. BMI, 23.18 kg/m^2; waist circumference, 82 cm. BP, 120/78 mmHg. He refused examination for HbA1c and C-peptide.

The Proband's Aunt (II7)

She is 40 years old; Han ethnicity. BMI, 22.60 kg/m^2; waist circumference, 73 cm. BP, 110/70 mmHg. OGTT (0–120 min): BS, 3.6–11.2 mmol/L; C-peptide, 0.571–3.23 nmol/L. HbA1c, 5.5%. At present, her diabetes is treated with diet and exercise; her blood sugar is well-controlled.

The Proband's Grandmother (I4)

She is 76 years old; Han ethnicity. She has a history of sequelae of cerebral infarction and hypertension for 5 years. BMI, 18.26 kg/m^2; waist circumference, 69 cm. BP, 110/80 mmHg. OGTT (0–120 min): BS. 4.7–13.2 mmol/L; C-peptide, 0.59–4.51 nmol/L. HbA1c, 5.4%. At present, her diabetes is treated with diet and exercise to control blood sugar and with amlodipine to control BP, both of which are well-controlled.

The Proband's Grandfather (I3)

He is 77 years old; Han ethnicity. He has had hypertension for 10 years. BMI, 25.96 kg/m^2; waist circumference, 92 cm. BP, 140/80 mmHg. OGTT (0–120 min): BS, 4.4–9.0 mmol/L; C-peptide, 0.488–3.67 nmol/L. HbA1c, 5.4%. At present, his diabetes is treated with diet and exercise; his blood sugar is well-controlled.

Genetic Analysis

The combination of negative autoantibodies for type 1 diabetes with inappropriately low C-peptide levels and a family history of diabetes or abnormal glucose tolerance prompted the molecular investigation for MODY. After obtaining informed consent, a venous blood (5 ml) was collected from the proband (III1) as well as his families and placed in an anti-coagulant tube containing ethylenediaminetetraacetic acid (EDTA).

DNA was extracted from the venous blood collected from the patient as well as from the patient's families using the QIAamp DNA Blood Midi kit (Qiagen, Germany), The quantity/quality of the DNA preparations was assessed using a NanoDrop 1000 spectrophotometer (Thermo Fisher, USA).

Exome enrichment was performed using the IDT xGenExome ResearchPanelv1.0 (Integrated DNA Technologies, Coralville, lowa, USA) and 150 base pair, paired end sequencing was performed using an Illumina HiSeq 4000 platform (San Diego, CA, USA). Mean sequencing depth and nucleotides with >20X sequencing depth were 159x and 99.61%, respectively. The raw sequencing reads were aligned by the We-Health BioMedical Technology (Shanghai, China) using the Burrows–Wheeler Aligner (BWA) and SAMtools. Polymorphic variants that showed >0.5% allele frequency in general populations were filtered out (based on the 1000 genomes database). The SIFT, PolyPhen2, MutationTaster were used to assist in predicting the functional impact of identified missense variants (8, 9).

The next-generation sequencing data were analyzed for mutations in known MODY-related gene (included the genes for *HNF4A, GCK, HNF1A,PDX1, HNF1B, NEUROD1, KLF11, CEL, PAX4, INS, BLK, ABCC8, KCNJ11, and APPL1*). The

sequencing data revealed a heterozygous missense mutation: c.C4544T (p.T1515M), in exon 37 of the *ABCC8* gene of the proband (III1) that was derived from his mother (II5). The amino acid changed from threonine to methionine (**Figure 2**); no mutations were detected for the remaining 13 genes. For the heterozygous mutation c.C4544T (p.T1515M) of the *ABCC8* gene detected in III1, we verified I3, I4, II4, II5, II6, II7, II8, II9, III1, and III2 using Sanger sequencing and found that III1, II5, II6, II7, and I4 all had the same mutation of the *ABCC8* gene.

Oligonucleotides flanking the genomic locations of identified variantswere designed using the Primer3Plus browser. Polymerase chainreactions (PCR) was performed with the following primers: 5′-CACCCCACAGGACTGAACAG-3′ and 5′- ATCTGCTCCACTCACAGCAC-3′. PCR products were sequenced bi-directionally using Big Dye Terminatorchemistry v3.1 and sequenced using an ABI 3730XL sequencer (AppliedBiosystems/Life Technologies, Carlsbad, CA, USA). Sequences were reviewed manually and compared using CodonCode Aligner to reference sequences: *ABCC8*(NM_000352).

This study was approved by the Ethics Committee of Hainan General Hospital. All subjects gave written informed consent in accordance with the Declaration of Helsinki.

DISCUSSION

Monogenic diabetes is a special type of diabetes caused by a single gene mutation or defect; it is genetically and clinically heterogeneous, and includes MODY, neonatal diabetes, congenital hyperinsulinemia, and Wolcott-Rallison syndrome (10). First-degree relatives of a MODY family member carrying genetic mutations for the 2 most common MODY subtypes, i.e., GCK-MODY2 or HNF1α-MODY3, could have 95% risk of developing diabetes (11), and patients in the same family are more likely to have similar clinical presentations. MODY is the most common form of monogenic diabetes (1–3, 12, 13). Previous studies agree that the diagnostic criteria of MODY are: (i) autosomal dominant inheritance, (ii) insulin independence within 2 years of onset, (iii) at least one family member diagnosed with diabetes before the age of 25 years, (iv) combined with islet β-cell dysfunction (14).

The identification of a MODY subtype is crucial for the choice of adequate treatment. However, with the maturing of genetic testing technology in recent years, an increasing number of patients with MODY discovered by genetic testing do not fully meet the above diagnostic criteria, and their clinical manifestations tend to be more diverse. Strict adherence to the above criteria may result in missed diagnosis of a large number of patients with MODY. A study from the UK has shown that a significant number of patients with MODY have a primary diagnosis of diabetes and the MODY diagnosis could be confirmed only by performing molecular genetic testing (15), which may lead to inappropriate treatment such as insulin and/or insulin sensitization treatment (16). Therefore, when the onset of diabetes in young patients is not typical type 1 or type 2 diabetes, it should prompt molecular investigation for MODY.

The *ABCC8* gene is located on chromosome 11p15.1 and encodes the sulfonylurea receptor 1 (SUR1) subunit of the ATP-sensitive potassium (K_{ATP}) channel in the pancreatic β-cell, which is involved in the electrical activity of the plasma membrane, thereby regulating insulin secretion (17). *ABCC8* gene mutations can cause a variety of phenotypes, resulting in overactivity or underactivity of the K_{ATP} channel, resulting in abnormal glucose metabolism. In 2012, Bowman et al. first reported that MODY12 is caused by *ABCC8* gene mutation, and its clinical manifestations are diverse, may be associated with overweight or obesity, and are usually with no significant hypertriglyceridemia and hypercholesterolemia. Further, such families may also have neonatal diabetic patients (18, 19). As sulfonylureas specifically bind to the SUR1 subunit and shut down the channel to release insulin in a non–ATP-dependent manner, this type of MODY is sensitive to sulfonylureas.

Initially, the present case was misclassified with type 1 diabetes because of his young age and ketosis, despite the negative islet β-cell autoantibodies. The possibility of considering the case as MODY was supported by the presence of diabetes within three generations, the stable C-peptide levels, and the obvious signs of overdose on relatively small insulin doses, which led to overweight. The characteristics of the family are: the proband's age is <25 years old with insulin deficiency, and his ketosis had precipitating factors and was easily eliminated. The diabetes-related antibodies (islet cell antibody [ICA], tyrosine phosphatase-like protein antigen-2 antibody [IA2A], glutamic acid decarboxylase antibody [GADA]) were negative, and a follow-up visit after 4 months on the regimen showed that his glycemic control had remarkably improved, with the vast majority of both fasting and postprandial glucose values within the target range and HbA1c of 5.7%; islet β-cell function was significantly improved, and even the overweight and insulin resistance appeared. All three generations in the family have diabetes or impaired glucose tolerance with autosomal dominant inheritance. In summary, our evidence supports the diagnosis of MODY. Genetic testing verified the presence of the *ABCC8* gene mutation (*ABCC8*: NM_000352: exon37: c.C4544T: p.T1515M) in the proband (III1), his mother (II5) and three maternal relatives (II6, II7, I4) with diabetes or impaired glucose tolerance with similar figures and islet β-cell function, but not in the other relatives (II8, II9, III1) who do not have diabetes or impaired glucose tolerance, suggesting that the above mutation and diabetes have obvious co-segregation in the family. In addition, the proband's uncle (II6) had early-onset diabetes and took glipizide for it without spontaneous ketosis. This mutation (*ABCC8*: NM_000352: exon37: c.C4544T: p.T1515M) can lead to the conserved amino acid residues of this site being replaced by different amino acids throughout the evolution process, resulting in congenital hyperinsulinemia (20), and it has been suggested that congenital hyperinsulinemia caused by *ABCC8* gene mutation can develop into MODY (21, 22), but since then, there has been no report of MODY12 caused by the above mutation. The SIFT score, PolyPhen2 score, and Mutation Taster score was 0, 1, and 1, all suggesting that it is damaging to the protein function. Based on the above predictions, the mutation is considered pathogenic. Therefore, we speculate that

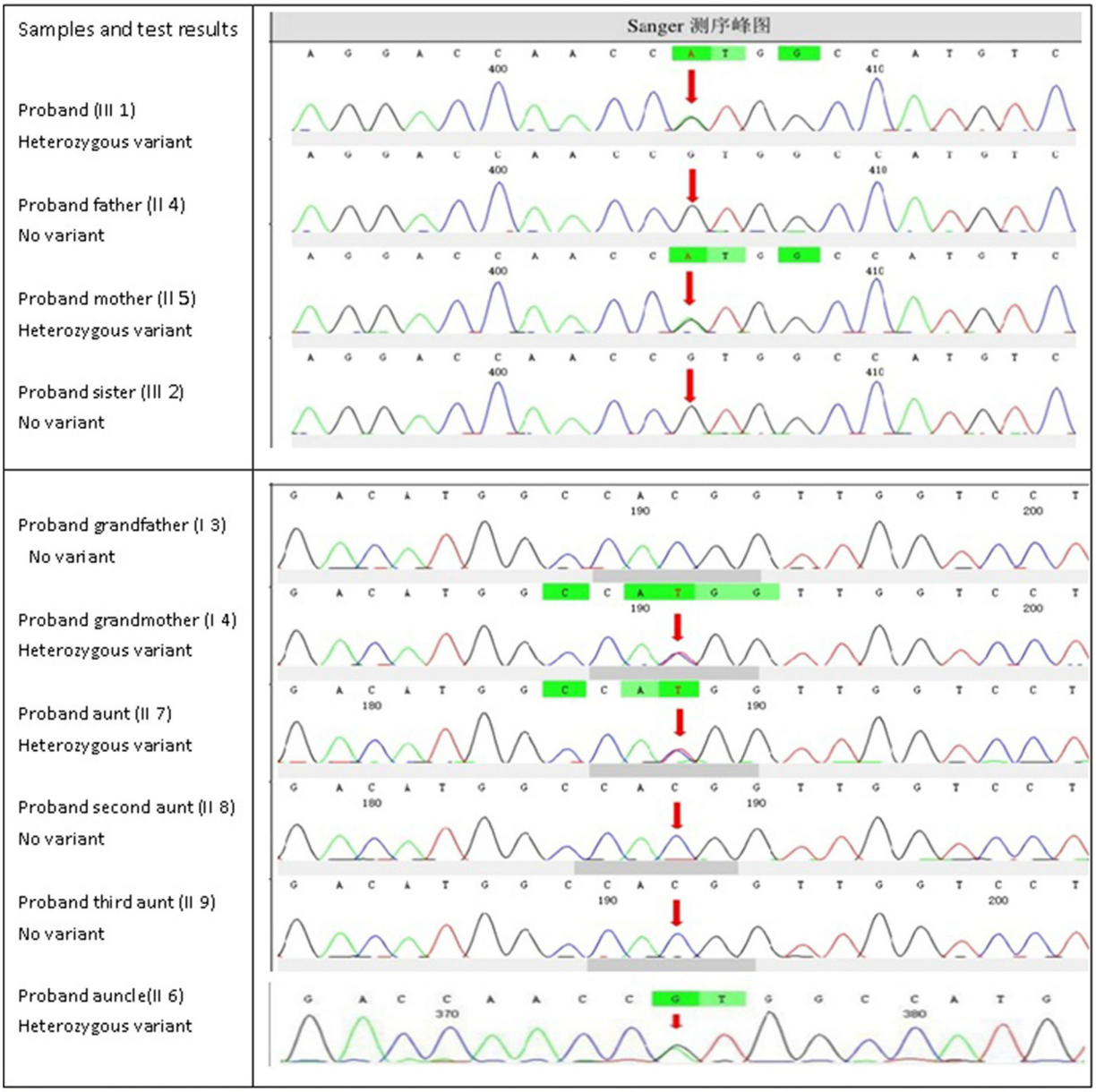

Gene	Locus (hg19)	dbSNP ID	Mutation desription	gnomAD_EAS allele frequency	ACMG variant assessment	合子类型
ABCC8	Chr11: 17415814	Rs769989185	ABCC8:NM_000352:exon37:c.C4544T:P.T1515M	0	Clinical significance unknown	Hetero-zygous

Relative verification results								
II 4	II 5	III 2	I 3	I 4	II 6	II 7	II 8	II 9
Not found	Hetero-zygous	Not found	Not found	Hetero-zygous	Hetero-zygous	Hetero-zygous	Not found	Not found

FIGURE 2 | Gene_sequencing results of proband and his family.

TABLE 1 | Clinical characteristics of family members with disease.

	Gender	Age at diagnosis (years)	BMI (kg/m^2)	Waistline (cm)	0'BS (mmol/L)	120'BS (mmol/L)	0'CP (nmol/L)	HbA1c (%)
III1	M	12	23.39	83	9.0	18.8	0.438	13.0
II5	F	45	23.18	78	4.3	10.6	0.488	5.4
II6	M	43	23.18	82	-	-	-	-
II7	F	40	22.60	73	3.6	11.2	0.571	5.5
I4	F	76	18.26	69	4.7	13.2	0.59	5.4
II4	M	55	28.03	96	6.1	11.8	1.020	6.3
II3	M	59	29.75	98	5.2	8.6	1.010	6.2
I2	F	80	-	-	-	-	-	-
I3	M	77	25.96	92	4.4	9.0	1.000	5.4

BMI, body mass index; BS, blood sugar; CP, C-peptide; HbA1c, glycated hemoglobin A1c. The "-" indicates not available.

this mutation site is the cause of diabetes or impaired glucose tolerance in the proband (III1), his mother (II5), and the three maternal relatives (II6, II7, I4), where the type of diabetes is considered MODY12. I3, II3, and II4 also have diabetes or impaired glucose tolerance, but unlike the proband, they do not have the above mutation, and have characteristics such as central obesity or overweight, insulin resistance, diabetes diagnosed at age >50 years, and whose diagnosis is more prone to type 2 diabetes, which are quite different from the proband (**Table 1**).

The prevalence of MODY subtypes varies widely between countries and ethnic groups. More than 80% of Caucasian patients with MODY are MODY3 or MODY2 (15, 23), but only 7.2–36.7% of Asian patients with MODY are diagnosed as MODY2 or MODY3 (24–27). In China, epidemiological research of MODY is in its infancy, and the distributions of different MODY subtypes are not so clear. Further genes related to MODY are likely to be found, as most patients with MODY have unknown mutations; this group is defined as MODYX. MODYX might be responsible for 80–90% of MODY in China, which is quite different from other populations (25, 26, 28, 29). A lack of awareness of MODY, as well as its similar clinical features to other types of diabetes, means that clinicians cannot often easily distinguish MODY from type 1 or type 2 diabetes without genetic testing, which may lead to misdiagnosis. In the present case, the proband was diagnosed with type 1 diabetes due to early onset (12 years old) with ketosis, the obvious signs of overweight on relatively small doses of insulin, significantly improved islet β-cell function, and even the appearance of insulin resistance. After family investigation and genetic testing, we revised the diagnosis of type 1 diabetes to MODY12, and attempted to discontinue insulin therapy and started treatment with 1.0 g/day metformin combined with diet and exercise therapy. The proband's blood glucose is well-controlled, and he has not gained any more weight. His relatives (II5, II6, II7, I4) with the same *ABCC8* gene mutation as the proband have similar habius, no central obesity, BMI within the 18–24 kg/m^2 range, mildly elevated blood glucose, and similar islet β-cell function. At present, they only require diet and exercise therapy. Therefore, the identification of a MODY subtype is crucial for the choice of adequate treatment. In the present case, verification of the diagnosis by genetic testing enabled the discontinuation of insulin therapy, which had produced obvious adverse effects, such as increased bodyweight.

In conclusion, we report a case of MODY12 caused by a single nucleotide mutation of cytosine to thymine at position 4,544 of the *ABCC8* gene. This mutation has not been reported to be associated with MODY in China or in other countries. It is a rare missense *ABCC8* gene mutation (dbSNP ID: rs769989185, and has not been reported in ClinVar database: https://www.ncbi.nlm.nih.gov/clinvar/), which might be useful for individualized selection of appropriate treatment and for genetic consulting. The described case also highlights the clinical expression of diabetes related to the *ABCC8* gene and underlines the value of genetic testing in young patients presenting with non-autoimmune diabetes.

DATA AVAILABILITY STATEMENT

This article contains previously unpublished data. The name of the repository and accession number(s) are not available.

ETHICS STATEMENT

Written informed consent was obtained from the individuals and minor's legal guardian for the publication of any potentially identifiable images or data included in this article.

AUTHOR CONTRIBUTIONS

LL collected, analyzed, and interpreted the patient data and was the major contributor to the writing of the manuscript. TF made substantial contributions to the data interpretation, manuscript revision, and conducted the work. HQ helped with manuscript revision in English. HQ, KC, DC, and DL assisted with the patient data analysis. All authors are in agreement with the contents of the manuscript.

FUNDING

We are grateful for the support of the Hainan Province family planning science and education health project (no. 19A200034) and the major research and development program of Hainan Province (nos. ZDYF2018130 and ZDYF2019156). Lastly, the authors are deeply grateful to the proband and his family for their support.

REFERENCES

1. Urakami T. Maturity-onset diabetes of the young (MODY): current perspectives on diagnosis and treatment. *Diabetes Metab Syndr Obes.* (2019) 12:1047–56. doi: 10.2147/DMSO.S179793
2. Oliveira SC, Neves JS, Pérez A, Carvalho D. Maturity-onset diabetes of the young: from a molecular basis perspective toward the clinical phenotype and proper management. *Endocrinol Diabetes Nutr.* (2020) 67:137–47. doi: 10.1016/j.endien.2020.03.001
3. Peixoto-Barbosa R, Reis AF, Giuffrida FMA. Update on clinical screening of maturity-onset diabetes of the young (MODY). *Diabetol Metab Syndr.* (2020) 12:50. doi: 10.1186/s13098-020-00557-9
4. Thomas ER, Brackenridge A, Kidd J, Kariyawasam D, Carroll P, Colclough K, et al. Diagnosis of monogenic diabetes: 10-Year experience in a large multi-ethnic diabetes center. *J Diabetes Investig.* (2016) 7:332–7. doi: 10.1111/jdi.12432
5. McDonald TJ, Ellard S. Maturity onset diabetes of the young:identification and diagnosis. *Ann Clin Biochem.* (2013) 50(Pt 5):403–15. doi: 10.1177/0004563213483458
6. Thanabalasingham G, Pal A, Selwood MP. Systematic assessment of etiology in adults with a clinical diagnosis of young-onset type 2 diabetes is a successful strategy for identifying maturity-onset diabetes of the young. *Diabetes Care.* (2012) 35:1206–12. doi: 10.2337/dc11-1243
7. Department of Noncommunicable Disease Surveillance. *Definition, Diagnosis, and Classification of Diabetes Mellitus and Its Complications: Report of a WHO Consultation. Part 1. Diagnosis and Classification of Diabetes Mellitus.* Geneva: World Health Organization (1999).
8. Schwarz JM, Cooper DN, Schuelke M, Seelow D. MutationTaster2: mutation prediction for the deep-se quencing age. *Nat Methods.* (2014) 11:361–2. doi: 10.1038/nmeth.2890
9. Vaser R, Adusumalli S, Leng SN, Sikic M, Ng PC. SIFT missense predictions for genomes. *Nat Protoc.* (2016) 11:1–9. doi: 10.1038/nprot.2015.123
10. Kleinberger JW, Pollin TI. Undiagnosed MODY: time for action. *Curr Diab Rep.* (2015) 15:110. doi: 10.1007/s11892-015-0681-7
11. Heuvel-Borsboom H, de Valk HW, Losekoot M, Westerink J. Maturity onset diabetes of the young: Seek and you will find. *Neth J Med.* (2016) 74:193–200.
12. Glaser B. Insulin mutations in diabetes: the clinical spectrum. *Diabetes.* (2008) 57:799–800. doi: 10.2337/db08-0116
13. Li J, Sun S, Wang X, Li Y, Zhu H, Zhang H, et al. A missense mutation in IRS1 is associated with the development of early-onset type 2 diabetes. *Int J Endocrinol.* (2020) 2020:9569126. doi: 10.1155/2020/9569126
14. Ellard S, Bellanne-Chantelot C, Hattersley AT. Best practice guidelines for the molecular genetic diagnosis of maturity-onset diabetes of the young. *Diabetologia.* (2008) 51:546–53. doi: 10.1007/s00125-008-0942-y
15. Shields BM, Hicks S, Shepherd MH, Colclough K, Hattersley AT, Ellard S. et al. Maturity-onset diabetes of the young(MODY):how many cases are we missing? *Diabetologia.* (2010) 53:2504–8. doi: 10.1007/s00125-010-1799-4
16. Chambers C, Fouts A, Dong F, Colclough K, Wang Z, Batish SD, et al. Characteristics of maturity onset diabetes of the young in a large diabetes center. *Pediatr Diabetes.* (2016) 17:360–7. doi: 10.1111/pedi.12289
17. Patch AM, Flanagan SE, Boustred C, Hattersley AT, Ellard S. Mutations in the ABCC8 gene encoding the SUR1 subunit of the KATP channel cause transient neonatal diabetes, permanent neonatal diabetes or permanent diabetes diagnosed outside the neonatal period. *Diabetes Obes Metab.* (2007) 9 (Suppl. 2):28–39. doi: 10.1111/j.1463-1326.2007.00772.x
18. Bowman P, Flanagan SE, Edghill EL, Damhuis A, ShepherdMH, Paisey R, et al. Heterozygous ABCC8 mutations are a cause of MODY. *Diabetologia.* (2012) 55:123–7. doi: 10.1007/s00125-011-2319-x
19. Hartemann-Heurtier A, Simon A, Bellanne-Chantelot C, Reynaud R, Cavé H, Polak M, et al. Mutations in the ABCC8 gene can cause autoantibody-negative insulin-dependent diabetes. *Diabetes Metab.* (2009) 35:233–35. doi: 10.1016/j.diabet.2009.01.003
20. Banerjee I, Skae M, Flanagan S E, Rigby L, Patel L, Didi M, et al. The contribution of rapid K ATP channel gene mutation analysis to the clinical management of children with congenital hyperinsulinism. *Eur J Endocrinol.* (2011) 164:733–40. doi: 10.1530/EJE-10-1136
21. Abdulhadi-Atwan M, Bushman J, Tornovsky-Babaey S, Perry A, Abu-Libdeh A, Glaser B, et al. Novel de novo mutation in sulfonylurea receptor 1 presenting as hyperinsulinism in infancy followed by oven diabetes in early adolescence. *Diabetes.* (2008) 57:1935–40. doi: 10.2337/db08-0159
22. Kapoor RR, Flanagan SE, James C, Shield J, Ellard S, Hussain K, et al. Hyperinsulinaemic hypoglycaemia. *Arch Dis Child.* (2009) 94:450–7. doi: 10.1136/adc.2008.148171
23. Frayling TM, Evans JC, Bulman MP, Pearson E, Allen L, Owen K, et al. Beta-cell genes and diabetes: molecular and clinical characterization of mutations in transcription factors. *Diabetes.* (2001) 50 (Suppl. 1):S94–S100. doi: 10.2337/diabetes.50.2007.S94
24. Yorifuji T, Fujimaru R, Hosokawa Y, Tamagawa N, Shiozaki M, Aizu K, et al. Comprehensive molecular analysis of Japanese patients with pediatric-onset MODY -type diabetes mellitus. *Pediatr Diabetes.* (2012) 13:26–32.16. doi: 10.1111/j.1399-5448.2011.00827.x
25. Hwang JS, Shin CH, Yang SW, Jung SY, Huh N. Genetic and clinical characteristics of Korean maturity-onset diabetes of the young (MODY) patients. *Diabetes Res Clin Pract.* (2006) 74:75–81. doi: 10.1016/j.diabres.2006.03.002
26. Mohan V, Radha V, Nguyen TT, Stawiski EW, Pahuja KB, Goldstein LD, et al. Comprehensive genomic analysis identifies pathogenic variants in maturity-onset diabetes of the young (mody) patients in south india. *BMC Med Genet.* (2018) 19:22. doi: 10.1186/s12881-018-0528-6
27. Xu JY, Dan QH, Chan V, Wat NMS, Tam S, Tiu SC, et al. Genetic and clinical characteristics of maturity-onset diabetes of the young in Chinese patients. *Eur J Hum Genet.* (2005) 13:422–7. doi: 10.1038/sj.ejhg.5201347
28. Hu C, Jia W. Diabetes in china: epidemiology and genetic risk factors and their clinical utility in personalized medication. *Diabetes.* (2018) 67:3–11. doi: 10.2337/dbi17-0013
29. Zhang M, Zhou JJ, Cui W, Li Y, Yang P, Chen X, et al. Molecular and phenotypic characteristics of matutity-onset diabetes of the young compared with early onset type 2 diabetes in China. *J Diabetes.* (2015) 7:858–63. doi: 10.1111/1753-0407.12253

Conflict of Interest: The authors declare that the research was conducted in the absence of any commercial or financial relationships that could be construed as a potential conflict of interest.

frontiers in Genetics

ORIGINAL RESEARCH
published: 30 September 2020
doi: 10.3389/fgene.2020.567191

Identification of Novel Potential Type 2 Diabetes Genes Mediating β-Cell Loss and Hyperglycemia Using Positional Cloning

*Heja Aga[1,2†], Nicole Hallahan[1,2†], Pascal Gottmann[1,2], Markus Jaehnert[1,2], Sophie Osburg[1,2], Gunnar Schulze[1,2], Anne Kamitz[1,2], Danny Arends[3], Gudrun Brockmann[3], Tanja Schallschmidt[2,4], Sandra Lebek[2,4], Alexandra Chadt[2,4], Hadi Al-Hasani[2,4], Hans-Georg Joost[1,2], Annette Schürmann[1,2,5] and Heike Vogel[1,2,6]**

OPEN ACCESS

Edited by:
Hanne Scholz, University of Oslo, Norway

Reviewed by:
Johanne Dubail, INSERM U1163 Institut Imagine, France
Naveed Wasif, University Hospital Schleswig-Holstein, Germany

***Correspondence:**
Heike Vogel
heikevogel@dife.de

[†]These authors have contributed equally to this work

Specialty section:
This article was submitted to Genetics of Common and Rare Diseases, a section of the journal Frontiers in Genetics

Received: *29 May 2020*
Accepted: *28 August 2020*
Published: *30 September 2020*

Citation:
Aga H, Hallahan N, Gottmann P, Jaehnert M, Osburg S, Schulze G, Kamitz A, Arends D, Brockmann G, Schallschmidt T, Lebek S, Chadt A, Al-Hasani H, Joost H-G, Schürmann A and Vogel H (2020) Identification of Novel Potential Type 2 Diabetes Genes Mediating β-Cell Loss and Hyperglycemia Using Positional Cloning. Front. Genet. 11:567191. doi: 10.3389/fgene.2020.567191

[1]*Department of Experimental Diabetology, German Institute of Human Nutrition Potsdam-Rehbrücke, Potsdam, Germany,* [2]*German Center for Diabetes Research (DZD), München-Neuherberg, Germany,* [3]*Animal Breeding Biology and Molecular Genetics, Albrecht Daniel Thaer-Institute for Agricultural and Horticultural Sciences, Humboldt University of Berlin, Berlin, Germany,* [4]*German Diabetes Center (DDZ), Medical Faculty, Institute for Clinical Biochemistry and Pathobiochemistry, Heinrich Heine University Düsseldorf, Düsseldorf, Germany,* [5]*Institute of Nutritional Science, University of Potsdam, Potsdam, Germany,* [6]*Molecular and Clinical Life Science of Metabolic Diseases, University of Potsdam, Potsdam, Germany*

Type 2 diabetes (T2D) is a complex metabolic disease regulated by an interaction of genetic predisposition and environmental factors. To understand the genetic contribution in the development of diabetes, mice varying in their disease susceptibility were crossed with the obese and diabetes-prone New Zealand obese (NZO) mouse. Subsequent whole-genome sequence scans revealed one major quantitative trait loci (QTL), *Nidd/DBA* on chromosome 4, linked to elevated blood glucose and reduced plasma insulin and low levels of pancreatic insulin. Phenotypical characterization of congenic mice carrying 13.6 Mbp of the critical fragment of DBA mice displayed severe hyperglycemia and impaired glucose clearance at week 10, decreased glucose response in week 13, and loss of β-cells and pancreatic insulin in week 16. To identify the responsible gene variant(s), further congenic mice were generated and phenotyped, which resulted in a fragment of 3.3 Mbp that was sufficient to induce hyperglycemia. By combining transcriptome analysis and haplotype mapping, the number of putative responsible variant(s) was narrowed from initial 284 to 18 genes, including gene models and non-coding RNAs. Consideration of haplotype blocks reduced the number of candidate genes to four (*Kti12*, *Osbpl9*, *Ttc39a*, and *Calr4*) as potential T2D candidates as they display a differential expression in pancreatic islets and/or sequence variation. In conclusion, the integration of comparative analysis of multiple inbred populations such as haplotype mapping, transcriptomics, and sequence data substantially improved the mapping resolution of the diabetes QTL *Nidd/DBA*. Future studies are necessary to understand the exact role of the different candidates in β-cell function and their contribution in maintaining glycemic control.

Keywords: type 2 diabetes, β-cell loss, insulin, positional cloning, transcriptomics, haplotype

INTRODUCTION

Type 2 diabetes (T2D) arises from a complex interplay of multiple genetic and environmental factors that contribute to inadequate insulin secretion, insulin resistance, or both (American Diabetes Association, 2005; Tallapragada et al., 2015). A high percentage of obese people become diabetic, and the majority will at least experience insulin resistance and some degree of β-cell dysfunction (Kahn et al., 2006). Genetic predisposition accounts for differences in T2D susceptibility; so called "protective" gene variants mitigate the progression of the disease either through increased insulin sensitivity or secretion, while susceptibility variants can otherwise predispose an individual to β-cell failure and loss (McCarthy and Zeggini, 2009). Genome-wide association studies (GWAS) typically utilize genetic variants in the human population in the search for novel pathogenic genes. Despite the enormous numbers of human participants recruited for GWAS, diversity in the genome and environmental influences typically confound datasets, particularly for complex traits such as blood glucose or insulin concentrations. Thus, carefully controlled animal studies which allow for the precise manipulation of both environment and genetic variance remain a critical tool in T2D research.

In the past, individual crossbreeding approaches of inbred strains that vary in their predisposition to T2D have been useful for the identification of diabetes risk genes. However, with advances in bioinformatics and increasing capacity to deal with large and complex datasets, particularly involving the availability of genome-wide sequence coverage of common laboratory mouse strains, it has been advantageous to perform multiple crosses in parallel. We have recently carried out a collective diabetes cross (Vogel et al., 2018) using four lean inbred mouse strains (B6, DBA, C3H, and 129P2), each with varying susceptibility to T2D, to be individually crossbred with the obese and diabetes-prone New Zealand obese (NZO) mouse. This strategy addresses the current gaps in the knowledge of the genetic basis for T2D. It confers several advantages, including the ability to use haplotype maps for higher resolution positional cloning (Schwerbel et al., 2020).

The NZO mouse is an inbred strain that portrays a phenotype reminiscent of the human metabolic syndrome, displaying hyperphagia, severe obesity, insulin resistance, dyslipidemia, vascular disease, β-cell failure, and hyperglycemia (Kluge et al., 2012). With respect to islet dysfunction, NZO males display a more severe phenotype than females, and this gender difference is largely attributed to the protective effect of female sex hormones, in particular, estrogen (Vogel et al., 2013; Lubura et al., 2015). DBA mice, in contrast, are lean and normoglycemic. However, when obesity is induced with the introduction of either leptin or leptin receptor knockout mutations (lep-*ob* and lep-*db*, respectively), both male and female DBA mice develop a diabetes-like phenotype due to β-cell failure, indicating the presence of diabetes risk genes in the DBA genome (Leiter, 1981; Chua et al., 2002).

Here, we focus on the diabetes quantitative trait loci (QTL) *Nidd/DBA* on chromosome 4 which we identified as most prominent diabetes QTL in the NZOxDBA cross (Vogel et al., 2018). In the past, several QTL have been identified in the mid-region of mouse chromosome 4 in the proximity of the leptin receptor gene (*Lepr*) relating to hyperglycemia and hypoinsulinemia (Leiter et al., 1998; Plum et al., 2002; Scherneck et al., 2009; Davis et al., 2012; Kluge et al., 2012). In each case, the presence of a single allele from a lean, non-diabetic donor strain was able to produce a strong diabetogenic phenotype on an obese background. More specifically, the mice developed chronic hyperglycemia accompanied by pancreatic β-cell loss. Despite the fact that this trait has appeared repeatedly in crossbreeding experiments over the last 19 years, the responsible variant has yet to be identified. Variants in the gene *Zfp69* were previously hypothesized to be responsible for the diabetogenic effects of this locus (Scherneck et al., 2009). However, results obtained from subsequent characterization of *Zfp69*-tg mice suggested that *Zfp69* alone was not sufficient to trigger the hyperglycemic phenotype observed for the *Nidd/SJL* QTL (Scherneck et al., 2009; Chung et al., 2015). Here, we describe the QTL *Nidd/DBA*, a diabetogenic allele which was contributed by DBA and enhanced hyperglycemia and β-cell loss. In order to re-address the issue of which variants on chromosome 4 are responsible for this trait, *Nidd/DBA* recombinant congenic lines were generated on an NZO background. In the process of this investigation, cross-strain (NZO, B6, 129P2, DBA, and C3H) comparisons and bioinformatic approaches have been utilized in order to identify putative T2D genes.

MATERIALS AND METHODS

Animals

Female NZO mice from our own colony (NZO/HIBomDife: German Institute of Human Nutrition, Nuthetal, Germany) and male DBA (DBA/2J: maintained in-house with breeders originating from Jackson Lab, Maine, United States) were crossed. Generation and phenotypical characterization of backcross mice were performed, as previously described (Vogel et al., 2018). Recombinant congenic mice were bred by repeated backcrossing of mice positive for the *Nidd/DBA* locus with NZO.

All congenic mice were maintained on chow diet (Ssniff, Soest, Germany; maintenance diet for rats and mice, product no. V153xR/M-H) containing 36% protein, 11% fat, and 53% carbohydrates. The animals were kept in accordance with EU Directive 2010/63/EU guidelines for the care and use of laboratory animals. All experiments were approved by the ethics committee of the State Agency of Environment, Health, and Consumer Protection (State of Brandenburg, Germany) under the permit numbers V3-2347-21-2012, 2347-10-2014, and 2347-13-2018.

Genotyping of *Nidd/DBA* Mice by KASP and Microsatellite Markers

Genomic DNA was extracted from mouse tail-tips using the Invisorb Genomic DNA Kit II (STRATEC Molecular GmbH, Berlin, Germany), following the manufacturer's instructions. Kompetitive allele-specific PCR (KASP) genotyping of N2

backcross mice was performed by LGC genomics (LGC group, Teddington, United Kingdom; Vogel et al., 2018). Recombinant congenic mice containing the *Nidd/DBA* locus were genotyped with KASP assays or by PCR with oligonucleotide primers obtained from Sigma (Sigma-Aldrich, Munich, Germany), and the microsatellite length was determined by non-denaturing polyacrylamide gel electrophoresis (**Supplementary Table 1**).

Blood Glucose and Plasma Insulin

Random blood glucose was determined in the morning between 7 and 10 AM with a Contour glucometer (Bayer, Leverkusen, Germany). Plasma insulin levels were determined by Mouse Ultrasensitive Insulin ELISA kit (Alpco, Salem, United States).

Oral Glucose Tolerance Test

Oral glucose tolerance tests (oGTTs) were performed at 6 and 12 weeks of age. Animals were fasted for a period of 6 h and received 2 mg glucose (Glucosteril® 20%, Fresenius Kabi, Bad Homburg, Germany) per gram of body weight by oral gavage, subsequently. At the indicated time points, blood glucose and plasma insulin were obtained from the tail tip.

Fasting-Refeeding Experiment

Fasting and refeeding experiments were performed at 13 weeks of age. After a 16 h overnight fasting period, blood glucose levels were determined and blood samples were collected. Subsequently, mice were refed for 2 h, and blood glucose levels and blood samples were collected.

Endpoint Organ Collection

Mice were fasted 6 h before sacrifice. Blood was obtained by heart puncture with a 0.29 G needle attached to 0.5 M ethylenediaminetetraacetic acid (EDTA) coated syringes. Plasma was extracted by centrifugation (10,000 × *g*, 15 min, 4°C). Tissues were extracted and snap-frozen in liquid nitrogen. All tissue samples were stored at −80°C.

Isolation of Pancreatic Islets

Islets were obtained from mouse pancreas following the protocol, as previously described (Kluth et al., 2015).

Glucose-Stimulated Insulin Secretion in Primary Islets

Glucose-stimulated insulin secretion (GSIS) was performed, as described (Kluth et al., 2019). Briefly, 30 isolated and 24 h recovered islets were equilibrated in Krebs-Ringer buffer for 30 min under low glucose (2.8 mM) conditions and transferred into perifusion chambers (PERI5-115, Biorep Technologies Inc., Miami Lakes, FL, United States) with a continuous flow of 100 µl/min. GSIS was measured continuously under low (2.8 mM) and high glucose (20 mM) conditions and finally with low glucose for indicated periods. Fractions were collected in 2–3 min intervals. Insulin levels were measured using Mouse Ultrasensitive Insulin ELISA (Alpco) and normalized to residual insulin.

Total Pancreatic Insulin

For detection of the pancreatic insulin content, whole pancreas was homogenized in ice-cold acidified ethanol (0.1 mol/L HCl in 70% ethanol) and incubated for 24 h at 4°C. After centrifugation (16,000 × *g*, 10 min), insulin was detected in 5 µl of the supernatant fraction using the Mouse High Range Insulin ELISA (Alpco) according to the manufacturer's instructions.

Immunohistochemistry and Immunofluorescence Staining

Embedded pancreatic sections were stained for insulin with the monoclonal mouse antibody K36AC10 (Sigma-Aldrich) by overnight incubation in a humid chamber at 4°C. For immunofluorescence staining, the secondary antibody 546 Alexa (Thermo Fisher Scientific Inc., Massachusetts, United States) and DAPI were applied at room temperature for 30 min. Next, biotinylated secondary antibody was applied and left at room temperature for 30 min. Subsequently, sections were treated with DAB substrate (DAB + Substrate Chromogen System, Agilent Technologies Inc.) for 2.5 min. Following staining of nuclei with hematoxylin and draining of the sections were performed in a Leica ST5020 Multistainer (Leica Biosystems, Wetzlar, Germany). For morphometric analysis, pancreatic sections were scanned with the MIRAX MIDI scanner (Carl Zeiss MicroImaging GmbH, Jena, Germany) and viewed with the MIRAX Viewer 1.12 software. Fluorescence images were examined with the confocal microscope Leica TCS SP8 (Leica Biosystems, Nussloch GmbH, Germany) and quantified by using the ImageJ software package [v1.52; Wayne Rasband (NIH)].

Linkage Analysis

Genome-wide scan of N2 mice (NZOxDBA, n = 288 males/299 females) was performed, as previously described (Vogel et al., 2018). In brief, genetic map, genotyping errors, and linkage between individual traits and genotypes were assessed with the software package R/qtl (version 1.04-8) using the expectation maximization (EM)-algorithm and 1,000 permutations (Broman et al., 2003).

Haplogroup Analysis

Haplogroup analysis was performed, as described (Schallschmidt et al., 2018). In brief, mouse single nucleotide polymorphism (SNPs) were used from the Wellcome Trust Sanger Institute Database.[1] The chromosomal region was dissected into intervals of 250 kb to determine the frequency of polymorphic SNPs between the mouse strains. A window of 250 kb exceeding the threshold of 100 SNPs was defined as polymorphic according to the assumption (B6 = NZO ≠ DBA). For the total number of SNPs between parental strains, SNPs were compared to the C57BL/6J as reference.

[1]https://www.sanger.ac.uk/sanger/Mouse_SnpViewer/rel-1303

RNA Isolation

Isolation of total RNA from islets of Langerhans was performed with the Micro RNA Isolation RNAqueous® Kit (Life Technologies™, Darmstadt, Germany). Lysis of islet cells was initially carried out by a 10-s ultrasonic pulse (Branson Sonifier 450, G. Heinemann Ultraschall- und Labortechnik, Schwäbisch Gmünd, Germany). All further steps were carried out according to the manufacturer's instructions.

Genome-Wide mRNA Gene Expression

Whole-genome RNA-deep sequencing was performed by LGC Genomics (LGC Group). First, for data processing, adapters were trimmed and reads were filtered for quality using the wrapper Trim Galore and Cutadapt. Second, FastQC was utilized to check quality of samples, and finally, alignment of reads to reference genome was performed with HISAT2, and fragments per kilobase of transcript per million mapped reads (FPKM) values for transcripts have been determined by Cufflinks.

Analysis of Putative Transcription Factor Binding Sites

For the identification of putative transcription factor binding sites (TFBSs) within the promotor region of differentially expressed genes, genetic variants (SNPs/Indels) between the parental strains NZO and DBA (Wellcome Trust Sanger Institute Database; REL-1505) were combined with position weight matrices (PWM) from the JASPAR database (Mathelier et al., 2014). TFBSs were predicted by R version 4.0 and the package TFBS tools (Tan and Lenhard, 2016).

Statistics

Data, if not indicated otherwise, are presented as mean ± standard error of the mean (SEM). Statistical analyses were performed by either unpaired *t*-test, one-way ANOVA, or two-way ANOVA (with or without Bonferroni post-tests), as appropriate. GraphPad Prism 8 software (GraphPad, San Diego, United States) was utilized for simultaneous graph creation and statistical analysis. Significance levels were set for $p < 0.05$ (*), 0.01 (**), and 0.005 (***).

RESULTS

Nidd/DBA, a Diabetes QTL, Contributed by DBA

Male parental NZO and DBA mice were characterized on a 45% kcal high-fat diet (HFD) until the age of 16 weeks. The mice were phenotyped for metabolic traits relating to obesity and diabetes according to a standardized protocol that was established for the DZD collective diabetes cross (Vogel et al., 2018). NZO males, in contrast to DBA mice, developed overt diabetes, incidentally the average male blood glucose reading at the earliest time point measured (week 6) was >16.6 mM and all mice reached severe hyperglycemia (**Figure 1A**) combined with body weight loss by the endpoint of 16 weeks (data not shown). This heterogeneity observed between the two strains provided the basis for the subsequent investigation of QTL arising from the cross of both inbred strains. Since the trait blood glucose also scattered widely in the backcross population of NZO and DBA [(NZOxDBA)N2, **Figure 1A**], we assume that genetic variations are causal for the effect.

Indeed, in the (NZOxDBA)N2 population, a major QTL for elevated blood glucose, reduced plasma insulin concentrations, and low levels of total pancreatic insulin was localized to chromosome 4 with logarithm of the odds (LOD) scores of 8, 3.7, and 6, respectively (**Figure 1B**). This locus was designated *Nidd/DBA* (non-insulin dependent diabetes from DBA). As mice heterozygous for *NZO/DBA* (*N/D*) had an increased propensity toward hyperglycemia and low circulating and pancreatic insulin compared to homozygous *NZO/NZO* (*N/N*) allele carriers (**Figure 1C**), we concluded that the DBA genome contributed the diabetogenic gene.

Characterization of the QTL *Nidd/DBA*

To analyze the phenotype conferred by the *Nidd/DBA* locus and to narrow down the critical region, recombinant congenic mice harboring one (RCS-I, *Nidd/DBA.13.6*$^{N/D}$) or two diabetogenic (*Nidd/DBA.13.6*$^{D/D}$) alleles from DBA on chromosome 4 (103.9–117.5 Mbp) on the NZO background

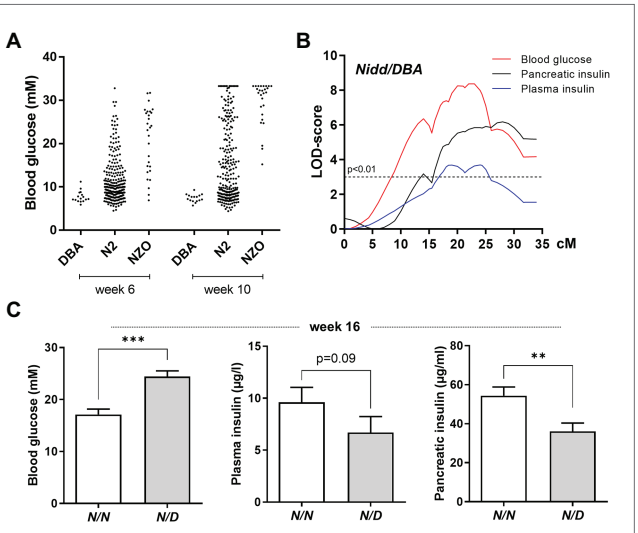

FIGURE 1 | Localization of susceptibility loci on chromosome 4. **(A)** Distribution of blood glucose levels in the (NZOxDBA)N2 cohort at the age of 6 (DBA, *n* = 16; N2, *n* = 282; NZO, *n* = 28) and 10 (DBA, *n* = 16; N2, *n* = 219; NZO, *n* = 27) weeks in comparison to the parental NZO and DBA strains. **(B)** Genome-wide linkage analysis for the traits blood glucose, plasma insulin, and total pancreatic insulin revealed a single quantitative trait loci (QTL) on chromosome 4. The analysis was performed with data from male mice of the (NZOxDBA)N2 population at 16 weeks of age. The horizontal line indicates the threshold of significance ($p < 0.01$). **(C)** Effect sizes of traits associated with the QTL *Nidd/DBA* in the (NZOxDBA)N2 cohort. The critical region of *Nidd/DBA* was defined within a region of 46 Mbp on chromosome 4, defined by border SNP markers rs3692661 and rs3674038. Blood glucose (*N/N*, *n* = 103; *N/D*, *n* = 103), plasma insulin (*N/N*, *n* = 83; *N/D*, *n* = 52), and total pancreatic insulin (*N/N*, *n* = 80; *N/D*, *n* = 58) of homozygous (*N/N*) vs. heterozygous (*N/D*) N2 male mice for the critical region of the QTL. Data are presented as means ± SEM and were analyzed with Student's *t*-test. $^{**}p < 0.01$; $^{***}p < 0.005$.

were characterized and compared to homozygous NZO (*Nidd/DBA.13.6*$^{N/N}$) controls (**Figure 2A**). From week 10 onward, blood glucose values were significantly higher in *Nidd/DBA.13.6*$^{D/D}$ mice compared to controls (**Figure 2A**). At the endpoint (16 weeks of age), approximately two-thirds (66.6%) of the *Nidd/DBA.13.6*$^{D/D}$ group was diabetic, as determined by blood glucose levels >16.6 mM and a stagnation or even drop in body weight, compared to 37.5% diabetic *Nidd/DBA.13.6*$^{N/D}$ and 8.3% *Nidd/DBA.13.6*$^{N/N}$ mice. Likewise, we observed an impaired glucose tolerance during oGTTs in homozygous *Nidd/DBA* allele carriers compared to controls. This effect worsened progressively from week 6 to week 12 (**Figure 2B**). However, the corresponding plasma insulin levels during the oral glucose tests were similar between the different groups (**Figure 2C**).

To further estimate glucose homeostasis and insulin sensitivity, we performed fasting-refeeding experiments in congenic mice at the age of 13 weeks. In the fasting state (16 h fasting), homozygous DBA mice had already higher blood glucose levels than heterozygous and homozygous NZO mice, whereas circulating insulin levels were identical between the different groups (**Figure 2D**). After 2 h refeeding, the homozygous *Nidd/DBA.13.6*$^{N/N}$ and heterozygous *Nidd/DBA.13.6*$^{N/D}$ mice showed significantly higher blood glucose and insulin levels compared to the corresponding fasting state. Although the homozygous *Nidd/DBA.13.6*$^{D/D}$ mice were hyperglycemic already in the fasting state, the mice were still able to secrete significantly more insulin under re-fed conditions (**Figure 2D**). Moreover, in isolated islets of 13-week-old *Nidd/DBA.13.6*$^{D/D}$ and *Nidd/*

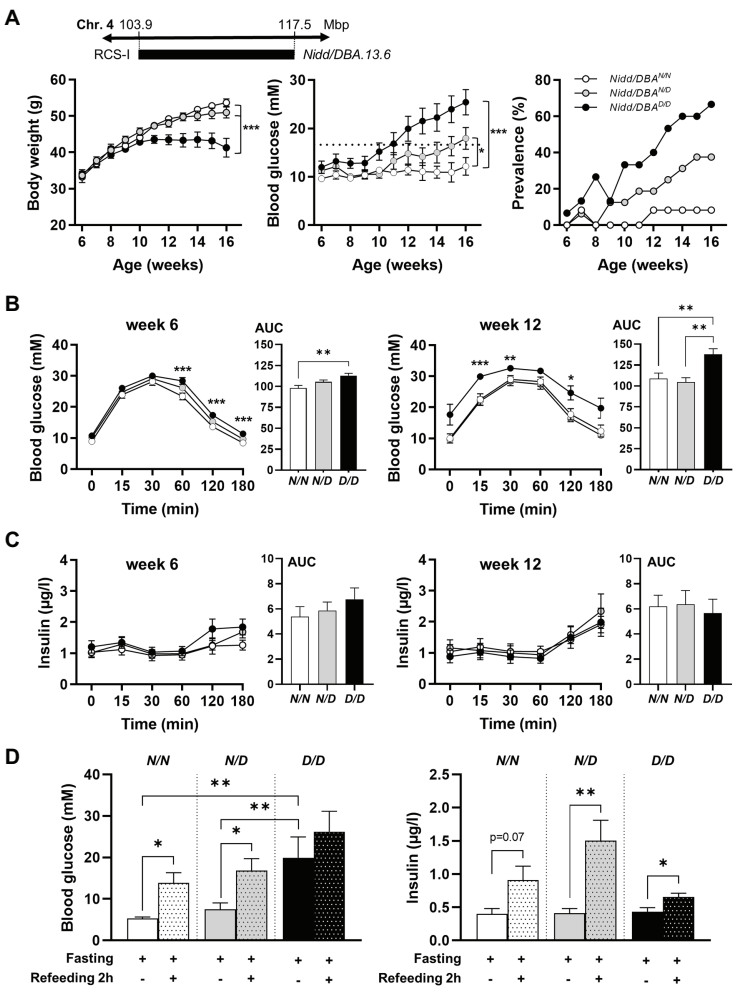

FIGURE 2 | Diabetes traits of *Nidd/DBA* mice. **(A)** Male mice carrying 13.6 Mbp of chromosome 4 from NZO or DBA (*N/N*, *N/D*, and *D/D*) on the NZO background were characterized for the development of body weight (left panel), blood glucose (middle panel), and prevalence of diabetes (blood glucose >16.6 mM; right panel) on chow diet until 16 weeks of age. **(B)** Blood glucose and **(C)** insulin levels with corresponding area under the curve (AUC, right panels) during oral glucose tolerance test (oGTT) in male congenic mice at week 6 and week 12 (*N/N*, n = 12–19, *N/D*, n = 16–35, *D/D*, n = 12–20). **(D)** Blood glucose and insulin levels in 13-week-old *Nidd/DBA* mice after 16 h overnight fast and 2 h-refeeding (*N/N*, n = 6–8, *N/D*, n = 8–11, *D/D*, n = 4–5). Data are presented as means ± SEM and were analyzed by one-way ANOVA (AUC: **B**–**D**) or two-way ANOVA **(A–C)**. *$p < 0.05$; **$p < 0.01$; ***$p < 0.0005$; *N/N*, *Nidd/DBA*$^{N/N}$ mice; *N/D*, *Nidd/DBA*$^{N/D}$ mice; *D/D*, *Nidd/DBA*$^{D/D}$ mice.

DBA.13.6$^{N/N}$ mice, we tested the capacity for GSIS. During the challenge, *Nidd/DBA.13.6*$^{D/D}$ and *Nidd/DBA.13.6*$^{N/N}$ islets displayed equivalent basal (2.8 mM media glucose concentration) insulin secretion capacity. In response to 20 mM glucose, *Nidd/DBA.13.6*$^{D/D}$ islets showed a tendency toward a reduced insulin secretion without reaching significance. No differences in the insulin secretion capacity were obtained in islets of 6 weeks old mice (**Figure 3**).

Nidd/DBA Mice Exhibited Marked β-Cell Loss and Islet Destruction

As we observed higher blood glucose concentrations in *Nidd/DBA.13.6*$^{D/D}$ mice, we isolated the pancreas of congenic mice at different time points to monitor the islet morphology. As shown in **Figure 4A** and **Supplementary Figure S1**, at 16 weeks of age, the islet area, as well as the number of islets, was significantly reduced in homozygous *Nidd/DBA.13.6*$^{D/D}$ mice compared to heterozygous allele carriers and tendentially also to homozygous controls (*Nidd/DBA.13.6*$^{N/N}$), assuming in combination with the hyperglycemic phenotype that *Nidd/DBA.13.6*$^{D/D}$ mice exhibited a marked loss in pancreatic β-cells. Immunofluorescent staining of pancreatic islets with an insulin specific antibody additionally highlighted the loss of β-cells in *Nidd/DBA.13.6*$^{D/D}$ mice (**Figure 4B**) with a gradual loss from week 6 to week 16. In order to validate the data obtained by immunohistochemistry, we determined the insulin content of total pancreas by immunoassay of acidic ethanol extracts (**Figure 4C**). A significant decrease of the insulin content in *Nidd/DBA.13.6*$^{D/D}$ mice was detected at the age of 16 weeks. Thus, a gradual decrease in total pancreatic insulin appeared to accompany the increase in fasting plasma glucose levels combined with a fall in fasting plasma insulin levels (**Figure 4C**).

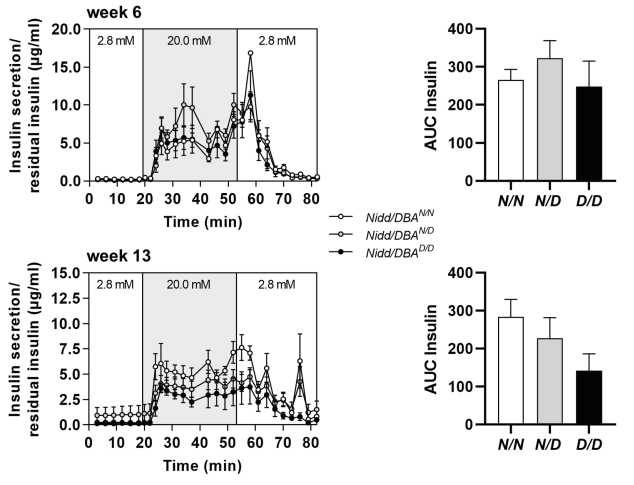

FIGURE 3 | Insulin secretion in *Nidd/DBA* islets *ex vivo*. Glucose-stimulated insulin secretion (GSIS) in primary islets of 6 (n = 3) and 13 weeks old homozygous NZO (*N/N*, n = 4), heterozygous (*N/D*, n = 6), or homozygous DBA (*D/D*, n = 3) allele carriers for the *Nidd/DBA* locus (RCS-III, *Nidd/DBA.6.3*) with corresponding AUC (right panel). Data are presented as means ± SEM and were analyzed by one-way ANOVA.

Fine Mapping of the Critical Diabetogenic Interval of *Nidd/DBA*

The region spanning 13.6 Mbp of the *Nidd/DBA* harbors 284 genes including 139 annotated genes, 78 gene models, and 67 non-coding RNAs (Yates et al., 2020). To identify the responsible gene variant(s), additional recombinant congenic lines, each carrying a distinct region of the initial *Nidd/DBA* locus, were generated by further backcrossing to NZO (**Figure 5A**). The characterization of these mice indicated that more than two-thirds of the heterozygous allele carriers of each line developed a diabetic phenotype at the endpoint of 16 weeks, compared to 33.3% diabetic *Nidd/DBA*$^{N/N}$ mice (**Figure 5B**). Heterozygous mice of each line developed hyperglycemia compared to normoglycemic controls, and the body weight already started to drop (**Figure 5C**). Thus, a 3.3 Mbp fragment with 61 genes including 28 annotated genes, 18 gene models, and 15 non-coding RNAs (Yates et al., 2020), comprising the diabetogenic allele, was defined to be located between 108.1 Mbp (rs233757491) and 111.4 Mbp (rs32727600).

Within the collective diabetes cross project, a backcross population of the NZO and B6 strain was conducted, where no QTL on chromosome 4 with similarities to the *Nidd/DBA* locus was defined. Thus, the causal gene variant(s) may be common between the NZO and B6 strain but different to DBA. According to this hypothesis, a haplotype map of the putative critical region on chromosome 4 was created based on NZO/HiltJ, DBA/2J, and C57BL/6J (B6) SNP information (Keane et al., 2011; Yalcin et al., 2011). A graphical representation of the polymorphic regions found in the *Nidd/DBA* locus is shown in **Figure 5D**, where several clusters of variants can be identified across the entire region. In total, 18 genes (11 annotated genes, one gene model, three processed pseudo genes, and three non-coding RNAs) were found to be unique for the DBA strain but different to NZO and B6.

Moreover, gene expression profiles of pancreatic islets were generated from congenic mice carrying the initial 13.6 Mbp fragment (RCS-I) of the *Nidd/DBA* locus. Six genes within the critical region were differentially expressed in pancreatic islets of homozygous *Nidd/DBA*$^{D/D}$ mice compared to homozygous *Nidd/DBA*$^{N/N}$ controls (**Figure 5F**), whereby only *Kti12*, *Osbpl9*, and *Ttc39a* are also located in a polymorphic haplotype block (**Figure 5E**). As the complete NZO and DBA genomic sequence is publicly available, we also screened for sequence variations in genes located within the polymorphic *Nidd/DBA* haplotype block. In total, two non-synonymous SNPs (**Table 1**) in association with *Ttc39a* [rs28150999; missense variant (P169L)] and *Calr4* (rs219833914; frameshift variant) were found to be common between NZO and B6 but different to DBA (**Table 1**; **Figure 5E**).

Next, we aimed to investigate the underlying genetic cause of the differential expression of *Ttc39a*, *Osbpl9*, and *Kti12*. An *in silico* approach using a PWM based TFBS prediction revealed

strong alterations for eight transcription factors (TFs) in a region 2 kbp upstream of *Ttc39a* (**Supplementary Table 2**). These variants lead to an altered core region in the DBA sequence, and it is possible that these sequence alterations and a likely difference in TF binding are causal for the low *Ttc39a* expression in DBA allele carriers.

Expression of Human Orthologues of *Nidd/DBA* Candidates in Patients With Type 2 Diabetes

The *Nidd/DBA* locus on mouse chromosome 4 is syntenic to the human genomic segment on chromosome 1 (**Figure 6A**). To clarify the importance of the genes with differential expression in mouse islets in the pathogenesis of T2D, we used transcriptomic data from human pancreatic islets of deceased donors with and without T2D (Fadista et al., 2014). As shown in **Figure 6B**, all three genes displayed a significantly different expression in islets of patients with and without T2D, whereby only the effect for *TTC39A* with a reduced expression in T2D patients was comparable with the data obtained in pancreatic islets of mice carrying the diabetogenic *Nidd/DBA* allele (**Figure 5F**).

DISCUSSION

The present data define a critical interval of the QTL *Nidd/DBA* on chromosome 4, a diabetogenic allele which was introduced by DBA. The QTL is characterized by hyperglycemia starting at 10 weeks of age, accompanied by hypoinsulinemia

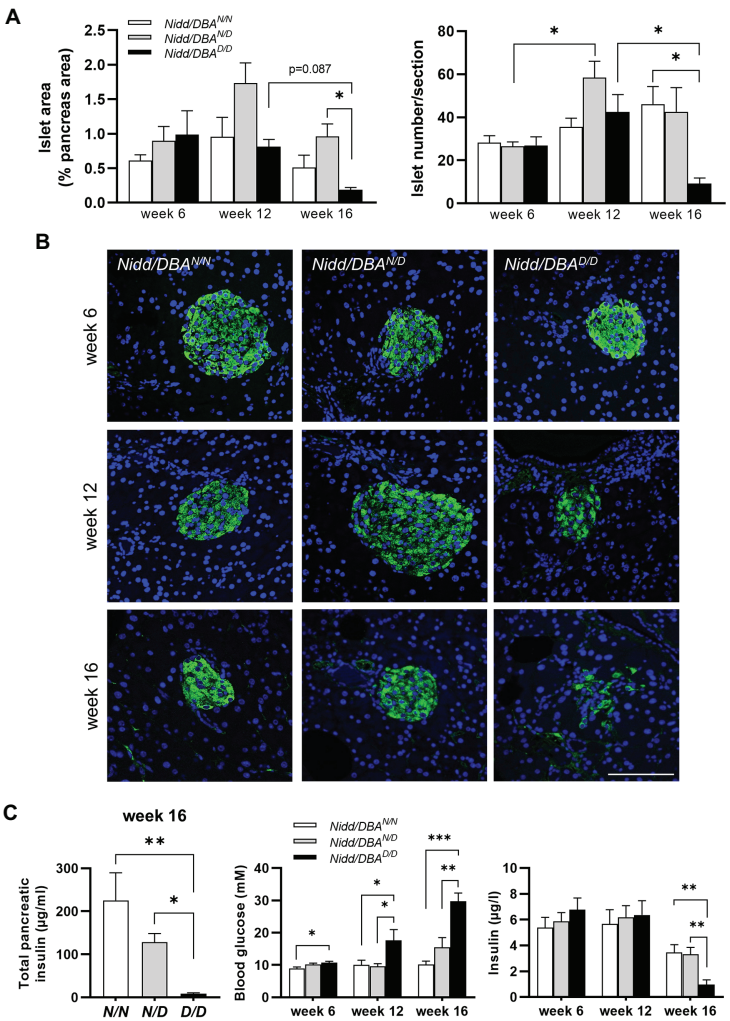

FIGURE 4 | *Nidd/DBA* mice exhibited marked β-cell loss and islet destruction. **(A)** Quantification of islet area (left panel) and islet number/section (right panel) at the indicated time points in male *Nidd/DBA*$^{N/N}$ (*N/N*), *Nidd/DBA*$^{N/D}$ (*N/D*), and *Nidd/DBA*$^{D/D}$ (*D/D*) mice (n = 3–8 animals/genotype). **(B)** Representative images of pancreatic sections of male *Nidd/DBA* (RCS-I) mice stained for insulin (green). Nuclei were stained with DAPI (blue); Scale bar: 100 µm. **(C)** Pancreatic insulin content in congenic mice (RCS-I) at the age of 16 weeks (n = 5–7) and 6 h fasting blood glucose and insulin values in RCS-I mice at different time points (*N/N*, n = 5–19, *N/D*, n = 6–35, *D/D*, n = 10–20). Data are presented as means ± SEM and were analyzed by one-way ANOVA. *$p < 0.05$; **$p < 0.01$; ***$p < 0.0005$.

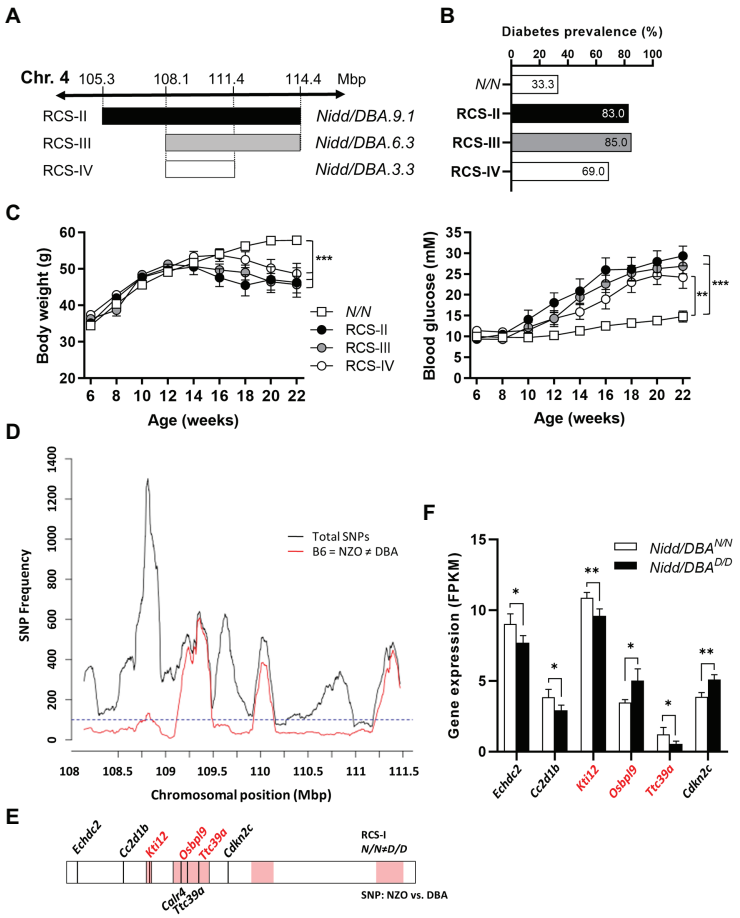

FIGURE 5 | Combined approach of haplotype and gene expression analysis in islets for the identification of DBA-specific gene variants within the *Nidd/DBA* locus. **(A)** Generation of congenic mice carrying different fragments of the QTL *Nidd/DBA*. **(B)** Diabetes prevalence (blood glucose >16.6 mM, week 16), **(C)** body weight, and blood glucose development in congenic mice carrying one heterozygous DBA allele for the *Nidd/DBA* locus compared to homozygous NZO controls. **(D)** Haplotype map of single nucleotide polymorphisms (SNPs) within the critical region of *Nidd/DBA* (108.8–111.4 Mbp). Black line: total number of SNPs (all SNPs annotated for the B6 reference genome with calls for NZO and DBA). Red line: SNPs according to B6 = NZO ≠ DBA. **(E)** QTL was dissected into windows of 250 kb. Red boxes indicate 100 SNPs per window polymorphic according to B6 = NZO ≠ DBA. Location of genes within the critical *Nidd/DBA* interval with a differential expression in pancreatic islets of 6 weeks old congenic mice (*N/N* ≠ *D/D*) and position of genes with non-synonymous coding variants between the parental strains NZO and DBA (REL-1505-GRCm38). **(F)** Genes within the critical *Nidd/DBA* interval displaying a differential expression in pancreatic islets of congenic mice (RCS-I, *Nidd/DBA.13.6*). Expression was analyzed *via* RNA-sequencing ($n = 4$). Genes with differential expression in pancreatic islets and location within a polymorphic *Nidd/DBA* haplotype block are indicated in red. Data are presented as means ± SEM and were analyzed with Student's *t*-test **(F)** or one-way ANOVA **(C)**. $*p < 0.05$; $**p < 0.01$; $***p < 0.001$.

and a loss of body weight and total pancreatic insulin levels at the endpoint of the study at 16 weeks. In order to identify the responsible variant(s) on chromosome 4, *Nidd/DBA* recombinant congenic lines were generated and combined with transcriptomics and different bioinformatic tools to finally define a critical QTL segment of 3.3 Mbp which contains four candidate genes for the observed diabetic phenotype.

The diabetogenic allele of *Nidd/DBA* mice induces severe hyperglycemia and impaired glucose clearance starting at 10 weeks of age and decreased glucose response in week 13. In week 6, *Nidd/DBA*$^{D/D}$ islets displayed equivalent basal as well as GSIS, whereas in week 13, carriers of the diabetogenic allele showed a tendency of an impaired insulin secretion capacity. Also, the unchanged insulin levels during the glucose tolerance tests which showed an impaired glucose clearance indicate that *Nidd/DBA*$^{D/D}$ mice exhibit a restricted insulin secretion. Histology of non-diabetic *Nidd/DBA*$^{N/N}$ and *Nidd/DBA*$^{D/D}$ mice at the age of 6 weeks did not indicate any early differences in islet morphology, whereas later immunostaining of pancreatic sections of diabetic *Nidd/DBA* mice revealed a loss of β-cells and reduced islet size to be a central element in the pathology of *Nidd/DBA* induced T2D. The time course data indicate that, presumably, due to a moderate and early impairment of insulin secretion, a fast β-cell loss occurs within a period of 3–4 weeks.

Many mouse-cross populations have been analyzed worldwide, but despite the fact that diabetes-related QTL on chromosome 4 have appeared several times in both DBA and NZO outcrosses (BKS-db/−xNZO: Togawa et al., 2006;

TABLE 1 | Summary of genetic variants in the critical region of *Nidd/DBA*, common between the New Zealand obese (NZO) and B6 strain but different to DBA (Keane et al., 2011; Yalcin et al., 2011).

Variant type	Number of SNPs	Number of InDels	Number of genes
Intron	1,139	489	29
Upstream	326	114	30
Missense	1	-	1
Splice region	-	2	2
Frameshift	-	1	1
Stop	-	-	-
Intergenic	433	152	0

The region defining upstream variants was set by 2 kbp upstream of the transcription start site.

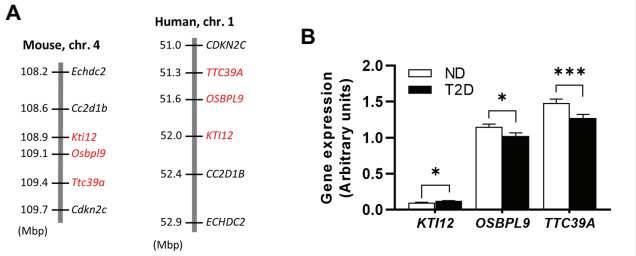

FIGURE 6 | Expression of *Nidd/DBA* candidate genes in human pancreatic islets. **(A)** Cluster of the critical *Nidd/DBA* region on mouse chromosome 4 and human chromosome 1. **(B)** Expression of candidate genes in pancreatic islets of T2D (n = 26) and normoglycemic controls (n = 51; Fadista et al., 2014). Data are presented as means ± SEM and were analyzed with Student's t-test. *$p < 0.05$; ***$p < 0.0005$.

NONxNZO: Leiter et al., 1998; NZOxSJL: Plum et al., 2002), the responsible variant has yet to be elucidated. The gene *Zfp69*, uniquely expressed in SJL and repressed in NZO due to the presence of a retrotransposon, is located on chromosome 4 at approximately 121 Mbp and was previously investigated as a T2D candidate, but does not account for islet dysfunction and β-cell loss (Scherneck et al., 2009; Chung et al., 2015). DBA mice carry an intact copy of *Zfp69*, however, characterization of recombinant congenic mice excluded the possibility that *Zfp69* is responsible for β-cell failure observed in *Nidd/DBA* mice, as *Zfp69* is located outside of the smallest critical *Nidd/DBA* fragment (108.1–111.4 Mbp) inducing hyperglycemia. In addition to SJL, QTL for elevated blood glucose were identified on chromosome 4 from parallel NZO crosses with C3H and 129P2 (Schallschmidt et al., 2018). The QTL derived from SJL, 129P2, and C3H were characterized not only by hyperglycemia but also by a lack of insulin, indicating that β-cell failure is underlying the diabetogenic effect of the QTL. However, it is not entirely clear whether the DBA, C3H, 129P2, and SJL strains harbor the same pathological variant on chromosome 4. Therefore, for haplotype mapping, we just included the sequence variants in the critical region of the *Nidd/DBA* between DBA and NZO as well as the B6 strain, as no QTL for hyperglycemia was detected on chromosome 4 in the (NZOxB6)N2 cross.

Of the 18 genes within the haplotype block that carry common variants between these strains, three genes located between 108.1 and 111.4 Mbp are differently expressed in islets of homozygous DBA compared to homozygous NZO mice. One of these genes, *Ttc39a* [tetratricopeptide repeat (TPR) domain] also carries a missense variant in the DBA genome. *Ttc39a* belongs to the structural family of TPR domain proteins, which comprises about 100 members characterized by repeats of a 34-amino-acid consensus (Dmitriev et al., 2009). The TPR-containing (TTC) proteins are involved in many important biological processes, such as intracellular transport, vesicle fusion, protein folding, cell cycle, and transcriptional regulation (Zeytuni and Zarivach, 2012; Xu et al., 2015). For *Ttc4*, it has been demonstrated that it is involved in the intraflagellar transport (IFT), a trafficking machinery essential for cilia formation and function (Hao and Scholey, 2009). Defects in cilia assembly and function result in severe disorders called ciliopathies (Xu et al., 2015). A subset of ciliopathies including Bardet-Biedl-Syndrome (BBS) and Alström Syndrome (ALMS) shows metabolic abnormalities including truncal obesity and higher susceptibility to diabetes (Volta and Gerdes, 2017). Cilia are present, e.g., in endocrine β-cells, and it has been reported that cilia play a role in insulin signaling, insulin secretion, and β-cell function (Gerdes et al., 2014). We recently reported that cilia-gene regulation has a strong impact on the presence and dynamics of cilia in islets which, in turn, determines diabetes susceptibility (Kluth et al., 2019). However, as there are multiple transcript variants described for *Ttc39a*, which encode distinct isoforms, the specific role of the differently expressed isoform in the pathogenesis of diabetes in mice has to be clarified. The second gene with a differential expression is *Kti12* (*KTI12 homolog, chromatin associated*). *Kti12* is known to be a vastly conserved ATPase and essential for transfer RNA (tRNA)-modification activity of the Elongator complex (Krutyhołowa et al., 2020). So far, *Kti12* was mainly described in plant cell biology, where it plays a role in the transcription by interacting with RNA polymerase II (Nelissen et al., 2003). Attempts to generate *Kti12*-KO models in mice resulted either in embryonic lethality (prior to organogenesis) or pre-weaning lethality (IMPC[2]). The gene *Osbpl9* (*oxysterol binding protein-like 9*) belongs to the oxysterol-binding protein family, which has been implicated in the function of, e.g., endoplasmic reticulum (ER) junctions, non-vesicular transport of lipids, integration of sterol and sphingomyelin metabolism, sterol transport, regulation of neutral lipid metabolism, and regulation of signaling cascades (Olkkonen et al., 2006). Familial loss-of-function variants of OSBPL1 in humans predisposed to impaired reverse cholesterol transport and low plasma high-density lipoprotein (HDL) levels (Motazacker et al., 2016). Studies on OSBPL10 suggested a suppressive function on hepatic lipogenesis and very low density lipoprotein (VLDL) production (Perttilä et al., 2009). Finally, the gene *Calr4* (*Calreticulin 4*) located within the critical *Nidd/DBA* segment carries a frameshift mutation within the first exon in the DBA strain. *Calr4* alongside with *Crt* (*calreticulin*), *Cnx* (*calnexin*), and *Clgn* (*calmegin*) belongs to the calreticulin protein family that is known to

[2]https://www.mousephenotype.org/

be involved in calcium binding. Genes of the calreticulin family encode for proteins located in the endoplasmic reticulum (ER; Michalak et al., 1992; Bergeron et al., 1994; Watanabe et al., 1994). *Crt* promotes folding and quality control of the ER by interactions with *Cnx* (Calreticulin/calnexin cycle; Raghubir et al., 2011). However, due to the fact that *Calr4* was not detected in islets by RNAseq, we concluded that its variant is not involved in the impaired β-cell function induced by *Nidd/DBA*. In addition, *Calr4* appears to only be expressed during embryonic development in mice, it is poorly conserved and only encoded as a pseudogene in humans.

In summary, the positional cloning of the QTL *Nidd/DBA* has identified four genes as potential T2D candidates as they display a differential expression in pancreatic islets and/or sequence variation. However, it cannot be excluded that genetic variants, including non-coding SNPs, indels, or copy number polymorphisms, may exert effects on regulatory circuits in the locus, thereby affecting islet cell function and glycemic control. Similarly, it must be considered that the *Nidd/DBA* locus may contain a diabetogenic variant not in a gene but rather in a regulatory region.

CONCLUSION

In conclusion, the integration of comparative analysis of multiple inbred populations with one common breeding partner, haplotype mapping, expression, and sequence data substantially improved the mapping resolution of the diabetes QTL *Nidd/DBA*. Within the critical fragment of 3.3 Mbp, four genes with differential expression in pancreatic islets and/or genetic variants were identified. Future studies are necessary to validate the role of the different candidates in β-cell function and for maintaining glycemic control. This information may finally contribute to our growing understanding of the pathomechanisms that lead to β-cell failure and provide new paths toward targeted therapies and prevention strategies.

DATA AVAILABILITY STATEMENT

The data discussed in this publication have been deposited in NCBI's Gene Expression Omnibus (Edgar et al., 2002) and are accessible through GEO Series accession number GSE152127 (https://www.ncbi.nlm.nih.gov/geo/query/acc.cgi?acc=GSE152127).

ETHICS STATEMENT

The animal study was reviewed and approved by State Agency of Environment, Health, and Consumer Protection (State of Brandenburg, Germany).

AUTHOR CONTRIBUTIONS

HA designed and performed the experiments, wrote and edited the manuscript. NH designed and performed the experiments and interpreted the data. HA and NH equally contributed on the composition and the analyses conducted in the manuscript. PG and MJ analyzed the data. SO performed the experiments. GS analyzed the data. AK performed the experiments and analyzed the data. DA analyzed the data and provided expertise. GB provided expertise. TS and SL performed the experiments and provided the data. AC, HA-H, and H-GJ were involved in designing the study. AS designed and directed the study and edited the manuscript. HV designed and directed the study, wrote and edited the manuscript. All authors contributed to the article and approved the submitted version.

FUNDING

The work was supported by the German Ministry of Education and Research (BMBF: DZD grant 82DZD00302) and the Brandenburg state.

ACKNOWLEDGMENTS

We gratefully thank the skillful technical assistance of Josefine Würfel, Ute Lehmann, Andrea Teichmann, Anett Helms, Arne Weigelt, and Julia Vogt.

SUPPLEMENTARY MATERIAL

The Supplementary Material for this article can be found online at: https://www.frontiersin.org/article/10.3389/fgene.2020.567191/full#supplementary-material

REFERENCES

American Diabetes Association (2005). Diagnosis and classification of diabetes mellitus. *Diabetes Care* 28, S37–S42. doi: 10.2337/diacare.28.suppl_1.S37

Bergeron, J. J. M., Brenner, M. B., Thomas, D. Y., and Williams, D. B. (1994). Calnexin: a membrane-bound chaperone of the endoplasmic reticulum. *Trends Biochem. Sci.* 19, 124–128. doi: 10.1016/0968-0004(94)90205-4

Broman, K. W., Wu, H., Sen, Ś., and Churchill, G. A. (2003). R/qtl: QTL mapping in experimental crosses. *Bioinformatics* 19, 889–890. doi: 10.1093/bioinformatics/btg112

Chua, S., Liu, S. M., Li, Q., Yang, L., Thassanapaff, V., and Fisher, P. (2002). Differential beta cell responses to hyperglycaemia and insulin resistance in two novel congenic strains of diabetes (FVB-Leprdb) and obese (DBA-Lepob) mice. *Diabetologia* 45, 976–990. doi: 10.1007/s00125-002-0880-z

Chung, B., Stadion, M., Schulz, N., Jain, D., Scherneck, S., Joost, H. -G., et al. (2015). The diabetes gene Zfp69 modulates hepatic insulin sensitivity in mice. *Diabetologia* 58, 2403–2413. doi: 10.1007/s00125-015-3703-8

Davis, R. C., van Nas, A., Castellani, L. W., Zhao, Y., Zhou, Z., Wen, P., et al. (2012). Systems genetics of susceptibility to obesity-induced diabetes in mice. *Physiol. Genomics* 44, 1–13. doi: 10.1152/physiolgenomics.00003.2011

Dmitriev, R. I., Okkelman, I. A., Abdulin, R. A., Shakhparonov, M. I., and Pestov, N. B. (2009). Nuclear transport of protein TTC4 depends on the cell cycle. *Cell Tissue Res.* 336, 521–527. doi: 10.1007/s00441-009-0785-y

Edgar, R., Domrachev, M., and Lash, A. E. (2002). Gene Expression Omnibus: NCBI gene expression and hybridization array data repository. *Nucleic Acids Res.* 30, 207–210. doi: 10.1093/nar/30.1.207

Fadista, J., Vikman, P., Laakso, E. O., Mollet, I. G., Esguerra, J. L., Taneera, J., et al. (2014). Global genomic and transcriptomic analysis of human pancreatic

islets reveals novel genes influencing glucose metabolism. *Proc. Natl. Acad. Sci. U S A.* 111, 13924–13929. doi: 10.1073/pnas.1402665111

Gerdes, J. M., Christou-Savina, S., Xiong, Y., Moede, T., Moruzzi, N., Karlsson-Edlund, P., et al. (2014). Ciliary dysfunction impairs beta-cell insulin secretion and promotes development of type 2 diabetes in rodents. *Nat. Commun.* 5:5308. doi: 10.1038/ncomms6308

Hao, L., and Scholey, J. M. (2009). Intraflagellar transport at a glance. *J. Cell Sci.* 122, 889–892. doi: 10.1242/jcs.023861

Kahn, S. E., Hull, R. L., and Utzschneider, K. M. (2006). Mechanisms linking obesity to insulin resistance and type 2 diabetes. *Nature* 444, 840–846. doi: 10.1038/nature05482

Keane, T. M., Goodstadt, L., Danecek, P., White, M. A., Wong, K., Yalcin, B., et al. (2011). Mouse genomic variation and its effect on phenotypes and gene regulation. *Nature* 477, 289–294. doi: 10.1038/nature10413

Kluge, R., Scherneck, S., Schürmann, A., and Joost, H. -G. (2012). Pathophysiology and genetics of obesity and diabetes in the New Zealand obese mouse: a model of the human metabolic syndrome. *Methods Mol. Biol.* 933, 59–73. doi: 10.1007/978-1-62703-068-7

Kluth, O., Matzke, D., Kamitz, A., Jähnert, M., Vogel, H., Scherneck, S., et al. (2015). Identification of four mouse diabetes candidate genes altering β-cell proliferation. *PLoS Genet.* 11:e1005506. doi: 10.1371/journal.pgen.1005506

Kluth, O., Stadion, M., Gottmann, P., Aga, H., Jähnert, M., Scherneck, S., et al. (2019). Decreased expression of cilia genes in pancreatic islets as a risk factor for type 2 diabetes in mice and humans. *Cell Rep.* 26, 3027–3036.e3. doi: 10.1016/j.celrep.2019.02.056

Krutyhołowa, R., Reinhardt-Tews, A., Chramiec-Głąbik, A., Breunig, K. D., and Glatt, S. (2020). Fungal Kti12 proteins display unusual linker regions and unique ATPase p-loops. *Curr. Genet.* 66, 823–833. doi: 10.1007/s00294-020-01070-2

Leiter, E. H. (1981). The influence of genetic background on the expression of mutations at the diabetes locus in the mouse IV. Male lethal syndrome in CBA/Lt mice. *Diabetes* 30, 1035–1044. doi: 10.2337/diabetes.30.12.1035

Leiter, E. H., Reifsnyder, P. C., Flurkey, K., Partke, H. J., Junger, E., and Herberg, L. (1998). NIDDM genes in mice: deleterious synergism by both parental genomes contributes to diabetogenic thresholds. *Diabetes* 47, 1287–1295.

Lubura, M., Hesse, D., Krämer, M., Hallahan, N., Schupp, M., von Loeffelholz, C., et al. (2015). Diabetes prevalence in NZO females depends on estrogen action on liver fat content. *Am. J. Physiol. Endocrinol. Metab.* 309, E968–E980. doi: 10.1152/ajpendo.00338.2015

Mathelier, A., Zhao, X., Zhang, A. W., Parcy, F., Worsley-Hunt, R., Arenillas, D. J., et al. (2014). JASPAR 2014: an extensively expanded and updated open-access database of transcription factor binding profiles. *Nucleic Acids Res.* 42, D142–D147. doi: 10.1093/nar/gkt997

McCarthy, M. I., and Zeggini, E. (2009). Genome-wide association studies in type 2 diabetes. *Curr. Diab. Rep.* 9, 164–171. doi: 10.1007/s11892-009-0027-4

Michalak, M., Milner, R. E., Burns, K., and Opas, M. (1992). Calreticulin. *Biochem. J.* 285, 681–692. doi: 10.1042/bj2850681

Motazacker, M. M., Pirhonen, J., van Capelleveen, J. C., Weber-Boyvat, M., Kuivenhoven, J. A., Shah, S., et al. (2016). A loss-of-function variant in OSBPL1A predisposes to low plasma HDL cholesterol levels and impaired cholesterol efflux capacity. *Atherosclerosis* 249, 140–147. doi: 10.1016/j.atherosclerosis.2016.04.005

Nelissen, H., Clarke, J. H., De Block, M., De Block, S., Vanderhaeghen, R., Zielinski, R. E., et al. (2003). DRL1, a homolog of the yeast TOT4/KTI12 protein, has a function in meristem activity and organ growth in plants. *Plant Cell* 15, 639–654. doi: 10.1105/tpc.007062

Olkkonen, V. M., Johansson, M., Suchanek, M., Yan, D., Hynynen, R., Ehnholm, C., et al. (2006). The OSBP-related proteins (ORPs): global sterol sensors for co-ordination of cellular lipid metabolism, membrane trafficking and signalling processes? *Biochem. Soc. Trans.* 34, 389–391. doi: 10.1042/BST0340389

Perttilä, J., Merikanto, K., Naukkarinen, J., Surakka, I., Martin, N. W., Tanhuanpää, K., et al. (2009). OSBPL10, a novel candidate gene for high triglyceride trait in dyslipidemic Finnish subjects, regulates cellular lipid metabolism. *J. Mol. Med.* 87, 825–835. doi: 10.1007/s00109-009-0490-z

Plum, L., Giesen, K., Kluge, R., Junger, E., Linnartz, K., Schürmann, A., et al. (2002). Characterisation of the mouse diabetes susceptibilty locus Nidd/SJL: islet cell destruction, interaction with the obesity QTL Nob1, and effect of dietary fat. *Diabetologia* 45, 823–830. doi: 10.1007/s00125-002-0796-7

Raghubir, R., Nakka, V. P., and Mehta, S. L. (2011). Endoplasmic reticulum stress in brain damage. *Methods Enzymol.* 489, 259–275. doi: 10.1016/B978-0-12-385116-1.00015-7

Schallschmidt, T., Lebek, S., Altenhofen, D., Damen, M., Schulte, Y., Knebel, B., et al. (2018). Two novel candidate genes for insulin secretion identified by comparative genomics of multiple backcross mouse populations. *Genetics* 210, 1527–1542. doi: 10.1534/genetics.118.301578

Scherneck, S., Nestler, M., Vogel, H., Blüher, M., Block, M. -D., Berriel Diaz, M., et al. (2009). Positional cloning of zinc finger domain transcription factor Zfp69, a candidate gene for obesity-associated diabetes contributed by mouse locus Nidd/SJL. *PLoS Genet.* 5:e1000541. doi: 10.1371/journal.pgen.1000541

Schwerbel, K., Kamitz, A., Krahmer, N., Hallahan, N., Jähnert, M., Gottmann, P., et al. (2020). Immunity-related GTPase induces lipophagy to prevent excess hepatic lipid accumulation. *J. Hepatol.* doi: 10.1016/j.jhep.2020.04.031 [Epub ahead of print]

Tallapragada, D. S. P., Bhaskar, S., and Chandak, G. R. (2015). New insights from monogenic diabetes for "common" type 2 diabetes. *Front. Genet.* 6:251. doi: 10.3389/fgene.2015.00251

Tan, G., and Lenhard, B. (2016). TFBSTools: an R/bioconductor package for transcription factor binding site analysis. *Bioinformatics* 32, 1555–1556. doi: 10.1093/bioinformatics/btw024

Togawa, K., Moritani, M., Yaguchi, H., and Itakura, M. (2006). Multidimensional genome scans identify the combinations of genetic loci linked to diabetes-related phenotypes in mice. *Hum. Mol. Genet.* 15, 113–128. doi: 10.1093/hmg/ddi433

Vogel, H., Kamitz, A., Hallahan, N., Lebek, S., Schallschmidt, T., Jonas, W., et al. (2018). A collective diabetes cross in combination with a computational framework to dissect the genetics of human obesity and type 2 diabetes. *Hum. Mol. Genet.* 27, 3099–3112. doi: 10.1093/hmg/ddy217

Vogel, H., Mirhashemi, F., Liehl, B., Taugner, F., Kluth, O., Kluge, R., et al. (2013). Estrogen deficiency aggravates insulin resistance and induces β-cell loss and diabetes in female New Zealand obese mice. *Horm. Metab. Res.* 45, 430–435. doi: 10.1055/s-0032-1331700

Volta, F., and Gerdes, J. M. (2017). The role of primary cilia in obesity and diabetes. *Ann. N. Y. Acad. Sci.* 1391, 71–84. doi: 10.1111/nyas.13216

Watanabe, D., Yamada, K., Nishina, Y., Tajima, Y., Koshimizu, U., Nagata, A., et al. (1994). Molecular cloning of a novel Ca(2+)-binding protein (calmegin) specifically expressed during male meiotic germ cell development. *J. Biol. Chem.* 269, 7744–7749.

Xu, Y., Cao, J., Huang, S., Feng, D., Zhang, W., Zhu, X., et al. (2015). Characterization of tetratricopeptide repeat-containing proteins critical for cilia formation and function. *PLoS One* 10:e0124378. doi: 10.1371/journal.pone.0124378

Yalcin, B., Wong, K., Agam, A., Goodson, M., Keane, T. M., Gan, X., et al. (2011). Sequence-based characterization of structural variation in the mouse genome. *Nature* 477, 326–329. doi: 10.1038/nature10432

Yates, A. D., Achuthan, P., Akanni, W., Allen, J., Allen, J., Alvarez-Jarreta, J., et al. (2020). Ensembl 2020. *Nucleic Acids Res.* 48, D682–D688. doi: 10.1093/nar/gkz966

Zeytuni, N., and Zarivach, R. (2012). Structural and functional discussion of the tetra-trico-peptide repeat, a protein interaction module. *Structure* 20, 397–405. doi: 10.1016/j.str.2012.01.006

Conflict of Interest: The authors declare that the research was conducted in the absence of any commercial or financial relationships that could be construed as a potential conflict of interest.

frontiers in Endocrinology

ORIGINAL RESEARCH
published: 30 October 2020
doi: 10.3389/fendo.2020.575469

Increased Plasma Soluble Interleukin-2 Receptor Alpha Levels in Patients With Long-Term Type 1 Diabetes With Vascular Complications Associated With *IL2RA* and *PTPN2* Gene Polymorphisms

Magdalena Keindl[1,2], Olena Fedotkina[1], Elsa du Plessis[1], Ruchi Jain[3], Brith Bergum[2,4], Troels Mygind Jensen[5,6], Cathrine Laustrup Møller[7], Henrik Falhammar[8,9], Thomas Nyström[10], Sergiu-Bogdan Catrina[8,9,11], Gun Jörneskog[12], Leif Groop[3,13], Mats Eliasson[14], Björn Eliasson[15], Kerstin Brismar[9], Peter M. Nilsson[3], Tore Julsrud Berg[16], Silke Appel[2,4] and Valeriya Lyssenko[1,3*]*

[1] Center for Diabetes Research, Department of Clinical Science, Faculty of Medicine, University of Bergen, Bergen, Norway, [2] Broegelmann Research Laboratory, Department of Clinical Science, Faculty of Medicine, University of Bergen, Bergen, Norway, [3] Department of Clinical Science, Lund University Diabetes Centre, Malmö, Sweden, [4] Flow Cytometry Core Facility, Department of Clinical Science, Faculty of Medicine, University of Bergen, Bergen, Norway, [5] Research Unit for General Practice & Danish Ageing Research Center, Department of Public Health, University of Southern Denmark, Odense, Denmark, [6] Clinical Epidemiology, Steno Diabetes Center Copenhagen (SDCC), Gentofte, Denmark, [7] Translational Pathophysiology, Steno Diabetes Center Copenhagen (SDCC), Gentofte, Denmark, [8] Department of Molecular Medicine and Surgery, Karolinska Institute, Stockholm, Sweden, [9] Department of Endocrinology, Metabolism and Diabetes, Karolinska University Hospital, Stockholm, Sweden, [10] Department of Clinical Science and Education, Division of Internal Medicine, Unit for Diabetes Research, Karolinska Institute, South Hospital, Stockholm, Sweden, [11] Center for Diabetes, Academica Specialist Centrum, Stockholm, Sweden, [12] Karolinska Institute, Department of Clinical Sciences, Danderyd University Hospital, Division of Internal Medicine, Stockholm, Sweden, [13] Institute for Molecular Medicine Finland (FIMM), University of Helsinki, Helsinki, Finland, [14] Department of Public Health and Clinical Medicine, Sunderby Research Unit, Umeå University, Umeå, Sweden, [15] Department of Medicine, University of Gothenburg, Gothenburg, Sweden, [16] Institute of Clinical Medicine, Faculty of Medicine, University of Oslo, Oslo, Norway

OPEN ACCESS

Edited by:
Shane T. Grey, Garvan Institute of Medical Research, Australia

Reviewed by:
Amelia K. Linnemann, Indiana University, United States
Marie-Sophie Nguyen-Tu, Imperial College London, United Kingdom

***Correspondence:**
Valeriya Lyssenko
valeriya.lyssenko@uib.no
Magdalena Keindl
magdalena.keindl@uib.no

Specialty section:
This article was submitted to Diabetes: Molecular Mechanisms, a section of the journal Frontiers in Endocrinology

Received: *23 June 2020*
Accepted: *06 October 2020*
Published: *30 October 2020*

Citation:
Keindl M, Fedotkina O, du Plessis E, Jain R, Bergum B, Mygind Jensen T, Laustrup Møller C, Falhammar H, Nyström T, Catrina S-B, Jörneskog G, Groop L, Eliasson M, Eliasson B, Brismar K, Nilsson PM, Berg TJ, Appel S and Lyssenko V (2020) Increased Plasma Soluble Interleukin-2 Receptor Alpha Levels in Patients With Long-Term Type 1 Diabetes With Vascular Complications Associated With IL2RA and PTPN2 Gene Polymorphisms. Front. Endocrinol. 11:575469. doi: 10.3389/fendo.2020.575469

Type 1 diabetes (T1D) is largely considered an autoimmune disease leading to the destruction of insulin-producing pancreatic β cells. Further, patients with T1D have 3–4-fold increased risk of developing micro- and macrovascular complications. However, the contribution of immune-related factors contributing to these diabetes complications are poorly understood. Individuals with long-term T1D who do not progress to vascular complications offer a great potential to evaluate end-organ protection. The aim of the present study was to investigate the association of inflammatory protein levels with vascular complications (retinopathy, nephropathy, cardiovascular disease) in individuals with long-term T1D compared to individuals who rapidly progressed to complications. We studied a panel of inflammatory markers in plasma of patients with long-term T1D with (n = 81 and 26) and without (n = 313 and 25) vascular complications from two cross-sectional Scandinavian cohorts (PROLONG and DIALONG) using Luminex technology. A subset of

PROLONG individuals (n = 61) was screened for circulating immune cells using multicolor flow cytometry. We found that elevated plasma levels of soluble interleukin-2 receptor alpha (sIL-2R) were positively associated with the complication phenotype. Risk carriers of polymorphisms in the *IL2RA* and *PTPN2* gene region had elevated plasma levels of sIL-2R. In addition, cell surface marker analysis revealed a shift from naïve to effector T cells in T1D individuals with vascular complications as compared to those without. In contrast, no difference between the groups was observed either in IL-2R cell surface expression or in regulatory T cell population size. In conclusion, our data indicates that *IL2RA* and *PTPN2* gene variants might increase the risk of developing vascular complications in people with T1D, by affecting sIL-2R plasma levels and potentially lowering T cell responsiveness. Thus, elevated sIL-2R plasma levels may serve as a biomarker in monitoring the risk for developing diabetic complications and thereby improve patient care.

Keywords: cardiovascular disease, Cluster of Differentiation 25 (CD25), diabetes complications, nephropathy, regulatory T cells, retinopathy, sIL-2R

INTRODUCTION

Type 1 diabetes (T1D) is characterised by T cell mediated autoimmune destruction of insulin-producing pancreatic β cells (1, 2), causing T1D individuals to become insulin-dependent throughout their life (3). Most of the patients with T1D develop macrovascular complications such as cardiovascular disease (CVD), and microvascular complications, including proliferative diabetic retinopathy (PDR), chronic kidney disease (CKD), and peripheral neuropathy (PN) (4). The rising prevalence of T1D and its associated long-term vascular complications clearly confer a humanistic (5) and socio-economic burden (6). Vascular complications in T1D individuals are a common cause of mortality related to end-organ damage as compared to the non-diabetic population (4, 7). Remarkably, few patients with T1D do not progress to these vascular complications despite long disease duration and chronic hyperglycaemia, and therefore exert great potential to evaluate end-organ protection (8).

Although T1D individuals with complications show considerable derangement in immunological processes like having elevated concentrations of C-reactive protein (CRP), a marker of inflammation, proinflammatory cytokines interleukin-6 (IL-6), and tumor necrosis factor alpha (TNF-α) as compared to individuals without complications (9), the extent of contribution of immunological factors to the development of vascular complications in patients with T1D is poorly understood.

Over the past decades, both genetic (10, 11) and immunological (12, 13) studies revealed IL-2 receptor (IL-2R) and its downstream signalling pathways as central players in the pathogenesis of T1D (14). Upon binding of IL-2 to its receptor IL-2R, a cascade of signalling events is initiated. These events are negatively regulated by the ubiquitously expressed phosphatase tyrosine-protein phosphatase non-receptor type 2 (PTPN2) (14, 15). IL-2 signalling is critical for the function of regulatory T cells (Tregs), a type of suppressive immune cell, which plays an indispensable role in maintaining immune homeostasis (16) and prevention of autoimmune diseases (17, 18). In addition, elevated levels of soluble IL-2R alpha (sIL-2R; alternative: IL-2RA, CD25) have been reported to be an important factor in the development of diabetic retinopathy in non-insulin-dependent diabetes patients (19) and coronary artery calcification in T1D patients (20). However, a limitation of both studies was that the patient group without complications had a considerably shorter diabetes duration compared to the patient group with the respective complications. Therefore, some of the patients in the complications-free group could have later progressed to vascular complications. Furthermore, Colombo et al. (2019) reported that elevated levels of sIL-2R were associated with a decline in estimated glomerular filtration rate (eGFR) in T1D patients (21).

The aim of the present study was to evaluate plasma levels of inflammatory proteins including but not limited to sIL-2R in long-term T1D individuals with and without vascular complications. Additionally, a subset of patients was screened for circulating immune cells to investigate cell populations associated with developing vascular complications in T1D individuals. Finally, plasma sIL-2R levels were correlated to genetic risk variants in *IL2RA* and *PTPN2*.

METHODS

Study Design

This immunological investigation forms a part of the PROtective genetic and non-genetic factors in diabetic complications and LONGevity (PROLONG) study, which was launched to identify protective factors against complications in long-term T1D individuals. Patients were recruited from seven departments of endocrinology/diabetes outpatient clinics in Sweden and at the Steno Diabetes Center in Denmark. As an extended collaborative effort, we included T1D individuals from a Norwegian cohort, DIALONG. The DIALONG study also included non-diabetic spouses or friends as a control group.

We classified T1D patients into two groups comparing their diabetes complications status. Non-progressors (NP) were

defined as patients with a T1D duration of over 30 years without having progressed to any of the specified complications. Patients who progressed to complications within 25 years of T1D diagnosis were defined as rapid progressors (RP). We defined late progressors (LP) as T1D patients that did progress to complications >25 years post diagnosis. For this study RPs and LPs were pooled into one group referred to as progressors (P).

In PROLONG, PDR was defined by the presence of proliferative retinopathy in at least one eye, confirmed laser treatment (panretinal photocoagulation) or blindness. For CKD we used the following inclusion criteria: presence of nighttime albuminuria over 200 µg/min, macroalbuminuria over 300 mg/g or a documented diabetic kidney disease diagnosis. None of the PROLONG participants were treated with SGLT2 inhibitors. Documented events including non-fatal myocardial infarction, stroke (haemorrhagic or ischemic), balloon angioplasty, or coronary artery bypass were defined as CVD. There was limited information on CVD, as the original focus of PROLONG was on microvascular complications.

In DIALONG (22) macro- and microvascular complications were defined using similar criteria as in PROLONG. PDR was defined by the presence of proliferative retinopathy or blindness. Laser treatment was not used as criteria here as it was not exclusively applied to proliferative retinopathy in this study. CKD was adjusted to include patients with persistent microalbuminuria or proteinuria. None of the DIALONG participants were treated with SGLT2 inhibitors. CVD was defined by stroke or myocardial infarction events, coronary artery bypass or percutaneous coronary intervention (PCI), diagnosed peripheral vascular disease or heart failure.

The regional ethical committees approved the studies (PROLONG: Denmark H-2-2013-073, Sweden 777/2009, Norway 2019/1324; DIALONG: Norway 2014/851) and all participants provided written informed consent.

Blood Sampling

Collected EDTA plasma was aliquoted and stored at -80°C for ~6 years (PROLONG) and ~3 years (DIALONG).

For peripheral blood mononuclear cells (PBMCs) isolation, peripheral blood from patients with T1D (PROLONG) with and without complications was collected in CPT tubes (BD Vacutainer) at the Steno Diabetes Center, Denmark. PBMCs were subsequently isolated by density gradient centrifugation and cryopreserved in human AB serum containing 10% DMSO at -80°C for ~5 years.

Cytokine Analysis

In DIALONG, plasma cytokines were measured in 79 individuals using an Invitrogen™ Human Cytokine 30-Plex kit (LHC6003M, Thermo Fisher Scientific) according to the manufacturer's instructions. The following adjustments were made to the protocol: (a) one additional standard was included in the serial dilution, making the standard range from 1:3 to 1:2,187; (b) undiluted plasma samples that underwent one freeze-thaw cycle were measured. The following biomarkers were detected in >90% of samples (CCL11, IFN-α, IL-12, sIL-2R, CXCL10, CCL2, CCL3, CCL4 and CCL5), whereas others were only detected in 40–75% (FGF basic, G-CSF, HGF, IL-13, IL-1RA, CXCL9, VEGF) and <17% of patients (EGF, IFN-γ, IL-10, IL-15, IL-17A, IL-1β, IL-2, IL-4, IL-6, TNF-α). GM-CSF, IL-5, IL-7, and IL-8 were not detected in any samples.

In PROLONG, we used a custom-designed ProCartaPlex™ Human Cytokine Panel (sIL-2R, CCL2, CCL11, IFN-α; Thermo Fisher Scientific) according to manufacturer's instructions to measure plasma cytokines. The following adjustments were made to the protocol: (a) one additional standard was included in the serial dilution, making the standard range from 1:4 to 1:32,768 (in pg/ml: sIL-2R 10.06–82,425; CCL2 0.45–3,650; CCL11 0.07–550; IFN-α 0.08–625); (b) undiluted plasma samples that underwent one freeze-thaw cycle were measured.

Data was acquired on a Luminex® 100™, counting 3,000 (DIALONG) and 600 (PROLONG) beads per well. The five-parameter logistic algorithm [weighted by 1/y, (V2.4)] and raw median fluorescence intensity values were used for the creation of standard curves.

Genetic Analysis

The DNA samples in the PROLONG study were genotyped using InfiniumCoreExome-24v1-1 array. Standard quality control steps for GWAS were performed. Imputation was performed using Michigan Imputation Server (https://imputationserver.sph.umich.edu/index.html) using Haplotype Reference Consortium Release 1.1 (HRC.r1-1, GRCh37) as a reference panel. Variants with minor allele frequency (MAF) <5% were excluded before imputation. In the present study, we extracted the region for the *IL2RA* (Chromosome 10: 6,052,652-6,104,288, build GRch37) and *PTPN2* gene (Chromosome 18: 12,785,477-12,929,642, build GRch37) for analysis. Only variants with imputation quality R^2 >0.4 and with MAF >5% were included in the analysis.

Principal component analysis (PCA) was performed on pruned, directly genotyped SNPs using 1,000 Genomes' reference panel version 5A. Population outliers were examined based on visual inspection of PC1 and PC2, and outliers were excluded from the further analysis. Only individuals with complete data on sIL-2R, sex, complication group, HbA1c and age at visit were included. In total, there were 330 individuals analyzed. We used linear regression adjusted for sex, age, and complication group to identify associations between genetic variants and log-transformed plasma levels of sIL-2R.

Antibodies Used for Flow Cytometry

We designed two flow cytometry panels using multiple fluorochrome-conjugated antibodies. Panel 1 includes 14 markers (14 colors), which can discriminate the main mononuclear immune cell types (B cells, T cells, NK cells, monocytes, dendritic cells), and endothelial progenitor cells. Panel 2 includes 16 markers (15 colors) and focuses specifically on different types of T cells. Pacific orange dye (250 ng/ml; Life Technologies) was used as a live/dead marker in both panels. The monoclonal antibodies used in the two panels during the flow cytometry protocol are listed in **Supplementary Table 1**.

Fluorescent Staining for Flow Cytometry

Before staining, cryopreserved PBMCs were rapidly thawed using a water bath set to 37°C and washed once in cold PBS (without calcium and magnesium, Lonza) containing 5% AB serum and Benzonase® Nuclease (1:10,000; Merck Millipore) by centrifugation at 450 x g for 5 min at 4°C. The PBMCs were then resuspended in cold PBS and stained with pacific orange (250 ng/ml; Life Technologies) for 20 min on ice in the dark. Following live/dead staining, cells were washed once, taken up in cold FACS-buffer (PBS containing 0.5% BSA) and incubated with 2 µl Fc receptor block (Miltenyi Biotec) per 1 x 10^6 cells for 10 min on ice. Cells were then subdivided into two parts and incubated for 30 min on ice in the dark with the respective antibody staining panel. The samples were subsequently washed once and re-suspended in FACS-buffer prior to analysis at the flow cytometer.

Flow Cytometry Analysis

Samples were acquired on a LSRI Fortessa flow cytometer (BD Biosciences) with BD FACSDiva™ Software (BD Biosciences) at the Bergen Flow Cytometry Core Facility, University of Bergen, Norway. The flow cytometer was equipped with 407, 488, 561, and 635 nm lasers, and emission filters for PerCP-Cy5.5 (Long Pass (LP): 685, Band Pass (BP): 695/40), Alexa Fluor 488 (LP: 505, BP: 530/30), PE-Cy7 (LP: 750, BP: 780/60), PE (LP: -, BP: 582/15), APC (LP: -, BP: 670/14), Pacific blue (LP: -, BP: 450/50), Pacific orange (LP: 570, BP: 585/42), and BV786 (LP: 750, BP: 780/60). The cytometer was routinely calibrated with BD cytometer setup and tracking beads (BD Biosciences). An average of 138,635 (panel 1) and 122,287 (panel 2) events were recorded in the intact single cell gate and mean percentage of live cells was 98 and 96% for panels 1 and 2, respectively. Flow cytometry data was analyzed in FlowJo™ 10 (Tree Star). Compensation beads (eBioscience) stained with the respective antibody were used as controls to calculate the compensation matrix. The representative gating strategies for both panels are shown in **Supplementary Figures 1** and **2** and were validated with the unsupervised gating method using the tSNE algorithm (**Supplementary Figures 3B, C**). For accurate gating, fluorescence minus one (FMO) controls were run regularly for both panels.

Statistical Analysis

sIL-2R was log2 transformed prior to analysis. Values above the ordinary range were removed by biological consideration and literature review. The Mann-Whitney U test was used in the comparison between the complication groups in the analyses of plasma cytokines. To evaluate the association between two variables we used the Pearson correlation formula. In flow cytometry analysis, multiple linear regression was applied and adjusted for the age and sex covariates. Differences were considered statistically significant when $p < 0.05$. The study was of exploratory nature and hence no correction was made for multiple comparisons. Comparisons between patient groups, correlations and the production of associated graphs were done using R Studio (Version 1.1.456). Figures were arranged in Adobe Illustrator CS6.

RESULTS

Elevated sIL-2R in T1D Individuals

Baseline characteristics of DIALONG study participants are given in **Table 1**. There were 26 T1D individuals with vascular complications (progressor, P), of whom 10 had CKD, 11 had CVD, and all apart from one had PDR. As the matching groups we included 25 T1D individuals without any vascular complications (non-progressors, NP) and 28 healthy controls. In brief, progressors had significantly higher BMI and slightly elevated HbA1c. The groups were balanced regarding age, sex, and eGFR.

There was a significant increase of sIL-2R ($p = 0.0011$) in T1D as compared to healthy individuals (**Figure 1A**). The increase was gradual in relation to vascular complication status, being highest in the progressor group (Control vs. NP: $p = 0.014$; Control vs. P: $p = 0.0021$; NP vs. P: $p = 0.47$) (**Supplementary Figure 4A**). None of the other analyzed cytokines showed significant differences between the T1D groups in relation to their complication status (**Supplementary Figure 5A**). An overview over the detection rate for each investigated cytokine is provided in **Supplementary Figure 5B**.

To investigate complication status further, we stratified progressors into those with CKD, CVD, or PDR. These analyses revealed that progressors with CVD had significantly elevated sIL-2R plasma levels ($p = 0.029$) as compared to NPs (**Supplementary Figure 4B**). Plasma sIL-2R was slightly increased in progressors with CKD ($p = 0.19$) as compared to NPs (**Supplementary Figure 4C**), and sIL-2R correlated negatively with eGFR (T1D: $R = -0.42$, $p = 0.0037$) (**Supplementary Figure 4D**). Adjusting for eGFR did not change the observed result with CKD ($p = 0.35$). Plasma sIL-2R was elevated in progressors with PDR compared to NPs ($p = 0.36$) (**Supplementary Figure 4E**). Monocyte chemotactic protein-1 (CCL2, alternative: MCP-1) plasma levels were significantly higher in progressors with CKD ($p = 0.021$) and CVD ($p = 0.013$) compared to NPs (**Supplementary Figures 4F, G**). CCL2 was slightly elevated in progressors with PDR compared to NPs ($p = 0.09$) (**Supplementary Figure 4H**).

Elevated sIL-2R in T1D Individuals with Vascular Complications

In order to confirm our cytokine findings in DIALONG in a larger and independent cohort, we measured 4 nominally associated cytokines (sIL-2R, CCL2, CCL11, IFN-α) in plasma from PROLONG patients with T1D with and without complications (n = 394). Clinical characteristics for this cohort are summarized in **Table 2**. We included 81 patients with T1D with vascular complications (progressors, P), of whom 40 had PDR, 58 had CKD, and on 2 we had information on CVD. Those individuals were compared to 313 T1D individuals without any vascular complications (non-progressors, NP). Progressors were significantly younger in age, displayed significantly higher BMI and HbA1c and lower eGFR and diabetes duration compared to NPs. The groups were balanced regarding sex.

TABLE 1 | Clinical characteristics of the DIALONG study participants.

Cohort	Healthy control	NP	Progressors	p-value
N	28	25	26	
Age (years)	62.2 ± 6.3	63.1 ± 6.5	62.2 ± 6.5	ns
BMI (kg/m^3)	26.6 ± 4.2[a]	25.1 ± 3.3	27.3 ± 3.9	3.66×10^{-2}
Diabetes duration (years)	NA	50.5 ± 3.4	51.3 ± 5.1	ns
Age at diagnosis (years)	NA	12.6 ± 5.6	10.8 ± 6.5	ns
Sex (% female)	57%	48%	54%	ns
HbA1c (%)	5.5 ± 0.2	7.3 ± 0.8	7.6 ± 0.8	ns
GAD AA positive (%)	7%	29%[b]	32%[c]	ns
IA-2 AA positive (%)	4%	8%[b]	16%[c]	ns
Insulin AA positive (%)	0%	71%[b]	68%[c]	ns
ZnT8 AA positive (%)	0%	4%[b]	8%[c]	ns
AA positive (%)	7%	75%[b]	80%[c]	ns
eGFR (ml/min/1.73 m^3)	83.4 ± 16.4	85.4 ± 15.1	78.5 ± 26.1	ns
C-peptide (nmol/L)	718.3 ± 225.3	undetectable	undetectable	ns
CRP (mg/L)	1.8 ± 2.3[d]	3.3 ± 6.1[e]	3.0 ± 3.3[e]	ns
Statins	6 (21%)	9 (36%)	17 (65%)	3.87×10^{-2}
Beta-blocker	1 (4%)	2 (8%)	10 (38%)	1.16×10^{-2}
ACEi/ARB	6 (21%)	7 (28%)	19 (73%)	1.49×10^{-3}
Antiplatelet agent	6 (21%)	1 (4%)	14 (54%)	1.16×10^{-4}
Loop diuretics	0 (0%)	1 (4%)	7 (27%)	2.69×10^{-2}
PDR/CKD/CVD (n)	NA	NA	25/10/11	

Values for continuous variables are presented as mean ± SD. P-values were calculated between NPs and progressors by Mann–Whitney U test. NP, non-progressor; BMI, body mass index; HbA1c, haemoglobin A1c; GAD, glutamic acid decarboxylase; AA, autoantibody; IA2, islet cell antigen-2; ZnT8, zink transporter 8; eGFR, estimated glomerular filtration rate; C-peptide, connecting peptide; CRP, C-reactive protein; ACEi, angiotensin-converting enzyme; ARB, angiotensin receptor blocker; PDR, proliferative diabetic retinopathy; CKD, chronic kidney disease; CVD, cardiovascular disease.

[a]n = 27, [b]n = 24; [c]n = 25, [d]n = 21, [e]n = 20.

Three cytokines were detected in 100% of samples (sIL-2R, CCL2, CCL11), while IFN-α was only detected <16% of samples (**Supplementary Figure 6B**). We observed a significant increase of sIL-2R (p = 0.0064) in progressors compared to NPs (**Figure 1B**). This observed difference was even more pronounced (p = 0.00084) when comparing NPs with progressors with PDR (**Figure 1C**). Additionally, sIL-2R was slightly increased in patients with CKD (p = 0.077) compared to NPs (**Supplementary Figure 6C**), and sIL-2R correlated negatively with eGFR (R = -0.12, p = 0.025) (**Supplementary Figure 6D**). Adjusting for eGFR using linear regression, resulted in a significant increase in sIL-2R between progressors with CKD and NPs (p = 0.041). Comparisons for CVD could not be made due to the small sample size of progressors with information on CVD (n = 2). As observed in the DIALONG cohort, there was no significant difference between the complication groups in CCL2 (p = 0.46), CCL11 (p = 0.25), and IFN- α (p = 0.40) (**Supplementary Figure 6A**). In PROLONG, CCL2 was not elevated in progressors with CKD (p = 0.39) (**Supplementary Figure 6E**). Progressors with PDR and NPs showed similar levels of CCL2 (p = 0.97) (**Supplementary Figure 6F**).

Association of sIL-2R Levels With IL2RA and PTPN2 Gene Variants

To identify associations between genetic variants in *IL2RA* and plasma levels of sIL-2R, we used linear regression adjusting for sex, age, and group. Plasma levels of sIL-2R were significantly associated with 68 SNPs in the *IL2RA* gene (**Table 3**), with rs12722489 showing the statistically strongest association (p = $5{,}19 \times 10^{-7}$). Two of our identified SNPs are located in exon 8, namely rs12722606 and rs12722605. The majority of the associated SNPs (n = 51) are located in the large intron 1 area of *IL2RA*.

Furthermore, sIL-2R levels were significantly associated with 53 intronic SNPs in the *PTPN2* gene region (**Table 4**). The variant rs12971201 showed the strongest association with plasma sIL-2R (p = 1.09×10^{-3}). When we conditioned this analysis for the T1D-associated SNP rs2104286 in *IL2RA*, we could still identify 42 *PTPN2* variants to be independently associated with sIL-2R (**Table 4**). Here rs592390 had the strongest association with plasma sIL-2R (p = 2.16×10^{-3}).

Cell-Surface Marker Analysis on PBMC of T1D Individuals

Our flow cytometry panels enabled us to investigate a range of different cell populations, which are summarized in **Supplementary Figure 3A**. The applied gating strategies are provided in **Supplementary Figure 1** and **2**. Baseline characteristics for this subset of PROLONG patients are provided in **Table 2**. In total, we performed flow cytometry analysis on 61 T1D samples, of which 17 were from progressors. The groups were balanced regarding age and sex.

We identified a significant decrease of $CD8^+$ naïve T cells ($CD3^+CD8^+CD45RA^+CCR7^+CCR5^-$) (p = 0.0046) and increase of $CD8^+$ effector T cells ($CD3^+CD8^+CD45RA^+CCR7^-$) (p = 0.070) in progressors compared to NPs (**Figures 2A, B**). Furthermore, progressors had significantly increased $CD4^+$ effector T cells ($CD3^+CD4^+CD45RA^+CCR7^-$) (p = 0.045) and decreased $CD4^+$ naïve T cells ($CD3^+CD4^+CD45RA^+CCR7^+CCR5^-$) (p = 0.14) compared to NPs (**Figures 2C, D**). To summarize, we observed

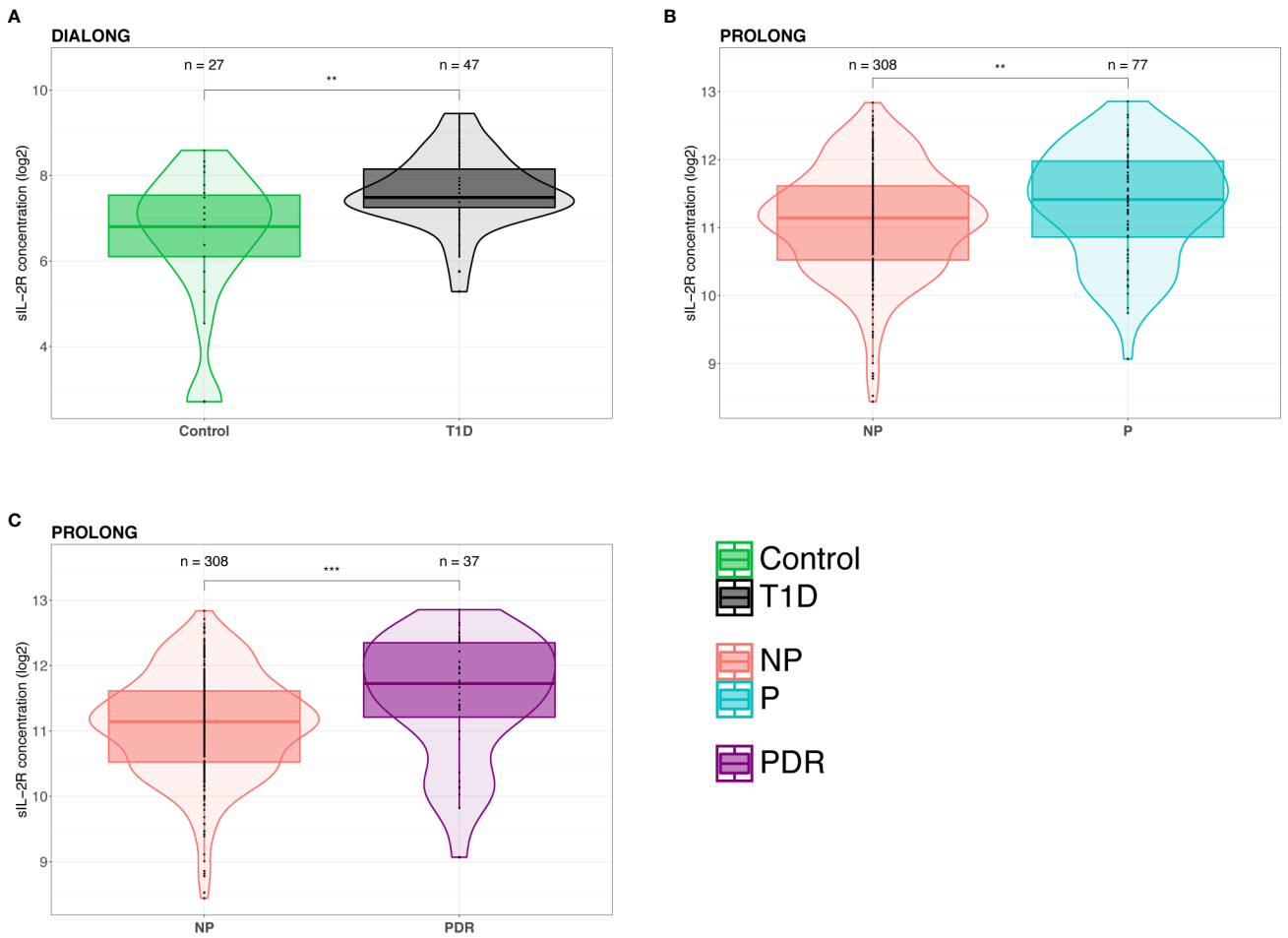

FIGURE 1 | Elevated plasma levels of sIL-2R in patients with type 1 diabetes (T1D). **(A)** Patients with T1D from the DIALONG cohort had significantly elevated sIL-2R plasma levels compared to healthy controls. **(B)** In PROLONG, sIL-2R plasma levels were significantly increased in T1D with vascular complications (progressors, P) compared to T1D patients without complications (non-progressors, NP). **(C)** PROLONG progressors with proliferative diabetic retinopathy (PDR) showed significantly higher sIL-2R plasma levels compared to progressors with other vascular complications. (The Mann-Whitney U test was used in the comparison between the different groups. **p < 0.01 and ***p < 0.001).

TABLE 2 | Clinical characteristics of the PROLONG participants.

Cohort	Cytokine assay			Flow cytometry		
	NP	Progressors	p-value	NP	Progressors	p-value
n	313	81		44	17	
Age (yrs.)	58.1 ± 10.6	44.6 ± 13.7[a]	1.08×10^{-13}	50.6 ± 7.2	50.8 ± 15.5	ns
BMI (kg/m^3)	24.8 ± 3.7[b]	26.4 ± 4.7	3.94×10^{-3}	25.3 ± 4.2	25.3 ± 4.7	ns
Diabetes duration (years)	40.6 ± 8.6	22.4 ± 8.3	$<2.2 \times 10^{-16}$	37.7 ± 5.1	29.9 ± 13.4	9.49×10^{-3}
Age at diagnosis (years)	17.5 ± 9.9	22.0 ± 14.4[a]	ns	12.9 ± 6.0	20.9 ± 13.2	4.63×10^{-2}
Sex (% female)	58%	53%	ns	59%	53%	ns
HbA1c (%)	7.6 ± 0.9	8.9 ± 1.5	3.33×10^{-14}	7.4 ± 0.9	8.5 ± 0.8	6.35×10^{-5}
GAD AA positive (%)	50%[c]	68%	8.15×10^{-3}	50%[d]	90%[e]	2.41×10^{-2}
eGFR (ml/min/1.73 m^3)	90.2 ± 15.5	97.4 ± 30.8[f]	3.66×10^{-3}	94.6 ± 16.6	93.3 ± 29.7	ns
C-peptide (nmol/L)	0.03 ± 0.07[g]	0.03 ± 0.05[h]	ns	0.01 ± 0.02[i]	0.02 ± 0.01[j]	3.37×10^{-2}
PDR/CKD/CVD (n)	NA	40/58/2		NA	10/12/0	

Values for continuous variables are presented as mean ± SD. P-values were calculated by Mann–Whitney U test. NP, non-progressor; BMI, body mass index; HbA1c, haemoglobin A1c; GAD, glutamic acid decarboxylase; AA, autoantibody; eGFR, estimated glomerular filtration rate; C-peptide, connecting peptide; PDR, proliferative diabetic retinopathy; CKD, chronic kidney disease; CVD, cardiovascular disease.

[a]n = 77; [b]n = 308; [c]n = 303; [d]n = 40; [e]n = 10; [f]n = 76; [g]n = 296; [h]n = 68; [i]n = 35; [j]n = 7.

TABLE 3 | Imputed *IL2RA* genotypes and their significant associations with sIL-2R in plasma.

Chr	SNP	bp*	Intron/Exon	A1	n	Beta (95% CI)	p-Value
10	rs12722489	6102012	Intron 1	T	330	–0.28 (–0.39, –0.17)	5.19×10^{-7}
10	rs12722517	6081040	Intron 1	C	330	–0.24 (–0.34, –0.14)	2.23×10^{-6}
10	rs9663421	6055604	Intron 7	T	330	0.25 (0.15, 0.35)	3.17×10^{-6}
10	rs12722553	6071284	Intron 1	A	330	–0.26 (–0.37, –0.15)	3.30×10^{-6}
10	rs12722551	6071379	Intron 1	T	330	–0.26 (–0.37, –0.15)	3.30×10^{-6}
10	rs791593	6083292	Intron 1	G	330	–0.23 (–0.33, –0.14)	4.22×10^{-6}
10	rs2104286	6099045	Intron 1	C	330	–0.24 (–0.33, –0.14)	4.63×10^{-6}
10	rs41294713	6080354	Intron 1	C	330	–0.25 (–0.36, –0.15)	5.23×10^{-6}
10	rs12722515	6081230	Intron 1	A	330	–0.25 (–0.36, –0.15)	5.23×10^{-6}
10	rs791590	6090322	Intron 1	T	330	–0.25 (–0.36, –0.15)	5.23×10^{-6}
10	rs2246031	6092210	Intron 1	T	330	–0.25 (–0.36, –0.15)	5.23×10^{-6}
10	rs7078614	6075831	Intron 1	T	330	–0.21 (–0.30, –0.12)	5.50×10^{-6}
10	rs7920946	6074634	Intron 1	C	330	–0.22 (–0.31, –0.13)	5.53×10^{-6}
10	rs4625363	6072504	Intron 1	G	330	–0.25 (–0.36, –0.15)	5.54×10^{-6}
10	rs12722527	6077328	Intron 1	T	330	–0.25 (–0.36, –0.15)	5.54×10^{-6}
10	rs12722523	6078390	Intron 1	A	330	–0.25 (–0.36, –0.15)	5.54×10^{-6}
10	rs12722561	6069893	Intron 1	T	330	–0.25 (–0.36, –0.15)	6.22×10^{-6}
10	rs12722559	6070273	Intron 1	A	330	–0.25 (–0.36, –0.15)	6.22×10^{-6}
10	rs12722606	6053133	Exon 8	A	330	0.25 (0.14, 0.36)	6.98×10^{-6}
10	rs11256335	6055222	Intron 7	A	330	0.25 (0.14, 0.36)	6.98×10^{-6}
10	rs12722605	6053163	Exon 8	A	330	0.29 (0.17, 0.42)	7.27×10^{-6}
10	rs12722497	6095928	Intron 1	A	330	0.35 (0.20, 0.50)	1.22×10^{-5}
10	rs11256464	6082558	Intron 1	T	330	0.32 (0.18, 0.47)	2.55×10^{-5}
10	rs11597237	6079017	Intron 1	T	330	–0.23 (–0.33, –0.12)	3.07×10^{-5}
10	rs11256416	6075359	Intron 1	T	330	–0.21 (–0.31, –0.11)	3.67×10^{-5}
10	rs7910961	6077796	Intron 1	T	330	0.20 (0.11, 0.30)	4.04×10^{-5}
10	rs4747837	6058735	Intron 7	G	330	–0.23 (–0.34, –0.12)	4.34×10^{-5}
10	rs7900385	6062748	Intron 4	A	330	–0.23 (–0.34, –0.12)	4.34×10^{-5}
10	rs12722588	6060433	Intron 6	T	330	–0.22 (–0.33, –0.11)	5.83×10^{-5}
10	rs12722587	6060630	Intron 6	T	330	–0.22 (–0.33, –0.11)	5.83×10^{-5}
10	rs7093069	6063319	Intron 4	T	330	–0.22 (–0.33, –0.11)	5.83×10^{-5}
10	rs11816044	6074082	Intron 1	A	330	0.20 (0.10, 0.30)	8.91×10^{-5}
10	rs7100984	6078539	Intron 1	A	330	0.20 (0.10, 0.30)	9.07×10^{-5}
10	rs12722574	6066462	Intron 2	A	330	–0.20 (–0.29, –0.10)	9.63×10^{-5}
10	rs4749894	6058323	Intron 7	G	330	0.22 (0.11, 0.33)	1.00×10^{-4}
10	rs4749924	6082396	Intron 1	C	330	0.20 (0.10, 0.29)	1.00×10^{-4}
10	rs6602398	6082953	Intron 1	T	330	0.20 (0.10, 0.29)	1.00×10^{-4}
10	rs7900744	6065611	Intron 3	G	330	–0.20 (–0.29, –0.10)	1.19×10^{-4}
10	rs791588	6089342	Intron 1	G	330	0.15 (0.06, 0.24)	7.71×10^{-4}
10	rs11256342	6057231	Intron 7	G	330	0.17 (.07, 0.26)	8.37×10^{-4}
10	rs12253981	6092346	Intron 1	G	330	0.16 (0.07, 0.25)	8.84×10^{-4}
10	rs2025345	6067688	Intron 2	G	330	0.16 (0.07, 0.26)	9.75×10^{-4}
10	rs12358961	6066195	Intron 3	A	330	0.16 (0.07, 0.26)	1.03×10^{-3}
10	rs1924138	6096158	Intron 1	A	330	0.16 (0.06, 0.25)	1.06×10^{-3}
10	rs11256497	6087794	Intron 1	A	330	0.15 (0.06, 0.25)	1.36×10^{-3}
10	rs10795752	6072354	Intron 1	T	330	0.15 (0.06, 0.25)	1.51×10^{-3}
10	rs2245675	6095577	Intron 1	A	330	0.16 (0.06, 0.25)	1.55×10^{-3}
10	rs2256852	6096923	Intron 1	A	330	0.16 (0.06, 0.25)	1.55×10^{-3}
10	rs791587	6088699	Intron 1	A	330	0.14 (0.05, 0.23)	1.62×10^{-3}
10	rs12251836	6091281	Intron 1	A	330	0.15 (0.06, 0.24)	1.65×10^{-3}
10	rs6602368	6062915	Intron 4	C	330	0.15 (0.06, 0.24)	1.67×10^{-3}
10	rs2476491	6095410	Intron 1	T	330	0.16 (0.06, 0.26)	1.74×10^{-3}
10	rs4749926	6085312	Intron 1	A	330	0.15 (0.05, 0.24)	2.60×10^{-3}
10	rs11256457	6080794	Intron 1	G	330	0.15 (0.05, 0.24)	2.72×10^{-3}
10	rs10905641	6072293	Intron 1	C	330	0.14 (0.05, 0.23)	3.41×10^{-3}
10	rs6602379	6073374	Intron 1	G	330	0.14 (0.05, 0.24)	3.51×10^{-3}
10	rs809356	6091148	Intron 1	C	330	0.13 (0.04, 0.22)	3.60×10^{-3}
10	rs2256774	6097165	Intron 1	C	330	0.14 (0.05, 0.23)	3.87×10^{-3}
10	rs1323657	6072427	Intron 1	A	330	0.13 (0.04, 0.23)	3.95×10^{-3}
10	rs7072398	6079846	Intron 1	A	330	0.13 (0.04. 0.22)	5.33×10^{-3}
10	rs10795763	6096199	Intron 1	G	330	0.13 (0.04. 0.22)	5.34×10^{-3}
10	rs7917726	6096600	Intron 1	G	330	0.13 (0.04. 0.22)	5.34×10^{-3}
10	rs706779	6098824	Intron 1	C	330	0.12 (0.03. 0.21)	7.97×10^{-3}

(Continued)

TABLE 3 | Continued

Chr	SNP	bp*	Intron/Exon	A1	n	Beta (95% CI)	p-Value
10	rs10905656	6086093	Intron 1	A	330	0.11 (0.02. 0.20)	1.51×10^{-2}
10	rs3793713	6059704	Intron 7	G	330	0.11 (0.01. 0.20)	2.56×10^{-2}
10	rs4749920	6071453	Intron 1	C	330	0.11 (0.01. 0.21)	3.73×10^{-2}
10	rs4749921	6071654	Intron 1	C	330	0.11 (0.01. 0.21)	3.73×10^{-2}
10	rs4747845	6074441	Intron 1	A	330	0.11 (0.01. 0.21)	3.73×10^{-2}

SNP positions according to the Genome Reference Consortium Human Build 37 (GRch37).

Linear regression model: p-value = adjusted for age, sex and complication group. Chr, chromosome; SNP, single nucleotide polymorphism; bp, base pair; A1, minor allele; CI, confidence interval.

a shift from naïve to effector T cells ($CD4^+$ and $CD8^+$) in PBMCs from T1D patients with vascular complications compared to those without.

Since we observed significant differences in plasma sIL-2R in the two PROLONG groups, we also investigated cell surface expression of interleukin-2 receptor alpha (CD25) on PBMCs. Remarkably, we did not see differences between NPs and progressors in neither $CD25^+$ T cells ($p = 0.84$) nor Tregs ($CD3^+CD4^+CD25^{++}CD127^-$) ($p = 0.27$) (**Supplementary Figures 7A, B**).

DISCUSSION

The present study revealed that plasma sIL-2R levels are reproducibly elevated in individuals with long-term T1D with severe vascular complications as compared to those who remained free from to vascular complications despite more than 30 years of diabetes duration. Further, plasma levels of sIL-2R were associated with SNPs in the *IL2RA* and *PTPN2* gene regions, which might suggest underlying genetic determinants and possibly biological causal inference. Finally, our results are in agreement with published studies confirming an increase of circulating sIL-2R in patients with T1D when compared to healthy controls, which might further emphasize that immune factors contributing to diabetes pathogenesis might early on govern progression to vascular complications (12, 23).

The biological function of sIL-2R is not yet completely understood, but there is evidence that it reflects an imbalance in Treg and effector T cell (T_{EFF}) activity (14, 24). It has been suggested that there is a reduced immunosuppressive function of Tregs due to impaired IL-2 signalling in T1D (24–28), a defect which may subsequently lead to a more aggressive immune destruction of pancreatic β cells by T_{EFF} (12, 28). In addition, defects in the intracellular IL-2 pathways and a decreased regulatory function have recently been reported in patients with type 2 diabetes (T2D) (29). In many autoimmune diseases, such as multiple sclerosis (MS) (30), rheumatoid arthritis (31), primary Sjögren's syndrome (32), scleroderma (33), and inflammatory myopathies (34), but also in various cancers (31), sIL-2R has been proposed to be a biomarker for disease activity.

Patients with T1D develop the disease at an early age and a large proportion of them will progress to devastating vascular complications representing a major problem because the tools for monitoring when and how disease deteriorates are not available (4). Diabetes retinopathy is the most common vascular complication of diabetes (35) and the proliferative form of diabetic retinopathy (PDR) is the leading cause of vision loss in adults (36). Previous studies show that several inflammatory cytokines are involved in the pathogenesis and progression of PDR, including sIL-2R (19), however, not all of the results have been replicated. In the present study, both PROLONG and DIALONG progressors with PDR had higher plasma levels of sIL-2R compared to NPs, supporting the notion that sIL-2R could emerge as a contributing player not only in the pathogenesis of T1D but also in disease progression.

An additional evidence in the present study to biological importance of sIL-2R were our findings that 68 *IL2RA* SNPs are associated with sIL-2R plasma levels in PROLONG patients with T1D and correlated with the elevated sIL-2R levels observed in progressors accordingly. *IL2RA* rs12722489 showed the strongest association with sIL-2R plasma levels in patients with T1D and is located in the large intron 1. This particular SNP has been identified as a risk factor for MS in several studies (37–39). However, a secondary association was suggested due to the nearby location of rs2104286 (Linkage disequilibrium D' = 1, $R^2 = 0.58$), which is a well-recognized T1D risk factor (11, 37) and also significantly associated with plasma sIL-2R in our dataset. Interestingly, one of our identified SNPs, rs2256774, was associated with higher levels of Rubella antibodies (40), and Rubella viral infections have been associated with the onset of T1D (41, 42). Additionally, multiple *IL2RA* variants have been shown to correlate with sIL-2R levels in T1D (10) and MS (37) and *IL2RA* gene variants are associated with susceptibility of T1D (10, 11, 43). Further, functional studies support these results by suggesting that specific *IL2RA* variants cause defects in immune homeostasis due to impaired IL-2 signalling in Tregs (25, 27, 44).

Interestingly, seventeen of our identified SNPs are positioned within the first 15 kb of the first intron of the *IL2RA* gene, which has been described as a super-enhancer region due to a cluster of histone 3 lysine 27 acetylation (H3K27ac) elements in this area (45). Notably, many of the *IL2RA* SNPs related to autoimmune diseases fall into this region and affect transcription factor binding and enhancer activity (46). Several of our identified SNPs have been reported to be associated with DNA methylation at the *IL2RA* promoter locus, particularly rs6602398 and rs4749926 (47). Despite having detected a number of *IL2RA* SNPs to be associated with sIL-2R, it is challenging to conclude the direct effect of those mostly intronic SNPs on the expression of IL-2R itself and in-depth research is scarce. However, it has

TABLE 4 | Imputed *PTPN2* genotypes and their significant associations with sIL-2R in plasma.

Chr	SNP	bp*	Intron/Exon	A1	n	Beta (95% CI)	p-Value$_a$	p-Value$_b$
18	rs12971201	12830538	Intron 4	A	330	0.16 (0.07, 0.26)	1.09×10^{-3}	3.01×10^{-3}
18	rs2542162	12820900	Intron 5	T	330	0.16 (0.06, 0.26)	1.13×10^{-3}	2.91×10^{-3}
18	rs2847281	12821593	Intron 5	G	330	0.16 (0.06, 0.26)	1.13×10^{-3}	2.91×10^{-3}
18	rs2852151	12841176	Intron 2	A	330	0.16 (0.06, 0.26)	1.16×10^{-3}	3.38×10^{-3}
18	rs3826557	12843263	Intron 2	T	330	0.16 (0.06, 0.26)	1.16×10^{-3}	3.38×10^{-3}
18	rs674222	12848349	Intron 2	C	330	0.16 (0.06, 0.26)	1.16×10^{-3}	3.38×10^{-3}
18	rs2847273	12856908	Intron 2	C	330	0.16 (0.06, 0.26)	1.16×10^{-3}	3.38×10^{-3}
18	rs641085	12824930	Intron 5	T	330	0.15 (0.06, 0.24)	1.61×10^{-3}	2.22×10^{-3}
18	rs592390	12822314	Intron 5	C	330	0.15 (0.06, 0.24)	1.67×10^{-3}	2.16×10^{-3}
18	rs12957037	12829065	Intron 4	G	330	0.15 (0.06, 0.24)	1.67×10^{-3}	2.16×10^{-3}
18	rs588447	12832842	Intron 3	C	330	0.15 (0.06, 0.24)	1.69×10^{-3}	2.48×10^{-3}
18	rs8087237	12834359	Intron 3	A	330	0.15 (0.06, 0.24)	1.69×10^{-3}	2.48×10^{-3}
18	rs478582	12835976	Intron 3	C	330	0.15 (0.06, 0.24)	1.69×10^{-3}	2.48×10^{-3}
18	rs559406	12857002	Intron 2	G	330	−0.14 (−0.24, −0.05)	1.94×10^{-3}	2.44×10^{-3}
18	rs960550	12827697	Intron 4	T	330	0.15 (0.06, 0.25)	2.08×10^{-3}	6.02×10^{-3}
18	rs4797709	12882359	Intron 1	C	330	0.15 (0.05, 0.24)	2.43×10^{-3}	6.64×10^{-3}
18	rs2292759	12884343	upstream	A	330	0.15 (0.05, 0.24)	2.43×10^{-3}	8.09×10^{-3}
18	rs2542157	12787247	Intron 10	G	330	0.14 (0.04, 0.23)	5.57×10^{-3}	4.98×10^{-3}
18	rs2847291	12808713	Intron 8	A	330	0.14 (0.04, 0.24)	6.86×10^{-3}	1.43×10^{-2}
18	rs11663472	12810471	Intron 8	A	330	0.14 (0.04, 0.24)	6.86×10^{-3}	1.43×10^{-2}
18	rs2847286	12817815	Intron 6	G	330	0.14 (0.04, 0.24)	6.86×10^{-3}	1.43×10^{-2}
18	rs2847285	12818224	Intron 6	A	330	0.14 (0.04, 0.24)	6.86×10^{-3}	1.43×10^{-2}
18	rs45456495	12792228	Intron 10	T	330	0.13 (0.03, 0.24)	9.11×10^{-3}	1.77×10^{-2}
18	rs2542167	12795849	Intron 9	T	330	0.13 (0.03, 0.24)	9.11×10^{-3}	1.77×10^{-2}
18	rs2847298	12800120	Intron 9	G	330	0.13 (0.03, 0.24)	9.11×10^{-3}	1.77×10^{-2}
18	rs2542160	12789246	Intron 10	C	330	0.13 (0.03, 0.23)	1.06×10^{-2}	1.94×10^{-2}
18	rs2847299	12801337	Intron 9	A	330	0.14 (0.03, 0.24)	1.10×10^{-2}	3.06×10^{-2}
18	rs7227207	12819616	Intron 5	T	330	−0.13 (−0.23, −0.03)	1.15×10^{-2}	2.13×10^{-2}
18	rs72872125	12876915	Intron 1	T	330	0.19 (0.04, 0.34)	1.24×10^{-2}	1.72×10^{-2}
18	rs60474474	12792736	Intron 10	T	330	−0.14 (−0.25, −0.03)	1.68×10^{-2}	2.03×10^{-2}
18	rs45450798	12792940	Intron 10	G	330	−0.14 (−0.25, −0.03)	1.68×10^{-2}	2.03×10^{-2}
18	rs60751993	12795420	Intron 9	A	330	−0.14 (−0.25, −0.03)	1.68×10^{-2}	2.03×10^{-2}
18	rs60735058	12795470	Intron 9	A	330	−0.14 (−0.25, −0.03)	1.68×10^{-2}	2.03×10^{-2}
18	rs8096138	12808140	Intron 8	G	330	−0.14 (−0.25, −0.03)	1.68×10^{-2}	2.03×10^{-2}
18	rs1893217	12809340	Intron 8	G	330	−0.14 (−0.25, −0.03)	1.68×10^{-2}	2.03×10^{-2}
18	rs11663253	12789556	Intron 10	G	330	−0.13 (−0.25, −0.02)	1.84×10^{-2}	2.12×10^{-2}
18	rs10502416	12822702	Intron 5	T	330	−0.13 (−0.24, −0.02)	2.01×10^{-2}	2.14×10^{-2}
18	rs78637414	12826836	Intron 4	A	330	−0.13 (−0.24, −0.02)	2.01×10^{-2}	2.14×10^{-2}
18	rs62097820	12834649	Intron 3	T	330	−0.13 (−0.24, −0.02)	2.01×10^{-2}	2.14×10^{-2}
18	rs8096327	12887750	Upstream	G	330	−0.10 (−0.19, −0.01)	2.91×10^{-2}	3.71×10^{-2}
18	rs3737361	12831324	Intron 3	C	330	−0.11 (−0.22, −0.01)	3.07×10^{-2}	5.45×10^{-2}
18	rs16939910	12837993	Intron 2	A	330	−0.11 (−0.22, −0.01)	3.07×10^{-2}	5.45×10^{-2}
18	rs3786158	12843275	Intron 2	A	330	−0.11 (−0.22, −0.01)	3.07×10^{-2}	5.45×10^{-2}
18	rs11080605	12847329	Intron 2	C	330	−0.11 (−0.22, −0.01)	3.07×10^{-2}	5.45×10^{-2}
18	rs62097858	12862581	Intron 1	A	330	−0.11 (−0.22, −0.01)	3.07×10^{-2}	$5.45 \times 10^{--2}$
18	rs8091720	12865186	Intron 1	T	330	−0.11 (−0.22, −0.01)	3.07×10^{-2}	5.45×10^{-2}
18	rs7244152	12854294	Intron 2	C	330	−0.11 (−0.22, −0.01)	3.23×10^{-2}	5.44×10^{-2}
18	rs11080606	12867969	Intron 1	C	330	−0.11 (−0.22, −0.01)	3.23×10^{-2}	5.44×10^{-2}
18	rs7242788	12820330	Intron 5	A	330	−0.11 (−0.22, −0.01)	3.30×10^{-2}	5.79×10^{-2}
18	rs12959799	12900695	Upstream	G	330	0.11 (0.01, 0.21)	4.01×10^{-2}	5.41×10^{-2}
18	rs80262450	12818922	Intron 6	A	330	−0.13 (−0.25, −0.01)	4.13×10^{-2}	3.45×10^{-2}
18	rs56946650	12916943	Upstream	T	330	−0.11 (−0.22, −0.00)	4.16×10^{-2}	6.45×10^{-2}
18	rs2847282	12819820	Intron 5	G	330	−0.09 (−0.19, −0.00)	4.79×10^{-2}	6.62×10^{-2}

**SNP positions according to the Genome Reference Consortium Human Build 37 (GRch37)*

Linear regression models: p-value$_a$ = adjusted for age, sex and complication group; p-value$_b$ = adjusted for age, sex, complication group and rs2104286. Chr, chromosome; SNP, single nucleotide polymorphism; bp, base pair; A1, minor allele; CI, confidence interval.

been reported that one of our identified SNPs, rs12251836, is associated with *IL2RA* expression on acutely triggered T_{EFF}, but not in Tregs (48), suggesting a likely biological causal inference of IL-2R gene locus in T1D.

Another exciting and supporting genetic observation included 53 *PTPN2* SNPs to be significantly associated with sIL-2R plasma levels, importantly 42 of which were associations independent of *IL2RA* variant rs2104286. Our most significant SNP in *PTPN2* is rs12971201, which has previously been associated with T1D, however a secondary association has been suggested due to rs1893217 (49). This particular variant is considered a risk variant for T1D and celiac disease (50, 51),

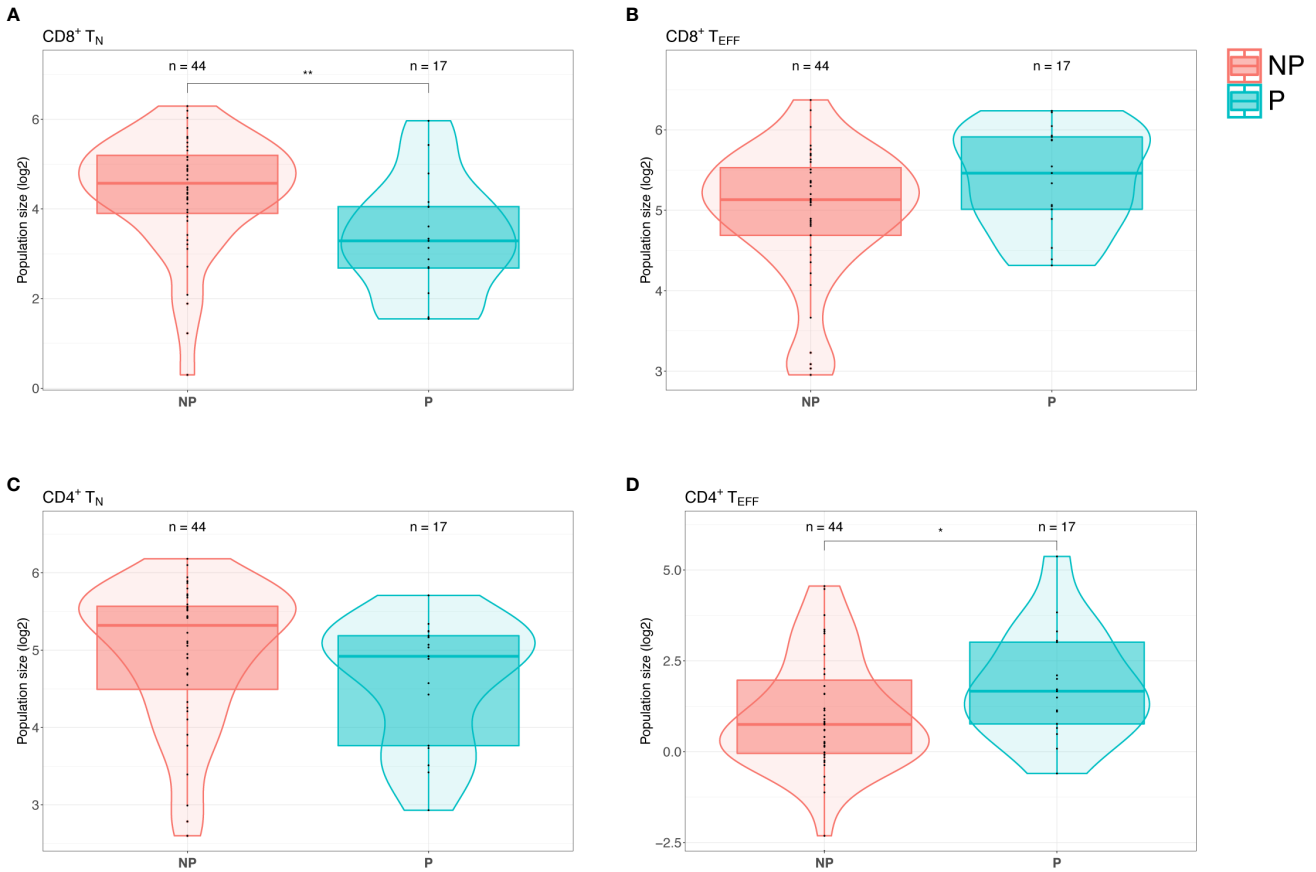

FIGURE 2 | Patients with type 1 diabetes (T1D) with complications display a shift from naïve T cells to effector T cells. **(A)** Flow cytometry screening of PBMCs from PROLONG patients revealed a significant decrease of $CD8^+$ naïve T (T_N) cells ($CD3^+CD4^+CD45RA^+CCR7^+CCR5^-$) in progressors (P) compared to non-progressors (NP). **(B)** Progressors displayed elevated $CD8^+$ effector T (T_{EFF}) cells ($CD3^+CD4^+CD45RA^+CCR7^-$) simultaneously (p = ns). **(C)** $CD4^+$ T_N cells were also declined in patients with T1D with complications as compared to NPs (p = ns). **(D)** In progressors $CD4^+$ T_{EFF} cells were significantly elevated compared to NPs. (For the comparison between the different groups, multiple linear regression was applied and adjusted for the age and sex covariates. *p < 0.05 and **p < 0.01).

and correlated with impaired IL-2 signalling in $CD4^+$ T cells as measured by decreased phosphorylation of STAT5 (pSTAT5) but also reduced PTPN2 expression (52). One of our identified SNPs, rs2847281, was shown to significantly associate with CRP levels along many other *PTPN2* variants (53). PTPN2 is a negative regulator in the IL-2 signalling cascade and several SNPs in the *PTPN2* gene region have been linked to different autoimmune diseases including T1D, rheumatoid arthritis and Crohn's disease (54, 55). Furthermore, different genetic variants in *PTPN2* were reported to be associated with diminished IL-2 responsiveness in naïve Tregs from patients with long-standing T1D (56). PTPN2 has been shown to modulate interferon gamma signal transduction in pancreatic β cells and regulate cytokine-induced apoptosis, which could potentially contribute to the pathogenesis of T1D (57).

As described above, elevated sIL-2R levels are likely to reflect an imbalance in Treg and T_{EFF} activity. PBMCs from PROLONG patients with T1D with vascular complications displayed a shift from naïve T cells (T_N) to T_{EFF}, however, we cannot distinguish whether this shift is the cause or the result of diabetic complications. The interpretation of these results was difficult due to the small and heterogeneous sample size in the progressors group. One can speculate that progressors have increased T_{EFF} due to impaired Treg suppression leading to a more destructive form of T1D, thereby more active course of the disease. This systemic long-term inflammation could subsequently drive the development of vascular complications by affecting tissues aside from the pancreas. Further studies testing suppression capacity of Tregs isolated from patients with T1D with and without complications are crucial to confirm this notion.

In PROLONG, we observed significantly higher levels of sIL-2R in progressors which associated with *IL2RA* SNPs, however the surface expression of IL-2R on circulating immune cells was similar between progressors and NPs. This may be confirmatory for the theory that it is not the number of cells expressing IL-2R making a difference, but the efficiency of IL-2 signalling within the cells themselves. Paradoxically, the IL-2/IL-2R signalling pathway is important in immunity and tolerance, which is further complicated by shedding of sIL-2R. How sIL-2R is involved in the pathogenesis of different diseases remains a

puzzle. The high-affinity receptor for IL-2 consists of 3 protein chains, namely IL-2Rα, IL-2Rβ, and IL-2Rγ. Upon proteolytic cleavage of the ectodomains of the membrane-bound IL-2Rα and release into the extracellular space, sIL-2R retains the ability to bind IL-2 with low affinity, which can lead to different outcomes. Firstly, sIL-2R may function as a decoy-receptor reducing the bioavailability of IL-2 and favor tolerance controlled by Tregs over immunity. Tregs constitutively express the high-affinity IL-2R, which enables them to out-compete conventional T cells with the intermediate-affinity receptor (IL-2Rβ and IL-2Rγ) when less IL-2 is available, thereby boosting immune tolerance (58). This difference in affinity is exploited in clinical trials in T1D where the administration of low-dose IL-2 has shown promising effects expanding and activating Tregs (59, 60). Alternatively, the binding of sIL-2R to IL-2 can enable *in trans* presentation of IL-2 to T-cells which only express the intermediate-affinity IL-2R. Overall, increased shedding of sIL-2R and it binding to IL-2 can have opposing effects depending on the cell type affected (58).

Stratified analysis of different vascular complications revealed increased sIL-2R and CCL2 levels in DIALONG patients with CVD in comparison to patients with T1D with other diabetic complications. Elevated sIL-2R has been described as a marker for coronary artery calcification progression in both individuals with and without T1D independent of traditional CVD risk factors (20). CCL2 plays a critical role in the development of atherosclerotic plaque formation by attracting monocytes to the vessel lumen where they will differentiate into macrophages and become foam cells by the uptake of low-density lipoprotein (61). Elevated plasma levels of CCL2 have also been associated with CVD (61–63). The observed increases in sIL-2R and CCL2 were based on a small sample set in DIALONG, however, the patient characterisation for CVD was performed thoroughly using computed tomography coronary angiography, which enabled the identification of asymptomatic coronary artery disease (64). Nevertheless, we were not able to investigate this finding in PROLONG due to the limited information on CVD.

Previously it was shown in the EURODIAB study that patients with T1D with complications have increased IL-6 and TNF-α as compared to individuals without complications (9). We could neither confirm nor confound this finding due to the low detection rate of IL-6 and TNF-α (< 20%) in our study, which statistically did not allow for reliable comparisons. In general, the detection rates in our cytokine screening were considerably low, where many of the investigated biomarkers were not detected at all. This could be due to technical differences and kit quality, however all kits used were validated for plasma usage by the respective providers, we followed manufacturer's instructions accordingly and did not experience technical issues during analysis.

Our future perspective is to unravel the role of IL-2R in the progression to diabetic complications in general, larger cohorts analyzing sIL-2R levels in other types of diabetes, such as T2D with no autoimmunity and latent autoimmune diabetes of adults, are of importance. To investigate the predictive power of sIL-2R levels in the development of diabetic complications, longitudinal studies in children and adolescents would be a great asset. Furthermore, it is of great interest to study the relationship between sIL-2R and IL-2 signalling efficacy and Treg function in patients with T1D.

In summary, we conclude that *IL2RA* and *PTPN2* gene variants may not only increase the risk of T1D, but in addition the development of diabetic complications possibly by influencing sIL-2R plasma levels and lowering T cell responsiveness. Thus, sIL-2R could potentially act as a biomarker for monitoring vascular complications in people with T1D thereby enabling early treatment and improving patient care.

DATA AVAILABILITY STATEMENT

The datasets presented in this article are not readily available because of GDPR and ethical restrictions. Requests to access the datasets should be directed to valeriya.lyssenko@uib.no.

ETHICS STATEMENT

The studies involving human participants were reviewed and approved by PROLONG-Sweden: Regional Ethics Review Board, Department 1, Lund, Sweden, Dnr 777/2009; PROLONG-Denmark: Scientific-Ethical Committee for the Capital Region of Denmark, Hillerød, Denmark, Dnr H-2-2013-073; DIALONG: Regional Committees for Medical and Health Research Ethics (REC), South-East regional health authority, panel D, Norway, 2014/851; Data analysis of both studies at University of Bergen: REC, West regional health authority, Norway 2019/1324. The patients/participants provided their written informed consent to participate in this study.

AUTHOR CONTRIBUTIONS

VL, RJ, and SA conceived the study, and MK and SA designed the immunological part of the study. TM, CL, HF, TN, S-BC, GJ, LG, ME, BE, KB, and PN contributed to the study design and data collection. VL is the PI of the PROLONG study. TB is the PI of the DIALONG study. MK conducted the flow cytometric and cytokine analysis and wrote the manuscript. MK, OF, EP, BB, and SA analyzed and processed the data. All authors contributed to the article and approved the submitted version.

FUNDING

Financial support was obtained from the Swedish Research Council (Dnr2015-03574, Dnr349-2006-237), the Novo Nordisk Foundation (NNF12OC1016467), the Family Erling-Person Foundation, the Steno Diabetes Center Copenhagen, the

Bergen Research Foundation (BFS811294), and the University of Bergen. The DIALONG study is supported by the Oslo Diabetes Research Centre and the Norwegian Diabetics' Centre.

ACKNOWLEDGMENTS

We thank all PROLONG and DIALONG patients and blood donors, nurses, and researchers involved in the planning and implementation of the studies. Additionally, we are grateful for the help from Karl A. Brokstad with the Luminex assay. We appreciate the help from the Flow Cytometry Core Facility, Department of Clinical Science, University of Bergen, where the flow cytometry analysis was performed. Furthermore, we acknowledge Richard Davies and Timothy Holmes for their continuous assistance designing, conducting, and analyzing multicolor flow cytometry measurements. We are very thankful for the help we received from Türküler Özgümüş with data analysis.

SUPPLEMENTARY MATERIAL

The Supplementary Material for this article can be found online at: https://www.frontiersin.org/articles/10.3389/fendo.2020.575469/full#supplementary-material

REFERENCES

1. Castano a L, Eisenbarth GS. Type-I Diabetes: A Chronic Autoimmune Disease of Human, Mouse, and Rat. *Annu Rev Immunol* (1990) 8(1):647–79. doi: 10.1146/annurev.iy.08.040190.003243
2. Roep BO. The role of T-cells in the pathogenesis of Type 1 diabetes: From cause to cure. *Diabetologia* (2003) 46(3):305–21. doi: 10.1007/s00125-003-1089-5
3. Tisch R, McDevitt H. Insulin-Dependent Diabetes Mellitus. *Cell* (1996) 85 (3):291–7. doi: 10.1016/S0092-8674(00)81106-X
4. Harcourt BE, Penfold SA, Forbes JM. Coming full circle in diabetes mellitus: from complications to initiation. *Nat Rev Endocrinol* (2013) 9:113. doi: 10.1038/nrendo.2012.236
5. Rydén A, Sörstadius E, Bergenheim K, Romanovschi A, Thorén F, Witt EA, et al. The Humanistic Burden of Type 1 Diabetes Mellitus in Europe: Examining Health Outcomes and the Role of Complications. *PLoS One* (2016) 11(11):e0164977. doi: 10.1371/journal.pone.0164977
6. Forlenza GP, Rewers M. The epidemic of type 1 diabetes: what is it telling us? *Curr Opin Endocrinol Diabetes Obes* (2011) 18(4):248–51. doi: 10.1097/MED.0b013e32834872ce
7. Park M, Katon WJ, Wolf FM. Depression and risk of mortality in individuals with diabetes: a meta-analysis and systematic review. *Gen Hosp Psychiatry* (2013) 35(3):217–25. doi: 10.1016/j.genhosppsych.2013.01.006
8. Sun JK, Keenan HA, Cavallerano JD, Asztalos BF, Schaefer EJ, Sell DR, et al. Protection from retinopathy and other complications in patients with type 1 diabetes of extreme duration: the joslin 50-year medalist study. *Diabetes Care* (2011) 34(4):968–74. doi: 10.2337/dc10-1675
9. Schram MT, Chaturvedi N, Schalkwijk C, Giorgino F, Ebeling P, Fuller JH, et al. Vascular Risk Factors and Markers of Endothelial Function as Determinants of Inflammatory Markers in Type 1 Diabetes. *EURODIAB Prospect Complications Study* (2003) 26(7):2165–73. doi: 10.2337/diacare.26.7.2165
10. Lowe CE, Cooper JD, Brusko T, Walker NM, Smyth DJ, Bailey R, et al. Large-scale genetic fine mapping and genotype-phenotype associations implicate polymorphism in the IL2RA region in type 1 diabetes. *Nat Genet* (2007) 39:1074. doi: 10.1038/ng2102
11. Tang W, Cui D, Jiang L, Zhao L, Qian W, Long SA, et al. Association of common polymorphisms in the IL2RA gene with type 1 diabetes: evidence of 32,646 individuals from 10 independent studies. *J Cell Mol Med* (2015) 19 (10):2481–8. doi: 10.1111/jcmm.12642
12. Downes K, Marcovecchio ML, Clarke P, Cooper JD, Ferreira RC, Howson JM, et al. Plasma concentrations of soluble IL-2 receptor α (CD25) are increased in type 1 diabetes and associated with reduced C-peptide levels in young patients. *Diabetologia* (2014) 57(2):366–72. doi: 10.1007/s00125-013-3113-8
13. Krause S, Beyerlein A, Winkler C, Gavrisan A, Kayser C, Puff R, et al. Soluble interleukin-2 receptor alpha in preclinical type 1 diabetes. *Acta Diabetol* (2014) 51(3):517–8. doi: 10.1007/s00592-013-0512-8
14. Hulme MA, Wasserfall CH, Atkinson MA, Brusko TM. Central role for interleukin-2 in type 1 diabetes. *Diabetes* (2012) 61(1):14–22. doi: 10.2337/db11-1213
15. Kovanen PE, Leonard WJ. Cytokines and immunodeficiency diseases: critical roles of the γc-dependent cytokines interleukins 2, 4, 7, 9, 15, and 21, and their signaling pathways. *Immunol Rev* (2004) 202(1):67–83. doi: 10.1111/j.0105-2896.2004.00203.x
16. Sakaguchi S, Yamaguchi T, Nomura T, Ono M. Regulatory T Cells and Immune Tolerance. *Cell* (2008) 133(5):775–87. doi: 10.1016/j.cell.2008.05.009
17. Lan Q, Fan H, Quesniaux V, Ryffel B, Liu Z, Zheng SG. Induced Foxp3(+) regulatory T cells: a potential new weapon to treat autoimmune and inflammatory diseases? *J Mol Cell Biol* (2012) 4(1):22–8. doi: 10.1093/jmcb/mjr039
18. Ye C, Brand D, Zheng SG. Targeting IL-2: an unexpected effect in treating immunological diseases. *Signal Transduct Targeted Ther* (2018) 3(1):2. doi: 10.1038/s41392-017-0002-5
19. Doganay S, Evereklioglu C, Er H, Türköz Y, Sevinç A, Mehmet N, et al. Comparison of serum NO, TNF-α, IL-1β, sIL-2R, IL-6 and IL-8 levels with grades of retinopathy in patients with diabetes mellitus. *Eye* (2002) 16(2):163–70. doi: 10.1038/sj.eye.6700095
20. Wadwa RP, Kinney GL, Ogden L, Snell-Bergeon JK, Maahs DM, Cornell E, et al. Soluble interleukin-2 receptor as a marker for progression of coronary artery calcification in type 1 diabetes. *Int J Biochem Cell Biol* (2006) 38(5):996–1003. doi: 10.1016/j.biocel.2005.09.015
21. Colombo M, Valo E, McGurnaghan SJ, Sandholm N, Blackbourn LAK, Dalton RN, et al. Biomarker panels associated with progression of renal disease in type 1 diabetes. *Diabetologia* (2019) 62(9):1616–27. doi: 10.1007/s00125-019-4915-0
22. Holte KB, Juel NG, Brox JI, Hanssen KF, Fosmark DS, Sell DR, et al. Hand, shoulder and back stiffness in long-term type 1 diabetes; cross-sectional association with skin collagen advanced glycation end-products. The Dialong study. *J Diabetes Complications* (2017) 31(9):1408–14. doi: 10.1016/j.jdiacomp.2017.06.007
23. Giordano C, Galluzzo A, Marco A, Panto F, Amato MP, Caruso C, et al. Increased soluble interleukin-2 receptor levels in the sera of type 1 diabetic patients. *Diabetes Res (Edinburgh Scotland)* (1988) 8(3):135–8.
24. Yu H, Paiva R, Flavell RA. Harnessing the power of regulatory T-cells to control autoimmune diabetes: overview and perspective. *Immunology* (2018) 153(2):161–70. doi: 10.1111/imm.12867
25. Garg G, Tyler JR, Yang JH, Cutler AJ, Downes K, Pekalski M, et al. Type 1 diabetes-associated IL2RA variation lowers IL-2 signaling and contributes to diminished CD4+CD25+ regulatory T cell function. *J Immunol (Baltimore Md 1950)* (2012) 188(9):4644–53. doi: 10.4049/jimmunol.1100272
26. Lawson JM, Tremble J, Dayan C, Beyan H, Leslie RD, Peakman M, et al. Increased resistance to CD4+CD25hi regulatory T cell-mediated suppression in patients with type 1 diabetes. *Clin Exp Immunol* (2008) 154(3):353–9. doi: 10.1111/j.1365-2249.2008.03810.x
27. Long SA, Buckner JH. CD4+FOXP3+ T regulatory cells in human autoimmunity: more than a numbers game. *J Immunol (Baltimore Md 1950)* (2011) 187(5):2061–6. doi: 10.4049/jimmunol.1003224
28. Hughson A, Bromberg I, Johnson B, Quataert S, Jospe N, Fowell DJ. Uncoupling of proliferation and cytokines from suppression within the CD4+CD25+Foxp3+ T-cell compartment in the 1st year of human type 1 diabetes. *Diabetes* (2011) 60(8):2125–33. doi: 10.2337/db10-1661
29. Sheikh V, Zamani A, Mahabadi-Ashtiyani E, Tarokhian H, Borzouei S, Alahgholi-Hajibehzad M. Decreased regulatory function of CD4+CD25+CD45RA+ T cells and impaired IL-2 signalling pathway in patients with type 2 diabetes mellitus. *Scand J Immunol* (2018) 88(4):e12711. doi: 10.1111/sji.12711

30. Sharief MK, Thompson EJ. Correlation of interleukin-2 and soluble interleukin-2 receptor with clinical activity of multiple sclerosis. *J Neurol Neurosurg Psychiatry* (1993) 56(2):169–74. doi: 10.1136/jnnp.56.2.169
31. Witkowska AM. On the role of sIL-2R measurements in rheumatoid arthritis and cancers. *Mediators Inflamm* (2005) 2005(3):121–30. doi: 10.1155/mi.2005.121
32. Akiyama M, Sasaki T, Kaneko Y, Yasuoka H, Suzuki K, Yamaoka K, et al. Serum soluble interleukin-2 receptor is a useful biomarker for disease activity but not for differential diagnosis in IgG4-related disease and primary Sjogren's syndrome adults from a defined population. *Clin Exp Rheumatol* (2018) 36 Suppl 112(3):157–64.
33. Uziel Y, Krafchik BR, Feldman B, Silverman ED, Rubin LA, Laxer RM. Serum levels of soluble interleukin-2 receptor. A marker of disease activity in localized scleroderma. *Arthritis Rheum* (1994) 37(6):898–901. doi: 10.1002/art.1780370618
34. Tournadre A, Dubost JJ, Soubrier M, Ruivard M, Souteyrand P, Schmidt J, et al. Soluble IL-2 receptor: a biomarker for assessing myositis activity. *Dis Markers* (2014) 2014:472624. doi: 10.1155/2014/472624
35. Hietala K, Harjutsalo V, Forsblom C, Summanen P, Groop PH. Age at onset and the risk of proliferative retinopathy in type 1 diabetes. *Diabetes Care* (2010) 33(6):1315–9. doi: 10.2337/dc09-2278
36. Semeraro F, Cancarini A, dell'Omo R, Rezzola S, Romano MR, Costagliola C. Diabetic Retinopathy: Vascular and Inflammatory Disease. *J Diabetes Res* (2015) 2015:582060. doi: 10.1155/2015/582060
37. Maier LM, Lowe CE, Cooper J, Downes K, Anderson DE, Severson C, et al. IL2RA Genetic Heterogeneity in Multiple Sclerosis and Type 1 Diabetes Susceptibility and Soluble Interleukin-2 Receptor Production. *PLoS Genet* (2009) 5(1):e1000322. doi: 10.1371/journal.pgen.1000322
38. Consortium IMSG, Hafler DA, Compston A, Sawcer S, Lander ES, Daly MJ, et al. Risk Alleles for Multiple Sclerosis Identified by a Genomewide Study. *N Engl J Med* (2007) 357(9):851–62. doi: 10.1056/NEJMoa073493
39. Alcina A, Fedetz M, Ndagire D, Fernández O, Leyva L, Guerrero M, et al. IL2RA/CD25 gene polymorphisms: uneven association with multiple sclerosis (MS) and type 1 diabetes (T1D). *PLoS One* (2009) 4(1):e4137. doi: 10.1371/journal.pone.0004137
40. Pankratz VS, Vierkant RA, O'Byrne MM, Ovsyannikova IG, Poland GA. Associations between SNPs in candidate immune-relevant genes and rubella antibody levels: a multigenic assessment. *BMC Immunol* (2010) 11(1):48. doi: 10.1186/1471-2172-11-48
41. Ramondetti F, Sacco S, Comelli M, Bruno G, Falorni A, Iannilli A, et al. Type 1 diabetes and measles, mumps and rubella childhood infections within the Italian Insulin-dependent Diabetes Registry. *Diabetic Med* (2012) 29(6):761–6. doi: 10.1111/j.1464-5491.2011.03529.x
42. Korkmaz HA, Ermiş Ç. A case of immune-mediated type 1 diabetes mellitus due to congenital rubella ınfection. *Ann Pediatr Endocrinol Metab* (2019) 24 (1):68–70. doi: 10.6065/apem.2019.24.1.68
43. Vella A, Cooper JD, Lowe CE, Walker N, Nutland S, Widmer B, et al. Localization of a type 1 diabetes locus in the IL2RA/CD25 region by use of tag single-nucleotide polymorphisms. *Am J Hum Genet* (2005) 76(5):773–9. doi: 10.1086/429843
44. Maier LM, Anderson DE, Severson CA, Baecher-Allan C, Healy B, Liu DV, et al. Soluble IL-2RA levels in multiple sclerosis subjects and the effect of soluble IL-2RA on immune responses. *J Immunol (Baltimore Md 1950)* (2009) 182(3):1541–7. doi: 10.4049/jimmunol.182.3.1541
45. Farh KK-H, Marson A, Zhu J, Kleinewietfeld M, Housley WJ, Beik S, et al. Genetic and epigenetic fine mapping of causal autoimmune disease variants. *Nature* (2014) 518:337. doi: 10.1038/nature13835
46. Schwartz AM, Demin DE, Vorontsov IE, Kasyanov AS, Putlyaeva LV, Tatosyan KA, et al. Multiple single nucleotide polymorphisms in the first intron of the IL2RA gene affect transcription factor binding and enhancer activity. *Gene* (2017) 602:50–6. doi: 10.1016/j.gene.2016.11.032
47. Belot M-P, Fradin D, Mai N, Le Fur S, Zélénika D, Kerr-Conte J, et al. CpG methylation changes within the IL2RA promoter in type 1 diabetes of childhood onset. *PLoS One* (2013) 8(7):e68093–e. doi: 10.1371/journal.pone.0068093
48. Ye CJ, Feng T, Kwon H-K, Raj T, Wilson MT, Asinovski N, et al. Intersection of population variation and autoimmunity genetics in human T cell activation. *Science* (2014) 345(6202):1254665–. doi: 10.1126/science.1254665
49. Onengut-Gumuscu S, Chen W-M, Burren O, Cooper NJ, Quinlan AR, Mychaleckyj JC, et al. Fine mapping of type 1 diabetes susceptibility loci and evidence for colocalization of causal variants with lymphoid gene enhancers. *Nat Genet* (2015) 47(4):381–6. doi: 10.1038/ng.3245
50. Johnson MB, Cerosaletti K, Flanagan SE, Buckner JH. Genetic Mechanisms Highlight Shared Pathways for the Pathogenesis of Polygenic Type 1 Diabetes and Monogenic Autoimmune Diabetes. *Curr Diabetes Rep* (2019) 19(5):20. doi: 10.1007/s11892-019-1141-6
51. Dubois PCA, Trynka G, Franke L, Hunt KA, Romanos J, Curtotti A, et al. Multiple common variants for celiac disease influencing immune gene expression. *Nat Genet* (2010) 42(4):295–302. doi: 10.1038/ng.543
52. Long SA, Cerosaletti K, Wan JY, Ho JC, Tatum M, Wei S, et al. An autoimmune-associated variant in PTPN2 reveals an impairment of IL-2R signaling in CD4+ T cells. *Genes Immun* (2010) 12:116. doi: 10.1038/gene.2010.54
53. Dehghan A, Dupuis J, Barbalic M, Bis JC, Eiriksdottir G, Lu C, et al. Meta-analysis of genome-wide association studies in >80 000 subjects identifies multiple loci for C-reactive protein levels. *Circulation* (2011) 123(7):731–8. doi: 10.1161/CIRCULATIONAHA.110.948570
54. Todd JA, Walker NM, Cooper JD, Smyth DJ, Downes K, Plagnol V, et al. Robust associations of four new chromosome regions from genome-wide analyses of type 1 diabetes. *Nat Genet* (2007) 39(7):857–64. doi: 10.1038/ng2068
55. Wellcome Trust Case Control C. Genome-wide association study of 14,000 cases of seven common diseases and 3,000 shared controls. *Nature* (2007) 447 (7145):661–78. doi: 10.1038/nature05911
56. Yang JH, Cutler AJ, Ferreira RC, Reading JL, Cooper NJ, Wallace C, et al. Natural Variation in Interleukin-2 Sensitivity Influences Regulatory T-Cell Frequency and Function in Individuals With Long-standing Type 1 Diabetes. *Diabetes* (2015) 64(11):3891–902. doi: 10.2337/db15-0516
57. Moore F, Colli ML, Cnop M, Esteve MI, Cardozo AK, Cunha DA, et al. PTPN2, a candidate gene for type 1 diabetes, modulates interferon-gamma-induced pancreatic beta-cell apoptosis. *Diabetes* (2009) 58(6):1283–91. doi: 10.2337/db08-1510
58. Damoiseaux J. The IL-2 – IL-2 receptor pathway in health and disease: The role of the soluble IL-2 receptor. *Clin Immunol* (2020) 218:108515. doi: 10.1016/j.clim.2020.108515
59. Rosenzwajg M, Churlaud G, Mallone R, Six A, Dérian N, Chaara W, et al. Low-dose interleukin-2 fosters a dose-dependent regulatory T cell tuned milieu in T1D patients. *J Autoimmun* (2015) 58:48–58. doi: 10.1016/j.jaut.2015.01.001
60. Yu A, Snowhite I, Vendrame F, Rosenzwajg M, Klatzmann D, Pugliese A, et al. Selective IL-2 Responsiveness of Regulatory T Cells Through Multiple Intrinsic Mechanisms Supports the Use of Low-Dose IL-2 Therapy in Type 1 Diabetes. *Diabetes* (2015) 64(6):2172–83. doi: 10.2337/db14-1322
61. Niu J, Kolattukudy P E. Role of MCP-1 in cardiovascular disease: molecular mechanisms and clinical implications. *Clin Sci* (2009) 117(3):95–109. doi: 10.1042/cs20080581
62. Piemonti L, Calori G, Lattuada G, Mercalli A, Ragogna F, Garancini MP, et al. Association between plasma monocyte chemoattractant protein-1 concentration and cardiovascular disease mortality in middle-aged diabetic and nondiabetic individuals. *Diabetes Care* (2009) 32(11):2105–10. doi: 10.2337/dc09-0763
63. Gonzalez-Quesada C, Frangogiannis NG. Monocyte chemoattractant protein-1/CCL2 as a biomarker in acute coronary syndromes. *Curr Atheroscl Rep* (2009) 11(2):131–8. doi: 10.1007/s11883-009-0021-y
64. Holte KB, Svanteson M, Hanssen KF, Haig Y, Solheim S, Berg TJ. Undiagnosed coronary artery disease in long-term type 1 diabetes. The Dialong study. *J Diabetes Complications* (2019) 33(5):383–9. doi: 10.1016/j.jdiacomp.2019.01.006

Conflict of Interest: The authors declare that the research was conducted in the absence of any commercial or financial relationships that could be construed as a potential conflict of interest. At the time when the data from Steno was collected, CLM was affiliated with Steno Diabetes Centre. During revisions and the finalization of the article, CLM have changed affiliation from Steno to Novo Nordisk as of 6-Jun-2016.

frontiers in Endocrinology

MINI REVIEW
published: 19 January 2021
doi: 10.3389/fendo.2020.614123

What Is the Sweetest UPR Flavor for the β-cell? That Is the Question

Alina Lenghel, Alina Maria Gheorghita, Andrei Mircea Vacaru and Ana-Maria Vacaru *

Institute for Cellular Biology and Pathology "Nicolae Simionescu", Bucharest, Romania

Unfolded protein response (UPR) is a process conserved from yeasts to mammals and, based on the generally accepted dogma, helps the secretory performance of a cell, by improving its capacity to cope with a burden in the endoplasmic reticulum (ER). The ER of β-cells, "professional secretory cells", has to manage tremendous amounts of insulin, which elicits a strong pressure on the ER intrinsic folding capacity. Thus, the constant demand for insulin production results in misfolded proinsulin, triggering a physiological upregulation of UPR to restore homeostasis. Most diabetic disorders are characterized by the loss of functional β-cells, and the pathological side of UPR plays an instrumental role. The transition from a homeostatic to a pathological UPR that ultimately leads to insulin-producing β-cell decay entails complex cellular processes and molecular mechanisms which remain poorly described so far. Here, we summarize important processes that are coupled with or driven by UPR in β-cells, such as proliferation, inflammation and dedifferentiation. We conclude that the UPR comes in different "flavors" and each of them is correlated with a specific outcome for the cell, for survival, differentiation, proliferation as well as cell death. All these greatly depend on the way UPR is triggered, however what exactly is the switch that favors the activation of one UPR as opposed to others is largely unknown. Substantial work needs to be done to progress the knowledge in this important emerging field as this will help in the development of novel and more efficient therapies for diabetes.

Keywords: unfolded protein response (UPR) pathway, β-cell proliferation, β-cell dedifferentiation, immune attack, heterogeneity

OPEN ACCESS

Edited by:
Vincent Poitout,
Université de Montréal, Canada

Reviewed by:
Feyza Engin,
University of Wisconsin-Madison, United States
Neha Shrestha,
University of Michigan, United States

***Correspondence:**
Ana Maria Vacaru
ana.vacaru@icbp.ro

Specialty section:
This article was submitted to Diabetes: Molecular Mechanisms, a section of the journal Frontiers in Endocrinology

Received: *05 October 2020*
Accepted: *24 November 2020*
Published: *19 January 2021*

Citation:
Lenghel A, Gheorghita AM, Vacaru AM and Vacaru A-M (2021) What Is the Sweetest Unfolded Protein Response Flavor for the β-cell? That Is the Question. Front. Endocrinol. 11:614123. doi: 10.3389/fendo.2020.614123

INTRODUCTION

Recently, increased stress of the endoplasmic reticulum (ER), or ER stress, has emerged as a critical regulator of transcription and translation events in diabetes (1–5). The ER supports correct protein folding that is essential to maintain protein homeostasis and cell survival; however, this process is remarkably sensitive as even minute modifications in the cellular milieu can result in protein misfolding (6, 7). Following nutrient stimulation, freshly transcribed insulin mRNA translated in the ER drives a 10-fold increase in insulin synthesis that represents about 50% of the total protein production by the β-cells (7, 8). This massive synthesis and its variations result in a constant hassle

of the ER. To deal with this challenge, β-cells continuously supervise protein folding in the ER through a well conserved mechanism, the unfolded protein response (UPR) (7, 9).

Over the next sections, we will present how UPR is actively present during important stages of β-cell existence in physiological and pathological circumstances. We will focus on processes that are relevant for the development of potential therapies that target UPR. As such, we will address the role of UPR in proliferation, inflammation/inflammatory attack and dedifferentiation of β-cells.

UPR AND DEVELOPMENT OF DIABETES

UPR is a cellular process consisting of an intricate network of transducers and downstream target genes ensuring correct protein folding in the ER. UPR comprises of three major sensors: Protein kinase RNA-like endoplasmic reticulum kinase (PERK), endoribonuclease/kinase inositol-requiring enzyme 1 (IRE1, or ERN1), and activating transcription factor 6 (ATF6) (10, 11). These factors are localized in the ER membrane and they are able to sense and monitor through their luminal domains the status of protein folding in the ER (12–17). If an accumulation of unfolded proteins occurs, these transducers signal *via* their cytosolic domains either by direct targeted catalytic activities or by specific post-translational modulation. The precise mechanism that triggers UPR is still under debate (18–22), and most probably there is not a single mechanism involved, but rather the multiple concerted action of several ones, depending on cell type (23–25). The downstream effectors converge at the nucleus and induce UPR targets, finally restoring homeostasis *via* various processes described below.

PERK, upon oligomerization followed by autophosphorylation (26–28), phosphorylates the translation initiation factor 2 (eIF2α) inducing inhibition of mRNA translation through activation of a signaling cascade, thus reducing the ER protein load, and increasing ATF4 translation (13, 27, 29, 30). This results in overexpression of chaperones, antioxidant genes, but also of proapoptotic genes, such as CHOP, GADD34, ATF3 and TRB3 that contribute to β-cell apoptosis during terminal UPR (31, 32). eIF2α has a central role in stress management, being also targeted by other kinases in response to various kinds of stresses (30, 33–36). This signaling cascade converging on eIF2α phosphorylation followed by ATF4 activation is an adaptive pathway for cellular homeostasis restoration commonly known as Integrated Stress Response (ISR) (37, 38).

IRE1 possesses both kinase and endoribonuclease activities. When UPR is induced, dimerization and trans-autophosphorylation of IRE1 activates its RNase domain and results in splicing of *Xbp1* pre-mRNA and overexpression of XBP1s, a transcription factor that induces genes-encoding chaperones, ER-associated protein degradation (ERAD), and lipid biosynthetic enzymes (12, 17, 39–41). Additionally, IRE1 presents a nonspecific RNase activity responsible for degradation of mRNAs from ER vicinity, thus reducing import of proteins into the ER (26, 42, 43). During increased stress, the kinase activity of IRE1 is activated and initiates the apoptosis cascade mediated by signal-regulating kinase 1 (ASK1)/cJun amino terminal kinase (JNK) (44).

Upon UPR activation, ATF6 is translocated to the Golgi apparatus, where it is processed by Site-1 and Site-2 proteases (S1P/S2P) (45, 46). Once the cytosolic fragment (nuclear ATF6, or nATF6) is generated, it travels to the nucleus and induces transcription of UPR target genes (47–49). Alone or in combination with XBP1s, nATF6 acts on increasing synthesis of chaperones to aid with the misfolded proteins, of proteins involved in lipid synthesis to increase ER volume, and of genes responsible for the ERAD pathway. They work for restoring homeostasis by modulating the amount of ER-mediated production of ER lipids and proteins necessary to accommodate variable requirements of ER protein folding and other functions in response to physiological and pathological conditions. If any of these mechanisms fail, the ER homeostasis is lost, a stressed UPR is induced and that ultimately results in cell apoptosis (11, 32, 50–52).

In diabetes, overactivation of UPR leads to phosphorylation of IRE1, which results in degradation of proinsulin mRNA (53–55) activation of JNK pathway, and splicing of XBP1 mRNA. XBP1s by itself or in cooperation with ATF6 induces expression of various ER chaperons, such as Herp1, EDEM, HRD1, p58IPK, and ERAD proteins, followed by swelling of the ER. Moreover, CHOP mRNA expression is induced by both ATF4 and XBP1s (5). By depleting CHOP in various diabetes models results in improved β-cell function and survival (56), although in NOD mice it is not the case (57). Surprisingly, TUDCA was able to increase the expression of Atf6 and XBP1 and increased β-cells survival, reduced islet inflammation and thus lower diabetes incidence in mouse models of diabetes (58). Therefore, in diabetes, the erroneous expression of ER chaperones may be responsible for the predisposition of the β-cell to a terminal UPR that culminates with cell death induced by CHOP.

PERK-eiF2α-ATF4 and IRE1-XBP1s/ATF6 arms of the UPR are activated differently by glucose. Surprisingly, low glucose concentrations result in maximal activation of the first arm, while protein synthesis, ATP levels and the concentration of Ca^{2+} in the ER are low, whereas the second arm is inactive. The response to high glucose concentration is the rapid inhibition of the ISR, the splicing of Xbp1 pre-mRNA and subsequent upregulation of XBP1s together with the downstream target genes to accommodate increased ER machinery load. Finely adjusting this adaptive response is indispensable to preserve the identity and function of β-cell (59).

UPR IS VERY DYNAMIC AND DRIVES HETEROGENIC INSULIN EXPRESSION

Xin and collaborators have shown that in healthy human subjects, β-cells go through different active states to accommodate insulin requirements that are characterized by different levels of UPR and insulin gene expression. They show that the transition between an active and prolonged insulin

secretory state results in induction of a stressed UPR that diminishes the levels of secreted insulin. After a certain time, the UPR of the β-cell recovers at a basal level and the cells restart the production of insulin. They describe several cyclical individual states of β-cell stress in correlation with insulin secretion, and low apoptosis and dedifferentiation markers (60). UPR was induced in a subpopulation of β-cells that express low insulin levels ($INS^{low}UPR^{hi}$) suggesting they represent a state of recovery from stress. Another population of β-cells was characterized by $INS^{hi}UPR^{low}$ and most likely represents a state of active production and secretion (60). Importantly, the insulin protein amounts are not always correlated with the mRNA levels. Apparently, in pancreases of type 1 diabetes (T1D) patients insulin protein levels were very low; nevertheless proinsulin and INS mRNA were still detected (61). It is not clear if this occurs due to dedifferentiation of β-cells or because more precursors of β-cells arise (61, 62). The characterization of different populations of β-cells based on their UPR and insulin levels is crucial in diabetes. It is important to know how these populations change during the disease progression, and where and when to intervene therapeutically to recover insulin homeostasis.

β-CELLS WITH ACTIVE UPR PROLIFERATE

One of the questions that puzzled scientists referred to how is β-cell mass regulation maintained? While it is already established that stem cells drive regeneration of tissues with fast turnover, such as skin, gut and blood, a stem cell pool has not yet been characterized for the pancreatic islets (63). Multiple studies demonstrated that β-cell mass adjusts in a dynamic way, in correlation with increased metabolic demand, or upon injury. Under most conditions, the major driver of postnatal islet cell expansion is the proliferation of already present β-cells (64).

Several studies suggested that UPR activation *in vivo* drives β-cell proliferation. Hodish and collaborators showed that overexpression of mutant proinsulin is correlated with both UPR activation and islet size increase (65). Inhibiting expression of PERK in adult mice resulted in increased proliferation of β-cells (66). In addition, another study established that ATF6 pathway that acts in response to the loss of PERK is regulating the pro-proliferative UPR mechanism rather than PERK. By using different murine models of diabetes (glucose-induced hyperglycemia mouse model; db/db mice and Akita mice) as well as β-cells isolated from pancreatic donors, they argue that mild UPR drives ATF6-induced proliferation of β-cells based on the insulin requirement. Moreover, they show that inhibition of ATF6 and IRE1 pathways reduce glucose-induced β-cell proliferation *in vitro*. However, chemical chaperones abrogated the proliferative effect on the β-cells (63). Human β-cells are less likely to respond well to stimulation, as they have a lower basal proliferation than mouse cells (67, 68). Importantly, there are studies showing proliferation of β-cells from donors upon UPR stimulation (63). A thorough study that characterized various β-cells subpopulation from healthy subjects showed that the majority of proliferating cells displayed low insulin expression correlated with activated UPR, with more proliferating cells in G1S cell cycle phase rather than in G2M (60).

UPR AND INFLAMMATION IN β-CELLS

The questions raised here are: does the dysregulated UPR from β-cells facilitate the immune attack, or vice-versa, the cytokines secreted by the immune cells induced upregulation of the UPR in β-cells, rendering them more susceptible to apoptosis? Many studies proved that both are true and mostly interdependent.

Inflammatory Environment Triggers UPR Activation

Recent work shows the importance of inflammation for UPR induction and β-cell fate in various diabetes contexts, especially in T1D (9, 69). There, the progressive invasion of inflammatory cells, like T-cells, macrophages, dendritic cells, and natural killer cells within the islets leads to insulitis (9, 70–72). Due to insulitis, the access of numerous proinflammatory molecules and reactive oxygen species (ROS) to β-cells, like interleukin-1β (IL1β), TNF, IFN-γ, IL17, and NO, is facilitated as these molecules are secreted by the invading immune cells. This results in apoptosis of β-cells (73, 74). Death of β-cells driven by cytokines entails induction of various transcription factors (NF-κB and STAT1), JNK, which in conjunction with a stressed UPR, end with activation of mitochondrial pathway of apoptosis (73, 75, 76). Moreover, upon stimulation by pro-inflammatory cytokines, β-cells start expressing and secreting more cytokines and chemokines, resulting in a cross-talk between the immune cells and the β-cells (77, 78). As a consequence, many T cells get infiltrated into the islets and cause destruction of the β-cells initiating diabetes (73, 79, 80).

The low grade inflammation present in the pancreas of T2D patients is responsible for recruitment of macrophages in the vicinity of the islets creating a pro-inflammatory milieu and inducing UPR (81, 82). A recent study provided direct evidence for the role of ER stress-induced inflammation in T2D. It revealed that by blocking IL23 and IL24, proinflammatory cytokines upregulated in the islets of T2D patients, the authors were able to partially decrease oxidative stress, UPR induction and restore glucose tolerance in obese mice. In addition, after reducing ROS with IL22, the improved UPR stress and β-cell function re-established glucose homeostasis (83).

UPR Facilitates Inflammatory Attack of β-Cells

This research topic got attention, as emerging data connects inflammatory responses to UPR in β-cells *via* the regulator of inflammation, NFκB (84, 85). Additionally, XBP1 seems to exert both pro- and anti-inflammatory effects in β-cells depending on the context established by the anti-apoptotic/anti-oxidative reaction as opposed to the pro-inflammatory response (47). Moreover, CHOP was shown to have a pro-inflammatory role in various disease models, upregulating pro-inflammatory

cytokines (such as IL1β, IL8) and chemokines (CCL2) in several tissues (86, 87). However, it is not clear how CHOP activates NF-κB. In β-cells, studies show that the transcription factor NF-κB is able to modulate the UPR upon activation by pro-inflammatory cytokines (88, 89). Reciprocally, the UPR was found to induce NF-κB activity in correlation with inflammatory responses, resulting in increased apoptosis and overexpression of cytokines and chemokines that may be responsible for β-cell death (74, 89, 90).

UPR IN DEDIFFERENTIATION OF β-CELLS

It has been established that every cell from any organism, β-cells included, are derived by differentiation from embryonic stem cells (91). Differentiation toward β-cells involves synchronized and rigorously controlled induction/downregulation of certain transcription factors and effectors in a timely manner (59). Importantly, cellular differentiation is not unidirectional (92). Recent data has shown that specific factors can induce mature β-cells to lose their identity and phenotype and backslide to an under-differentiated state, or in a progenitor-like condition. This phenomena is called dedifferentiation and has been involved in the pathology of diabetes (93–96), being a significant contributor of the reduction of functional β-cell mass (62, 97). Dedifferentiation of β-cells is characterized by reduced expression of β-cell-specific genes, that include essential transcription factors, insulin, genes responsible for glucose metabolism, genes required for protein processing and genes of the secretory pathway, accompanied by induction of genes that are usually repressed or lowly expressed in mature β-cell, such as the embryonic endocrine progenitor genes. Expression of these later genes is found in diabetic animals, in the islets (59, 62, 94). The mechanisms involved in the dedifferentiation process are still under investigation and here, we will underline some possible implications of UPR.

In a recent study, Zhu and collaborators have demonstrated that overexpression of miR24 reduced ER stress-induced β-cells apoptosis and blocked INS mRNA degradation, though it induced dedifferentiation of β-cells (98). MiR24 was found to inactivate the IRE1 sensor. Importantly, they speculated that one of the downstream effectors of IRE1 was CHOP. As ATF4 was not affected by miR24, the assumption was that CHOP was not upregulated *via* the PERK/ATF4 pathway. Surprisingly, they demonstrated that XBP1s, effector downstream of IRE1, is responsible for the apoptosis of β-cells under terminal ER stress (98). In a T1D model, work from Engin's group has shown that downregulating IRE1 before insulitis appearance results in temporary dedifferentiation of β-cells proved to be beneficial as it made β-cells more resistant to the immune attack (99). These dedifferentiated β-cells expressed lower levels of autoantigens and of MHC class I molecules and upregulated their immune inhibitory markers (99, 100). It became apparent that interference with TGFβ signaling resulted in induction of several markers of β-cells maturation (101, 102) and reversed dedifferentiation (103). The E3 ligase Hsd1 and the cofactor Sel1L represent well-conserved ERAD machinery (104) that has recently been linked to the preservation of β-cells identity *via* inhibition TGFβ pathway, while their survival and proliferation were not affected (105).

CONCLUSIONS AND PERSPECTIVES

The correlation between activation of UPR and their insulin gene expression was shown to divide β-cells into several populations that evolve from dynamic insulin secretion states to a stress recovery state when insulin production is decreased (60). This is an important aspect when developing new therapies that have a scope to mimic the heterogeneity of the β-cells. Strategies for regenerating β-cells should consider the importance to reintroduce these differences in the newly-emerged cells.

In the β-cells, there are functions of UPR that are ER stress-independent. Hassler and collaborators, by using mice with inducible β-cells-specific deletion of IRE1α, established the importance IRE1α/XBP1s pathway for glucose-stimulated insulin synthesis. The study revealed that this pathway regulates recruitment and structure of the ribosome, translation of pro-insulin mRNA, cleavage of the signal peptide, and inhibition of oxidative/inflammatory stress. Early activation of this UPR pathway appears to happen separately of ER stress and precedes the glucose-stimulated insulin synthesis (47).

Prolonged upregulation of a stressed UPR induces apoptosis, a process that involves JNK activation by the pro-inflammatory cytokines that act upon pancreatic β-cells through the progression of diabetes. It is not clear though the definitive mechanisms that pro-inflammatory cytokines use to induce IRE1α and JNK in human β-cells. This will help build new strategies to inhibit the UPR-driven pro-apoptotic signals without disturbing the other homeostatic functions (70).

We previously defined the ER stress as a stressed/terminal/decompensated UPR, the ultimate stage of UPR, with no recovery, when the cell enters the apoptosis pathway. One of the questions here is how do the cells get to the terminal UPR. What are the stages that precede it and can be targeted through therapies? We and others have challenged two different models for UPR activation: 1) the "rheostat model", when the UPR sensors and targets get activated in a concerted fashion and they are correlated with the level of stress - the more stress, the higher the UPR. This model is described by different subclasses that are characterized by the type and extent of the stress (52, 106). 2) Some stressors induce a UPR subclass that causes a specific outcome, physiological or pathological. This could vary from "adaptive" to the "terminal" UPR, when the cell sees many facets of UPR through a combination of different arms that are activated differently. These are such broad definitions, and future thorough characterizations are necessary to address the precise role of each of them in the β-cells fate.

Possible therapies that use UPR for restoring β-cells homeostasis should consider the existing β-cell stress level and

action inside a narrow safe range to overcome the excess and cell death. One possibility is employing agents that recover β-cell stress from terminal stage to the adaptive stage thus to facilitate the increase of β-cell mass through the mild stress. Therefore, there is a need for more tools for measuring and modulating β-cell stress *in vivo*.

AUTHOR CONTRIBUTIONS

AL, AG, AMV, and AnaMV read and reviewed the final version of the work, and participated in bibliographical research and design. AL assisted in the writing. AnaMV designed the concept and wrote the manuscript. All authors contributed to the article and approved the submitted version.

FUNDING

The research leading to these results has received funding from the NO Grants 2014-2021, under Project contract no. 21/2020 (RO-NO-2019-0544; BETAUPREG to AnaMV) and from a project co-financed by European Regional Development Fund through the Competitiveness Operational Program 2014–2020 (POC-A.1-A.1.1.4-E-2015, ID: P_37_668; DIABETER) and by Romanian Academy.

ACKNOWLEDGMENTS

The authors are grateful to Madalina Dumitrescu for productive discussions. We apologize to the many researchers whose work we could not cite due to space limitations.

REFERENCES

1. Herbert TP, Laybutt DR. A Reevaluation of the Role of the Unfolded Protein Response in Islet Dysfunction: Maladaptation or a Failure to Adapt? *Diabetes* (2016) 65:1472–80. doi: 10.2337/db15-1633
2. Laybutt DR, Preston AM, Akerfeldt MC, Kench JG, Busch AK, Biankin AV, et al. Endoplasmic reticulum stress contributes to beta cell apoptosis in type 2 diabetes. *Diabetologia* (2007) 50:752–63. doi: 10.1007/s00125-006-0590-z
3. Marhfour I, Lopez XM, Lefkaditis D, Salmon I, Allagnat F, Richardson SJ, et al. Expression of endoplasmic reticulum stress markers in the islets of patients with type 1 diabetes. *Diabetologia* (2012) 55:2417–20. doi: 10.1007/s00125-012-2604-3
4. Plaisance V, Brajkovic S, Tenenbaum M, Favre D, Ezanno H, Bonnefond A, et al. Endoplasmic Reticulum Stress Links Oxidative Stress to Impaired Pancreatic Beta-Cell Function Caused by Human Oxidized LDL. *PLoS One* (2016) 11:e0163046. doi: 10.1371/journal.pone.0163046
5. Rabhi N, Salas E, Froguel P, Annicotte JS. Role of the unfolded protein response in beta cell compensation and failure during diabetes. *J Diabetes Res* (2014) 2014:795171. doi: 10.1155/2014/795171
6. Araki K, Nagata K. Protein folding and quality control in the ER. *Cold Spring Harb Perspect Biol* (2011) 3:a007526. doi: 10.1101/cshperspect.a007526
7. Scheuner D, Kaufman RJ. The unfolded protein response: a pathway that links insulin demand with beta-cell failure and diabetes. *Endocr Rev* (2008) 29:317–33. doi: 10.1210/er.2007-0039
8. Liu M, Weiss MA, Arunagiri A, Yong J, Rege N, Sun J, et al. Biosynthesis, structure, and folding of the insulin precursor protein. *Diabetes Obes Metab* (2018) 20(Suppl 2):28–50. doi: 10.1111/dom.13378
9. Brozzi F, Eizirik DL. ER stress and the decline and fall of pancreatic beta cells in type 1 diabetes. *Ups J Med Sci* (2016) 121:133–9. doi: 10.3109/03009734.2015.1135217
10. Schroder M, Kaufman RJ. The mammalian unfolded protein response. *Annu Rev Biochem* (2005) 74:739–89. doi: 10.1146/annurev.biochem.73.011303.074134
11. Schroder M, Kaufman RJ. ER stress and the unfolded protein response. *Mutat Res* (2005) 569:29–63. doi: 10.1016/j.mrfmmm.2004.06.056
12. Cox JS, Walter P. A novel mechanism for regulating activity of a transcription factor that controls the unfolded protein response. *Cell* (1996) 87:391–404. doi: 10.1016/S0092-8674(00)81360-4
13. Harding HP, Novoa I, Zhang Y, Zeng H, Wek R, Schapira M, et al. Regulated translation initiation controls stress-induced gene expression in mammalian cells. *Mol Cell* (2000) 6:1099–108. doi: 10.1016/S1097-2765(00)00108-8
14. Harding HP, Zhang Y, Bertolotti A, Zeng H, Ron D. Perk is essential for translational regulation and cell survival during the unfolded protein response. *Mol Cell* (2000) 5:897–904. doi: 10.1016/S1097-2765(00)80330-5
15. Sidrauski C, Walter P. The transmembrane kinase Ire1p is a site-specific endonuclease that initiates mRNA splicing in the unfolded protein response. *Cell* (1997) 90:1031–9. doi: 10.1016/S0092-8674(00)80369-4
16. Yoshida H, Haze K, Yanagi H, Yura T, Mori K. Identification of the cis-acting endoplasmic reticulum stress response element responsible for transcriptional induction of mammalian glucose-regulated proteins. Involvement of basic leucine zipper transcription factors. *J Biol Chem* (1998) 273:33741–9. doi: 10.1074/jbc.273.50.33741
17. Yoshida H, Matsui T, Yamamoto A, Okada T, Mori K. XBP1 mRNA is induced by ATF6 and spliced by IRE1 in response to ER stress to produce a highly active transcription factor. *Cell* (2001) 107:881–91. doi: 10.1016/S0092-8674(01)00611-0
18. Acosta-Alvear D, Karagoz GE, Frohlich F, Li H, Walther TC, Walter P. The unfolded protein response and endoplasmic reticulum protein targeting machineries converge on the stress sensor IRE1. *Elife* (2018) 7:e43036. doi: 10.7554/eLife.43036
19. Carrara M, Prischi F, Nowak PR, Ali MM. Crystal structures reveal transient PERK luminal domain tetramerization in endoplasmic reticulum stress signaling. *EMBO J* (2015) 34:1589–600. doi: 10.15252/embj.201489183
20. Karagoz GE, Acosta-Alvear D, Nguyen HT, Lee CP, Chu F, Walter P. An unfolded protein-induced conformational switch activates mammalian IRE1. *Elife* (2017) 6:e30700. doi: 10.7554/eLife.30700
21. Kopp MC, Larburu N, Durairaj V, Adams CJ, Ali MMU. UPR proteins IRE1 and PERK switch BiP from chaperone to ER stress sensor. *Nat Struct Mol Biol* (2019) 26:1053–62. doi: 10.1038/s41594-019-0324-9
22. Kopp MC, Nowak PR, Larburu N, Adams CJ, Ali MM. In vitro FRET analysis of IRE1 and BiP association and dissociation upon endoplasmic reticulum stress. *Elife* (2018) 7:e30257. doi: 10.7554/eLife.30257
23. Adams CJ, Kopp MC, Larburu N, Nowak PR, Ali MMU. Structure and Molecular Mechanism of ER Stress Signaling by the Unfolded Protein Response Signal Activator IRE1. *Front Mol Biosci* (2019) 6:11. doi: 10.3389/fmolb.2019.00011
24. Karagoz GE, Acosta-Alvear D, Walter P. The Unfolded Protein Response: Detecting and Responding to Fluctuations in the Protein-Folding Capacity of the Endoplasmic Reticulum. *Cold Spring Harb Perspect Biol* (2019) 11:a033886. doi: 10.1101/cshperspect.a033886
25. Pobre KFR, Poet GJ, Hendershot LM. The endoplasmic reticulum (ER) chaperone BiP is a master regulator of ER functions: Getting by with a little help from ERdj friends. *J Biol Chem* (2019) 294:2098–108. doi: 10.1074/jbc.REV118.002804
26. Bertolotti A, Zhang Y, Hendershot LM, Harding HP, Ron D. Dynamic interaction of BiP and ER stress transducers in the unfolded-protein response. *Nat Cell Biol* (2000) 2:326–32. doi: 10.1038/35014014
27. Harding HP, Zhang Y, Ron D. Protein translation and folding are coupled by an endoplasmic-reticulum-resident kinase. *Nature* (1999) 397:271–4. doi: 10.1038/16729
28. Marciniak SJ, Garcia-Bonilla L, Hu J, Harding HP, Ron D. Activation-dependent substrate recruitment by the eukaryotic translation initiation factor 2 kinase PERK. *J Cell Biol* (2006) 172:201–9. doi: 10.1083/jcb.200508099

29. Harding HP, Zhang Y, Zeng H, Novoa I, Lu PD, Calfon M, et al. An integrated stress response regulates amino acid metabolism and resistance to oxidative stress. *Mol Cell* (2003) 11:619–33. doi: 10.1016/S1097-2765(03)00105-9
30. Suragani RN, Zachariah RS, Velazquez JG, Liu S, Sun CW, Townes TM, et al. Heme-regulated eIF2alpha kinase activated Atf4 signaling pathway in oxidative stress and erythropoiesis. *Blood* (2012) 119:5276–84. doi: 10.1182/blood-2011-10-388132
31. Lin JH, Li H, Yasumura D, Cohen HR, Zhang C, Panning B, et al. IRE1 signaling affects cell fate during the unfolded protein response. *Science* (2007) 318:944–9. doi: 10.1126/science.1146361
32. Lu M, Lawrence DA, Marsters S, Acosta-Alvear D, Kimmig P, Mendez AS, et al. Opposing unfolded-protein-response signals converge on death receptor 5 to control apoptosis. *Science* (2014) 345:98–101. doi: 10.1126/science.1254312
33. Balachandran S, Roberts PC, Brown LE, Truong H, Pattnaik AK, Archer DR, et al. Essential role for the dsRNA-dependent protein kinase PKR in innate immunity to viral infection. *Immunity* (2000) 13:129–41. doi: 10.1016/S1074-7613(00)00014-5
34. Gal-Ben-Ari S, Barrera I, Ehrlich M, Rosenblum K. PKR: A Kinase to Remember. *Front Mol Neurosci* (2018) 11:480. doi: 10.3389/fnmol.2018.00480
35. Vazquez de Aldana CR, Wek RC, Segundo PS, Truesdell AG, Hinnebusch AG. Multicopy tRNA genes functionally suppress mutations in yeast eIF-2 alpha kinase GCN2: evidence for separate pathways coupling GCN4 expression to unchanged tRNA. *Mol Cell Biol* (1994) 14:7920–32. doi: 10.1128/MCB.14.12.7920
36. Zhou Y, Shu F, Liang X, Chang H, Shi L, Peng X, et al. Ampelopsin induces cell growth inhibition and apoptosis in breast cancer cells through ROS generation and endoplasmic reticulum stress pathway. *PLoS One* (2014) 9:e89021. doi: 10.1371/journal.pone.0089021
37. Costa-Mattioli M, Walter P. The integrated stress response: From mechanism to disease. *Science* (2020) 368(6489):eaat5314. doi: 10.1126/science.aat5314
38. Pakos-Zebrucka K, Koryga I, Mnich K, Ljujic M, Samali A, Gorman AM. The integrated stress response. *EMBO Rep* (2016) 17:1374–95. doi: 10.15252/embr.201642195
39. Acosta-Alvear D, Zhou Y, Blais A, Tsikitis M, Lents NH, Arias C, et al. XBP1 controls diverse cell type- and condition-specific transcriptional regulatory networks. *Mol Cell* (2007) 27:53–66. doi: 10.1016/j.molcel.2007.06.011
40. Lee KP, Dey M, Neculai D, Cao C, Dever TE, Sicheri F. Structure of the dual enzyme Ire1 reveals the basis for catalysis and regulation in nonconventional RNA splicing. *Cell* (2008) 132:89–100. doi: 10.1016/j.cell.2007.10.057
41. Sriburi R, Jackowski S, Mori K, Brewer JW. XBP1: a link between the unfolded protein response, lipid biosynthesis, and biogenesis of the endoplasmic reticulum. *J Cell Biol* (2004) 167:35–41. doi: 10.1083/jcb.200406136
42. Hollien J, Lin JH, Li H, Stevens N, Walter P, Weissman JS. Regulated Ire1-dependent decay of messenger RNAs in mammalian cells. *J Cell Biol* (2009) 186:323–31. doi: 10.1083/jcb.200903014
43. Hollien J, Weissman JS. Decay of endoplasmic reticulum-localized mRNAs during the unfolded protein response. *Science* (2006) 313:104–7. doi: 10.1126/science.1129631
44. Urano F, Wang X, Bertolotti A, Zhang Y, Chung P, Harding HP, et al. Coupling of stress in the ER to activation of JNK protein kinases by transmembrane protein kinase IRE1. *Science* (2000) 287:664–6. doi: 10.1126/science.287.5453.664
45. Haze K, Yoshida H, Yanagi H, Yura T, Mori K. Mammalian transcription factor ATF6 is synthesized as a transmembrane protein and activated by proteolysis in response to endoplasmic reticulum stress. *Mol Biol Cell* (1999) 10:3787–99. doi: 10.1091/mbc.10.11.3787
46. Ye J, Rawson RB, Komuro R, Chen X, Dave UP, Prywes R, et al. ER stress induces cleavage of membrane-bound ATF6 by the same proteases that process SREBPs. *Mol Cell* (2000) 6:1355–64. doi: 10.1016/S1097-2765(00)00133-7
47. Hassler JR, Scheuner DL, Wang S, Han J, Kodali VK, Li P, et al. The IRE1alpha/XBP1s Pathway Is Essential for the Glucose Response and Protection of beta Cells. *PLoS Biol* (2015) 13:e1002277. doi: 10.1371/journal.pbio.1002277
48. Hong M, Li M, Mao C, Lee AS. Endoplasmic reticulum stress triggers an acute proteasome-dependent degradation of ATF6. *J Cell Biochem* (2004) 92:723–32. doi: 10.1002/jcb.20118
49. Hong M, Luo S, Baumeister P, Huang JM, Gogia RK, Li M, et al. Underglycosylation of ATF6 as a novel sensing mechanism for activation of the unfolded protein response. *J Biol Chem* (2004) 279:11354–63. doi: 10.1074/jbc.M309804200
50. Engin F, Nguyen T, Yermalovich A, Hotamisligil GS. Aberrant islet unfolded protein response in type 2 diabetes. *Sci Rep* (2014) 4:4054. doi: 10.1038/srep04054
51. Marre ML, Piganelli JD. Environmental Factors Contribute to beta Cell Endoplasmic Reticulum Stress and Neo-Antigen Formation in Type 1 Diabetes. *Front Endocrinol (Lausanne)* (2017) 8:262. doi: 10.3389/fendo.2017.00262
52. Vacaru AM, Di Narzo AF, Howarth DL, Tsedensodnom O, Imrie D, Cinaroglu A, et al. Molecularly defined unfolded protein response subclasses have distinct correlations with fatty liver disease in zebrafish. *Dis Model Mech* (2014) 7:823–35. doi: 10.1242/dmm.014472
53. Lipson KL, Ghosh R, Urano F. The role of IRE1alpha in the degradation of insulin mRNA in pancreatic beta-cells. *PLoS One* (2008) 3:e1648. doi: 10.1371/journal.pone.0001648
54. Tsuchiya Y, Saito M, Kadokura H, Miyazaki JII, Tashiro F, Imagawa Y, et al. IRE1-XBP1 pathway regulates oxidative proinsulin folding in pancreatic beta cells. *J Cell Biol* (2018) 217:1287–301. doi: 10.1083/jcb.201707143
55. Tsuchiya Y, Saito M, Kohno K. Pathogenic Mechanism of Diabetes Development Due to Dysfunction of Unfolded Protein Response. *Yakugaku Zasshi* (2016) 136:817–25. doi: 10.1248/yakushi.15-00292-4
56. Song B, Scheuner D, Ron D, Pennathur S, Kaufman RJ. Chop deletion reduces oxidative stress, improves beta cell function, and promotes cell survival in multiple mouse models of diabetes. *J Clin Invest* (2008) 118:3378–89. doi: 10.1172/JCI34587
57. Satoh T, Abiru N, Kobayashi M, Zhou H, Nakamura K, Kuriya G, et al. CHOP deletion does not impact the development of diabetes but suppresses the early production of insulin autoantibody in the NOD mouse. *Apoptosis* (2011) 16:438–48. doi: 10.1007/s10495-011-0576-2
58. Engin F, Yermalovich A, Nguyen T, Hummasti S, Fu W, Eizirik DL, et al. Restoration of the unfolded protein response in pancreatic beta cells protects mice against type 1 diabetes. *Sci Transl Med* (2013) 5:211ra156. doi: 10.1126/scitranslmed.3006534
59. Bensellam M, Jonas JC, Laybutt DR. Mechanisms of beta-cell dedifferentiation in diabetes: recent findings and future research directions. *J Endocrinol* (2018) 236:R109–43. doi: 10.1530/JOE-17-0516
60. Xin Y, Dominguez Gutierrez G, Okamoto H, Kim J, Lee AH, Adler C, et al. Pseudotime Ordering of Single Human beta-Cells Reveals States of Insulin Production and Unfolded Protein Response. *Diabetes* (2018) 67:1783–94. doi: 10.2337/db18-0365
61. Wasserfall C, Nick HS, Campbell-Thompson M, Beachy D, Haataja L, Kusmartseva I, et al. Persistence of Pancreatic Insulin mRNA Expression and Proinsulin Protein in Type 1 Diabetes Pancreata. *Cell Metab* (2017) 26:568–75.e563. doi: 10.1016/j.cmet.2017.08.013
62. Talchai C, Xuan S, Lin HV, Sussel L, Accili D. Pancreatic beta cell dedifferentiation as a mechanism of diabetic beta cell failure. *Cell* (2012) 150:1223–34. doi: 10.1016/j.cell.2012.07.029
63. Sharma RB, O'Donnell AC, Stamateris RE, Ha B, McCloskey KM, Reynolds PR, et al. Insulin demand regulates beta cell number via the unfolded protein response. *J Clin Invest* (2015) 125:3831–46. doi: 10.1172/JCI79264
64. Cigliola V, Thorel F, Chera S, Herrera PL. Stress-induced adaptive islet cell identity changes. *Diabetes Obes Metab* (2016) 18(Suppl 1):87–96. doi: 10.1111/dom.12726
65. Hodish I, Absood A, Liu L, Liu M, Haataja L, Larkin D, et al. In vivo misfolding of proinsulin below the threshold of frank diabetes. *Diabetes* (2011) 60:2092–101. doi: 10.2337/db10-1671
66. Wang R, Munoz EE, Zhu S, McGrath BC, Cavener DR. Perk gene dosage regulates glucose homeostasis by modulating pancreatic beta-cell functions. *PLoS One* (2014) 9:e99684. doi: 10.1371/journal.pone.0099684
67. Bernal-Mizrachi E, Kulkarni RN, Scott DK, Mauvais-Jarvis F, Stewart AF, Garcia-Ocana A. Human beta-cell proliferation and intracellular signaling

part 2: still driving in the dark without a road map. *Diabetes* (2014) 63:819–31. doi: 10.2337/db13-1146
68. Kulkarni RN, Mizrachi EB, Ocana AG, Stewart AF. Human beta-cell proliferation and intracellular signaling: driving in the dark without a road map. *Diabetes* (2012) 61:2205–13. doi: 10.2337/db12-0018
69. Garg AD, Kaczmarek A, Krysko O, Vandenabeele P, Krysko DV, Agostinis P. ER stress-induced inflammation: does it aid or impede disease progression? *Trends Mol Med* (2012) 18:589–98. doi: 10.1016/j.molmed.2012.06.010
70. Brozzi F, Gerlo S, Grieco FA, Juusola M, Balhuizen A, Lievens S, et al. Ubiquitin D Regulates IRE1alpha/c-Jun N-terminal Kinase (JNK) Protein-dependent Apoptosis in Pancreatic Beta Cells. *J Biol Chem* (2016) 291:12040–56. doi: 10.1074/jbc.M115.704619
71. Campbell-Thompson M, Fu A, Kaddis JS, Wasserfall C, Schatz DA, Pugliese A, et al. Insulitis and beta-Cell Mass in the Natural History of Type 1 Diabetes. *Diabetes* (2016) 65:719–31. doi: 10.2337/db15-0779
72. Coppieters KT, Dotta F, Amirian N, Campbell PD, Kay TW, Atkinson MA, et al. Demonstration of islet-autoreactive CD8 T cells in insulitic lesions from recent onset and long-term type 1 diabetes patients. *J Exp Med* (2012) 209:51–60. doi: 10.1084/jem.20111187
73. Eizirik DL, Colli ML, Ortis F. The role of inflammation in insulitis and beta-cell loss in type 1 diabetes. *Nat Rev Endocrinol* (2009) 5:219–26. doi: 10.1038/nrendo.2009.21
74. Montane J, Cadavez L, Novials A. Stress and the inflammatory process: a major cause of pancreatic cell death in type 2 diabetes. *Diabetes Metab Syndr Obes* (2014) 7:25–34. doi: 10.2147/DMSO.S37649
75. Demine S, Schiavo AA, Marin-Canas S, Marchetti P, Cnop M, Eizirik DL. Pro-inflammatory cytokines induce cell death, inflammatory responses, and endoplasmic reticulum stress in human iPSC-derived beta cells. *Stem Cell Res Ther* (2020) 11:7. doi: 10.1186/s13287-019-1523-3
76. Gurzov EN, Eizirik DL. Bcl-2 proteins in diabetes: mitochondrial pathways of beta-cell death and dysfunction. *Trends Cell Biol* (2011) 21:424–31. doi: 10.1016/j.tcb.2011.03.001
77. Russell MA, Morgan NG. The impact of anti-inflammatory cytokines on the pancreatic beta-cell. *Islets* (2014) 6:e950547. doi: 10.4161/19382014.2014.950547
78. Tyka K, Jorns A, Turatsinze JV, Eizirik DL, Lenzen S, Gurgul-Convey E. MCPIP1 regulates the sensitivity of pancreatic beta-cells to cytokine toxicity. *Cell Death Dis* (2019) 10:29. doi: 10.1038/s41419-018-1268-4
79. Grieco FA, Vendrame F, Spagnuolo I, Dotta F. Innate immunity and the pathogenesis of type 1 diabetes. *Semin Immunopathol* (2011) 33:57–66. doi: 10.1007/s00281-010-0206-z
80. Ryan GA, Wang CJ, Chamberlain JL, Attridge K, Schmidt EM, Kenefeck R, et al. B1 cells promote pancreas infiltration by autoreactive T cells. *J Immunol* (2010) 185:2800–7. doi: 10.4049/jimmunol.1000856
81. Cucak H, Mayer C, Tonnesen M, Thomsen LH, Grunnet LG, Rosendahl A. Macrophage contact dependent and independent TLR4 mechanisms induce beta-cell dysfunction and apoptosis in a mouse model of type 2 diabetes. *PloS One* (2014) 9:e90685. doi: 10.1371/journal.pone.0090685
82. Eguchi K, Manabe I. Macrophages and islet inflammation in type 2 diabetes. *Diabetes Obes Metab* (2013) 15(Suppl 3):152–8. doi: 10.1111/dom.12168
83. Hasnain SZ, Borg DJ, Harcourt BE, Tong H, Sheng YH, Ng, et al. Glycemic control in diabetes is restored by therapeutic manipulation of cytokines that regulate beta cell stress. *Nat Med* (2014) 20(12):1417–26. doi: 10.1038/nm.3705
84. Cardozo AK, Ortis F, Storling J, Feng YM, Rasschaert J, Tonnesen M, et al. Cytokines downregulate the sarcoendoplasmic reticulum pump Ca2+ ATPase 2b and deplete endoplasmic reticulum Ca2+, leading to induction of endoplasmic reticulum stress in pancreatic beta-cells. *Diabetes* (2005) 54:452–61. doi: 10.2337/diabetes.54.2.452
85. Ortis F, Naamane N, Flamez D, Ladriere L, Moore F, Cunha DA, et al. Cytokines interleukin-1beta and tumor necrosis factor-alpha regulate different transcriptional and alternative splicing networks in primary beta-cells. *Diabetes* (2010) 59:358–74. doi: 10.2337/db09-1159
86. DeZwaan-McCabe D, Riordan JD, Arensdorf AM, Icardi MS, Dupuy AJ, Rutkowski DT. The stress-regulated transcription factor CHOP promotes hepatic inflammatory gene expression, fibrosis, and oncogenesis. *PloS Genet* (2013) 9:e1003937. doi: 10.1371/journal.pgen.1003937
87. Suzuki T, Gao J, Ishigaki Y, Kondo K, Sawada S, Izumi T, et al. ER Stress Protein CHOP Mediates Insulin Resistance by Modulating Adipose Tissue Macrophage Polarity. *Cell Rep* (2017) 18:2045–57. doi: 10.1016/j.celrep.2017.01.076
88. Diana J, Gahzarian L, Simoni Y, Lehuen A. Innate immunity in type 1 diabetes. *Discovery Med* (2011) 11:513–20.
89. Meyerovich K, Ortis F, Cardozo AK. The non-canonical NF-kappaB pathway and its contribution to beta-cell failure in diabetes. *J Mol Endocrinol* (2018) 61:F1–6. doi: 10.1530/JME-16-0183
90. Meyerovich K, Ortis F, Allagnat F, Cardozo AK. Endoplasmic reticulum stress and the unfolded protein response in pancreatic islet inflammation. *J Mol Endocrinol* (2016) 57:R1–R17. doi: 10.1530/JME-15-0306
91. Keller G. Embryonic stem cell differentiation: emergence of a new era in biology and medicine. *Genes Dev* (2005) 19:1129–55. doi: 10.1101/gad.1303605
92. Swisa A, Glaser B, Dor Y. Metabolic Stress and Compromised Identity of Pancreatic Beta Cells. *Front Genet* (2017) 8:21. doi: 10.3389/fgene.2017.00021
93. Cinti F, Bouchi R, Kim-Muller JY, Ohmura Y, Sandoval PR, Masini M, et al. Evidence of beta-Cell Dedifferentiation in Human Type 2 Diabetes. *J Clin Endocrinol Metab* (2016) 101:1044–54. doi: 10.1210/jc.2015-2860
94. Efrat S. Beta-Cell Dedifferentiation in Type 2 Diabetes: Concise Review. *Stem Cells* (2019) 37:1267–72. doi: 10.1002/stem.3059
95. Hunter CS, Stein RW. Evidence for Loss in Identity, De-Differentiation, and Trans-Differentiation of Islet beta-Cells in Type 2 Diabetes. *Front Genet* (2017) 8:35. doi: 10.3389/fgene.2017.00035
96. Weir GC, Aguayo-Mazzucato C, Bonner-Weir S. beta-cell dedifferentiation in diabetes is important, but what is it? *Islets* (2013) 5:233–7. doi: 10.4161/isl.27494
97. Rahier J, Guiot Y, Goebbels RM, Sempoux C, Henquin JC. Pancreatic beta-cell mass in European subjects with type 2 diabetes. *Diabetes Obes Metab* (2008) 10(Suppl 4):32–42. doi: 10.1111/j.1463-1326.2008.00969.x
98. Zhu Y, Sun Y, Zhou Y, Zhang Y, Zhang T, Li Y, et al. MicroRNA-24 promotes pancreatic beta cells toward dedifferentiation to avoid endoplasmic reticulum stress-induced apoptosis. *J Mol Cell Biol* (2019) 11:747–60. doi: 10.1093/jmcb/mjz004
99. Lee H, Lee YS, Harenda Q, Pietrzak S, Oktay HZ, Schreiber S, et al. Beta Cell Dedifferentiation Induced by IRE1alpha Deletion Prevents Type 1 Diabetes. *Cell Metab* (2020) 31:822–36.e825. doi: 10.1016/j.cmet.2020.03.002
100. Starling S. beta-cell dedifferentiation prior to insulitis prevents T1DM. *Nat Rev Endocrinol* (2020) 16:301. doi: 10.1038/s41574-020-0358-4
101. Lin HM, Lee JH, Yadav H, Kamaraju AK, Liu E, Zhigang D, et al. Transforming growth factor-beta/Smad3 signaling regulates insulin gene transcription and pancreatic islet beta-cell function. *J Biol Chem* (2009) 284:12246–57. doi: 10.1074/jbc.M805379200
102. Rezania A, Riedel MJ, Wideman RD, Karanu F, Ao Z, Warnock GL, et al. Production of functional glucagon-secreting alpha-cells from human embryonic stem cells. *Diabetes* (2011) 60:239–47. doi: 10.2337/db10-0573
103. Blum B, Roose AN, Barrandon O, Maehr R, Arvanites AC, Davidow LS, et al. Reversal of beta cell de-differentiation by a small molecule inhibitor of the TGFbeta pathway. *Elife* (2014) 3:e02809. doi: 10.7554/eLife.02809
104. Sun S, Shi G, Han X, Francisco AB, Ji Y, Mendonca N, et al. Sel1L is indispensable for mammalian endoplasmic reticulum-associated degradation, endoplasmic reticulum homeostasis, and survival. *Proc Natl Acad Sci USA* (2014) 111:E582–91. doi: 10.1073/pnas.1318114111
105. Shrestha N, Liu T, Ji Y, Reinert RB, Torres M, Li X, et al. Sel1L-Hrd1 ER-associated degradation maintains beta cell identity via TGF-beta signaling. *J Clin Invest* (2020) 130:3499–510. doi: 10.1172/JCI134874
106. Matus S, Lisbona F, Torres M, Leon C, Thielen P, Hetz C. The stress rheostat: an interplay between the unfolded protein response (UPR) and autophagy in neurodegeneration. *Curr Mol Med* (2008) 8:157–72. doi: 10.2174/156652408784221324

Conflict of Interest: The authors declare that the research was conducted in the absence of any commercial or financial relationships that could be construed as a potential conflict of interest.

frontiers in Endocrinology

MINI REVIEW
published: 03 February 2021
doi: 10.3389/fendo.2020.619150

Cell Heterogeneity and Paracrine Interactions in Human Islet Function: A Perspective Focused in β-Cell Regeneration Strategies

Eva Bru-Tari, Daniel Oropeza and Pedro L. Herrera *

Department of Genetic Medicine and Development, Faculty of Medicine, University of Geneva, Geneva, Switzerland

The β-cell regeneration field has shown a strong knowledge boost in the last 10 years. Pluripotent stem cell differentiation and direct reprogramming from other adult cell types are becoming more tangible long-term diabetes therapies. Newly generated β-like-cells consistently show hallmarks of native β-cells and can restore normoglycemia in diabetic mice in virtually all recent studies. Nonetheless, these cells still show important compromises in insulin secretion, cell metabolism, electrical activity, and overall survival, perhaps due to a lack of signal integration from other islet cells. Mounting data suggest that diabetes is not only a β-cell disease, as the other islet cell types also contribute to its physiopathology. Here, we present an update on the most recent studies of islet cell heterogeneity and paracrine interactions in the context of restoring an integrated islet function to improve β-cell replacement therapies.

Keywords: human islet, beta-cell regeneration, paracrine signaling, cell heterogeneity, glucose homeostasis

OPEN ACCESS

Edited by:
Hanne Scholz,
University of Oslo, Norway

Reviewed by:
Weiping Han,
*Singapore Bioimaging Consortium (A*STAR), Singapore*
Hail Kim,
Korea Advanced Institute of Science and Technology, South Korea

***Correspondence:**
Pedro L. Herrera
pedro.herrera@unige.ch

Specialty section:
This article was submitted to Cellular Endocrinology, a section of the journal Frontiers in Endocrinology

Received: *19 October 2020*
Accepted: *14 December 2020*
Published: *03 February 2021*

Citation:
Bru-Tari E, Oropeza D and Herrera PL (2021) Cell Heterogeneity and Paracrine Interactions in Human Islet Function: A Perspective Focused in β-Cell Regeneration Strategies. Front. Endocrinol. 11:619150. doi: 10.3389/fendo.2020.619150

INTRODUCTION

The islets of Langerhans are complex micro-organs composed of different endocrine cell types whose principal function is the maintenance of glucose homeostasis and feeding behavior through coordinated hormone secretion and paracrine interactions. Different studies have estimated the human islet to be comprised mainly by insulin-secreting β-cells in the range of 52–75% (1–5). Following in number, glucagon-secreting α-cells and somatostatin-secreting δ-cells comprise some 40 and 10% of the islet. Pancreatic polypeptide (PP)-secreting γ-cells and ghrelin-secreting ϵ-cells are the minor cell types comprising about 5% and less than 1% of the islet, respectively. Islets cells are characterized by an exquisite secretory capacity and cell mass modulation that efficiently adapts to diverse metabolic stresses or pathologies like pregnancy and obesity. Defects in this adaptive capacity are at the core of certain impairments in nutrient metabolism and diabetes development (6–8).

The different islet cell types are arranged in an intricate network that facilitates cell proximity and direct contacts that fine-tune hormone secretion to robustly control glucose homeostasis. In human islets, there is a predominance of heterologous contacts between β- and α-cells, suggesting their direct interaction is crucial for glycaemia management (9). Indeed, paracrine α-cell signaling establishes a set point for insulin secretion and glycemia throughout different animal species (10). Dysregulation of islet paracrine interactions and non-β-cell function contribute substantially to diabetes symptomatology (11–17). This could be one of the reasons why conventional diabetes

therapies relying solely on exogenous insulin do not maintain stable normoglycemia. It is becoming apparent that diabetes is a disease concerning the whole islet, yet regenerative approaches have for the most part focused mainly on restoring a functional β-cell mass and basal insulin secretion with little regard on achieving a balanced islet secretory output. Here, we present an update on recent studies highlighting the importance of islet paracrine interactions and cell heterogeneity for a highly malleable human islet function that achieves optimal glucose homeostasis and withstands the range of stresses present in the ever-changing physiologic and cellular environment.

DIABETES AFFECTS ALL ISLET ENDOCRINE CELL TYPES

Mounting data shows that the complex islet cytoarchitecture, gene expression, and function of non-β-cells are also significantly compromised throughout diabetes progression. Both T1D and T2D patients present hyperglucagonemia in postprandial conditions or upon oral glucose challenge, that exacerbates hyperglycemia (11–15). The reasons are not fully understood, yet i) lack of intra-islet insulin, ii) dysfunctional α-cell glucose sensing, or iii) increases in the functional α-cell mass may be underlying mechanisms. A convoluted combination of these defects may also be possible, as T2D patients present hyperglucagonemia even in the fasting state (16, 17) while T1D patients present a defective α-cell response to hypoglycemia (18).

In T1D, α-cell mass is maintained in the early stages of the disease (19) while it clearly decreases in advanced stages (20). For T2D, most published studies do not specify the stage of the disease, and report conflicting results depending on the analytical method, with a higher α- to β-cell ratio in long-standing T2D pancreas (9, 21, 22) or a decrease of the total glucagon+ area in all regions of the pancreas (23), but no differences in α-cell mass (22). This suggests that α-cell defects may not be due to an increased cell mass. In concordance, recent studies with islets from T2D donors show no inhibition of glucagon secretion *in vitro* at high glucose concentrations (24). Moreover, transplantation of islets from T2D donors into a novel Glucagon knockout-NSG mouse model showed increased glucagon secretion during fasting and upon insulin-induced hypoglycemia, suggesting that hyperglucagonemia in T2D is caused by local islet defects that are not resolved when transplanted into a non-diabetic environment (25). Nonetheless, the effect of induced hyperglycemia was not tested in this study. In addition, single cell RNA sequencing (scRNA-seq) of α- and δ-cells from T2D donors showed a downregulation of energy metabolism and protein synthesis genes (26, 27). In contrast, islets from T1D donors show decreased glucagon secretion at low glucose concentrations *in vitro* (28), underlying the high risk of severe hypoglycemia after insulin administration in T1D patients (18, 28). α-cells from T1D donors also show differential gene expression, including in electrical activity and exocytosis, as well as master regulators of α-cell identity, *ARX* and *MAFB* (28).

Only few studies tested the effect of diabetes on the minor islet cell types, yet it is likely they are also significantly affected. ϵ-cells show a reduction in their number that could be linked to lower plasma ghrelin levels in T2D (29). Yet, this is unlikely since most ghrelin-secreting cells are extrapancreatic (gastric fundus). In δ-cells, islets from T2D donors showed blunted *in vitro* somatostatin secretion in response to glucose while some donors show hypersecretion at low glucose (30). While there are no reports on δ-cells from T1D donors, recent findings in diabetic mice indicate that increased somatostatin signaling may be reducing counter-regulatory glucagon secretion during insulin-induced hypoglycemia (31). Finally, T2D patients present high plasma levels of PP after an oral glucose challenge (32). As PP inhibits somatostatin secretion in human islets (33), is possible that increased levels of PP contribute to diabetic hyperglucagonemia by decreasing the somatostatin inhibitory effect on α-cells.

Collectively, these studies suggest that diabetes eventually becomes an islet disease affecting all islet cells or that the degree of initial non-β-cell dysfunction is a contributing factor accelerating the progression or the severity of diabetes. Whether non-β-cell defects are intrinsic or solely the result of the decrease in β-cells and local insulin, is still the focus of intense research. Little is known about the role of non-β-cell function in glucose intolerance, prediabetes or the initial stages of diabetes. δ-Cell electrical oscillatory activity in response to glucose stimulation is impaired in insulin resistant mice treated with high fat diet (34) and non-human primates show decreased proportion of δ-cells per islet that progresses with mounting hyperglycemia, possibly caused by δ-cell apoptosis (35). Alterations in δ-cell secretory function during the progression of type 2 diabetes may exacerbate β-cell exhaustion due to a lack of inhibitory signals exerted by somatostatin or could be an adaptation to the higher insulin demand during prediabetes. In the case of α-cells, insulin resistant and glucose intolerant mice under high fat diet present α-cell hypertrophy and lack of suppression of glucagon release upon intraperitoneal glucose injection (36). Studies with obese subjects also observed hyperglucagonemia upon postprandial conditions (37) and in non-human primates α-cell mass tends to increase with the duration and severity of obesity (38). It has been postulated that α-cell insulin resistance (39), intrinsic defects in α-cell glucose sensing or a reduced somatostatin signaling may lead to α-cell functional alterations at this stage (40). Nonetheless, these observations also highlight that defects in non-β-cells may appear in the eventual progression to T2D.

Analysis of non-β-cell numbers and circulating levels of their corresponding hormones in prediabetes or the initial stages of diabetes is needed to understand when these defects start and their contribution to diabetes before β-cell function is impaired. Likewise, whether defective α-cell function in diabetes is completely restored by the regeneration of a functional β-cell mass is still not clear. T1D recipients of islet transplants showed an absence or only partial restoration of glucagon secretion upon insulin-induced hypoglycemia (41–43). The combination of mouse diabetic models showing dysregulated glucagon secretion (44, 45) that allow the measurement of human

plasmatic glucagon (25) and transplantation of purified human α-cells alone or in combination with other islets cells will be needed to address this issue.

HUMAN ISLET ARCHITECTURE FAVORS HETEROLOGOUS CONTACTS BETWEEN ENDOCRINE CELLS: IMPLICATIONS IN THE COUNTER-REGULATORY ISLET RESPONSE TO HYPOGLYCEMIA

In 1982, pioneering studies described a poor responsiveness of isolated single rat β-cells to glucose, an effect that was linked to the lack of α-cell contacts and glucagon, revealing the crucial role of the islet architecture in the optimal functional cooperation between islet cells (46). Since then, most studies have focused on the core-mantle arrangement of rodent islets that clusters β-cells in the center surrounded by peripheral non-β-cells (4). This favors homologous β-to-β cell contacts shown to be critical in mice for regulating *in vivo* insulin secretory dynamics and glucose homeostasis through gap-junction coupling (47), which drives β-cell synchronization in terms of electrical activity and intracellular calcium concentration. However, it is broadly accepted that human islet cell types are distributed more randomly (3, 4). Recent studies show that the human islet involves a more intricate structure that depends on islet size. Small human islets (40-60 μm in diameter), which are more frequent during childhood, display the core-mantle structure of rodent islets, while large islets are formed by multiple subunits of β-cell clusters surrounded by non-β cells, containing a lower proportion of β-cells than the smaller ones (48). A similar trend is observed between juvenile and aged mice. This unique arrangement presents a higher rate of heterologous contacts, while maintaining homologous contacts between β-cells (9). In the case of humans, β-cells seem to be less synchronized than in mice in response to stimulatory glucose concentrations (4), possibly due to their organization within the islet, which can prime them to have a weaker β-cell electrical coupling. Indeed, synchronous intracellular calcium oscillations in response to stimulatory glucose concentrations have been recorded only in β-cells within the same islet region (49). The higher rate of heterologous contacts within the human islet suggests that counter-regulatory paracrine interactions might play a more important role in human than in mouse islets for the fine tuning of insulin secretion and glycemia maintenance. **Figure 1** summarizes paracrine interactions between human islet cell types.

In humans, α-cell signaling potentiates insulin secretion throughout a wide range of glucose concentrations (50), establishes the glycemic set point for insulin secretion (10) and enhances insulin secretion when β-cells are in contact with α-cells (51). This is classically known to be mediated by glucagon signaling (10), which activates human β-cell G protein-coupled receptors (GPCR) of class B, including glucagon receptor (GCGR), and glucagon-like peptide 1 receptor (GLP-1R), promoting insulin secretion by an increase in cyclic AMP and the recruitment of insulin granules (50). However, GLP-1 is also secreted by human α-cells (52–54) and necessary for insulin secretion in human islets, as GLP-1R antagonism blunted glucose stimulated insulin secretion (GSIS) *in vitro* (54). Moreover, GLP-1 can elicit synchronous intracellular calcium oscillations in human whole islets (55), suggesting an important role of this hormone and the location of α-cells within the islet to obtain pulsatile and synchronized insulin secretion. Human α-cells also amplify GSIS through the parasympathetic neurotransmitter acetylcholine, which is co-secreted with glucagon (56, 57) and acts through the activation of the muscarinic receptor M3 in β-cells (57). It has been postulated that this mechanism aids in maintaining β-cell responsiveness to the subsequent rise in glucose produced by glucagon action (56). Subsequently, excessive insulin release and hypoglycemia are avoided by a paracrine negative feedback loop between β- and δ-cells (58), mediated by urocortin-3 (UCN3), which is released by β-cells along with insulin. UCN3 activates type 2 corticotropin-releasing hormone receptors specifically borne by δ-cells within the human islet and stimulates somatostatin secretion (58), which directly inhibits insulin secretion through somatostatin receptor 2 (SSTR2) activation (59). Recent data shows that human δ-cells have long filopodia containing secretory granules that allow for direct contact with multiple β- and α-cells (34), and suggests that human β- and δ-cells are coupled by gap junctions (60), as somatostatin secretion follows the same pulsatile and coordinated response of insulin secretion in isolated islets (61).

Recent data is also starting to shed light on how paracrine interactions control α- and δ-cell secretory outputs. The activation of somatostatin secretion by β-cells, directly inhibits glucagon secretion through SSTR2 in α-cells (31) and *in vitro* chemical inhibition of insulin or somatostatin signaling in whole human islets induces glucagon secretion at non-stimulatory glucose concentrations (24). Isolated human α-cells also activate glucagon secretion at non-stimulatory glucose concentrations, which was corrected by reaggregation with purified β-cells but not by incubation with β-cell secreted factors (62). Lastly, ghrelin has been recently shown to suppress insulin secretion in human islets (29) and potentiate somatostatin release (63), thus suggesting a novel role for ϵ-cells in the control of hypoglycemia. Conversely, γ-cells seem to enhance human insulin secretion through an inhibition in somatostatin secretion caused by the PP activation of NPYR4 receptor in δ-cells (33). PP also activates the PPYR1 receptor (which is present in human α-cells) in mouse α-cells and inhibits glucagon secretion (64).

Knowledge about how human islet structure and the integrated input of paracrine signaling control synchronization of β-cells and islet hormone secretion is scarce and fragmented in comparison with the mouse islet. While mouse islets present tightly synchronized β-cell function and less heterologous cell contacts, non-β-cells might play a more important role in human islets. New techniques employing high yields of purified primary human islet cells will be necessary to study the contribution of

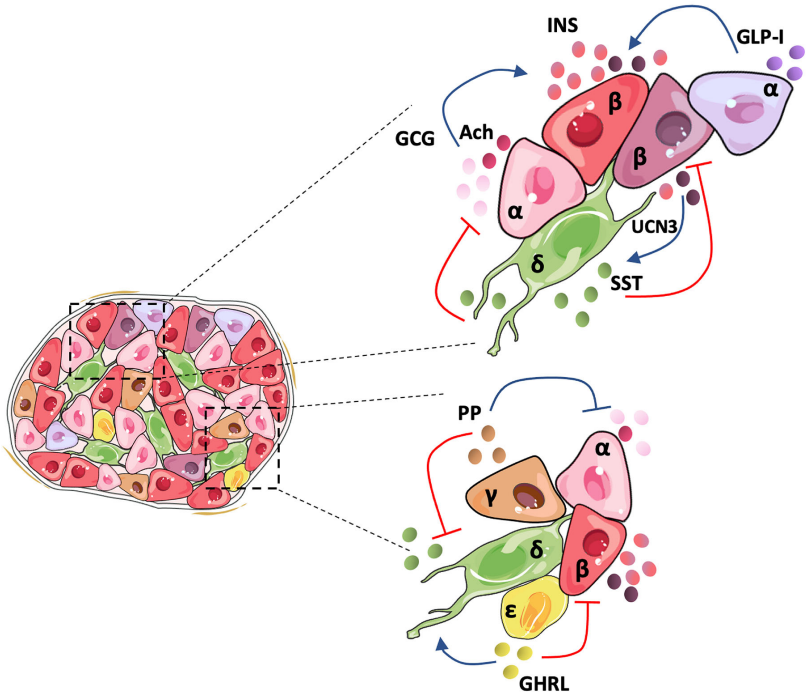

FIGURE 1 | Human islet architecture favors heterologous contacts and holds a tightly regulated cellular inter-communication network. In the human islet, β-and non-β-cells present frequent contacts favoring paracrine signaling between the cells. Human α-cells secrete mainly glucagon (GCG), acetylcholine (Ach), and GLP-I, which activates insulin secretion by β-cells. It has been postulated that an α-cell subpopulation holds the intra-islet secretion of GLP-I. Human pancreatic β-cells comprise a heterogeneous population and may hold differences in the amount of insulin (INS) secreted depending on the subpopulation. UCN3 is secreted along with INS and activates somatostatin (SST) release by δ-cells. SST inactivates GLC and INS secretion, closing the loop of paracrine signaling between the main islet cell types. Although less studied, the minor islet cell types also contribute to the regulation of the islet hormone secretion. Pancreatic polypeptide (PP) secreted by γ-cells suppresses both GCG and SST release, and ghrelin (GHRL), produced by ϵ-cells, seems to activate SST and inhibit INS release.

each cell type to integrated islet function. Systematic and high-resolution secretory profiling under various metabolic stresses, using isolated as well as reaggregated human islet cells in different combinations, will help dissect the bewildering interplay of interactions that coordinate optimal islet secretion. A recent study employing reaggregated human islets and a microfluidic system that measures secretion concurrently with intracellular signaling dynamics highlights the importance of developing new tools to study human islet cells, as it revealed G_i GPCR signaling decreases insulin and glucagon secretion while G_q GPCRs stimulate glucagon secretion but have dual effects on insulin secretion (65).

HUMAN ISLETS ARE COMPRISED OF HETEROGENEOUS CELL POPULATIONS: RELEVANCE IN β-CELL FUNCTION AND STRESS ADAPTATION

A higher level of complexity stems from recently identified β- and α-cell subpopulations based on physiological (66–68), transcriptomic (27, 67, 69–72), and proteomic differences (73–75). Upon stimulatory conditions, human β-cells located in discrete islet regions synchronize calcium flux and electrophysiology (4, 49, 76). Shedding light on whether this is due to their location in the islet, their specific β-β physical interactions or to intrinsic features, employing functional cell mapping with optogenetics, "hub" β-cells (10% of the human islet) were identified as first-responders that engage other β-cells into insulin secretion (66). These cells are considered immature based on low *Pdx1* and *Nkx6.1* expression and low insulin content (66). In mouse islets, "hub" β-cell function is not affected by the inhibition of glucagon signaling or by their location within the islet (66). However, these features have not been explored in human cells, neither whether "hub" cells have a higher number of contacts with α-cells or δ-cells, which could hint at which cell type has a bigger functional influence on this β-cell subpopulation.

Interestingly, "hub" β-cells are more susceptible to glucolipotoxicity, resulting in reduced numbers and high glucokinase protein levels (66). The genes involved in responses to different metabolic insults [including unfolded protein response (UPR), endoplasmic reticulum (ER) stress, and oxidative stress] efficiently cluster β-cells into subpopulations (69–71). This is one of the most relevant features across different scRNA-seq analyses of β-cell heterogeneity, although there is no consensus on the transcriptomic identity of β-cell subpopulations (27, 69–71).

In one instance, three β-cell sub clusters where observed matching low UPR with low insulin expression, low UPR with high insulin, and high UPR with low insulin (69). These groups might be transiently moving between a state high insulin production and secretion to fulfill the requirements that maintain normoglycemia, and a state of UPR-mediated recovery from ER stress due to high insulin production, taking the role of hub cells that orchestrate secretion from neighboring cells (69). Importantly, the heterogeneity in UPR responses may have a significant impact on the survival of β-cells to metabolic insults as chronic UPR activation is present in islets from T2D donors and those at risk to suffer the disease (77). However, other studies have not observed differences in UPR-related genes or correlation of any of these β-cell subpopulations with obesity or T2D (27, 72).

In the case of human α-cells, several scRNA-seq analyses identified human α-cell subpopulations with a proliferative profile (27, 69, 72), which have also been reported in pancreatic sections of adolescents (78) and can be correlated with a lower expression of UPR genes (69). At the functional level, GLP-1 secretion has been linked to specific α-cell subgroups that are more prevalent in T2D, indicating a possible α-cell adaptation to higher insulin demand (68). At the structural level, α-cells can be divided into subsets containing different ranges of glucagon granules (75), which suggest distinct secretory properties, yet no heterogeneity in glucagon secretion has been reported (68). However, studies in mice have shown that α-cell subsets vary in calcium flux and membrane capacitance upon stimulatory conditions (45, 79), which may correlate with granule density.

Studies that connect transcriptionally distinct subpopulations with β- and α-cell function are scarce due to technical limitations. Initial reports linked the lack of cell surface markers CD9 and ST8SIA1 with a β-cell subpopulation showing decreased insulin secretion (73). More recently, a study combining scRNA-seq with patch-clamp electrophysiological measurements of vesicle exocytosis and ion-channel activity, found improved excitability properties in a subpopulation of low-expressing *RBP4* β-cells in non-diabetic donors, as well as α-cell electrophysiological heterogeneity correlated with differential expression of ER stress markers in non-diabetic and T2D samples (67). Novel methods to inactivate specific subpopulations will unravel the role of heterogeneity in islet function.

CONCLUDING REMARKS: TARGETING ISLET PARACRINE INTERACTIONS AND HETEROGENEITY FOR OPTIMAL AND ROBUST ISLET FUNCTION IN β-CELL REGENERATION STRATEGIES

Available data suggests that diabetes affects all islet cell types. Islet paracrine interactions and heterogeneity are key features that allow adaptation to a wide spectrum of physiological challenges. Consequently, β-cell regeneration strategies must consider these factors to restore optimal islet secretory capacity. Indeed, islet transplantation, which would partially replenish a functional islet mass, restores circulating insulin to comparable levels of healthy individuals (80, 81), although efficient glucagon secretion upon hypoglycemia is only partially restored (41, 42). It is unclear if transplanting only β-cells to diabetic patients would give similar results, but analogous experiments could be performed in diabetic mice using different combinations of purified human islet populations. *De novo* generation of surrogate or replacement β-cells from stem cells (SC-β), or other cell sources, has focused in achieving insulin production and secretion comparable to native β-cells under stable conditions. Recent protocols yield SC-β cells that reverse hyperglycemia in mice for up to 45 days, with detectable human C-peptide within 3–14 days after transplantation (82–86). Despite this amazing progress, SC-β cells do not achieve the biphasic insulin release nor the magnitude of insulin secretion of cadaveric islets *in vitro*, possibly because of a disconnection in glucose sensing (87). Moreover, long-term analysis or the whole range of metabolic stresses including pregnancy, obesity, pathogenic infection, or extreme fasting [where β-cells undergo major modifications which must be quickly reversed after refeeding (88)] have not been explored. Besides, the impact of cell heterogeneity in SC-β strategies remains elusive, with only one report indicating that β-cell subpopulations were not detected after SC-β transplantation in mice (89). Although there are not such studies in human, heterogeneity is crucial in mice for β-cell adaptation to pathological stressors like obesogenic diets (90).

The signals coming from a diverse non-β-cell population might be pivotal to maintain robust insulin content and secretion throughout all these conditions. As described above, while mouse islets seem to rely on homologous β-cell contacts to achieve a synchronized function, in humans, non-β-cells may play a fundamental role as heterologous contacts are more prevalent and GLP-I signaling elicits a coordinated β-cell activation (55). Moreover, functional non-β-cells could also be required for the maturation, as glucagon receptor KO mice show lower expression of Pdx1, Glut2, and MafA in β-cells (91). Additionally, decreased insulin content occurs in glucagon-GFP knock-in mice that lack proglucagon derived peptides (92) and human insulin promoter activity is stimulated by GLP-1 (93). The implications of the cellular architecture and cell diversity in the generation of functional SC-β-cells has been studied recently by the generation of human islet-like organoids (94), containing some 60% of cells co-expressing insulin and other key β-cell markers, along with glucagon, somatostatin, and PP-positive cells (94). This improved functional maturation of SC-β-cells in terms of GSIS and, after the transplantation in mice, allowed for controlled insulin secretion upon a cycle of feeding, fasting, and refeeding (94). Although controls with only SC-β cells is needed to prove if this tuned insulin secretion is driven by adjacent non-β cells, the presence of UCN3 at protein level in β-cells, suggests that paracrine signaling may be restored (94).

Overall, non-β-cell paracrine signaling is key for optimal islet hormone secretion and any disruption to this balanced cell system may exacerbate diabetes symptomatology and compromise β-cell function. In diabetes, non-β-cells present

defects that may be not rectified by the sole reestablishment of insulin signaling *via* β-cell regeneration approaches. This data supports the idea that non-β-cells should be included in the regenerative strategies to treat diabetes. Likewise, the capacity of adaptation of newly generated β-cells and the role cell heterogeneity may play in coping mechanisms that respond to different physiological and pathological metabolic challenges *in vivo* is also an open question. Experiments that resolve these matters would highlight pivotal pitfalls in β-cell regeneration approaches aimed at restoring integrated islet function.

AUTHOR CONTRIBUTIONS

EB-T, DO, and PH wrote the mini-review. All authors contributed to the article and approved the submitted version.

FUNDING

DO was funded by the Hjelt Foundation and PH by the Swiss National Science Foundation (310030_L92496), the Fondation Aclon and the European Research Council (884449-Merlin).

REFERENCES

1. Yoon KH, Ko SH, Cho JH, Lee JM, Ahn YB, Song KH, et al. Selective beta-cell loss and alpha-cell expansion in patients with type 2 diabetes mellitus in Korea. *J Clin Endocrinol Metab* (2003) 88(5):2300–8. doi: 10.1210/jc.2002-020735
2. Butler AE, Janson J, Bonner-Weir S, Ritzel R, Rizza RA, Butler PC. Beta-cell deficit and increased beta-cell apoptosis in humans with type 2 diabetes. *Diabetes* (2003) 52(1):102–10. doi: 10.2337/diabetes.52.1.102
3. Brissova M, Fowler MJ, Nicholson WE, Chu A, Hirshberg B, Harlan DM, et al. Assessment of human pancreatic islet architecture and composition by laser scanning confocal microscopy. *J Histochem Cytochem* (2005) 53 (9):1087–97. doi: 10.1369/jhc.5C6684.2005
4. Cabrera O, Berman DM, Kenyon NS, Ricordi C, Berggren PO, Caicedo A. The unique cytoarchitecture of human pancreatic islets has implications for islet cell function. *Proc Natl Acad Sci U S A* (2006) 103(7):2334–9. doi: 10.1073/pnas.0510790103
5. Pisania A, Weir GC, O'Neil JJ, Omer A, Tchipashvili V, Lei J, et al. Quantitative analysis of cell composition and purity of human pancreatic islet preparations. *Lab Invest* (2010) 90(11):1661–75. doi: 10.1038/labinvest.2010.124
6. Ellenbroek JH, Töns HAM, Hanegraaf MAJ, Rabelink TJ, Engelse MA, Carlotti F, et al. Pancreatic α-cell mass in obesity. *Diabetes Obes Metab* (2017) 19(12):1810–3. doi: 10.1111/dom.12997
7. Cohrs CM, Panzer JK, Drotar DM, Enos SJ, Kipke N, Chen C, et al. Dysfunction of Persisting β Cells Is a Key Feature of Early Type 2 Diabetes Pathogenesis. *Cell Rep* (2020) 31(1):107469. doi: 10.1016/j.celrep.2020.03.033
8. Baeyens L, Hindi S, Sorenson RL, German MS. β-Cell adaptation in pregnancy. *Diabetes Obes Metab* (2016) 18(Suppl 1):63–70. doi: 10.1111/dom.12716
9. Bosco D, Armanet M, Morel P, Niclauss N, Sgroi A, Muller YD, et al. Unique Arrangement of α- and β-Cells in Human Islets of Langerhans, in. *Diabetes* (2010) 1202–10. doi: 10.2337/db09-1177
10. Rodriguez-Diaz R, Molano RD, Weitz JR, Abdulreda MH, Berman DM, Leibiger B, et al. Paracrine Interactions within the Pancreatic Islet Determine the Glycemic Set Point. *Cell Metab* (2018) 27(3):549–58.e4. doi: 10.1016/j.cmet.2018.01.015
11. Brown RJ, Sinaii N, Rother KI. Too much glucagon, too little insulin: time course of pancreatic islet dysfunction in new-onset type 1 diabetes. *Diabetes Care* (2008) 31(7):1403–4. doi: 10.2337/dc08-0575
12. Kramer CK, Borgoño CA, Van Nostrand P, Retnakaran R, Zinman B. Glucagon response to oral glucose challenge in type 1 diabetes: lack of impact of euglycemia. *Diabetes Care* (2014) 37(4):1076–82. doi: 10.2337/dc13-2339
13. Thivolet C, Marchand L, Chikh K. Inappropriate glucagon and GLP-1 secretion in individuals with long-standing type 1 diabetes: effects of residual C-peptide. *Diabetologia* (2019) 62(4):593–7. doi: 10.1007/s00125-018-4804-y
14. Shah P, Vella A, Basu A, Basu R, Schwenk WF, Rizza RA. Lack of suppression of glucagon contributes to postprandial hyperglycemia in subjects with type 2 diabetes mellitus. *J Clin Endocrinol Metab* (2000) 85(11):4053–9. doi: 10.1210/jc.85.11.4053
15. Bagger JI, Knop FK, Lund A, Holst JJ, Vilsbøll T. Glucagon responses to increasing oral loads of glucose and corresponding isoglycaemic intravenous glucose infusions in patients with type 2 diabetes and healthy individuals. *Diabetologia* (2014) 57(8):1720–5. doi: 10.1007/s00125-014-3264-2
16. Gastaldelli A, Baldi S, Pettiti M, Toschi E, Camastra S, Natali A, et al. Influence of obesity and type 2 diabetes on gluconeogenesis and glucose output in humans: a quantitative study. *Diabetes* (2000) 49(8):1367–73. doi: 10.2337/diabetes.49.8.1367
17. Demant M, Bagger JI, Suppli MP, Lund A, Gyldenløve M, Hansen KB, et al. Determinants of Fasting Hyperglucagonemia in Patients with Type 2 Diabetes and Nondiabetic Control Subjects. *Metab Syndr Relat Disord* (2018) 16 (10):530–6. doi: 10.1089/met.2018.0066
18. Siafarikas A, Johnston RJ, Bulsara MK, O'Leary P, Jones TW, Davis EA. Early loss of the glucagon response to hypoglycemia in adolescents with type 1 diabetes. *Diabetes Care* (2012) 35(8):1757–62. doi: 10.2337/dc11-2010
19. Sayama K, Imagawa A, Okita K, Uno S, Moriwaki M, Kozawa J, et al. Pancreatic beta and alpha cells are both decreased in patients with fulminant type 1 diabetes: a morphometrical assessment. *Diabetologia* (2005) 48(8):1560–4. doi: 10.1007/s00125-005-1829-9
20. Bonnet-Serrano F, Diedisheim M, Mallone R, Larger E. Decreased α-cell mass and early structural alterations of the exocrine pancreas in patients with type 1 diabetes: An analysis based on the nPOD repository. *PLoS One* (2018) 13(1): e0191528. doi: 10.1371/journal.pone.0191528
21. Fujita Y, Kozawa J, Iwahashi H, Yoneda S, Uno S, Eguchi H, et al. Human pancreatic α- to β-cell area ratio increases after type 2 diabetes onset. *J Diabetes Invest* (2018) 9(6):1270–82. doi: 10.1111/jdi.12841
22. Henquin JC, Rahier J. Pancreatic alpha cell mass in European subjects with type 2 diabetes. *Diabetologia* (2011) 54(7):1720–5. doi: 10.1007/s00125-011-2118-4
23. Kilimnik G, Zhao B, Jo J, Periwal V, Witkowski P, Misawa R, et al. Altered Islet Composition and Disproportionate Loss of Large Islets in Patients with Type 2 Diabetes. *PLoS One* (2011) 6(11):e27445. doi: 10.1371/journal.pone.0027445
24. Omar-Hmeadi M, Lund P-E, Gandasi NR, Tengholm A, Barg S. Paracrine control of α-cell glucagon exocytosis is compromised in human type-2 diabetes. *Nat Commun* (2020) 11(1):1896. doi: 10.1038/s41467-020-15717-8
25. Tellez K, Hang Y, Gu X, Chang CA, Stein RW, Kim SK. In vivo studies of glucagon secretion by human islets transplanted in mice. *Nat Metab* (2020) 2 (6):547–57. doi: 10.1038/s42255-020-0213-x
26. Lawlor N, George J, Bolisetty M, Kursawe R, Sun L, Sivakamasundari V, et al. Single-cell transcriptomes identify human islet cell signatures and reveal cell-type-specific expression changes in type 2 diabetes. *Genome Res* (2017) 27 (2):208–22. doi: 10.1101/gr.212720.116
27. Segerstolpe Å, Palasantza A, Eliasson P, Andersson EM, Andréasson AC, Sun X, et al. Single-Cell Transcriptome Profiling of Human Pancreatic Islets in Health and Type 2 Diabetes. *Cell Metab* (2016) 24(4):593–607. doi: 10.1016/j.cmet.2016.08.020
28. Brissova M, Haliyur R, Saunders D, Shrestha S, Dai C, Blodgett DM, et al. α Cell Function and Gene Expression Are Compromised in Type 1 Diabetes. *Cell Rep* (2018) 22(10):2667–76. doi: 10.1016/j.celrep.2018.02.032
29. Lindqvist A, Shcherbina L, Prasad RB, Miskelly MG, Abels M, Martínez-Lopéz JA, et al. Ghrelin suppresses insulin secretion in human islets and type 2 diabetes patients have diminished islet ghrelin cell number and lower plasma ghrelin levels. *Mol Cell Endocrinol* (2020) 511:110835. doi: 10.1016/j.mce.2020.110835

30. Vergari E, Denwood G, Salehi A, Zhang Q, Adam J, Alrifaiy A, et al. Somatostatin secretion by Na(+)-dependent Ca(2+)-induced Ca(2+) release in pancreatic delta-cells. *Nat Metab* (2020) 2(1):32–40. doi: 10.1038/s42255-019-0158-0
31. Vergari E, Knudsen JG, Ramracheya R, Salehi A, Zhang Q, Adam J, et al. Insulin inhibits glucagon release by SGLT2-induced stimulation of somatostatin secretion. *Nat Commun* (2019) 10(1):139. doi: 10.1038/s41467-018-08193-8
32. Chia CW, Odetunde JO, Kim W, Carlson OD, Ferrucci L, Egan JM. GIP contributes to islet trihormonal abnormalities in type 2 diabetes. *J Clin Endocrinol Metab* (2014) 99(7):2477–85. doi: 10.1210/jc.2013-3994
33. Kim W, Fiori JL, Shin YK, Okun E, Kim JS, Rapp PR, et al. Pancreatic polypeptide inhibits somatostatin secretion. *FEBS Lett* (2014) 588(17):3233–9. doi: 10.1016/j.febslet.2014.07.005
34. Arrojo e Drigo R, Jacob S, García-Prieto CF, Zheng X, Fukuda M, Nhu HTT, et al. Structural basis for delta cell paracrine regulation in pancreatic islets. *Nat Commun* (2019) 10(1):3700. doi: 10.1038/s41467-019-11517-x
35. Guardado Mendoza R, Perego C, Finzi G, La Rosa S, Capella C, Jimenez-Ceja LM, et al. Delta cell death in the islet of Langerhans and the progression from normal glucose tolerance to type 2 diabetes in non-human primates (baboon, Papio hamadryas). *Diabetologia* (2015) 58(8):1814–26. doi: 10.1007/s00125-015-3625-5
36. Merino B, Alonso-Magdalena P, Lluesma M, Ñeco P, Gonzalez A, Marroquí L, et al. Pancreatic alpha-cells from female mice undergo morphofunctional changes during compensatory adaptations of the endocrine pancreas to diet-induced obesity. *Sci Rep* (2015) 5(1):11622. doi: 10.1038/srep11622
37. Calanna S, Piro S, Di Pino A, Maria Zagami R, Urbano F, Purrello F, et al. Beta and alpha cell function in metabolically healthy but obese subjects: Relationship with entero-insular axis. *Obesity* (2013) 21(2):320–5. doi: 10.1002/oby.20017
38. Guardado-Mendoza R, Jimenez-Ceja L, Majluf-Cruz A, Kamath S, Fiorentino TV, Casiraghi F, et al. Impact of obesity severity and duration on pancreatic β- and α-cell dynamics in normoglycemic non-human primates. *Int J Obes* (2013) 37(8):1071–8. doi: 10.1038/ijo.2012.205
39. Tsuchiyama N, Takamura T, Ando H, Sakurai M, Shimizu A, Kato K, et al. Possible role of alpha-cell insulin resistance in exaggerated glucagon responses to arginine in type 2 diabetes. *Diabetes Care* (2007) 30(10):2583–7. doi: 10.2337/dc07-0066
40. Kellard JA, Rorsman NJG, Hill TG, Armour SL, van de Bunt M, Rorsman P, et al. Reduced somatostatin signalling leads to hypersecretion of glucagon in mice fed a high-fat diet. *Mol Metab* (2020) 40:101021. doi: 10.1016/j.molmet.2020.101021
41. Rickels MR, Schutta MH, Mueller R, Markmann JF, Barker CF, Naji A, et al. Islet cell hormonal responses to hypoglycemia after human islet transplantation for type 1 diabetes. *Diabetes* (2005) 54(11):3205–11. doi: 10.2337/diabetes.54.11.3205
42. Rickels MR, Peleckis AJ, Markmann E, Dalton-Bakes C, Kong SM, Teff KL, et al. Long-Term Improvement in Glucose Control and Counterregulation by Islet Transplantation for Type 1 Diabetes. *J Clin Endocrinol Metab* (2016) 101 (11):4421–30. doi: 10.1210/jc.2016-1649
43. Paty BW, Ryan EA, Shapiro AM, Lakey JR, Robertson RP. Intrahepatic islet transplantation in type 1 diabetic patients does not restore hypoglycemic hormonal counterregulation or symptom recognition after insulin independence. *Diabetes* (2002) 51(12):3428–34. doi: 10.2337/diabetes.51.12.3428
44. Bru-Tari E, Cobo-Vuilleumier N, Alonso-Magdalena P, Dos Santos RS, Marroqui L, Nadal A, et al. Pancreatic alpha-cell mass in the early-onset and advanced stage of a mouse model of experimental autoimmune diabetes. *Sci Rep* (2019) 9(1):9515. doi: 10.1038/s41598-019-45853-1
45. Huang YC, Rupnik MS, Karimian N, Herrera PL, Gilon P, Feng ZP, et al. In situ electrophysiological examination of pancreatic α cells in the streptozotocin-induced diabetes model, revealing the cellular basis of glucagon hypersecretion. *Diabetes* (2013) 62(2):519–30. doi: 10.2337/db11-0786
46. Pipeleers D, in't Veld PI, Maes E, Van De Winkel M. Glucose-induced insulin release depends on functional cooperation between islet cells. *Proc Natl Acad Sci U S A* (1982) 79(23):7322–5. doi: 10.1073/pnas.79.23.7322
47. Head WS, Orseth ML, Nunemaker CS, Satin LS, Piston DW, Benninger RKP. Connexin-36 Gap Junctions Regulate In Vivo First- and Second-Phase Insulin Secretion Dynamics and Glucose Tolerance in the Conscious Mouse. *Diabetes* (2012) 61(7):1700. doi: 10.2337/db11-1312
48. Bonner-Weir S, Sullivan BA, Weir CG. Human Islet Morphology Revisited: Human and Rodent Islets Are Not So Different After All. *J Histochem Cytochem* (2015) 63(8):604–12. doi: 10.1369/0022155415570969
49. Quesada I, Todorova MG, Alonso-Magdalena P, Beltrá M, Carneiro EM, Martin F, et al. Glucose induces opposite intracellular Ca2+ concentration oscillatory patterns in identified alpha- and beta-cells within intact human islets of Langerhans. *Diabetes* (2006) 55(9):2463–9. doi: 10.2337/db06-0272
50. Capozzi ME, Svendsen B, Encisco SE, Lewandowski SL, Martin MD, Lin H, et al. β Cell tone is defined by proglucagon peptides through cAMP signaling. *JCI Insight* (2019) 4(5):e126742. doi: 10.1172/jci.insight.126742
51. Wojtusciszyn A, Armanet M, Morel P, Berney T, Bosco D. Insulin secretion from human beta cells is heterogeneous and dependent on cell-to-cell contacts. *Diabetologia* (2008) 51(10):1843. doi: 10.1007/s00125-008-1103-z
52. Marchetti P, Lupi R, Bugliani M, Kirkpatrick CL, Sebastiani G, Grieco FA, et al. A local glucagon-like peptide 1 (GLP-1) system in human pancreatic islets. *Diabetologia* (2012) 55(12):3262–72. doi: 10.1007/s00125-012-2716-9
53. Linnemann AK, Neuman JC, Battiola TJ, Wisinski JA, Kimple ME, Davis DB. Glucagon-Like Peptide-1 Regulates Cholecystokinin Production in β-Cells to Protect From Apoptosis. *Mol Endocrinol (Baltimore Md)* (2015) 29(7):978–87. doi: 10.1210/me.2015-1030
54. de Souza AH, Tang J, Yadev AK, Saghafi ST, Kibbe CR, Linnemann AK, et al. Intra-islet GLP-1, but not CCK, is necessary for β-cell function in mouse and human islets. *Sci Rep* (2020) 10(1):2823. doi: 10.1038/s41598-020-59799-2
55. Hodson DJ, Mitchell RK, Bellomo EA, Sun G, Vinet L, Meda P, et al. Lipotoxicity disrupts incretin-regulated human β cell connectivity. *J Clin Invest* (2013) 123(10):4182–94. doi: 10.1172/JCI68459
56. Rodriguez-Diaz R, Dando R, Jacques-Silva MC, Fachado A, Molina J, Abdulreda MH, et al. Alpha cells secrete acetylcholine as a non-neuronal paracrine signal priming beta cell function in humans. *Nat Med* (2011) 17 (7):888–92. doi: 10.1038/nm.2371
57. Molina J, Rodriguez-Diaz R, Fachado A, Jacques-Silva MC, Berggren PO, Caicedo A. Control of insulin secretion by cholinergic signaling in the human pancreatic islet. *Diabetes* (2014) 63(8):2714–26. doi: 10.2337/db13-1371
58. van der Meulen T, Donaldson CJ, Cáceres E, Hunter AE, Cowing- Zitron C, Pound LD, et al. Urocortin3 mediates somatostatin-dependent negative feedback control of insulin secretion. *Nat Med* (2015) 21(7):769–76. doi: 10.1038/nm.3872
59. Kailey B, van de Bunt M, Cheley S, Johnson PR, MacDonald PE, Gloyn AL, et al. SSTR2 is the functionally dominant somatostatin receptor in human pancreatic β- and α-cells. *Am J Physiol Endocrinol Metab* (2012) 303(9): E1107–16. doi: 10.1152/ajpendo.00207.2012
60. Briant LJB, Reinbothe TM, Spiliotis I, Miranda C, Rodriguez B, Rorsman P. δ-cells and β-cells are electrically coupled and regulate α-cell activity via somatostatin. *J Physiol* (2018) 596(2):197–215. doi: 10.1113/JP274581
61. Hellman B, Salehi A, Gylfe E, Dansk H, Grapengiesser E. Glucose generates coincident insulin and somatostatin pulses and antisynchronous glucagon pulses from human pancreatic islets. *Endocrinology* (2009) 150(12):5334–40. doi: 10.1210/en.2009-0600
62. Liu W, Kin T, Ho S, Dorrell C, Campbell SR, Luo P, et al. Abnormal regulation of glucagon secretion by human islet alpha cells in the absence of beta cells. *EBioMedicine* (2019) 50:306–16. doi: 10.1016/j.ebiom.2019.11.018
63. DiGruccio MR, Mawla AM, Donaldson CJ, Noguchi GM, Vaughan J, Cowing-Zitron C, et al. Comprehensive alpha, beta and delta cell transcriptomes reveal that ghrelin selectively activates delta cells and promotes somatostatin release from pancreatic islets. *Mol Metab* (2016) 5(7):449–58. doi: 10.1016/j.molmet.2016.04.007
64. Aragón F, Karaca M, Novials A, Maldonado R, Maechler P, Rubí B. Pancreatic polypeptide regulates glucagon release through PPYR1 receptors expressed in mouse and human alpha-cells. *Biochim Biophys Acta* (2015) 1850(2):343–51. doi: 10.1016/j.bbagen.2014.11.005
65. Walker JT, Haliyur R, Nelson HA, Ishahak M, Poffenberger G, Aramandla R, et al. Integrated human pseudoislet system and microfluidic platform demonstrate differences in GPCR signaling in islet cells. *JCI Insight* (2020) 5 (10):e137017. doi: 10.1172/jci.insight.137017
66. Johnston NR, Mitchell RK, Haythorne E, Pessoa MP, Semplici F, Ferrer J, et al. Beta Cell Hubs Dictate Pancreatic Islet Responses to Glucose. *Cell Metab* (2016) 24(3):389–401. doi: 10.1016/j.cmet.2016.06.020

67. Camunas-Soler J, Dai XQ, Hang Y, Bautista A, Lyon J, Suzuki K, et al. Patch-Seq Links Single-Cell Transcriptomes to Human Islet Dysfunction in Diabetes. *Cell Metab* (2020) 31(5):1017–31.e4. doi: 10.1016/j.cmet.2020.04.005
68. Campbell SA, Golec DP, Hubert M, Johnson J, Salamon N, Barr A, et al. Human islets contain a subpopulation of glucagon-like peptide-1 secreting α cells that is increased in type 2 diabetes. *Mol Metab* (2020) 39:1010–4. doi: 10.1016/j.molmet.2020.101014
69. Xin Y, Dominguez Gutierrez G, Okamoto H, Kim J, Lee AH, Adler C, et al. Pseudotime Ordering of Single Human β-Cells Reveals States of Insulin Production and Unfolded Protein Response. *Diabetes* (2018) 67(9):1783–94. doi: 10.2337/db18-0365
70. Baron M, Veres A, Wolock SL, Faust AL, Gaujoux R, Vetere A, et al. A Single-Cell Transcriptomic Map of the Human and Mouse Pancreas Reveals Inter- and Intra-cell Population Structure. *Cell Syst* (2016) 3(4):346–60.e4. doi: 10.1016/j.cels.2016.08.011
71. Muraro MJ, Dharmadhikari G, Grün D, Groen N, Dielen T, Jansen E, et al. A Single-Cell Transcriptome Atlas of the Human Pancreas. *Cell Syst* (2016) 3 (4):385–94.e3. doi: 10.1016/j.cels.2016.09.002
72. Fang Z, Weng C, Li H, Tao R, Mai W, Liu X, et al. Single-Cell Heterogeneity Analysis and CRISPR Screen Identify Key β-Cell-Specific Disease Genes. *Cell Rep* (2019) 26(11):3132–44.e7. doi: 10.1016/j.celrep.2019.02.043
73. Dorrell C, Schug J, Canaday PS, Russ HA, Tarlow BD, Grompe MT, et al. Human islets contain four distinct subtypes of β cells. *Nat Commun* (2016) 7 (1):11756. doi: 10.1038/ncomms11756
74. Wang YJ, Golson ML, Schug J, Traum D, Liu C, Vivek K, et al. Single-Cell Mass Cytometry Analysis of the Human Endocrine Pancreas. *Cell Metab* (2016) 24(4):616–26. doi: 10.1016/j.cmet.2016.09.007
75. Ghazvini Zadeh EH, Huang Z, Xia J, Li D, Davidson HW. ZIGIR, a Granule-Specific Zn2+ Indicator, Reveals Human Islet α Cell Heterogeneity. *Cell Rep* (2020) 32(2):107904. doi: 10.1016/j.celrep.2020.107904
76. Almaça J, Liang T, Gaisano HY, Nam HG, Berggren PO, Caicedo A. Spatial and temporal coordination of insulin granule exocytosis in intact human pancreatic islets. *Diabetologia* (2015) 58(12):2810–8. doi: 10.1007/s00125-015-3747-9
77. Huang C-j, Lin C-y, Haataja L, Gurlo T, Butler AE, Rizza RA, et al. High Expression Rates of Human Islet Amyloid Polypeptide Induce Endoplasmic Reticulum Stress–Mediated β-Cell Apoptosis, a Characteristic of Humans With Type 2 but Not Type 1 Diabetes. *Diabetes* (2007) 56(8):2016. doi: 10.2337/db07-0197
78. Lam CJ, Cox AR, Jacobson DR, Rankin MM, Kushner JA. Highly Proliferative α-Cell-Related Islet Endocrine Cells in Human Pancreata. *Diabetes* (2018) 67 (4):674–86. doi: 10.2337/db17-1114
79. Le Marchand SJ, Piston DW. Glucose suppression of glucagon secretion: metabolic and calcium responses from alpha-cells in intact mouse pancreatic islets. *J Biol Chem* (2010) 285(19):14389–98. doi: 10.1074/jbc.M109.069195
80. Barton FB, Rickels MR, Alejandro R, Hering BJ, Wease S, Naziruddin B, et al. Improvement in Outcomes of Clinical Islet Transplantation: 1999–2010. *Diabetes Care* (2012) 35(7):1436. doi: 10.2337/dc12-0063
81. Warnock GL, Thompson DM, Meloche RM, Shapiro RJ, Ao Z, Keown P, et al. A Multi-Year Analysis of Islet Transplantation Compared With Intensive Medical Therapy on Progression of Complications in Type 1 Diabetes. *Transplantation* (2008) 86(12):1762–66. doi: 10.1097/TP.0b013e318190b052
82. Nair GG, Liu JS, Russ HA, Tran S, Saxton MS, Chen R, et al. Recapitulating endocrine cell clustering in culture promotes maturation of human stem-cell-derived β cells. *Nat Cell Biol* (2019) 21(2):263–74. doi: 10.1038/s41556-018-0271-4
83. Velazco-Cruz L, Song J, Maxwell KG, Goedegebuure MM, Augsornworawat P, Hogrebe NJ, et al. Acquisition of Dynamic Function in Human Stem Cell-Derived β Cells. *Stem Cell Rep* (2019) 12(2):351–65. doi: 10.1016/j.stemcr.2018.12.012
84. Ghazizadeh Z, Kao D-I, Amin S, Cook B, Rao S, Zhou T, et al. ROCKII inhibition promotes the maturation of human pancreatic beta-like cells. *Nat Commun* (2017) 8(1):298–8. doi: 10.1038/s41467-017-00129-y
85. Pagliuca FW, Millman JR, Gürtler M, Segel M, Van Dervort A, Ryu JH, et al. Generation of functional human pancreatic β cells in vitro. *Cell* (2014) 159 (2):428–39. doi: 10.1016/j.cell.2014.09.040
86. Rezania A, Bruin JE, Arora P, Rubin A, Batushansky I, Asadi A, et al. Reversal of diabetes with insulin-producing cells derived in vitro from human pluripotent stem cells. *Nat Biotechnol* (2014) 32(11):1121–33. doi: 10.1038/nbt.3033
87. Davis JC, Alves TC, Helman A, Chen JC, Kenty JH, Cardone RL, et al. Glucose Response by Stem Cell-Derived β Cells In Vitro Is Inhibited by a Bottleneck in Glycolysis. *Cell Rep* (2020) 31(6):107623–3. doi: 10.1016/j.celrep.2020.107623
88. Boland BB, Brown CJr., Alarcon C, Demozay D, Grimsby JS, Rhodes CJ, et al. β-Cell Control of Insulin Production During Starvation-Refeeding in Male Rats. *Endocrinology* (2018) 159(2):895–906. doi: 10.1210/en.2017-03120
89. Redick SD, Leehy L, Rittenhouse AR, Blodgett DM, Derr AG, Kucukural A, et al. Recovery of viable endocrine-specific cells and transcriptomes from human pancreatic islet-engrafted mice. *FASEB J* (2020) 34(1):1901–11. doi: 10.1096/fj.201901022RR
90. Ellenbroek JH, Töns HA, de Graaf N, Loomans CJ, Engelse MA, Vrolijk H, et al. Topologically heterogeneous beta cell adaptation in response to high-fat diet in mice. *PLoS One* (2013) 8(2):e56922. doi: 10.1371/journal.pone.0056922
91. Vuguin PM, Kedees MH, Cui L, Guz Y, Gelling RW, Nejathaim M, et al. Ablation of the glucagon receptor gene increases fetal lethality and produces alterations in islet development and maturation. *Endocrinology* (2006) 147 (9):3995–4006. doi: 10.1210/en.2005-1410
92. Takagi Y, Kinoshita K, Ozaki N, Seino Y, Murata Y, Oshida Y, et al. Mice Deficient in Proglucagon-Derived Peptides Exhibit Glucose Intolerance on a High-Fat Diet but Are Resistant to Obesity. *PLoS One* (2015) 10(9):e0138322–e0138322. doi: 10.1371/journal.pone.0138322
93. Hay CW, Sinclair EM, Bermano G, Durward E, Tadayyon M, Docherty K. Glucagon-like peptide-1 stimulates human insulin promoter activity in part through cAMP-responsive elements that lie upstream and downstream of the transcription start site. *J Endocrinol* (2005) 186(2):353–65. doi: 10.1677/joe.1.06205
94. Yoshihara E, O'Connor C, Gasser E, Wei Z, Oh TG, Tseng TW, et al. Immune-evasive human islet-like organoids ameliorate diabetes. *Nature* (2020) 586:606–11. doi: 10.1038/s41586-020-2631-z

Conflict of Interest: The authors declare that the research was conducted in the absence of any commercial or financial relationships that could be construed as a potential conflict of interest.

frontiers in Endocrinology

ORIGINAL RESEARCH
published: 09 February 2021
doi: 10.3389/fendo.2020.534362

Identification of Maturity-Onset Diabetes of the Young Caused by Mutation in *FOXM1 via* Whole-Exome Sequencing in Northern China

Liang Zhong[1,2,3], *Zengyi Zhao*[1,2], *Qingshan Hu*[1,2], *Yang Li*[1,2,3], *Weili Zhao*[1,2,3], *Chuang Li*[1,2], *Yunqiang Xu*[1], *Ruijuan Rong*[1,2,3], *Jing Zhang*[1,2,3], *Zifeng Zhang*[1,2,3], *Nan Li*[1,2,3] *and Zanchao Liu*[1,2,3]*

[1] The Shijiazhuang Second Hospital, Shijiazhuang, China, [2] Hebei Provincial Key Laboratory of Basic Medicine for Diabetes, The Shijiazhuang Second Hospital, Shijiazhuang, China, [3] Shijiazhuang Technology Innovation Center of Precision Medicine for Diabetes, The Shijiazhuang Second Hospital, Shijiazhuang, China

OPEN ACCESS

Edited by:
Hanne Scholz,
University of Oslo, Norway

Reviewed by:
Inês Cebola,
Imperial College London, United Kingdom
Senta Georgia,
Children's Hospital of Los Angeles, United States
Claire C. Morgan,
Centre for Genomic Regulation (CRG), Spain

***Correspondence:**
Zanchao Liu
liuzanchao2007@163.com

Specialty section:
This article was submitted to Diabetes: Molecular Mechanisms, a section of the journal Frontiers in Endocrinology

Received: 12 May 2020
Accepted: 27 November 2020
Published: 09 February 2021

Citation:
Zhong L, Zhao Z, Hu Q, Li Y, Zhao W, Li C, Xu Y, Rong R, Zhang J, Zhang Z, Li N and Liu Z (2021) Identification of Maturity-Onset Diabetes of the Young Caused by Mutation in FOXM1 via Whole-Exome Sequencing in Northern China. Front. Endocrinol. 11:534362. doi: 10.3389/fendo.2020.534362

Diabetes mellitus is a highly heterogeneous disorder encompassing different types with particular clinical manifestations, while maturity-onset diabetes of the young (MODY) is an early-onset monogenenic diabetes. Most genetic predisposition of MODY has been identified in European and American populations. A large number of Chinese individuals are misdiagnosed due to defects of unknown genes. In this study, we analyzed the genetic and clinical characteristics of the Northern China. A total of 200 diabetic patients, including 10 suspected MODY subjects, were enrolled, and the mutational analysis of monogenic genes was performed by whole-exome sequencing and confirmed by familial information and Sanger sequencing. We found that clinical features and genetic characteristics have varied widely between MODY and other diabetic subjects in Northern China. *FOXM1*, a key molecule in the proliferation of pancreatic β-cells, has a rare mutation rs535471991, which leads to instability within the phosphorylated domain that impairs its function. Our findings indicate that *FOXM1* may play a critical role in MODY, which could reduce the misdiagnose rate and provide promising therapy for MODY patients.

Keywords: maturity-onset diabetes of the young (MODY), diabetes, whole-exome sequencing (WES), SNP, FoxM1

INTRODUCTION

Maturity-onset diabetes of the young (MODY) is a kind of monogenic diabetes mellitus that is characterized by early-onset, autosomal dominant, non-insulin dependent diabetes. Pancreatic β-cell dysfunction reduces glucose-stimulated insulin secretion during early age due to monogenic variation (1, 2). However, MODY not only manifests a distinct clinical phenotype but also emerges metabolically and genetically heterogeneously due to the various MODY-associated genes. To date, 14 genes (*HNF4A, GCK, HNF1A, PDX1, TCF2, NEUROD1, KLF11, CEL, PAX4, INS, BLK, ABCC8, KCNJ11, and APPL1*) have been identified, and their mutations are responsible for the initiation of MODY (3–5). Despite previous intensive linkage analyses for MODY, there are still diagnosed cases

that remain genetically inexplicable (6). In addition, different studies suggest that the prevalence of specific mutations of MODY genes differs considerably among various ethnic groups (7). Without characteristic features and pedigreed awareness, most MODY patients are misdiagnosed with type 1 or type 2 diabetes in Chinese populations, who may potentially receive inappropriate therapy.

The emergence of next-generation sequencing has greatly enhanced the identification of novel mutated genes related to complicated diseases. In particular, whole-exome sequencing (WES) is a more useful and efficient strategy for identifying unknown causative genes in complex disorders, such as GCK-MODY (8) PAX4-MODY (9), and KCNJ11-MODY (10). According to Bonnefond's finding, WES also provides a clinical tool to assess patients presenting with other monogenic diabetes (6). With regard to MODY, geography and ethnicity specific detection rates have been determined in previous studies (11). Moreover, the low detection rate of given mutations previously reported in Chinese patients suggests that the MODY-X gene may play a major role in these populations (12–14).

The aim of this study was to investigate the prevalence of the diabetic population and novel mutations responsible for MODY, especially in Northern of China. Ten diagnosed and suspected MODY patients underwent WES analysis to elucidate the molecular genotype. Focusing on monogenic diabetes enhances the understanding of pancreatic β-cell dysfunction and insulin resistance, which will promote the criterion of clinical typing and reduce misdiagnosis, finally leading to precise and effective therapy.

MATERIALS AND METHODS

Experimental Subjects

Diabetes subjects were recruited from the Bio-resource Center of The Shijiazhuang Second Hospital (Shijiazhuang, China). The suspected clinical diagnoses of MODY patients were selected based on (1) the early onset of diabetes (< 25 years of age); (2) negative pancreatic autoantibodies; (3) persistently detectable C-peptide; (4) nonketotic hyperglycaemia; and (5) non-pedigreed information. The study was approved by the ethical committee of the The Shijiazhuang Second Hospital and all the patients provided their written informed consent to participate in this study.

Whole-Exome Sequencing

Five to 10 ml venous blood was collected in plastic EDTA bottles or >5 μg DNA. DNA extraction was performed using the Gentra Puregene Blood Kit (Qiagen) according to the manufacturer's instructions. DNA was quantified for each sample using the Nanodrop (Thermo Fisher Scientific). Whole-exome libraries were constructed using the TruSeq Exome Library Preparation Kit (Illumina, CA). Sequencing was performed using the XTen system (Illumina, San Diego, CA, USA) to generate 2×150 bp paired-end reads. The depth of each sample was over 100X.

Variant Calling

Sequenced raw reads were mapped against the human reference genome (GRCh38) with Burrows-Wheeler Aligner (BWA, v0.78) (15). Variant identification was performed with Genome Analysis Toolkit (GATK, v4.1.2.0) (16). Duplicate alignments were marked and removed with Picard tool (v2.2). Variant quality filters were applied by a set of criteria (QUAL > 30, 5 < DP) and parameters as recommended by GATK (17). The annotation of variants was performed and ANNOVAR (18).

Genome-Wide Association Analysis

Variation and phenotype data were analyzed by PLINK (v1.9) (19). The variants with a minor allele frequency (MAF) of less than 0.05, missing call frequencies greater than 0.1 and Hardy-Weinberg equilibrium exact test p-value less than 0.00001 were excluded. The three diabetic groups, MODY group used as case and the T1DM and T2DM used as control, C-peptide and FPG, were selected as phenotypes to perform GWAS (Genome Wide Association Analysis) analysis.

Gene-Based Rare Variant Association Tests

To test differences burden of the MODY and MODY-X genes, total 56 genes used for burden test were selected by their potential pathogenicity in MODY or the dysfunction of pancreas. RVTESTS was used for the gene-based association by combined multivariate and collapsing (CMC) method (20). Common variants were removed with the following criteria: MAF more than 0.005 in any public database (ExAC, GnomAD, 1000 Genomes) or more than 0.01 in samples of this study; call rate of less than 0.9 in the study samples. The significance threshold here was set to 0.0167 (comparisons between the 3 groups, 0.0167 = 0.05/3), in accordance with Bonferroni correction.

Statistics

Statistical analysis was conducted by R and related packages. Wilcoxon test was used for pairwise comparison of quantitative traits, and Fisher's exact test was used for qualitative traits. Kruskal-Wallis H test was used for one-way analysis of variance among groups. The p-value was adjusted by Benjamini & Hochberg method, which is also known as false discovery rate (FDR) (21).

RESULTS

Clinical Characteristics of Diabetes Subjects

We sequenced a total of 200 diagnosed diabetes subjects in this study and found significant differences among the 3 groups (**Figure 1**), such as age ($P = 2.60 \times 10^{-8}$, Kruskal-Wallis test) fasting plasma glucose (FPG) ($P = 0.00028$, Kruskal-Wallis test), fasting plasma C-peptide (FPGC-peptide) ($P = 2.80 \times 10^{-7}$, Kruskal-Wallis test), insulin ($P = 0.0023$, Kruskal-Wallis test), HbA_1c ($P = 0.0015$, Kruskal-Wallis test), and body mass index

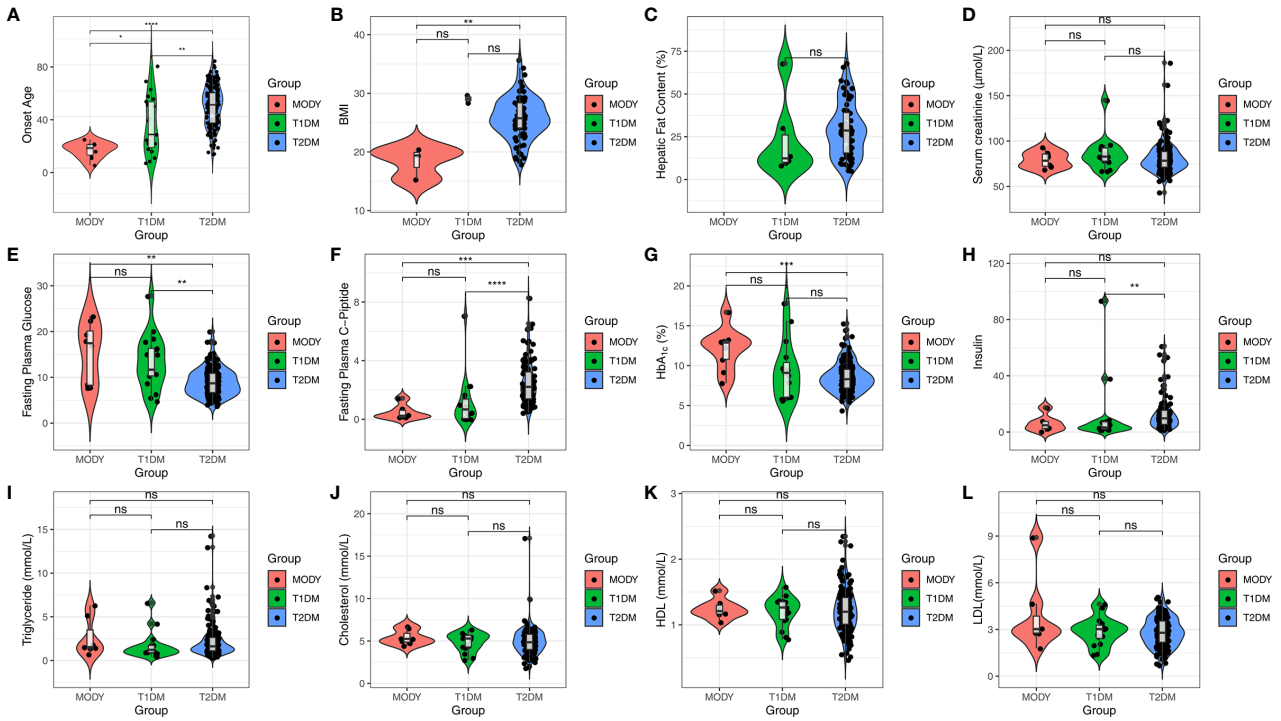

FIGURE 1 | Clinical characteristics of subjects. X axis indicates the clinical characteristics of subjects, which including age, BMI, hepatic fat content, serum creatinine, FPG, FPGC-piptide, HbA_1c, insulin, triglyceride, cholesterol, HDL, and LDL. And the colors of figure represent three diabetic group, MODY (red), T1DM (green), and T2DM (blue), respectively. The box plot is inside violin plot and the asterisk represents the significance between pairwised comparison. ns, p > 0.05; *p <= 0.05; **p <= 0.01; ***p <= 0.001; ****p <= 0.0001.

(BMI) (P = 0.0079, Kruskal-Wallis test). There were 130 males (65%) and 70 females (35%), and the average physical age was 53.67 ± 16.83, which ranged from 2 to 87 years. We unexpectedly found significant differences between the suspected MODY group and T1DM or T2DM group within onset age; however, we found that there were significant differences in BMI (P = 0.023, Wilcoxon test), HbA_1c (P = 0.00072, Wilcoxon test), FPGC-peptide (P = 0.00044, Wilcoxon test), and FPG (P = 0.017, Wilcoxon test) between the suspected MODY group and T2DM group, whereas those results did not show a remarkable alteration within the MODY group and T2DM group. Comparatively, the T1DM group also differed from T2DM group in FPGC-peptide ($P = 3.90 \times 10^{-5}$, Wilcoxon test), FPG (P = 0.006, Wilcoxon test), and insulin (P = 0.0037, Wilcoxon test) (**Table 1**). These finding suggested that a number of clinical characteristics have varied widely among various diabetic subjects.

Identification and Annotation of Variations

To investigate the relationship between genetic polymorphism and different types of diabetes, we performed whole-exome sequencing of the 200 diabetic cases, including T1DM, T2DM and MODY. The depth of WES achieved >100× coverage for all samples. The joint variants distributed in the genome shown in **Figure 2A** and the consequence type of variants are displayed in **Figure 2B**, including total 1,941,129 variants called from WES data, of which 417,468 remained after stringent filtering criteria were applied. We used SIFT (22) and PolyPhen2 (23) to predict whether an amino acid substitution could have an impact on the biological function of proteins, which showed that 23.8 and 26.82% variants might have a deleterious effect on the protein function (**Figures 2C, D**). However, according to ACMG guidelines, we found only eight likely pathogenic variants and six pathogenic variants that annotated by InterVar (24), unfortunately, none of those 14 variants was associated with diabetes.

Then, principal component analysis (PCA) was conducted on the genotypes from our cases and 1000 Genomes Project phase 3 samples (25). The PCA results showed that our 200 cases were mostly close to the East Asian (EAS) samples, as expected confirming the ethnicity of the cases used in this study (**Figure S1**). Since MODY was a monogenic disease, we assessed the previously reported pathogenic gene of MODY in our cases. Intriguingly, we found that the variants of MODY genes were usually accompanied by rarity and functional impact in suspected MODY cases, while other type diabetes cases were not observed.

Based on the significant difference in the clinical phenotype among the three diabetic groups, we also performed GWAS analysis. FPG, FPGC-peptide, and diabetic groups were selected to investigate the genotypic and phenotypic relationships. As displayed in **Figure 2E**, several significant sites ($P < 10 \times 10^{-7}$,

TABLE 1 | Clinical characteristics of diabetes subjects.

	MODY	T1DM	T2DM	P-value	Significance
Sex(female male)	0\10	12\10	58\110	0.011	*
Age	22.6 ± 15.04	41.86 ± 18.75	57.07 ± 13.9	2.60E-08	****
FPG	15.49 ± 6.57	13.4 ± 5.88	9 ± 3.01	0.00028	***
Insulin	6.22 ± 6.11	12.15 ± 24.23	12.83 ± 11.75	0.0023	**
FPGC-peptide	0.49 ± 0.51	1.13 ± 1.7	2.5 ± 1.46	2.80E-07	****
HbA_1c	12.12 ± 2.59	9.41 ± 3.7	8.59 ± 1.9	0.0015	**
Hepatic Fat Content	NA	23.45 ± 23.16	29.09 ± 15.55	0.2	ns
Triglyceride	2.63 ± 2.18	1.72 ± 1.59	2.24 ± 1.94	0.15	ns
Cholesterol	5.42 ± 0.86	4.87 ± 1.08	4.95 ± 1.54	0.48	ns
HDL	1.24 ± 0.15	1.21 ± 0.23	1.22 ± 0.32	0.92	ns
LDL	3.85 ± 2.39	2.89 ± 0.91	2.82 ± 0.91	0.57	ns
Serum creatinine	79.34 ± 8.83	86.01 ± 18.91	81.2 ± 17.06	0.5	ns
BMI	18.38 ± 2.71	29.06 ± 0.93	25.76 ± 3.49	0.0079	**

[1]*The one-way analysis of variance was performed by the Kruskal–Wallis test. The P value was adjusted by the Benjamini & Hochberg (FDR) method.*
[2]*ns, p > 0.05; *p <= 0.05; **p <= 0.01; ***p <= 0.001; ****p <= 0.0001.*

Fisher's exact test) were found in all three association results, suggesting that those sites were highly correlated with diabetes (**Table S1**). Enrichment analysis was performed and confirmed that those genes are relevant to diabetes (**Tables S2, S3**).

Potential Pathogenic Variants in Suspected Maturity-Onset Diabetes of the Young Cases

Since the allele frequency and population prevalence of MODY were lower than those in T2DM, burden analysis of rare variants across MODY and MODY-X genes was performed. Gene-based burden test was more efficient and justified for identifying associated monogenic traits than GWAS, as a single variant might show negative result due to the low frequency and the heterogeneity of pathogenic genes (26). Based on previous reports, 14 specific MODY type genes and 40 MODY-X genes were collected for the burden test. From **Figure 3**, we found that the mutations in *HNF1A*, *ABCC8*, and *BLK* were more numerous than the others among 14 MODY genes. **Table 2** presents the mutation count of MODY and MODY-X genes in 10 suspected subjects; however, the percentage of non-synonymous mutations in MODY-X genes was higher than that of MODY genes. This implied that the prevalence of MODY in Northern China may be caused by other pathogenic genes, since the 14 types of MODY were first and widely reported among populations in Europe and America.

To deduce the pathogenesis of MODY in Northern China with MODY and MODY-X genes, comprehensive analyses were performed to evaluate the potential sites in those genes. Sites with allele frequencies >0.01 in the 1000 Genome Project, gnomAD-ALL and gnomAD-EAS databases were removed, and burden test was applied with RVTESTS (27) on the remaining mutations between three diabetic groups. Six genes (*PAX4, FoxA3, Nr5a2, Hnf4a, Ada, Foxm1*) reached the significance level ($P < 0.1$, adjusted by Bonferroni method) for the burden test of association (**Table S4**). However, only the sites in *ADA* and *FOXM1* annotated with non-synonymous mutations, which could potentially impact the function of proteins. Thus, several single nucleotide variants of those genes were prioritized in the subjects as potential candidates for MODY.

Maturity-Onset Diabetes of the Young-*X* *Gene: FOXM1 Induced* Maturity-Onset Diabetes of the Young

As the single-variant association test of these three potential candidates did not show the association with MODY sufficiently, to address whether those variants in the genes that showed a positive result from the burden test were responsible for the pathogenesis of MODY, the impact of each mutation was thoroughly researched using clinical, population or functional databases. Fortunately, there were two pedigreed subjects among the 10 suspected cases, which was only detected in the father and the son. However, we did not find any pathogenic variant in 14 MODY genes, then extend out our sight to MODY-X genes which were collected from OMIM (Online Mendelian Inheritance in Man) annotation related with diabetes. Finally, rs535471991 was revealed as a heterozygous missense mutation (NM_202002; c.T1895G) in the coding region of *FOXM1*. This variant was then verified by Sanger sequencing (**Figures 4A, B**, **Figure S2**).

This mutation leads to an alteration in the amino acid sequence (p.Val632Gly). The allele frequency in the 1000 Genomes, Exome Aggregation Consortium (ExAC) (28) and Genome Aggregation Database (gnomAD) (29) was 2.00×10^{-5}, 9.48×10^{-5} and 1.80×10^{-5} respectively, but it was not found in the Exome Sequencing Project (ESP) (30). The pathogenic prediction of SIFT, MutationTaster (31), CADD (32), and gerp ++ indicated that this mutation was a deleterious mutation. Furthermore, we found that the mutation was located in vanadium-containing chloroperoxidase domain 2, which was annotated by a protein structure classification database (CATH) (33) (**Figure 4C**). That particular domain played a major role in phosphorylation, and the mutation existed exactly among a series of phosphorylation sites. A single nucleotide polymorphism at codon 1895, leading to the substitution of valine (Val) for glycine (Gly) in FOXM1, implicated the stability of the protein. The alteration caused the loss of isopropyl group and decreased the stability of FOXM1 (34). Furthermore, the hydrophobic state also changed from hydrophobicity to hydrophilicity, which played an important role in cell cycle and insulin signaling pathway, especially in pancreatic cell

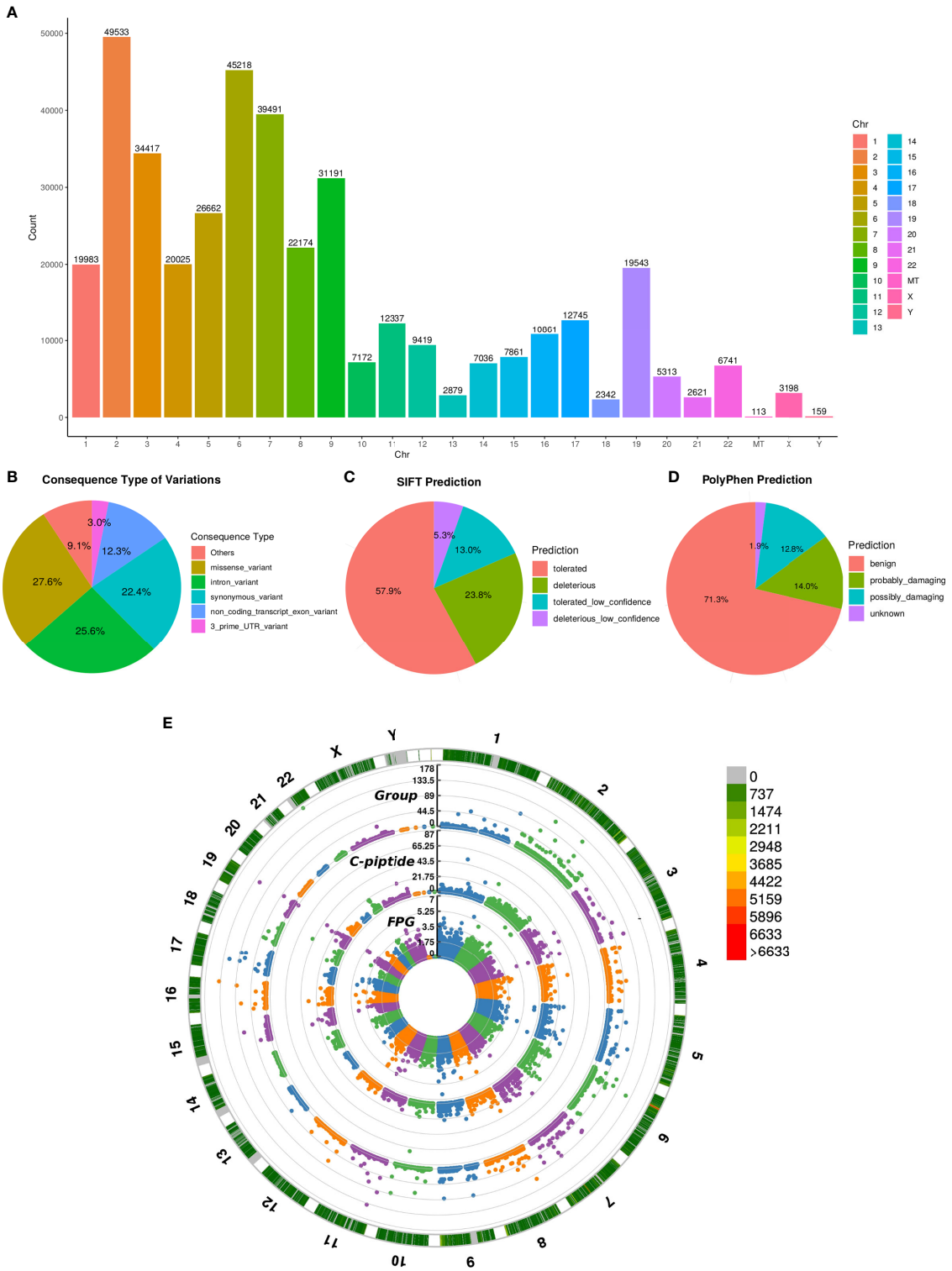

FIGURE 2 | Variant annotation and GWAS analysis. **(A)** The count of mutation distributed in each chromosome, the X axis indicates the name of chromosome and the Y axis is the count of mutation. **(B)** Consequence type of identified variations, top five categories of variations are listed. **(C, D)** The pie chart of pathogenic prediction, variations annotated by Sift and PolyPhen2. **(E)** Manhattan plot of GWAS results, the most outside track indicates the density of mutation, colors represent the count. The 3 tracks of manhattan plot are the GWAS results calculated by diabetic group, C-piptide and FPG, respectively. The vertical axis of 3 tracks represents the -Log10(P-value).

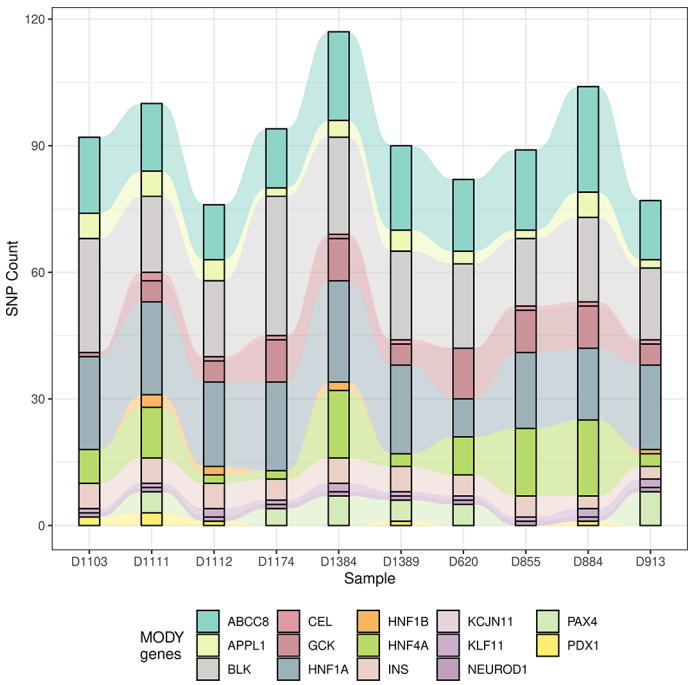

FIGURE 3 | The count of mutation in 14 MODY genes. The alluvial diagram drawed by the count of mutation in 14 MODY genes. X axis indicates the name subjects and Y axis indicates the count of mutation. Different colors represent different genes.

TABLE 2 | Variation count of MODY-related genes.

	MODY	MODY non synonymous	MODY-X	MODY-X non synonymous
D620	82	1(1.22%)	35	3(8.57%)
D855	89	4(4.49%)	45	5(11.11%)
D884	104	4(3.85%)	38	4(10.53%)
D913	77	2(2.6%)	31	2(6.45%)
D1103	92	2(2.17%)	22	5(22.73%)
D1111	100	5(5%)	53	9(16.98%)
D1112	76	5(6.58%)	30	7(23.33%)
D1174	94	2(2.13%)	32	3(9.38%)
D1384	117	4(3.42%)	44	7(15.91%)
D1389	90	4(4.44%)	33	3(9.09%)

proliferation (35). These findings extrapolate that rs535471991 may behave as a potentially pathogenic variant in *FOXM1*.

DISCUSSION

Two hundred diagnosed diabatic subjects were analyzed from northern China. However, multiple susceptibility genes involved in diabetes, particularly T1DM or T2DM, presented a distinguishing feature of polygenic inheritance and differed from MODY or neonatal diabetes mellitus (NDM), since WES could provide an accurate molecular diagnosis for monogenic disease.

Clinically, we found that BMI, FPG, C-peptide, and HbA_1c had a significant difference between suspected MODY patients and T2DM, while no difference was observed with T1DM. MODY patients usually do not associate with obesity, which is consistent with previous reports. It is interesting to note that FPG and HbA_1c were higher than T2DM and C-peptide was lower than T2DM in this study and that phenomenon also occurred in the research of Zhang (12) and Anuradha (36), despite general acceptance that patients with MODY have better glycemic control than patients with T2DM. Based on the phenotypic distinctions, GWAS and gene-based burden test were performed, however, the number of MODY patient was not large enough to obtain a convincing statistical results, which bring a limitation on this study. Besides,

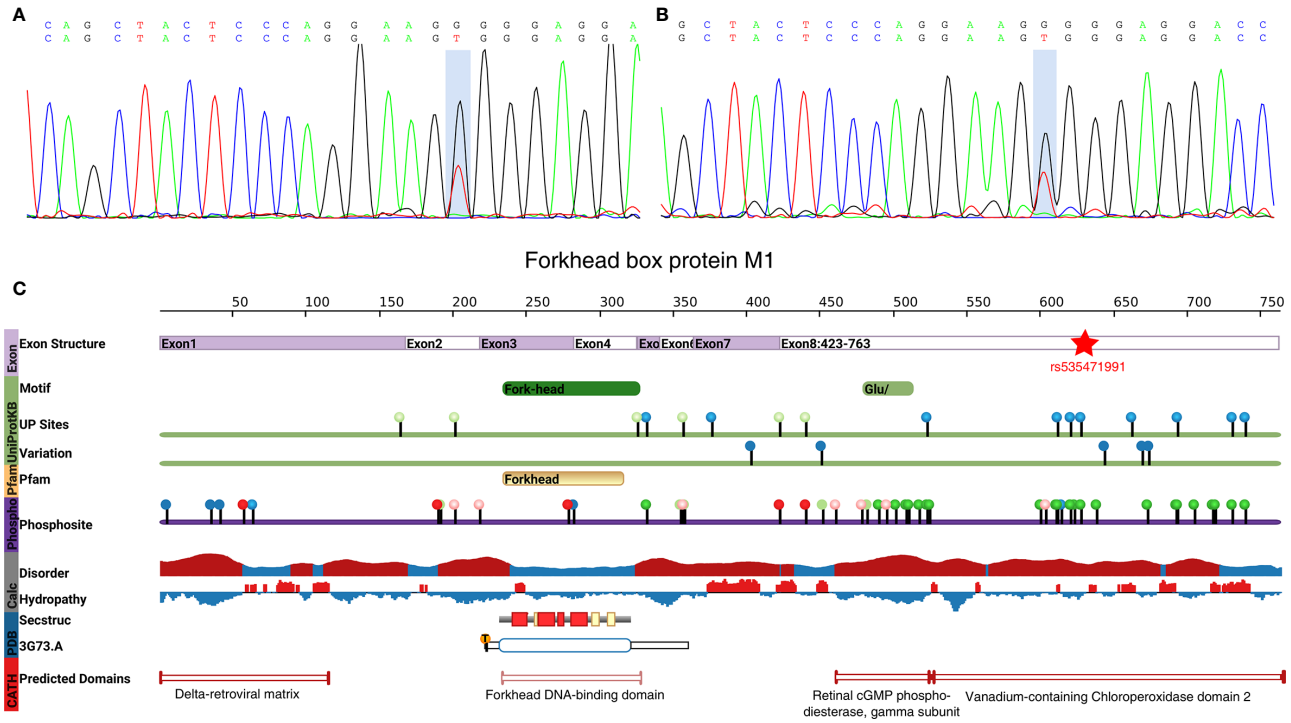

FIGURE 4 | rs535471991 identified in *FOXM1*. **(A, B)** Results of Sanger sequencing of rs535471991 in *FOXM1* of the subjects. The highlighted position indicates c.T1895G and the results showed the mutation on complementary strand. **(C)** The vertical color bar on the left side indicates data provenance, the top part in lavender color indicates the genomic exon structure; the green part indicates the motif and variation information from UniProtKB, UP sites shows the Uniprot annotated amino acid modifications and Variation shows non-genetic variation from ExPASy and dbSNP; the oranges part indicates the domain information from Pfam; purple part indicates the phosphorylation annotation from PhosphoSite; the grey part indicates the disorder (red: potentially disordered region, blue: probably ordered region) and hydropathy (red: hydrophobic, blue: hydrophilic) information; the blue part indicates the annotation from PDB, Secstruc shows the secondary structure and 3G73.A shows the structure from PDB; the red part indicates homology models predicted by CATH.

we use MODY group as case and T1DM and T2DM as control, some significantly differential traits might also stick out in the association results, such as BMI. Thus, we chose FPG and insulin data as covariates for association analysis to adjust the result. Fortunately, 2 MODY patients was a pair of father and son, which brought us a pedigreed information for investigating the potential pathogenic loci credibly. Since MODY-X might be the main component in China, and the relevant genes could impact the glycemic control even worse than that regulated by other diabetic genes. Therefore, the percentage of non-synonymous 14 MODY genes was sharply less than that of MODY-X genes, indirectly suggesting that the prevalence in China was distinctive, which was also comparable with previous studies (11–13).

Moreover, we also found a missence mutation in *ADA* except *FOXM1*. *ADA* is located in 20q12-q13.1 and has been reported as a MODY-associated region identified by genetic map of chromosomes (37). However, the mutation of emphADA only occurred in one suspected patient, unlike *FOXM1* without pedigreed information, and we could not verify as a pathogenic site based on a solitary case. In contrast, the mutation in *FOXM1* occurred in two paternity samples. *FOXM1* appears to be a transcription factor that regulates the expression of cell cycle proteins and is essential for proper mitotic progression (38, 39). During mitosis, cyclinA-dependent binding of CDK1 (cyclin-dependent kinase 1) affects the phosphorylation of FOXM1 within the vanadium-containing chloroperoxidase domain and then regulates the S/G2 transition (40). Though the vanadium-containing chloroperoxidase domain was annotated as a disordered region that did not have a stable three-dimensional structure but had good plasticity, the disordered region modulated the stability depending on the degree of aromaticity and phosphorylation status (41). In addition, receptor-mediated insulin signaling promotes the expression and binding between *FOXM1* and *CENPA* and *PLK1* in pancreatic β-cell to enable proliferation (35). These findings suggest that the mutation in *FOXM1* most likely affects the risk of MODY.

In summary, the study focused on MODY in the Northern China population. Based on WES analysis, we report a mutation in *FOXM1* caused MODY potentially. Furthermore, we validated the genetic findings with an alternative sequencing method and performed *in silico* analysis that suggest that rs535471991 may be relevant to the development of MODY. Therefore, elucidation of the molecular genetics of *FOXM1* is likely to result in better an understanding of the pathogenesis of MODY.

DATA AVAILABILITY STATEMENT

Raw reads of whole-exome sequencing data has been submitted to the NCBI Sequence Read Archive (SRA; http://www.ncbi.nlm.nih.gov/sra/) under accession number SRP227138.

ETHICS STATEMENT

The study was approved by the ethical committee of The Shijiazhuang Second Hospital, Shijiazhuang, China, and all the patients provided their written informed consent to participate in this study.

AUTHOR CONTRIBUTIONS

LZ, CL, and ZZ designed the experiment. LZ analyzed the data and wrote the manuscript. YL, QH, CL, and YX collected the samples. WZ tidied up the clinical information. NL, ZZ, and RR constructed the sequencing library. All authors contributed to the article and approved the submitted version.

FUNDING

We thank the patients and the stuff in The Shijiazhuang Second Hospital in this research. This work was supported by the National Natural Science Foundation of China (81400884), Key Research and Development Program Projects in Hebei Province (20190156), and Key Research and Development Program Self-Financing Projects in Hebei Province (172777120).

SUPPLEMENTARY MATERIAL

The Supplementary Material for this article can be found online at: https://www.frontiersin.org/articles/10.3389/fendo.2020.534362/full#supplementary-material

REFERENCES

1. Tattersall RB. Mild familial diabetes with dominant inheritance. *Q J Med* (1974) 43:339–57.
2. Tattersall RB, Fajans SS. A difference between the inheritance of classical juvenile onset and maturity-onset type diabetes of young people. *Diabetes* (1975) 24:44–53. doi: 10.2337/diab.24.1.44
3. Craig ME. Monogenic diabetes: advances in diagnosis and treatment. *Medicographia* (2016) 38:98–107. doi: 10.1046/j.1464-5491.1999.00188.x
4. Prudente S, Jungtrakoon P, Marucci A, Ludovico O, Buranasupkajorn P, Mazza T, et al. Loss-of-Function Mutations in APPL1 in Familial Diabetes Mellitus. *Am J Hum Genet* (2015) 97:177–85. doi: 10.1016/j.ajhg.2015.05.011
5. Firdous P, Nissar K, Ali S, Ganai BA, Shabir U, Hassan T, et al. Genetic testing of maturity-onset diabetes of the young current status and future perspectives. *Front Endocrinol* (2018) 9:253. doi: 10.3389/fendo.2018.00253
6. Bonnefond A, Durand E, Sand O, de Graeve F, Gallina S, Busiah K, et al. Molecular diagnosis of neonatal diabetes mellitus using next-generation sequencing of the whole exome. *PLoS One* (2010) 5. doi: 10.1371/journal.pone.0013630
7. Hattersley AT. Maturity-onset diabetes of the young: clinical heterogeneity explained by genetic heterogeneity. *Diabet Med* (1998) 15:15–24. doi: 10.1002/(SICI)1096-9136(199801)15:1<15::AID-DIA562>3.0.CO;2-M
8. Bonnefond A, Philippe J, Durand E, Dechaume A, Huyvaert M, Montagne L, et al. Whole-exome sequencing and high throughput genotyping identified KCNJ11 as the thirteenthMODY gene. *PLoS One* (2012) 7. doi: 10.1371/journal.pone.0037423
9. Deng M, Xiao X, Zhou L, Wang T. First Case Report of Maturity-Onset Diabetesof the Young Type 4 Pedigree in a Chinese Family. *Front Endocrinol* (2019) 10:406. doi: 10.3389/fendo.2019.00406
10. Bamshad MJ, Ng SB, Bigham AW, Tabor HK, Emond MJ, Nickerson DA, et al. Exome sequencing as a tool for Mendelian disease gene discovery. *Nat Rev Genet* (2011) 12:745–55. doi: 10.1038/nrg3031
11. Kleinberger JW, Pollin TII. Undiagnosed MODY: Time for Action. *Curr Diabetes Rep* (2015) 15:110. doi: 10.1007/s11892-015-0681-7
12. Zhang M, Zhou JJ, Cui W, Li Y, Yang P, Chen X, et al. Molecular and phenotypic characteristics of maturity-onset diabetes of the young compared with early onset type 2 diabetes in China. *J Diabetes* (2015) 7:858–63. doi: 10.1111/1753-0407.12253
13. Ng MC, Cockburn BN, Lindner TH, Yeung VT, Chow CC, So WY, et al. Molecular genetics of diabetes mellitus in Chinese subjects: identification of mutations in glucokinase and hepatocyte nuclear factor-1alpha genes in patients with early-onset type 2 diabetes mellitus/MODY. *Diabet Med* (1999) 16:956–63.
14. Xu JY, Dan QH, Chan V, Wat NMS, Tam S, Tiu SC, et al. Genetic and clinical characteristics of maturity-onset diabetes of the young in Chinese patients. *Eur J Hum Genet EJHG* (2005) 13:422–7. doi: 10.1038/sj.ejhg.5201347
15. Li H, Durbin R. Fast and accurate long-read alignment with Burrows-Wheeler transform. *Bioinformatics* (2010) 26:589–95. doi: 10.1093/bioinformatics/btp698
16. McKenna A, Hanna M, Banks E, Sivachenko A, Cibulskis K, Kernytsky A, et al. The Genome Analysis Toolkit: a MapReduce framework for analyzing next-generation DNA sequencing data. *Genome Res* (2010) 20:1297–303. doi: 10.1101/gr.107524.110
17. DePristo MA, Banks E, Poplin R, Garimella KV, Maguire JR, Hartl C, et al. Aframework for variation discovery and genotyping using next-generation DNA sequencing data. *Nat Genet* (2011) 43:491–8. doi: 10.1038/ng.806
18. Wang K, Li M, Hakonarson H. ANNOVAR: Functional annotation of genetic variants from high-throughput sequencing data. *Nucleic Acids Res* (2010) 38:1–7. doi: 10.1093/nar/gkq603
19. Purcell S, Neale B, Todd-Brown K, Thomas L, Ferreira MA, Bender D, et al. PLINK: A Tool Set for Whole-Genome Association and Population-Based Linkage Analyses. *Am J Hum Genet* (2007) 81:559–75. doi: 10.1086/519795
20. Li B, Leal SM. Methods for Detecting Associations with Rare Variants for Common Diseases: Application to Analysis of Sequence Data. *Am J Hum Genet* (2008) 83:311–21. doi: 10.1016/j.ajhg.2008.06.024
21. Benjamini Y, Hochberg Y. Controlling the False Discovery Rate: A Practical and Powerful Approach to Multiple Testing. *J R Stat Soc Ser B (Methodol)* (1995) 57:289–300. doi: 10.1111/j.2517-6161.1995.tb02031.x
22. Ng PC, Henikoff S. Predicting deleterious amino acid substitutions. *Genome Res* (2001) 11:863–74. doi: 10.1101/gr.176601
23. Adzhubei IA, Schmidt S, Peshkin L, Ramensky VE, Gerasimova A, Bork P, et al. A method and server for predicting damaging missense mutations. *Nat Methods* (2010) 7:248–9. doi: 10.1038/nmeth0410-248
24. Li Q, Wang K. InterVar: Clinical Interpretation of Genetic Variants by the 2015 ACMG-AMP Guidelines. *Am J Hum Genet* (2017) 100:267–80. doi: 10.1016/j.ajhg.2017.01.004
25. Auton A, Abecasis GR, Altshuler DM, Durbin RM, Abecasis GR, Bentley DR, et al. A global reference for human genetic variation. *Nature* (2015) 526:68–74. doi: 10.1038/nature15393
26. Visscher PM, Wray NR, Zhang Q, Sklar P, McCarthy MII, Brown MA, et al. 10 Years of GWAS Discovery: Biology, Function, and Translation. *Am J Hum Genet* (2017) 101:5–22. doi: 10.1016/j.ajhg.2017.06.005

27. Zhan X, Hu Y, Li B, Abecasis GR, Liu DJ. RVTESTS: An efficient and comprehensive tool for rare variant association analysis using sequence data. *Bioinformatics* (2016) 32:1423–6. doi: 10.1093/bioinformatics/btw079
28. Walsh R, Thomson KL, Ware JS, Funke BH, Woodley J, McGuire KJ, et al. Reassessment of Mendelian gene pathogenicity using 7,855 cardiomyopathy cases and 60,706 reference samples. *Genet Med* (2017) 19:192–203. doi: 10.1038/gim.2016.90
29. Lek M, Karczewski KJ, Minikel EV, Samocha KE, Banks E, Fennell T, et al. Analysis of protein-coding genetic variation in 60,706 humans. *Nature* (2016) 536:285–91. doi: 10.1038/nature19057
30. Fu W, O'Connor TD, Jun G, Kang HM, Abecasis G, Leal SM, et al. Analysis of 6,515 exomes reveals the recent origin of most human protein-coding variants. *Nature* (2013) 493:216–20. doi: 10.1038/nature11690
31. Schwarz JM, Cooper DN, Schuelke M, Seelow D. MutationTaster2: mutation prediction for the deep-sequencing age. *Nat Methods* (2014) 11:361–2. doi: 10.1038/nmeth.2890
32. Rentzsch P, Witten D, Cooper GM, Shendure J, Kircher M. CADD: Predicting the deleteriousness of variants throughout the human genome. *Nucleic Acids Res* (2019) 47:D886–94. doi: 10.1093/nar/gky1016
33. Dawson NL, Lewis TE, Das S, Lees JG, Lee D, Ashford P, et al. CATH: An expanded resource to predict protein function through structure and sequence. *Nucleic Acids Res* (2017) 45:D289–95. doi: 10.1093/nar/gkw1098
34. Pace CN, Fu H, Fryar KL, Landua J, Trevino SR, Shirley BA, et al. Contribution of Hydrophobic Interactions to Protein Stability. *J Mol Biol* (2011) 408:514–28. doi: 10.1016/j.jmb.2011.02.053
35. Shirakawa J, Fernandez M, Takatani T, El Ouaamari A, Jungtrakoon P, Okawa ER, et al. Insulin Signaling Regulates the FoxM1/PLK1/CENP-A Pathway to Promote Adaptive Pancreatic _ Cell Proliferation. *Cell Metab* (2017) 25:868–82.e5. doi: 10.1016/j.cmet.2017.02.004
36. Anuradha S, Radha V, Deepa R, Hansen T, Carstensen B, Pedersen O, et al. A prevalent amino acid polymorphism at codon 98 (Ala98Val) of the hepatocyte nuclear factor-1alpha is associated with maturity-onset diabetes of the young and younger age at onset of type 2 diabetes in Asian Indians. *Diabetes Care* (2005) 28:2430–5. doi: 10.2337/diacare.28.10.2430
37. Rothschild CB, Akots G, Hayworth R, Pettenati MJ, Rao PN, Wood P, et al. A genetic map of chromosome 20q12-q13.1: Multiple highly polymorphic microsatellite and RFLP markers linked to the maturity-onset diabetes of the young (MODY) locus. *Am J Hum Genet* (1993) 52:110–23. doi: 10.1016/0378-1119(94)90254-2
38. Wang X, Kiyokawa H, Dennewitz MB, Costa RH. The Forkhead Box m1b transcription factor is essential for hepatocyte DNA replication and mitosis during mouse liver regeneration. *Proc Natl Acad Sci USA* (2002) 99:16881–6. doi: 10.1073/pnas.252570299
39. Laoukili J, Kooistra MRH, Bras A, Kauw J, Kerkhoven RM, Morrison A, et al. FoxM1 is required for execution of the mitotic programme and chromosome stability. *Nat Cell Biol* (2005) 7:126–36. doi: 10.1038/ncb1217
40. Saldivar JC, Hamperl S, Bocek MJ, Chung M, Bass TE, Cisneros-Soberanis F, et al. An intrinsic S/G2 checkpoint enforced by ATR. *Science* (2018) 361:806–10. doi: 10.1126/science.aap9346
41. Lin Y, Currie SL, Rosen MK. Intrinsically disordered sequences enable modulation of protein phase separation through distributed tyrosine motifs. *J Biol Chem* (2017) 292:19110–20. doi: 10.1074/jbc.M117.800466

Conflict of Interest: The authors declare that the research was conducted in the absence of any commercial or financial relationships that could be construed as a potential conflict of interest.

frontiers in Genetics

ORIGINAL RESEARCH
published: 10 March 2021
doi: 10.3389/fgene.2021.630109

A Dual Systems Genetics Approach Identifies Common Genes, Networks, and Pathways for Type 1 and 2 Diabetes in Human Islets

Simranjeet Kaur[1], *Aashiq H. Mirza*[2], *Anne J. Overgaard*[1], *Flemming Pociot*[1,3,4] *and Joachim Størling*[1,5]*

[1] Department of Translational T1D Research, Steno Diabetes Center Copenhagen, Gentofte, Denmark, [2] Department of Pharmacology, Weill Cornell Medicine, New York, NY, United States, [3] Pediatric Department E, University Hospital, Herlev, Denmark, [4] Faculty of Health and Medical Sciences, University of Copenhagen, Copenhagen, Denmark, [5] Department of Biomedical Sciences, University of Copenhagen, Copenhagen, Denmark

OPEN ACCESS

Edited by:
Luiza Ghila,
University of Bergen, Norway

Reviewed by:
Hannah Maude,
Imperial College London, United Kingdom
Alex M. Mawla,
University of California, Davis, United States
Santiago A. Rodriguez-Segui,
Consejo Nacional de Investigaciones Científicas y Técnicas (CONICET), Argentina

***Correspondence:**
Joachim Størling
Joachim.stoerling@regionh.dk

Specialty section:
This article was submitted to Genetics of Common and Rare Diseases, a section of the journal Frontiers in Genetics

Received: *16 November 2020*
Accepted: *16 February 2021*
Published: *10 March 2021*

Citation:
Kaur S, Mirza AH, Overgaard AJ, Pociot F and Størling J (2021) A Dual Systems Genetics Approach Identifies Common Genes, Networks, and Pathways for Type 1 and 2 Diabetes in Human Islets. Front. Genet. 12:630109. doi: 10.3389/fgene.2021.630109

Type 1 and 2 diabetes (T1/2D) are complex metabolic diseases caused by absolute or relative loss of functional β-cell mass, respectively. Both diseases are influenced by multiple genetic loci that alter disease risk. For many of the disease-associated loci, the causal candidate genes remain to be identified. Remarkably, despite the partially shared phenotype of the two diabetes forms, the associated loci for T1D and T2D are almost completely separated. We hypothesized that some of the genes located in risk loci for T1D and T2D interact in common pancreatic islet networks to mutually regulate important islet functions which are disturbed by disease-associated variants leading to β-cell dysfunction. To address this, we took a dual systems genetics approach. All genes located in 57 T1D and 243 T2D established genome-wide association studies (GWAS) loci were extracted and filtered for genes expressed in human islets using RNA sequencing data, and then integrated with; (1) human islet expression quantitative trait locus (eQTL) signals in linkage disequilibrium (LD) with T1D- and T2D-associated variants; or (2) with genes transcriptionally regulated in human islets by pro-inflammatory cytokines or palmitate as *in vitro* models of T1D and T2D, respectively. Our *in silico* systems genetics approaches created two interaction networks consisting of densely-connected T1D and T2D loci genes. The "T1D-T2D islet eQTL interaction network" identified 9 genes (*GSDMB, CARD9, DNLZ, ERAP1, PPIP5K2, TMEM69, SDCCAG3, PLEKHA1*, and *HEMK1*) in common T1D and T2D loci that harbor islet eQTLs in LD with disease-associated variants. The "cytokine and palmitate islet interaction network" identified 4 genes (*ASCC2, HIBADH, RASGRP1*, and *SRGAP2*) in common T1D and T2D loci whose expression is mutually regulated by cytokines and palmitate. Functional annotation analyses of the islet networks revealed a number of significantly enriched pathways and molecular functions including cell cycle regulation, inositol phosphate metabolism, lipid metabolism, and cell death and survival. In summary, our study has identified a number of new plausible common candidate genes and pathways for T1D and T2D.

Keywords: type 1 diabetes, type 2 diabetes, genetics, network analysis, human islets

INTRODUCTION

Type 1 (T1D) and 2 diabetes (T2D) are complex metabolic traits characterized by complete or relative insulin deficiency, respectively, due to destruction or failure of the β-cells in the pancreatic islets of Langerhans. In T1D, the β-cells are destroyed by both innate and adaptive immune mechanisms in which pro-inflammatory cytokines are believed to play key roles (Berchtold et al., 2016). During the process of immune-mediated β-cell killing, the β-cells are not just passive bystanders but actively participate in their own demise through the interface with the immune system via e.g., MHC class I expression and production of chemokines favoring islet infiltration of immune cells, and through their inherent "fragility" to immune damage (Soleimanpour and Stoffers, 2013; Mallone and Eizirik, 2020). β-cell failure in T2D may be caused by prolonged metabolic stress exerted by e.g., free fatty acids (FFA) such as palmitate, and by the persistent increased demand for insulin production due to peripheral insulin resistance ultimately leading to β-cell failure (Prentki and Nolan, 2006; Oh et al., 2018; Wysham and Shubrook, 2020). Hence, although different mechanisms lead to β-cell failure in T1D and T2D, the loss of functional β-cell mass is a common key mechanism and, in both cases the β-cells seem to play an active role (Eizirik et al., 2020).

Both T1D and T2D are polygenetic and disease risk is influenced by multiple genetic variants. To date, genome-wide association studies (GWAS) genotyping thousands of single nucleotide polymorphisms (SNPs) have established more than 50 and 200 risk loci for T1D and T2D, respectively (Barrett et al., 2009; Bradfield et al., 2011; Morris et al., 2012; Onengut-Gumuscu et al., 2015; Mahajan et al., 2018)[1] Remarkably, the GWAS signals in T1D and T2D are starkly separated with only a few shared loci (Basile et al., 2014; Aylward et al., 2018) indicating vastly different genetic architectures. Among the few known common risk genes that have also been functionally validated is *GLIS3* which plays an important role in the β-cells by regulating proliferation and apoptosis (Nogueira et al., 2013; Wen and Yang, 2017). Based on its functional role, *GLIS3* has been suggested as an important predisposing factor of β-cell fragility in both forms of diabetes (Nogueira et al., 2013; Liston et al., 2017). Of note, the causal genetic variant(s) and gene(s) for most of the GWAS loci in T1D and T2D have not been identified. Better insight into the differences and putative commonalities of diabetes genetics may shed new light onto the pathogeneses of both diabetes forms.

Traditionally the gene located in closest physical proximity to the GWAS SNP in the disease locus has been considered the candidate risk gene (Slatkin, 2008). However, for complex polygenetic traits it has been reported that disease-associated SNPs are enriched for variants that have gene expression regulatory effects as determined by expression quantitative trait locus (eQTL) analyses (Westra and Franke, 2014; Fagny et al., 2017). eQTL analyses therefore represent an attractive way to link disease-associated SNPs to potential causal risk genes. Importantly, genetic variants can exert eQTL effects on genes that are physically distant to the disease-associated SNP underlining the complexity of disease genetics (Kumar et al., 2014). Based on this, it is plausible that many causal variants in T1D and T2D increase disease risk through changes in gene expression of nearby and distant genes. Notably, eQTLs can be highly tissue-specific emphasizing the necessity to examine eQTLs in relevant disease-affected tissue such as pancreatic islets in the case of T1D and T2D (Fagny et al., 2017).

In the present study, we aimed to take current knowledge of T1D and T2D genetics a step further by applying a systems genetics approach integrating GWAS data with human islet eQTLs and *in vitro* pathogenesis models to identify plausible causal risk genes, networks, and pathways shared between T1D and T2D at the pancreatic islet level. We identified a number of hitherto unreported common genes and pathways thereby advancing our understanding of shared genetic and pathogenic mechanisms in T1D and T2D. From our findings, novel hypotheses can be generated and tested in experimental disease models.

MATERIALS AND METHODS

T1D and T2D Loci and Associated Genes

T1D loci; GWAS signals and candidate genes were retrieved from ImmunoBase[1]. ImmunoBase provides curated and integrated datasets of summary case/control association studies from 12 immunologically related human diseases including T1D originally targeted by the ImmunoChip consortium. T2D loci; GWAS signals and candidate genes were retrieved from Mahajan et al. (2018). All genes located ± 500 kb from GWAS-significant SNPs were extracted using bedtools (Quinlan and Hall, 2010). This window to retrieve loci-associated genes was selected based on published studies (Alasoo et al., 2019; Stacey et al., 2019). Previously pin-pointed/suggested causative candidate genes for each locus were retrieved as reported (Onengut-Gumuscu et al., 2015; Mahajan et al., 2018)[1].

Islet eQTLs and LD Analysis

Recently, Viñuela et al. (2020) profiled and genotyped human islet samples from 420 human organ donors as a part of Integrated Network for Systematic analysis of Pancreatic Islet RNA Expression (InsPIRE) consortium (Viñuela et al., 2020). The study aggregated previous islet studies and retrieved data from 196 individuals (Fadista et al., 2014; van de Bunt et al., 2015; Varshney et al., 2017). The samples were jointly mapped and reprocessed (median sequence-depth per sample ∼60 M reads). We retrieved both exon- and gene-based islet eQTLs from this study to identify islet eQTLs associated with T1D-T2D loci.

Islet eQTLs in linkage disequilibrium (LD) ($r^2 \geq 0.8$) with nominally associated disease variants (both T1D and T2D variants) were identified using SNIPA (Arnold et al., 2015). The variant set used for LD calculation was 1,000 Genome, Phase 3 v5 (GRCh37 genome build), European population. For T1D and T2D, 20,669 and 5,270 nominally associated SNPs were obtained ($p < 0.05$), respectively. The summary statistics from a BMI-adjusted European dataset were used to retrieve T2D SNPs from Mahajan et al. (2018).

[1] *I*mmunobase. Available online at: https://www.immunobase.org/.

All the islet eQTL variants were annotated with Islet Regulome chromatin classes (including islet enhancers, promoters, and CTCF binding sites) retrieved from Mularoni et al. (2017) and Miguel-Escalada et al. (2019) using intersectBed feature of Bedtools (Quinlan and Hall, 2010). The T1D/T2D variants in LD with islet eQTLs were also annotated with islet regulome features.

Total RNAseq datasets from FACS-purified human α-, β-, and exocrine cells from 8 organ donors without diabetes were retrieved from GEO (GSE50386 and GSE76268) (Bramswig et al., 2013; Ackermann et al., 2016). The datasets included libraries that were single-end sequenced to 100 bp on an Illumina hiSeq2000. The raw fastq files were trimmed, cropped, and adapters removed using Trimmomatic v.0.36 (Bolger et al., 2014). The filtered reads after pre-processing (trimming and adapter removal) were aligned to a human genome (GRCh38) using tophat 2.1 (Trapnell et al., 2009) using the following parameters: Library-type = fr-firststrand, no-coverage-search, m 2, p 10. The raw read counts at gene level were calculated using htseqcount and further normalized to counts per million (CPM) and logCPM in EdgeR (Robinson et al., 2010).

Genes Transcriptionally Modified by Cytokines or Palmitate in Human Islets

The differentially expressed genes after cytokine (IL-1β + IFNγ) or palmitate exposure for 48 h in human islets were retrieved from GEO datasets GSE35296 and GSE53949, respectively (Eizirik et al., 2012; Cnop et al., 2014). Both datasets included five human islet preparations obtained from organ donors without diabetes, treated, and handled under similar conditions, with comparable human islet collection and handling protocols. In both studies, paired-end total RNA-sequencing was performed using polyA-selected mRNA and the datasets were processed using similar methods. Briefly, the authors mapped the paired end reads to human genome (GRCh37) using Genomic Multitool (GEM) suite (https://bio.tools/gemmapper) and transcripts were quantified into RPKM values using Flux Capacitor (http://flux.sammeth.net) (Eizirik et al., 2012; Cnop et al., 2014). The differentially expressed genes were identified using Fisher's exact test and p-values were corrected using Benjamini-Hochberg method. A difference in gene expression was considered significant if the adjusted $p < 0.05$ and if the expression changed significantly in one direction in at least four out of the five islet preparations (Eizirik et al., 2012; Cnop et al., 2014). In total 3,019 genes were found to be modulated by cytokines whereas 1,236 genes were modified by palmitate. Of these, 494 genes were regulated by both cytokines and palmitate.

PPI Network and Pathway Analysis

ToppCluster within ToppGene Suite (Chen et al., 2009) was used to identify protein-protein interactions (PPIs) between the T1D and T2D loci genes. Cytoscape v3.7.0 (http://www.cytoscape.org) (Smoot et al., 2011) was used to visualize the PPI network. A network topological analysis was performed using NetworkAnalyzer v2.7 which is a part of Cytoscape to assess various topological features. For every node in a network, NetworkAnalyzer computes its degree, the number of self-loops, and a variety of other parameters.

Ingenuity pathway analysis (IPA, Qiagen Inc.) was used to predict the downstream effects of the selected genes from the PPI networks. IPA has the most comprehensive, manually curated QIAGEN Knowledge Base that includes data derived from "omics" experiments including RNAseq, small RNAseq, metabolomics, proteomics, microarrays, and small-scale experiments from published studies[2]. IPA core analysis was performed to identify enriched pathways and molecular and cellular functions for the T1D and T2D loci genes in the PPI networks.

Pathway analysis was also performed using ClueGO plug-in v2.5.3 (Bindea et al., 2009) in Cytoscape. ClueGO integrates GO terms and pathways into a PPI network and creates a functional annotation map that represents the associations between terms. Pathway based clustering was performed with following settings: minimum number of genes within each cluster = 3, pathway network connectivity measure (κ score) = 0.4. The κ score defines the term-term interrelations and creates functional groups based on shared genes between the terms. The p-values were calculated using two-sided hypergeometric test and adjusted using Bonferroni step-down method. The minimum percentage of genes and terms for group merge was 50%. KEGG, Reactome, and WikiPathway annotations were used for pathway-based enrichment analyses in ClueGO.

STRING database and STRING enrichment app (Doncheva et al., 2019) in Cytoscape were used for expanding the network for the selected shared genes. The extended network in STRING was created using the following parameters: A confidence score cutoff of 0.5, selectivity of interactors 0.5 and the total number of interactors to expand the network was set to 50. The KEGG and Reactome pathway annotations were used to perform STRING enrichment analysis. The significant pathways were selected based on an FDR value < 0.05.

RESULTS

Selection and Integration of T1D and T2D Loci Genes and Islet eQTLs

A systems genetics approach was applied to pinpoint likely causal T1D and T2D risk genes and to examine their putative interactions in joint networks in human islets—the common "diseased tissue" in T1D and T2D (**Figure 1**). We divided our overall approach into two sub-approaches integrating; (1) T1D and T2D loci genes with human islet eQTL data, and (2) T1D and T2D loci genes with cytokine- or palmitate-modified human islet gene expressional changes. First, all genes located within ± 500 kb from 107 and 380 genome-wide significant signals for T1D and T2D, respectively, were extracted from publicly available data from ImmunoBase and Mahajan et al. (2018)[1]. These signals corresponded to 57 T1D and 243 T2D genomic loci of which 5 were overlapping. The genomic loci were defined based on conditionally independent signals that reach the GWAS significance ± 500 kb surrounding the lead SNP (Mahajan et al., 2018)[1]. If the minimum distance between any distinct signals

[2]IPA (QIAGEN Inc). Available online at: https://digitalinsights.qiagen.com/plugins/ingenuity-pathway-analysis/.

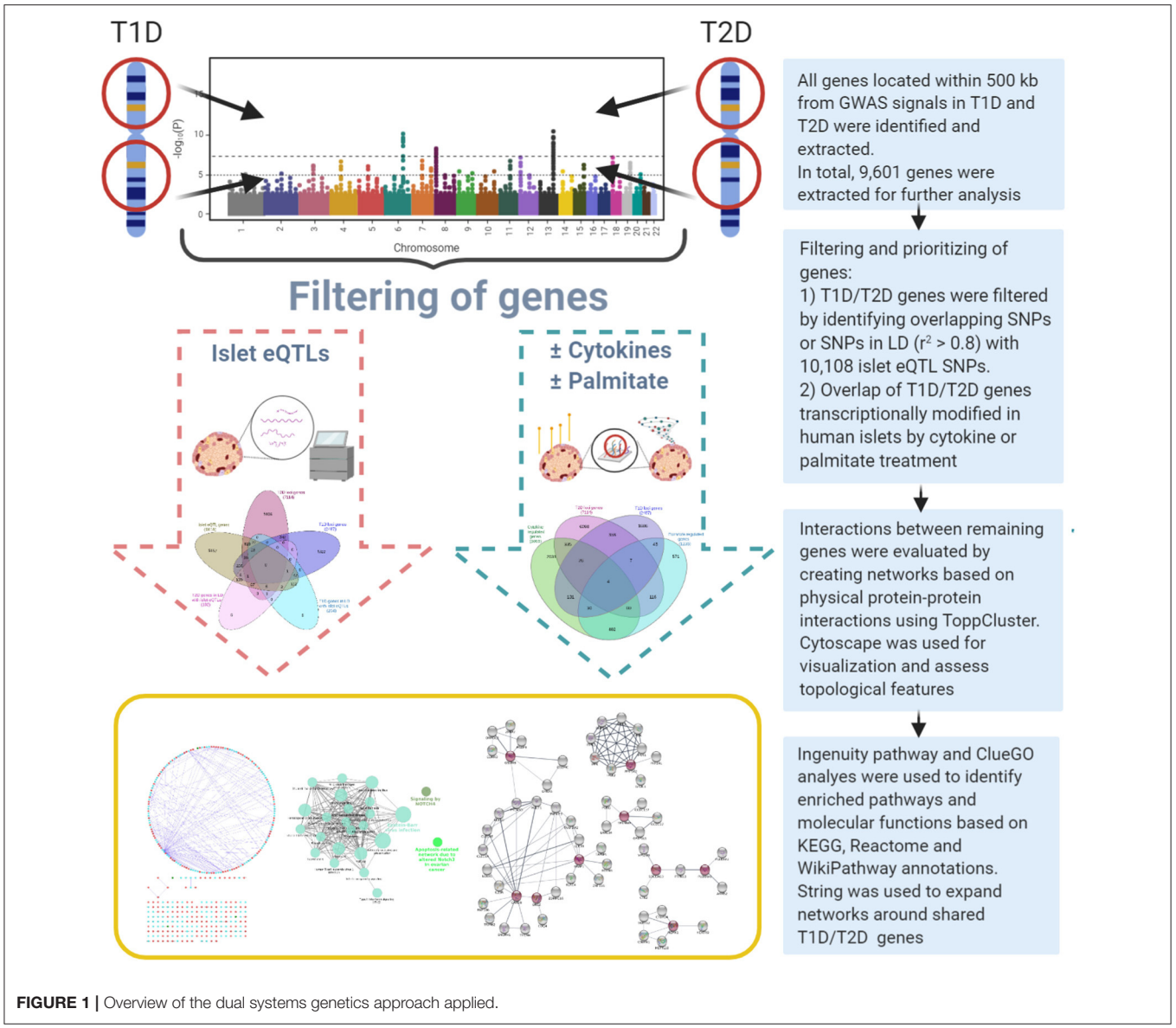

FIGURE 1 | Overview of the dual systems genetics approach applied.

from two separate loci was <500 kb, additional conditional analysis taking both regions (encompassing ± 500 kb from both ends) were performed to assess the independence of each signal (Mahajan et al., 2018). Of the total 403 identified distinct signals by Mahajan et al. 380 remained after excluding 23 signals that were not amenable to fine mapping (Mahajan et al., 2018). In total, 2,487 and 7,114 genes were retrieved for the T1D and T2D loci, respectively (**Figure 2A**).

Leveraging on a study by Vinuela and colleagues (Viñuela et al., 2020) that profiled gene expression and performed genotyping of human islets from 420 individual donors, we retrieved islet eQTLs. Both exon and gene-level *cis*-eQTLs corresponding to 4,312 and 6,039 genes, respectively (FDR < 1%; *cis* defined as within 1 Mb of the transcription start site [TSS]), were combined that resulted in a total of 10,108 islet eQTL associations for 6,618 genes (Table 1.1 in **Supplementary File 1**). The majority of the islet eQTL signals were associated with protein-coding genes (n = 9,627), while a much lower fraction was associated with long non-coding RNA genes (n = 842). We annotated the islet eQTL variants with Islet regulome features to identify enrichment for islet regulatory elements including islet enhancers, promoters, open chromatin regions, and CTCF binding sites etc. Only 12% (1,282 SNPs) of the islet eQTLs showed overlap with islet regulatory features, whereas the majority of the islet eQTL SNPs did not show any overlap (Table 2.1 in **Supplementary File 2**).

To further filter and prioritize the islet eQTL genes, we performed LD analysis to identify T1D and T2D GWAS SNPs that either themselves have islet eQTL effects or are in strong LD (r^2 > 0.8) with islet eQTL SNPs. For this analysis, we included all nominally associated SNPs for both T1D and T2D with a p < 0.05. Using a LD cutoff of r^2 >

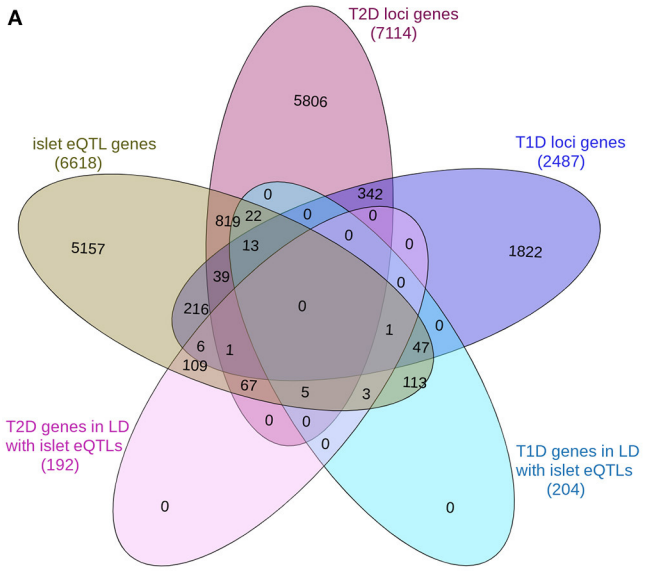

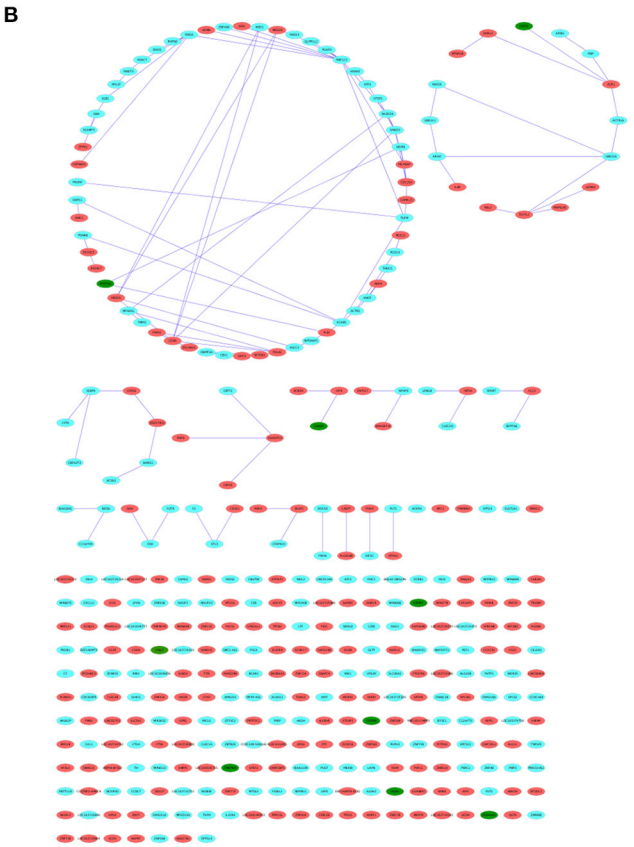

C

Top Canonical Pathways

Name	p-value	Overlap
Cell Cycle: G1/S Checkpoint Regulation	3.92E-04	6.0 % 4/67
PEDF Signaling	8.44E-04	4.9 % 4/82
Osteoarthritis Pathway	9.65E-04	2.7 % 6/220
Cell Cycle Control of Chromosomal Replication	2.99E-03	5.4 % 3/56
RhoA Signaling	3.73E-03	3.3 % 4/123

Molecular and Cellular Functions

Name	p-value range	# Molecules
Cell-To-Cell Signaling and Interaction	1.02E-02 - 2.23E-05	18
Cell Cycle	1.02E-02 - 2.75E-05	28
Cell Morphology	1.02E-02 - 3.62E-05	23
Lipid Metabolism	1.02E-02 - 7.57E-05	10
Molecular Transport	1.02E-02 - 7.57E-05	11

FIGURE 2 | The "T1D-T2D islet eQTL interaction network." The "T1D-T2D islet eQTL interaction network" is derived from islet eQTLs in linkage disequilibrium (LD $\geq$0.8) with nominally associated disease variants (both T1D and T2D variants). **(A)** Venn diagram of the genes filtered for. **(B)** The 'T1D-T2D islet eQTL interaction network' as visualized by Cytoscape. T1D ($n = 204$) and T2D genes ($n = 192$) are shown as cyan and red nodes, respectively. The edges (blue lines) represent the physicial interactions between the nodes. The network consists of 361 nodes, of which 9 are shared (shown in green). **(C)** Functional annotation of the "T1D-T2D islet eQTL interaction network" (117 nodes with a node degree $\geq$1) based on IPA analysis. Top canonical pathways and molecular and cellular processes are shown for the selected nodes.

0.8, 242,191 proxy SNPs were retrieved for the 10,108 islet eQTL SNPs.

For the T1D loci, 247 islet eQTLs SNPs (associated with 204 genes) were in LD with 1,735 T1D-associated SNPs. Of these, 55 of the T1D-associated SNPs directly acted as islet eQTL signals for T1D loci genes (Table 1.2 in **Supplementary File 1**). For the T2D loci, 223 islet eQTLs SNPs (associated with 192 genes) were in LD with 176 T2D SNPs. Of these, 19 of the T2D-associated SNPs directly acted as islet eQTL signals for T2D loci genes (Table 1.3 in **Supplementary File 1**). The annotation of these T1D and T2D SNPs in LD with islet eQTL SNPs with islet regulome features and Variant Effect Predictor (VEP) are shown in (Tables 2.2, 2.3 in **Supplementary File 2**).

Generation of a Common T1D-T2D Islet eQTL Interaction Network Based on Genes in LD With Disease Variants

We created a "T1D-T2D islet eQTL interaction network" based on the genes with islet eQTLs in LD with nominally associated T1D and T2D SNPs, i.e., the 204 T1D and 192 T2D loci-associated genes (**Figures 2A,B**).

Figure 2B (see **Supplementary File 3** for a high resolution image) shows the generated network which consists in total of 361 nodes, of which 9 are shared between T1D and T2D (shown as green nodes). These shared genes are *GSDMB*, *CARD9*, *DNLZ*, *ERAP1*, *PPIP5K2*, *TMEM69*, *SDCCAG3*,

PLEKHA1, and *HEMK1* and are covered in detail in the following section.

Pathway-based functional annotation was performed on the 117 nodes with a node degree ≥1 (i.e., with at least one physical interaction partner) in the "T1D-T2D islet eQTL interaction network." The top canonical pathways based on IPA pathway analysis included "Cell Cycle: G1/S checkpoint regulation," "PEDF Signaling," "Osteoarthritis Pathway," "Cell cycle control of chromosomal regulation," and "RhoA signaling" (**Figure 2C**). The identified molecular and cellular processes included "Cell-to-cell signaling and interaction," "Cell cycle," "Cell morphology," and "Lipid metabolism."

We also performed ClueGO pathway analysis of the "T1D-T2D islet eQTL interaction network" which identified 10 highly significant pathways that grouped into 5 clusters (Figure 1 in **Supplementary File 1**). The representative pathways and genes for these 5 clusters were "Sphingolipid metabolism" (with 3 genes involved: *CERS2*, *GBA*, *GLB1*), "Transcriptional regulation of white adipocyte differentiation" (with 4 genes involved: *CDK8, MED1, MED28, MED31*), "G1 to S cell cycle control" (with 3 genes involved: *CDC25A, POLA2, PRIM1*), "Ethanol effects on histone modifications" (with 4 genes involved: *ACSS2, ATF2, MED1, HDAC7*) and "Chromosomal and microsatellite instability in colorectal cancer" (with 6 genes involved: *RHOA, SMAD3, TCF7L2, CDK8, ATF2, PLEC*). All the 10 significant pathways are listed in Table 1.4 in **Supplementary File 1** along with their clusters and *p*-values.

Extended Network of Shared Genes and Pathway Analysis

The 9 shared genes between T1D and T2D found in the "T1D-T2D islet eQTL interaction network" (**Figure 2B**) were explored further in relation to; (1) their shared eQTL signals for T1D and T2D; (2) their neighboring interacting partners; and (3) their associated pathways. **Table 1** lists the 9 shared genes and their islet eQTL associations with T1D- and T2D-associated SNPs. The genes with islet eQTLs in LD with highly significant (GWAS $p < 2E\text{-}08$) T1D- and T2D-associated SNPs were *GSDMB* and *CRAD9* (**Table 1**).

We extended the network of the 9 shared T1D/T2D genes by including neighboring genes to create a larger network allowing identification of their associated pathways. **Figure 3A** shows the extended network of the 9 shared genes. The extended network was expanded by allowing a maximum of 50 interactors shown in gray nodes (**Figure 3A**). The STRING enrichment analysis identified 17 significant pathways and an overall PPI enrichment score of 1.0E-16. A PPI enrichment score <0.05 indicates that the proteins are more likely to be biologically connected as a group. The top 5 pathways for the extended network included "inositol phosphate metabolism," "synthesis of pyrophosphates in the cytosol," "phosphatidylinositol signaling system," "synthesis of IPs in the nucleus," and "c-type lectin receptors (CLRs)" (**Table 2**). We then analyzed the expression of the genes in the extended network using RNAseq data from FACS-purified α-, β-, and exocrine cells derived from human islets. **Figure 3B** shows

TABLE 1 | Islet eQTL SNPs in LD with disease-associated SNPs for the 9 shared genes within the "T1D-T2D islet eQTL interaction network."

Islet eQTLs							**T1D-associated SNP in LD (r2>0.8)**		**T2D-associated SNP in LD(r2>0.8)**	
Gene name	**eQTL SNP**	**A1**	**A2**	**MAF**	**chrSNP**	**StartSNP**	**SNP**	**P-value**	**SNP**	***P***
HEMK1	rs12493985	T	G	0.14	3	50544715	rs1034405	2.39E-03	rs1034405	0.022
GSDMB	**rs870829**	A	C	0.42	17	38068382	**rs870829**	2.42E-08		
	rs12939565	A	T	0.47	17	38038389	rs12453507	1.05E-08	rs11557467	0.019
ERAP1	**rs7063**	A	T	0.29	5	96110211	**rs7063**	0.014		
	rs146341958	C	T	0.13	5	96125159			rs72773968	0.007
PPIP5K2	rs1898673	G	C	0.33	5	102293380	rs3776855	0.016	rs34813	0.00064
	rs27489	C	T	0.28	5	102555746	rs3776855	0.016	rs34813	0.00064
TMEM69	rs28597977	A	G	0.32	1	46181206	rs6694302	0.040	rs28375469	0.049
DNLZ	rs57052773	T	C	0.04	9	139385701	rs78270318	0.012	rs3812561	0.002
	rs28679497	G	A	0.28	9	139246594			rs60980157	2.02E-15
	rs4442263	C	T	0.04	9	139322775	rs78270318	0.012	rs3812561	0.002
SDCCAG3	rs34619169	G	A	0.27	9	139327277	rs11146021	0.021	rs3812594	0.0051
CARD9	rs57052773	T	C	0.04	9	139385701	rs78270318	0.012	rs3812561	0.002
	rs61386106	G	A	0.28	9	139246768			rs60980157	2.02E-15
	rs4442263	C	T	0.04	9	139322775	rs78270318	0.012	rs3812561	0.002
PLEKHA1	rs4752689	G	A	0.4	10	124131176			rs1045216	9.80E-06
	rs71486610	G	C	0.49	10	124134803	rs2280141	0.030		
							rs7097701	0.0270		

The table shows the 9 shared genes in the "T1D-T2D islet eQTL interaction network." eQTLs that are disease-associated SNPs themselves are shown in bold. T1D/T2D SNPs in LD with islet eQTL SNPs are listed. In case of multiple disease-associated SNPs in LD with an eQTL SNP, the most significant disease-associated SNP is listed. The disease-associated SNPs with GWAS significance are highlighted in bold.

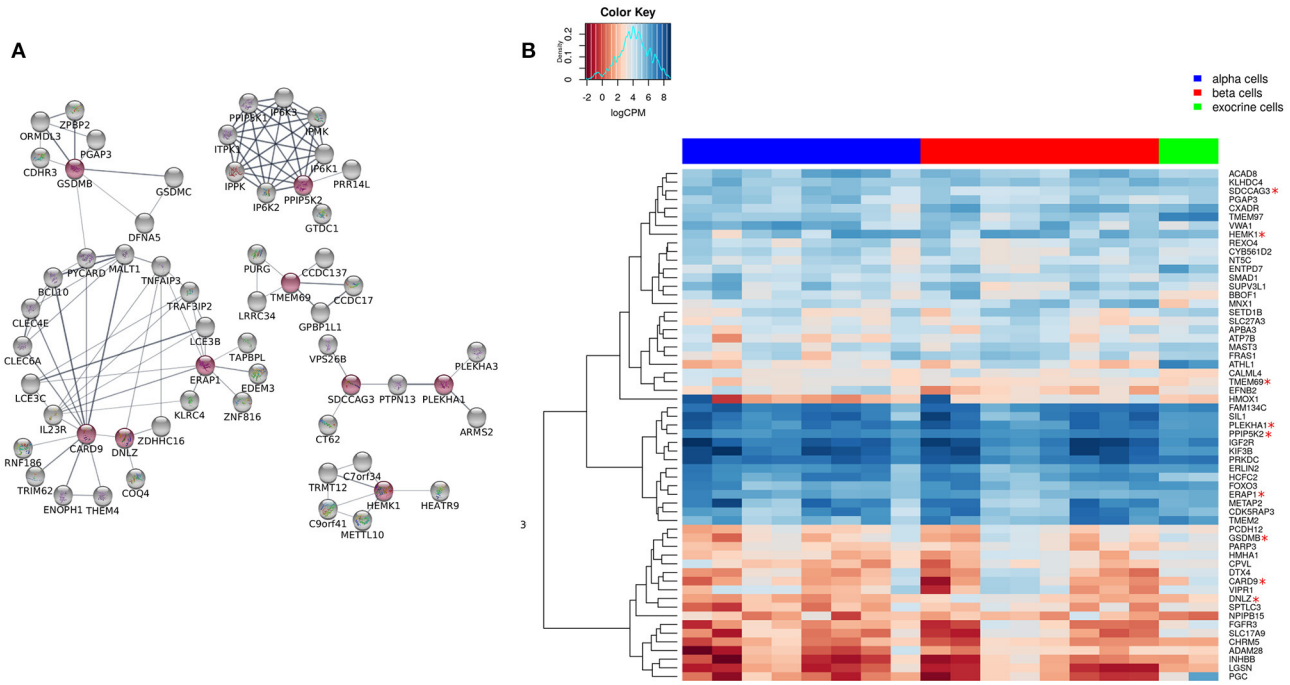

FIGURE 3 | Extended network of the 9 shared genes within the "T1D-T2D islet eQTL interaction network." **(A)** The 9 shared genes within the "T1D-T2D islet eQTL interaction network" are shown as red nodes. The network was extended based on physical interactions to allow 50 neighboring genes (shown in gray nodes) using STRING app in Cytoscape. **(B)** Expression of the genes within the extended network ($n = 59$) in FACS-purified α, β, and exocrine cells derived from human islets. The heatmap shows unsupervised clustering of log2CPM values for α-cells ($n = 8$), β-cells ($n = 8$), and exocrine cells ($n = 2$) samples. The clustering was done using Euclidean distance with complete linkage method.

a heatmap of the expression values of the genes in the three cell types.

Generation of a Common T1D-T2D Islet Interaction Network Based on Cytokine- and Palmitate-Regulated Loci Genes

As eQTLs may not be present under basal, non-disease conditions, but only in the disease state or the phase preceding disease, we sought to take an additional approach to investigate interactions between islet expressed T1D and T2D loci genes. We therefore next created a network of T1D and T2D loci genes whose expression in human islets is modulated by pro-inflammatory cytokines as an *in vitro* model of a T1D environment and/or by the FFA palmitate as an *in vitro* model of a T2D environment using published RNAseq datasets (Eizirik et al., 2012; Cnop et al., 2014) (**Figures 4A,B**). In total, cytokines modulated the expression of 191 T1D loci genes whereas palmitate modulated the expression of 187 T2D loci genes. Interestingly, among these, 4 genes (*ASCC2, HIBADH, RASGRP1, and SRGAP2*) were commonly regulated by cytokines and palmitate and were also located in shared T1D and T2D loci (Table 1.5 in **Supplementary File 1**). **Figure 4B** (see **Supplementary File 4** for a high resolution image) depict the derived network with a total of 372 nodes, the 4 shared genes are shown in green nodes.

IPA pathway analysis of the "cytokine and palmitate islet interaction network" identified "Antigen presentation" and "Th1 and Th2 activation" as top canonical pathways (**Figure 4C**). The top molecular and cellular processes included "Cellular movement," "Cell death and survival," and "Cell proliferation and growth."

Functional annotation of the "cytokine and palmitate islet interaction network" using ClueGO revealed 3 clusters of 24 highly significant pathways (Figure 2 and Table 1.6 in **Supplementary File 1**). The representative terms and genes for these 3 clusters are "Signaling by NOTCH4" (with 6 genes involved: *ACTA2, FBXW7, NOTCH2, PSMB1, PSMB8, PSMB9*), "Apoptosis-related network due to altered Notch3 in ovarian cancer" (with 5 genes involved: *APOE, AXIN1, ERBB3, ERN1, IL7R*) and "Epstein-Barr virus infection" (with 35 genes involved: *HLA-DMA, HLA-DMB, HLA-DPA1, HLA-DRA, HLA-DRB5, ITGB3, TAP1, TAP2, TUBA4A, CIITA, IL2RA, IL7R, NOTCH2, RARA, PTPRN2, EEF1A2, SOCS1, ICAM1, KRT40, CEBPG, CTSD, LSP1, IKBKE, KPNA2, OAS3, ADCY5, CDKN2C, FOSL1, MYC, DDB2, TNFAIP3, RAC2, AP1B1, AP2M1, PSMB9*).

DISCUSSION

In this study, we employed a systems genetics approach integrating RNAseq data, eQTL signals and cytokine/palmitate-regulated genes to look for PPIs between probable causal risk genes in T1D and T2D GWAS loci at the human pancreatic islet level. We were able to create a PPI network that contained interactions between multiple T1D and

TABLE 2 | Pathway-based functional annotation of the extended network of the 9 shared genes within the "T1D-T2D islet eQTL interaction network."

Annotation Source	# Background genes	# Genes	Description	Genes	FDR Value
Reactome	48	8	Inositol phosphate metabolism	ITPK1, IPPK, IP6K2, IPMK, IP6K3, PPIP5K1, IP6K1, **PPIP5K2**	4.31E-10
Reactome	10	6	Synthesis of pyrophosphates in the cytosol	ITPK1, IPPK, IP6K3, PPIP5K1, IP6K1, **PPIP5K2**	4.31E-10
KEGG	97	8	Phosphatidylinositol signaling system	ITPK1, IPPK, IP6K2, IPMK, IP6K3, PPIP5K1, IP6K1, **PPIP5K2**	2.81E-08
Reactome	4	4	Synthesis of IPs in the nucleus	IPPK, IP6K2, IPMK, IP6K1	1.65E-07
Reactome	134	6	C-type lectin receptors (CLRs)	PYCARD, CLEC4E, MALT1, BCL10, **CARD9**, CLEC6A	9.48E-05
Reactome	94	4	CLEC7A (Dectin-1) signaling	PYCARD, MALT1, BCL10, **CARD9**	0.0042
Reactome	6	2	CLEC7A/inflammasome pathway	PYCARD, MALT1	0.0042
Reactome	53	3	Synthesis of PIPs at the plasma membrane	PLEKHA3, **PLEKHA1**, PTPN13	0.0089
Reactome	54	3	Nucleotide-binding domain, leucine rich repeat containing receptor (NLR) signaling pathways	PYCARD, **CARD9**, TNFAIP3	0.0089
Reactome	2032	15	Metabolism	PLEKHA3, ITPK1, ENOPH1, IPPK, IP6K2, THEM4, **PLEKHA1**, IPMK, C9orf41, ORMDL3, PTPN13, IP6K3, PPIP5K1, IP6K1, **PPIP5K2**	0.009
Reactome	1925	14	Immune System	PYCARD, TRIM62, ERAP1, CLEC4E, MALT1, IL23R, IP6K2, THEM4, BCL10, **CARD9**, CLEC6A, ORMDL3, PTPN13, TNFAIP3	0.0145
Reactome	84	3	PI Metabolism	PLEKHA3, **PLEKHA1**, PTPN13	0.0202
KEGG	73	3	Inositol phosphate metabolism	ITPK1, IPPK, IPMK	0.0241
KEGG	93	3	NF-kappa B signaling pathway	MALT1, BCL10, TNFAIP3	0.0241
KEGG	172	4	Tuberculosis	CLEC4E, MALT1, BCL10, **CARD9**	0.0241
Reactome	26	2	Dectin-2 family	CLEC4E, CLEC6A	0.0258
Reactome	35	2	NOD1/2 Signaling Pathway	**CARD9**, TNFAIP3	0.0413

The functional annotations of the extended network of the 9 shared genes are shown in the table. KEGG and Reactome pathway annotations were used for the pathway enrichment analysis using the STRING app in CytoScape. The 9 shared genes associated with the enriched pathways are highlighted in bold.

T2D loci genes that associated with SNPs in LD with islet eQTL SNPs. IPA pathway analysis of the interacting nodes pointed toward important cellular processes such as regulation of cell cycle processes. Considering that loss of functional β-cell mass is a key mechanism in both T1D and T2D, it is plausible to think that disease-associated variants linked to altered gene expression of genes involved in cell cycle control could negatively affect the replicative capacity of the β-cells thereby favoring a loss of functional β-cell mass.

Interestingly, we identified 9 shared genes within the "T1D-T2D islet eQTL interaction network" and an extension of the network surrounding these shared genes revealed highly interconnected nodes that are putatively involved in regulating common processes leading to either type of disease. Among the 9 shared genes (*HEMK1, GSDMB, ERAP1, PPIP5K2, TMEM69, DNLZ, SDCCAG3, CARD9, and PLEKHA1*), two of them, *GSDMB* (gasdermin B) and PLEKHA1 (pleckstrin homology domain-containing family A member 1) were previously identified as candidate genes for T1D (Morris et al., 2012) and T2D (Mahajan et al., 2018), respectively. *GSDMB* and *CARD9* (caspase recruitment domain family member 9), both have implications in the inflammatory pathways leading to apoptosis (Hara et al., 2007; Ruan, 2019). Three genes encode for enzymes with different functions, *ERAP1* (endoplasmic reticulum aminopeptidase 1) an amino peptidase involved in the processing of HLA class I-binding precursors (Rock et al., 2002), a histidine acid phosphatase, *PPIP5K2* (diphosphoinositol pentakisphosphate kinase 2), regulating bioenergetic homeostasis (Nair et al., 2018), and *HEMK1* (methyl

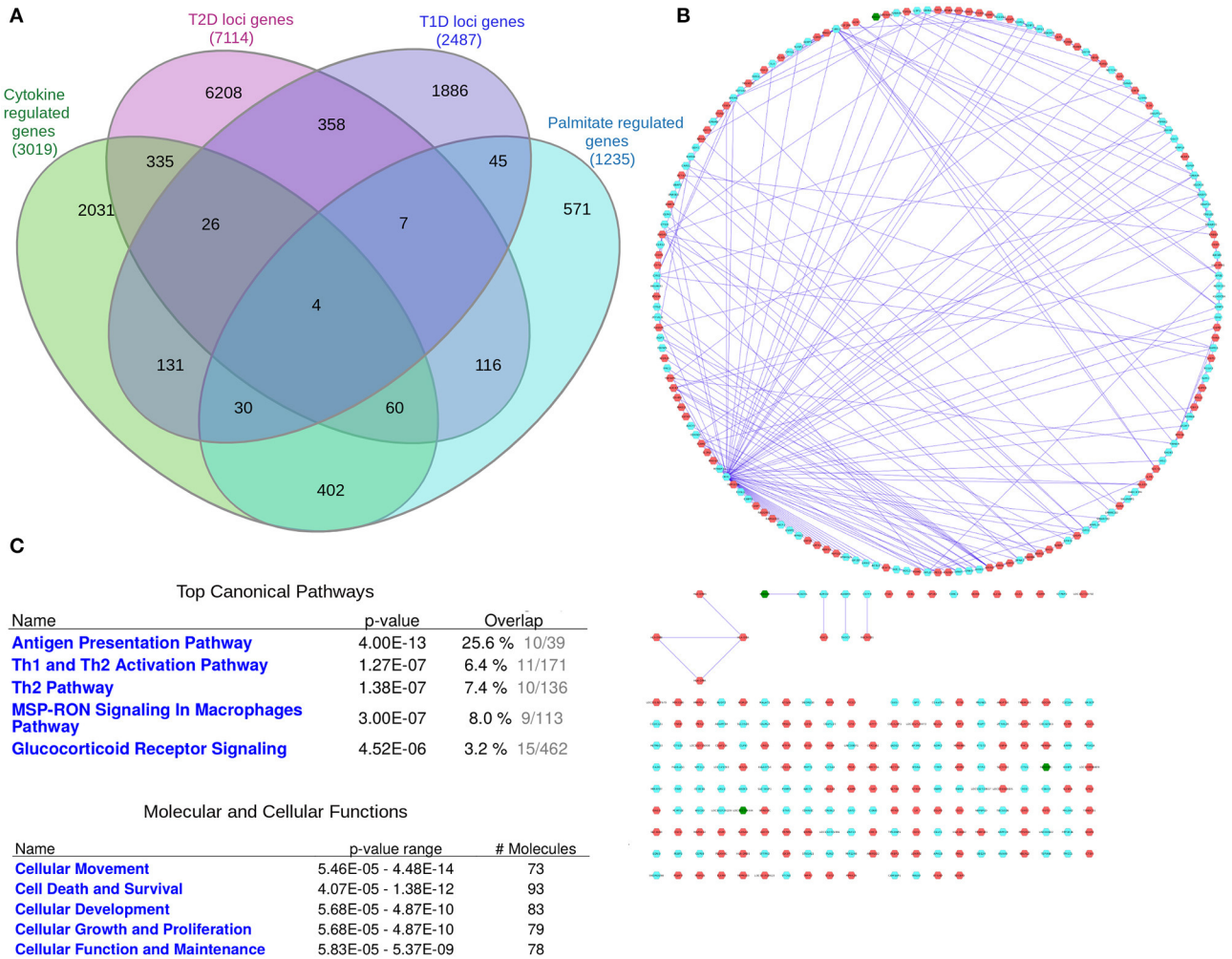

FIGURE 4 | The "cytokine and palmitate islet interaction network." The "cytokine and palmitate islet interaction network" is derived from overlap of T1D and T2D loci genes with cytokine- and/or palmitate-regulated genes. **(A)** Venn diagram of the genes filtered for. **(B)** The "cytokine and palmitate islet interaction network" as visualized by Cytoscape. The T1D loci genes subject to cytokine regulation ($n = 191$) and T2D loci genes subject to palmitate regulation ($n = 187$) are shown in cyan and red nodes, respectively. The edges (blue lines) represent the physicial interactions between the nodes. The network consists of 372 nodes, of which 4 are shared (shown in green). **(C)** Functional annotation of the "cytokine and palmitate islet interaction network" (181 nodes with node degree ≥ 1) based on IPA analysis. Top canonical pathways and molecular and cellular processes are shown for the selected nodes.

transferase family member 1), responsible for the methylation of glutamine residues. Further, *PLEKHA1* (pleckstrin homology domain containing A1) is involved in signaling complexes in the plasma membrane. *SDCCAG3* (serologically defined colon cancer antigen 3) is potentially related to protein trafficking and secretion (Neznanov et al., 2005).

The enriched pathways for the extended network of the 9 shared genes included interesting categories such as "inositol phosphate metabolism," "immune system," "inflammasome pathway," and "NOD1/2 signaling." Broadly speaking, most if not all these pathway functions seem rational in terms of regulating cellular mechanisms that could be important for diabetes at the islet level. For instance, with regard to "inositol phosphate metabolism," it is well-recognized that inositol phosphate compounds are intimately involved in the stimulus-secretion coupling process in β-cells through the regulation of calcium signaling (Barker et al., 2002). Remarkably, there was as many as 6 enriched pathways in total related to inositol in the extended network inferring that inositol signaling and metabolism may play prime roles in both T1D and T2D.

Identifying protein complexes from PPIs is an important area of research for gaining insights into genetic pathways and identification and prioritization of disease genes (Lage et al., 2007; Taylor and Wrana, 2012). An increasing number of studies have employed PPI networks to explore the molecular basis of complex diseases (Oti et al., 2006; Bergholdt et al., 2007; Lage et al., 2007; Jaeger and Aloy, 2012). Genes causing the same or similar diseases tend to lie close to one another in a network of PPIs or functional interactions and display a high degree of connectivity (Oti et al., 2006; Vanunu et al.,

2010). Previous studies combining PPIs and genetic interactions predicted disease genes for genetically heterogeneous diseases and proved helpful in identifying associations between disease genes and other genes for specific protein complexes (Oti et al., 2006; Bergholdt et al., 2007, 2009; Lage et al., 2007; Vanunu et al., 2010).

An important part of our study design of the first approach was the gene filtering based on regulatory islet eQTLs. Lappalainen et al. (2013) provided a detailed landscape of regulatory SNPs in 1,000 Genomes data and demonstrated how eQTL data can be used to identify potential causal variants. In a recent study, Fagny et al. (2017) constructed tissue-level eQTL networks in 13 human tissues and observed tissue-specific regulatory roles of common variants and their collective impact on biological pathways underlining the necessity to look for eQTLs in the specific tissue of interest, i.e., in islets in our current study, to obtain meaningful and (patho)physiologically relevant information.

In our second part of analyses, we also selected for loci genes that were subject to differential regulation by cytokines and/or palmitate as *in vitro* models of T1D and T2D. This analysis revealed 4 commonT1D and T2D loci genes (*ASCC2, HIBADH, RASGRP1, and SRGAP2*) that are all regulated by both cytokines and palmitate in human islets. *RASGRP1* (RAS guanyl releasing protein 1) was previously identified as a candidate gene for both T1D and T2D (Mahajan et al., 2018), and *ASCC2* (activating signal cointegrator 1 complex subunit 2) and *SRGAP2* (SLIT-ROBO Rho GTPase-activating protein 2) were identified as T2D candidate genes (Mahajan et al., 2018)[1]. Interestingly, two of the genes, *ASCC2* and *HIBADH*, were also associated with islet eQTLs, and even more remarkably, we found that *ASCC2* eQTL SNPs were in strong LD with T1D-associated SNPs (data not shown). *ASCC2* is involved in ubiquitin binding activity which might be responsible for commonly regulating β-cell function in human islets and contributing to both T1D and T2D (López-Avalos et al., 2006), which deserves further investigation in future studies. *HIBADH* (3-hydroxyisobutyrate dehydrogenase) has been previously implicated in insulin resistance and risk of incident type 2 diabetes and gestational diabetes mellitus (Nilsen et al., 2020). Although the selection of genes based on their regulation by cytokines and/or palmitate does not necessarily identify causal genes, but merely identifies genes whose expression level correlate with cytokine/palmitate exposure. It is also important to keep in mind that the genes observed to be differentially expressed at a specific time point only reflect a snapshot of the gene regulatory effects exerted by cytokines and palmitate. Despite these drawbacks, we do believe that this approach is a valid alternative approach to the eQTL/LD selection criteria in our first part of the analyses.

Our finding that risk genes for T1D and T2D interact in shared networks at the islet level supports the concept that despite the overall lack of genetic commonality in T1D and T2D, and that different mechanisms underlie the loss of functional β-cell mass in T1D and T2D, at least some candidate risk genes of both diabetes forms seem to cooperate in common pathways to regulate various islet processes that could be relevant for promoting disease. The common networks identified by our analyses adds to our current knowledge and may offer an opening to pinpoint potential commonality between T1D and T2D. It is worth noticing, however, that although both diseases are heterogenous, T2D is probably more heterogenous than T1D and can be classified into multiple subtypes according to clinical parameters and phenotype, and genetics most likely play an important underlying role in this (Udler, 2019). Future studies comparing T1D genetics with the various subclasses of T2D categorized by genetic profiles would be of interest.

A limitation of our study may be that the GWAS datasets used to define the disease-associated loci are from European populations only. We therefore might have missed potential GWAS signals that could be present in other ethnicities. Another limitation is that it was not possible to use PPIs obtained from human islets as such data currently does not exist. It is therefore not possible to apply tissue specificity at this point. In general, however, PPIs are not tissue-specific, though, but, obviously, rely on the expression of the protein-coding genes that interact at the protein level. We applied islet gene expression filtering that indirectly added some tissue specificity for the PPI analyses, but it would have been further advantageous if PPI data for human islets existed. Additional studies are highly warranted to validate the results and to explore the roles of the identified common candidate genes for normal and dysfunctional islet mass.

In summary, by a dual systems genetics approach, we report the identification of novel plausible causal T1D and T2D risk genes that are common between both diabetes forms. Our study further suggests that some genes located in T1D and T2D risk loci interact in shared islet networks where they regulate critical cellular functions such as cell cycle processes and lipid metabolism in human islets. From our findings novel testable hypotheses can be formulated thereby setting the groundwork for future experimental follow up and functional characterization of the shared and interacting T1D and T2D candidate genes in *in vitro* and *in vivo* models. Moreover, it would be imperative to experimentally validate the identified PPIs in human islets and in β-cells by appropriate methods. These studies are highly warranted as they could shed further light onto causal and pathogenic mechanisms and offer new clues about how genetic factors set the scene for immune- and metabolic stress-mediated β-cell loss in T1D and T2D.

DATA AVAILABILITY STATEMENT

The original contributions presented in the study are included in the article/**Supplementary Material**, further inquiries can be directed to the corresponding author.

AUTHOR CONTRIBUTIONS

JS suggested the overall hypothesis. SK and JS designed the study and researched the data. SK, JS, and AO drafted the manuscript. FP and AM revised the manuscript critically for important intellectual content. All authors contributed to the article and approved the submitted version.

FUNDING

This project has received funding from the Innovative Medicines Initiative 2 Joint Undertaking under grant agreement No 115797 (INNODIA) and No 945268 (INNODIA HARVEST). This Joint Undertaking receives support from the Union's Horizon 2020 research and innovation programme, EFPIA, JDRF, and The Leona M. and Harry B. Helmsley Charitable Trust.

SUPPLEMENTARY MATERIAL

The Supplementary Material for this article can be found online at: https://www.frontiersin.org/articles/10.3389/fgene.2021.630109/full#supplementary-material

Supplementary File 1. |

Supplementary Table 1.1 | Annotation of islet eQTL signals and biotype of islet eQTL genes. The islet eQTL associations were retrieved from Viñuela et al. (2020). Both exon and gene-level *cis*-eQTLs corresponding to 4,312 and 6,039 genes, respectively (FDR<1%; *cis* defined as within 1 Mb of the transcription start site [TSS]), were combined that resulted in a total of 10,108 islet eQTL associations for 6,618 islet eQTL genes.

Supplementary Table 1.2 | T1D-associated SNPs as islet eQTLs. The table lists 55 T1D-associated SNPs that act as islet eQTLs. T1D GWAS summary statistics were retrieved from Onengut-Gumuscu et al. (2015). All nominally associated SNPs ($p < 0.05$) were compared against the significant exon and gene level islet eQTLs from Viñuela et al. (2020). OR, log odds ratio for the effect allele. T1D GWAS Alleles (Min>Maj); Islet eQTL Alleles (Ref>Alt).

Supplementary Table 1.3 | T2D-associated SNPs as islet eQTLs. The table lists 19 T2D-associated SNPs that act as islet eQTLs. The T2D GWAS summary statistics were retrieved from Mahajan et al. (2019) (European BMI adjusted dataset). All nominally associated SNPs ($p < 0.05$) were compared against the significant exon and gene level islet eQTLs from Viñuela et al. (2020). Beta: log odds ratio for the effect allele; T2D GWAS Alleles (Effect allele > other allele); Islet eQTL Alleles (Ref>Alt).

Supplementary Table 1.4 | Pathway-based annotation analysis of the "T1D-T2D islet eQTL interaction network." The pathway-based annotations were performed using KEGG, Reactome, and Wiki pathway annotations in ClueGo app in Cytoscape. P-values were corrected with Bonferroni step down.

Supplementary Table 1.5 | Shared genes in the "cytokine and palmitate islet interaction network".

Supplementary Table 1.6 | Pathway-based annotation analysis of the "cytokine and palmitate islet interaction network." The pathway-based annotation was performed using KEGG, Reactome, and Wiki pathway annotations in ClueGo app in Cytoscape. P-values are corrected with Bonferroni step down.

Supplementary Figure 1 | Pathway based functional annotation of "T1D-T2D islet eQTL interaction network" (117 nodes with node degree ≥1) using CytoScape plugin ClueGO.

Supplementary Figure 2 | Pathway based functional annotation of "cytokine and palmitate islet interaction network" (181 nodes with node degree ≥1) using CytoScape plugin ClueGO.

Supplementary File 2. |

Supplementary Table 2.1 | Annotation of islet eQTL SNPs based on islet regulome features. A total of 1,282 islet eQTL SNPs intersect with islet regulome features derived from Miguel-Escalada et al. (2019). All the coordinates are based on the GRCh37 version of the human genome.

Supplementary Table 2.2 | Annotation of T1D-associated SNPs in LD with islet eQTL SNPs based on islet regulome features. 140 T1D-associated SNPs in LD with islet eQTLs intersect with islet regulome features derived from Miguel-Escalada et al. (2019). All the coordinates are based on the GRCh37 version of the human genome.

Supplementary Table 2.3 | Annotation of T2D-associated SNPs in LD with islet eQTL SNPs based on islet regulome features. 22 T2D SNPs in LD with islet eQTLs intersect with islet regulome features derived from Miguel-Escalada et al. (2019). All the coordinates are based on the GRCh37 version of the human genome.

Supplementary File 3. | High resolution view of the 'T1D-T2D islet eQTL interaction network' as visualized by Cytoscape. T1D ($n = 204$) and T2D genes ($n = 192$) are shown as cyan and red nodes, respectively. The edges (blue lines) represent the physicial interactions between the nodes. The network consists of 361 nodes, of which 9 are shared (shown in green).

Supplementary File 4. | High resolution view of the 'cytokine and palmitate islet interaction network' as visualized by Cytoscape. The T1D loci genes subject to cytokine regulation ($n = 191$) and T2D loci genes subject to palmitate regulation ($n = 187$) are shown in cyan and red nodes, respectively. The edges (blue lines) represent the physicial interactions between the nodes. The network consists of 372 nodes, of which 4 are shared (shown in green).

REFERENCES

Ackermann, A. M., Wang, Z., Schug, J., Naji, A., and Kaestner, K. H. (2016). Integration of ATAC-seq and RNA-seq identifies human alpha cell and beta cell signature genes. *Mol. Metab.* 5, 233–244. doi: 10.1016/j.molmet.2016.01.002

Alasoo, K., Rodrigues, J., Danesh, J., Freitag, D. F., Paul, D. S., and Gaffney, D. J. (2019). Genetic effects on promoter usage are highly context-specific and contribute to complex traits. *Elife* 8:e41673. doi: 10.7554/eLife.41673

Arnold, M., Raffler, J., Pfeufer, A., Suhre, K., and Kastenmüller, G. (2015). SNiPA: an interactive, genetic variant-centered annotation browser. *Bioinformatics* 31, 1334–1336. doi: 10.1093/bioinformatics/btu779

Aylward, A., Chiou, J., Okino, M.-L., Kadakia, N., and Gaulton, K. J. (2018). Shared genetic risk contributes to type 1 and type 2 diabetes etiology. *Hum Mol Genet.* 2018:ddy314. doi: 10.1093/hmg/ddy314

Barker, C. J., Leibiger, I. B., Leibiger, B., and Berggren, P.-O. (2002). Phosphorylated inositol compounds in beta -cell stimulus-response coupling. *Am. J. Physiol. Endocrinol. Metab.* 283, E1113–E1122. doi: 10.1152/ajpendo.00088.2002

Barrett, J. C., Clayton, D. G., Concannon, P., Akolkar, B., Cooper, J. D., Erlich, H. A., et al. (2009). Genome-wide association study and meta-analysis find that over 40 loci affect risk of type 1 diabetes. *Nat. Genet.* 41, 703–707. doi: 10.1038/ng.381

Basile, K. J., Guy, V. C., Schwartz, S., and Grant, S. F. A. (2014). Overlap of genetic susceptibility to type 1 diabetes, type 2 diabetes, and latent autoimmune diabetes in adults. *Curr. Diab. Rep.* 14:550. doi: 10.1007/s11892-014-0550-9

Berchtold, L. A., Prause, M., Størling, J., and Mandrup-Poulsen, T. (2016). Cytokines and pancreatic β-cell apoptosis. *Adv. Clin. Chem.* 75, 99–158. doi: 10.1016/bs.acc.2016.02.001

Bergholdt, R., Brorsson, C., Lage, K., Nielsen, J. H., Brunak, S., and Pociot, F. (2009). Expression profiling of human genetic and protein interaction networks in type 1 diabetes. *PLoS ONE* 4:e6250. doi: 10.1371/journal.pone.0006250

Bergholdt, R., Størling, Z. M., Lage, K., Karlberg, E. O., Olason, P. I., Aalund, M., et al. (2007). Integrative analysis for finding genes and networks involved in diabetes and other complex diseases. *Genome Biol.* 8:R253. doi: 10.1186/gb-2007-8-11-r253

Bindea, G., Mlecnik, B., Hackl, H., Charoentong, P., Tosolini, M., Kirilovsky, A., et al. (2009). ClueGO: a Cytoscape plug-in to decipher functionally grouped gene ontology and pathway annotation networks. *Bioinformatics* 25, 1091–1093. doi: 10.1093/bioinformatics/btp101

Bolger, A. M., Lohse, M., and Usadel, B. (2014). Trimmomatic: a flexible trimmer for Illumina sequence data. *Bioinformatics* 30, 2114–2120. doi: 10.1093/bioinformatics/btu170

Bradfield, J. P., Qu, H.-Q., Wang, K., Zhang, H., Sleiman, P. M., Kim, C. E., et al. (2011). A genome-wide meta-analysis of six type 1 diabetes

cohorts identifies multiple associated loci. *PLoS Genet*. 7:e1002293. doi: 10.1371/journal.pgen.1002293

Bramswig, N. C., Everett, L. J., Schug, J., Dorrell, C., Liu, C., Luo, Y., et al. (2013). Epigenomic plasticity enables human pancreatic α to β cell reprogramming. *J. Clin. Invest*. 123, 1275–1284. doi: 10.1172/JCI66514

Chen, J., Bardes, E. E., Aronow, B. J., and Jegga, A. G. (2009). ToppGene Suite for gene list enrichment analysis and candidate gene prioritization. *Nucleic Acids Res.* 37, W305–W311. doi: 10.1093/nar/gkp427

Cnop, M., Abdulkarim, B., Bottu, G., Cunha, D. A., Igoillo-Esteve, M., Masini, M., et al. (2014). RNA sequencing identifies dysregulation of the human pancreatic islet transcriptome by the saturated fatty acid palmitate. *Diabetes* 63, 1978–1993. doi: 10.2337/db13-1383

Doncheva, N. T., Morris, J. H., Gorodkin, J., and Jensen, L. J. (2019). Cytoscape stringapp: network analysis and visualization of proteomics data. *J. Proteome Res*. 18, 623–632. doi: 10.1021/acs.jproteome.8b00702

Eizirik, D. L., Pasquali, L., and Cnop, M. (2020). Pancreatic β-cells in type 1 and type 2 diabetes mellitus: different pathways to failure. *Nat. Rev. Endocrinol*. 16, 349–362. doi: 10.1038/s41574-020-0355-7

Eizirik, D. L., Sammeth, M., Bouckenooghe, T., Bottu, G., Sisino, G., Igoillo-Esteve, M., et al. (2012). The human pancreatic islet transcriptome: expression of candidate genes for type 1 diabetes and the impact of pro-inflammatory cytokines. *PLoS Genet.* 8:e1002552. doi: 10.1371/journal.pgen.1002552

Fadista, J., Vikman, P., Laakso, E. O., Mollet, I. G., Esguerra, J. L., Taneera, J., et al. (2014). Global genomic and transcriptomic analysis of human pancreatic islets reveals novel genes influencing glucose metabolism. *Proc. Natl. Acad. Sci. U.S.A*. 111, 13924–13929. doi: 10.1073/pnas.1402665111

Fagny, M., Paulson, J. N., Kuijjer, M. L., Sonawane, A. R., Chen, C.-Y., Lopes-Ramos, C. M., et al. (2017). Exploring regulation in tissues with eQTL networks. *Proc. Natl. Acad. Sci. U.S.A*. 114, E7841–E7850. doi: 10.1073/pnas.1707375114

Hara, H., Ishihara, C., Takeuchi, A., Imanishi, T., Xue, L., Morris, S. W., et al. (2007). The adaptor protein CARD9 is essential for the activation of myeloid cells through ITAM-associated and Toll-like receptors. *Nat. Immunol*. 8, 619–629. doi: 10.1038/ni1466

Jaeger, S., and Aloy, P. (2012). From protein interaction networks to novel therapeutic strategies. *IUBMB Life* 64, 529–537. doi: 10.1002/iub.1040

Kumar, V., Wijmenga, C., and Xavier, R. J. (2014). Genetics of immune-mediated disorders: from genome-wide association to molecular mechanism. *Curr. Opin. Immunol.* 31, 51–57. doi: 10.1016/j.coi.2014.09.007

Lage, K., Karlberg, E. O., Størling, Z. M., Olason, P. I., Pedersen, A. G., Rigina, O., et al. (2007). A human phenome-interactome network of protein complexes implicated in genetic disorders. *Nat. Biotechnol*. 25, 309–316. doi: 10.1038/nbt1295

Lappalainen, T., Sammeth, M., Friedländer, M. R.,'t Hoen, P. A. C., Monlong, J., Rivas, M. A., et al. (2013). Transcriptome and genome sequencing uncovers functional variation in humans. *Nature* 501, 506–511. doi: 10.1038/nature12531

Liston, A., Todd, J. A., and Lagou, V. (2017). Beta-cell fragility as a common underlying risk factor in type 1 and type 2 diabetes. *Trends Mol Med* 23, 181–194. doi: 10.1016/j.molmed.2016.12.005

López-Avalos, M. D., Duvivier-Kali, V. F., Xu, G., Bonner-Weir, S., Sharma, A., and Weir, G. C. (2006). Evidence for a role of the ubiquitin-proteasome pathway in pancreatic islets. *Diabetes* 55, 1223–1231. doi: 10.2337/db05-0450

Mahajan, A., Taliun, D., Thurner, M., Robertson, N. R., Torres, J. M., Rayner, N. W., et al. (2018). Fine-mapping type 2 diabetes loci to single-variant resolution using high-density imputation and islet-specific epigenome maps. *Nat. Genet*. 50, 1505–1513. doi: 10.1038/s41588-018-0241-6

Mallone, R., and Eizirik, D. L. (2020). Presumption of innocence for beta cells: why are they vulnerable autoimmune targets in type 1 diabetes? *Diabetologia* 63, 1999–2006. doi: 10.1007/s00125-020-05176-7

Miguel-Escalada, I., Bonàs-Guarch, S., Cebola, I., Ponsa-Cobas, J., Mendieta-Esteban, J., Atla, G., et al. (2019). Human pancreatic islet three-dimensional chromatin architecture provides insights into the genetics of type 2 diabetes. *Nat. Genet*. 51, 1137–1148. doi: 10.1038/s41588-019-0457-0

Morris, A. P., Voight, B. F., Teslovich, T. M., Ferreira, T., Segrè, A. V., Steinthorsdottir, V., et al. (2012). Large-scale association analysis provides insights into the genetic architecture and pathophysiology of type 2 diabetes. *Nat. Genet.* 44, 981–990. doi: 10.1038/ng.2383

Mularoni, L., Ramos-Rodríguez, M., and Pasquali, L. (2017). The pancreatic islet regulome browser. *Front. Genet*. 8:13. doi: 10.3389/fgene.2017.00013

Nair, V. S., Gu, C., Janoshazi, A. K., Jessen, H. J., Wang, H., and Shears, S. B. (2018). Inositol pyrophosphate synthesis by diphosphoinositol pentakisphosphate kinase-1 is regulated by phosphatidylinositol(4,5)bisphosphate. *Biosci. Rep*. 38:BSR20171549. doi: 10.1042/BSR20171549

Neznanov, N., Neznanova, L., Angres, B., and Gudkov, A. V. (2005). Serologically defined colon cancer antigen 3 is necessary for the presentation of TNF receptor 1 on cell surface. *DNA Cell Biol*. 24, 777–785. doi: 10.1089/dna.2005.24.777

Nilsen, M. S., Jersin, R. Å., Ulvik, A., Madsen, A., McCann, A., Svensson, P.-A., et al. (2020). 3-Hydroxyisobutyrate, a strong marker of insulin resistance in type 2 diabetes and obesity that modulates white and brown adipocyte metabolism. *Diabetes* 69, 1903–1916. doi: 10.2337/db19-1174

Nogueira, T. C., Paula, F. M., Villate, O., Colli, M. L., Moura, R. F., Cunha, D. A., et al. (2013). GLIS3, a susceptibility gene for type 1 and type 2 diabetes, modulates pancreatic beta cell apoptosis via regulation of a splice variant of the BH3-only protein Bim. *PLoS Genet*. 9:e1003532. doi: 10.1371/journal.pgen.1003532

Oh, Y. S., Bae, G. D., Baek, D. J., Park, E.-Y., and Jun, H.-S. (2018). Fatty acid-induced lipotoxicity in pancreatic beta-cells during development of type 2 Diabetes. *Front. Endocrinol.* 9:384. doi: 10.3389/fendo.2018.00384

Onengut-Gumuscu, S., Chen, W.-M., Burren, O., Cooper, N. J., Quinlan, A. R., Mychaleckyj, J. C., et al. (2015). Fine mapping of type 1 diabetes susceptibility loci and evidence for colocalization of causal variants with lymphoid gene enhancers. *Nat. Genet.* 47, 381–386. doi: 10.1038/ng.3245

Oti, M., Snel, B., Huynen, M. A., and Brunner, H. G. (2006). Predicting disease genes using protein-protein interactions. *J. Med. Genet*. 43, 691–698. doi: 10.1136/jmg.2006.041376

Prentki, M., and Nolan, C. J. (2006). Islet beta cell failure in type 2 diabetes. *J. Clin. Invest*. 116, 1802–1812. doi: 10.1172/JCI29103

Quinlan, A. R., and Hall, I. M. (2010). BEDTools: a flexible suite of utilities for comparing genomic features. *Bioinformatics* 26, 841–842. doi: 10.1093/bioinformatics/btq033

Robinson, M. D., McCarthy, D. J., and Smyth, G. K. (2010). edgeR: a Bioconductor package for differential expression analysis of digital gene expression data. *Bioinformatics* 26, 139–140. doi: 10.1093/bioinformatics/btp616

Rock, K. L., York, I. A., Saric, T., and Goldberg, A. L. (2002). Protein degradation and the generation of MHC class I-presented peptides. *Adv. Immunol.* 80, 1–70. doi: 10.1016/S0065-2776(02)80012-8

Ruan, J. (2019). Structural insight of gasdermin family driving pyroptotic cell death. *Adv. Exp. Med. Biol*. 1172, 189–205. doi: 10.1007/978-981-13-9367-9_9

Slatkin, M. (2008). Linkage disequilibrium–understanding the evolutionary past and mapping the medical future. *Nat Rev Genet* 9, 477–485. doi: 10.1038/nrg2361

Smoot, M. E., Ono, K., Ruscheinski, J., Wang, P.-L., and Ideker, T. (2011). Cytoscape 2.8: new features for data integration and network visualization. *Bioinformatics* 27, 431–432. doi: 10.1093/bioinformatics/btq675

Soleimanpour, S. A., and Stoffers, D. A. (2013). The pancreatic β cell and type 1 diabetes: innocent bystander or active participant? *Trends Endocrinol. Metab*. 24, 324–331. doi: 10.1016/j.tem.2013.03.005

Stacey, D., Fauman, E. B., Ziemek, D., Sun, B. B., Harshfield, E. L., Wood, A. M., et al. (2019). ProGeM: a framework for the prioritization of candidate causal genes at molecular quantitative trait loci. *Nucleic Acids Res* 47:e3. doi: 10.1093/nar/gky837

Taylor, I. W., and Wrana, J. L. (2012). Protein interaction networks in medicine and disease. *Proteomics* 12, 1706–1716. doi: 10.1002/pmic.201100594

Trapnell, C., Pachter, L., and Salzberg, S. L. (2009). TopHat: discovering splice junctions with RNA-Seq. *Bioinformatics* 25, 1105–1111. doi: 10.1093/bioinformatics/btp120

Udler, M. S. (2019). Type 2 diabetes: multiple genes, multiple diseases. *Curr. Diab. Rep*. 19:55. doi: 10.1007/s11892-019-1169-7

van de Bunt, M., Manning Fox, J. E., Dai, X., Barrett, A., Grey, C., Li, L., et al. (2015). Transcript expression data from human islets links regulatory signals from genome-wide association studies for type 2 diabetes and glycemic traits to their downstream effectors. *PLoS Genet*. 11:e1005694. doi: 10.1371/journal.pgen.1005694

Vanunu, O., Magger, O., Ruppin, E., Shlomi, T., and Sharan, R. (2010). Associating genes and protein complexes with disease via network propagation. *PLoS Comput. Biol.* 6:e1000641. doi: 10.1371/journal.pcbi.1000641

Varshney, A., Scott, L. J., Welch, R. P., Erdos, M. R., Chines, P. S., Narisu, N., et al. (2017). Genetic regulatory signatures underlying islet gene expression and type 2 diabetes. *Proc. Natl. Acad. Sci. U.S.A.* 114, 2301–2306. doi: 10.1073/pnas.1621192114

Viñuela, A., Varshney, A., van de Bunt, M., Prasad, R. B., Asplund, O., Bennett, A., et al. (2020). Genetic variant effects on gene expression in human pancreatic islets and their implications for T2D. *Nat. Commun.* 11:4912. doi: 10.1038/s41467-020-18581-8

Wen, X., and Yang, Y. (2017). Emerging roles of GLIS3 in neonatal diabetes, type 1 and type 2 diabetes. *J. Mol. Endocrinol.* 58, R73–R85. doi: 10.1530/JME-16-0232

Westra, H.-J., and Franke, L. (2014). From genome to function by studying eQTLs. *Biochim. Biophys. Acta* 1842, 1896–1902. doi: 10.1016/j.bbadis.2014.04.024

Wysham, C., and Shubrook, J. (2020). Beta-cell failure in type 2 diabetes: mechanisms, markers, and clinical implications. *Postgrad. Med.* 132, 676–686. doi: 10.1080/00325481.2020.1771047

Conflict of Interest: The authors declare that the research was conducted in the absence of any commercial or financial relationships that could be construed as a potential conflict of interest.

frontiers in Endocrinology

ORIGINAL RESEARCH
published: 14 June 2021
doi: 10.3389/fendo.2021.624309

SNAPIN Regulates Cell Cycle Progression to Promote Pancreatic β Cell Growth

Mengxue Jiang[1], Zhijian Kuang[2], Yaohui He[2], Yin Cao[2], Tingyan Yu[1], Jidong Cheng[1], Wen Liu[2]* and Wei Wang[1]**

[1] Department of Endocrinology, Xiang'an Hospital of Xiamen University, School of Medicine, Xiamen University, Xiamen, China, [2] Fujian Provincial KeyLaboratory of Innovative Drug Target Research, School of Pharmaceutical Sciences, Xiamen University, Xiamen, China

In diabetes mellitus, death of β cell in the pancreas occurs throughout the development of the disease, with loss of insulin production. The maintenance of β cell number is essential to maintaining normoglycemia. SNAPIN has been found to regulate insulin secretion, but whether it induces β cell proliferation remains to be elucidated. This study aimed to explore the physiological roles of SNAPIN in β cell proliferation. SNAPIN expression increases with the age of mice and SNAPIN is down-regulated in diabetes. KEGG pathway and GO analysis showed that SNAPIN- interacting proteins were enriched in cell cycle regulation. B cell cycle was arrested in the S phase, and cell proliferation was inhibited after SNAPIN knockdown. The expression of CDK2, CDK4 and CCND1 proteins in the S phase of the cell cycle were reduced after SNAPIN knockdown, whereas they were increased after overexpression of SNAPIN. In addition, insulin protein and mRNA levels also increased or decreased after SNAPIN knockdown or overexpression, respectively. Conclusions: Our data indicate that SNAPIN mediates β cells proliferation and insulin secretion, and provide evidences that SNAPIN might be a pharmacotherapeutic target for diabetes mellitus.

Keywords: SNAPIN, β cells, proliferation, cell cycle, diabetes

OPEN ACCESS

Edited by:
Luiza Ghila,
University of Bergen, Norway

Reviewed by:
Karim Bouzakri,
Université de Strasbourg, France
Sarah Tersey,
University of Chicago, United States

****Correspondence:***
Jidong Cheng
jidongcheng36@hotmail.com
Wen Liu
w2liu@xmu.edu.cn
Wei Wang
wwei19742007@hotmail.com

Specialty section:
This article was submitted to Diabetes: Molecular Mechanisms, a section of the journal Frontiers in Endocrinology

Received: *31 October 2020*
Accepted: *13 May 2021*
Published: *14 June 2021*

Citation:
Jiang M, Kuang Z, He Y, Cao Y, Yu T, Cheng J, Liu W and Wang W (2021) SNAPIN Regulates Cell Cycle Progression to Promote Pancreatic β Cell Growth. Front. Endocrinol. 12:624309. doi: 10.3389/fendo.2021.624309

INTRODUCTION

Diabetes is a prevalent disease worldwide, and it has become a serious social health problem (1). It ultimately results in a deficiency of functional pancreatic β cells (2).The maintenance of β-cell number and islet mass is essential for maintaining normoglycemia (3, 4). Human β cell replication rates are very low, and the cells are only capable of replication for a brief period after birth (5).

Type 1 diabetes mellitus (T1DM) is associated with impaired β cell mass (6).The pathogenesis of type 2 diabetes is more variable, and it consists of insulin resistance and defective insulin secretion (6). More specifically, type 2 diabetes mellitus (T2DM) is associated with genetic predisposition and environmental factors, such as obesity and diet (7). During pregnancy and the early stages of diabetes, compensatory proliferation of pancreatic β cells occurs in response to changes in blood glucose (8, 9). Glucose itself is able to stimulate β cell replication (10), and several lines of evidence indicate that the terminally differentiated pancreatic β cells retain significantly proliferative capacity

in vivo (11, 12). This proliferative capacity has attracted considerable research attention in terms of developing therapeutic strategies for diabetes mellitus. Although a number of studies concerning differentiated β-like cells from embryonic stem cells or induced pluripotent (adult) stem cells are in progress, the low conversion efficiency of β cells from stem cells remains a challenge for developing cell-based therapies (13). Glucokinase signaling, carbohydrate response element-binding protein (ChREBP), nuclear factor of activated T-cells (NFAT), platelet-derived growth factor (PDGF), CDK4/6 and TCF7L2 have all been reported to stimulate human β cells proliferation (14–19). Therefore, the mechanisms regulating β cell mass have been revealed that underlie the development of T1DM and T2DM, which is important for developing novel therapeutic approaches for diabetes. This proliferative capacity has attracted considerable research attention in terms of developing therapeutic strategies for diabetes mellitus.

SNAPIN is a protein that interacts with SNARE complexes during synaptic transmission and was first reported by Jeffrey M. Ilardi in 1999 and it was first identified in neurons and located on synaptic vesicle Membranes (20). It is also a component member of the BLOC-1 complex and BORC complex (21). The BLOC-1 complex is required for normal biogenesis of lysosome-related organelles (LRO), such as platelet-dense granules and melanosomes (22), and the BORC is required for lysosome positioning in mammalian cells (21). Increasing evidence shows that SNAPIN is important for retrograde axonal transport (23), late endosomal-lysosomal trafficking (24), and glucose-induced insulin exocytosis (25). It is also believed to be involved in a variety of signal transduction and intracapsular transport/fusion functions (26).

SNAPIN is specifically expressed in the endocrine department of the pancreas. Diffuse cytoplasmic staining has been observed, and the cells were clustered into punctate structures, which co-located with insulin-secreting granules (27).The insulin secretion may be caused by the interaction between the c-terminal H2 region of SNAPIN and sn-1 region of snap-25 in the SNARE complex (27, 28), which initiates the process of insulin secretion particle targeting, tethering, initiation and membrane fusion (27, 29). These exocytosis processes are mediated by the Munc18/SNARE complex (30).

In addition, SNAPIN is a target of protein kinase A (PKA) (31), which is a critical regulator of glucose-stimulated insulin exocytosis in pancreatic β cells by promoting the interaction and assembly of insulin secretory vesicle-associated proteins Snap25 and TMEM27 (32). SNAPIN is significantly correlated with the TMEM27 gene, which codes a membrane protein cleaved and shed by pancreatic beta cells that have been proposed as a beta cell mass biomarker (33). This indicates that SNAPIN may also be a biomarker for beta cells. The function of SNAPIN in β cell growth is poorly understood, and our findings reveal that the overexpression of SNAPIN in Min6 cells can promote cell proliferation and is promising in achieving the goals of regenerative medicine for diabetes treatment.

MATERIALS AND METHODS

Cloning Procedures

Snapin full length was PCR-amplified from cDNAs and cloned at XhoI and BamHI sites of PCDH-3xFlag-3xHA-EF1-puromycin vector. Primers were designed using the Primer Premier 5.0 software (Premier Biosoft International, Palo Alto, CA).

Lentivirus Packaging and Infection

HEK293T cells were seeded in culture plates for 12 hrs and transfected with lentiviral vectors together with packaging vectors, pMDL, VSVG, and REV, at a ratio of 10:5:3:2 using Lipofectamine 2000 for 48 hrs. Virus was collected, filtered and added to β cells in the presence of 10 μg/mL polybrene (Sigma, H9268), followed by centrifugation for 30 mins at 1,500 g at 37°C. Medium was replaced 12 hrs later. The transduction efficiency was evaluated by immunoblotting analysis.

shRNA Infection

The packaging process of lentiviruses particles was the same as above. Primers sequences were in the **Table 1**. The transient transfection of plasmids into the cells was performed by using Lipofactamine 2000 reagents (Invitrogen) according to the manufacturer's instructions.

Cell Lines

The mouse pancreatic Min6, the rat pancreatic INS1 and the HEK-293T cell lines were obtained from ATCC. Min6 cells were maintained in high-glucose DMEM medium(BI) supplemented with 15% v/v fetal bovine serum (FBS, BI), 50 mmol/L 2-mercaptoethanol, and 1% penicillin-streptomycin at 37°C and 5% CO2 in a humidified atmosphere in an incubator. HEK-293T

TABLE 1 | shRNA targeting sequencing and primers for SNAPIN cloning.

Gene	Forward (*5′→ 3′*)	Reverse (*5′→ 3′*)
shRNA-1	CCGGCAACCTAGCTACAGAACTGTGCTC	AATTCAAAAACAACCTAGCTACAGAACTG
(plko.1)	GAGCACAGTTCTGTAGCTAGGTTGTTTTTG	TGCTCGAGCACAGTTCTGTAGCTAGGTTG
shRNA-2	CCGGGAACAAATTGACAACCTAGCTCTC	AATTCAAAAAAGAACAAATTGACAACCTA
(plko.1)	GAGAGCTAGGTTGTCAATTTGTTCTTTTTG	GCTCTCGAGAGCTAGGTTGTCAATTTGTTC
shRNA-1	TCGACAACCTAGCTACAGAACTGTGTTCAAG	GATC GAAAAAACAACCTAGCTACAGAACT
(psicor)	AGACACAGTTCTGTAGCTAGGTTGTTTTTTC	GTGTCTCTTGAACACAGTTCTGTAGCTAGGTTG
shRNA-2	TCGAGAACAAATTGACAACCTAGCT TTCAA	GATC GAAAAAAGAACAAATTGACAACCTA
(psicor)	GAGAAGCTAGGTTGTCAATTTGTTC TTTTTTC	GCTTCTCTTGAAAGCTAGGTTGTCAATTTGTTC
SNAPIN	AGAGAATTCGGATCCATGGCCGCGGCTGGTT	CTTCCATGGCTCGAGTTTGCTTGGAGAACCAGG
(PCDH)		

was cultured in DMEM medium supplemented with 10% v/v fetal bovine serum (FBS, BI) and 1% penicillin-streptomycin in an incubator at 37°C and 5% CO2 in a humidified atmosphere in an incubator. The rat pancreatic INS1 cells were cultured in RPMI1640 (Hyclone) containing 10% v/v fetal bovine serum (FBS, BI), 1% penicillin-streptomycin 1% glutamine, 1 mM sodium pyruvate, and 50 μM β-mercaptoethanol (sigma).

Animal

Male KM mice weighing approximately 18–25 g were purchased from the Animal Center of Xiamen University. Mice were humanely housed at 22 ± 2°C with 12-h light/dark cycles. All animals had free access to food and water. All animal studies were approved by the ethical review committee of Xiamen University and followed the regulations of the National Institutes of Health guidelines on the care and welfare of laboratory animals. Db/Db and HFD mice were obtained from Li Ming Yu lab at Xiamen University.

Immunohistochemistry

SNAPIN and insulin were analyzed by immunohistochemical staining of frozen sections from adult mouse pancreas fixed O/N in 4% PFA in PBS at RT, pH 7.4, cryoprotected in 30% sucrose in PBS, embedded in Tissue-Tek (Sakura; Værlose, Denmark), and cut into 9-μm sections on a Leica cryostat. Antigen retrieval was performed by microwave treatment for 4 mins at 600 W in 200 mL 0.01 M citrate buffer, followed by 15 mins at 250 W, and finally left to cool for 20 mins. Tissue sections were rinsed in TBS, quenched in 3% H2O2 for 5 mins, and rinsed again. Then, 10% goat serum was used for blocking for 1 hr before overnight incubation with the purified rabbit anti-SNAPIN antibodies diluted 1:200 and rabbit anti-insulin antibodies diluted 1:400 in 10% goat serum blocking buffer. Sections were washed three times for 5 mins each in TBS between incubations with primary antibody and the following incubations with biotinylated secondary antibody (Zymed; Aarhus, Denmark) for 30 mins. Bound antibodies were visualized with the DAB after a 3 mins incubation period and a subsequent wash in TBS, and the slides were counterstained with hematoxylin. Images were collected with an Olympus (Tokyo, Japan) BX51 microscope and captured using a chilled Hamamatsu C5810 CCD camera (Hamamatsu City, Japan) and Image Pro Plus 4.5 software.

Nuclear Extraction of Cells

SNAPIN was overexpressed in Min6 cells. All steps were performed on ice with ice-cold reagents in pre-centrifuge tubes. We first used ice-cold 1xPBS to wash cells and scrape cells gently into a 15mL tube. They were centrifuged for 5 mins at 500 rpm, 4°C. Then the pellet was resuspended in 1 mL ice cold BUFFER1 (1 M HEPES, PH 8.0, 1 M Mgcl2, 1 M KCl and 1 M DTT) and incubated for 15 mins on ice to allow cells to swell. Np40 was added to vortex for 10 S. Cells were centrifuged for 3 mins at maximum speed, then supernatant was aspirated with pipet, which was the cytoplasmic fraction. The pellet was resuspended in cold BUFFER2 (1 M HEPES, PH 8.0, 1 M Mgcl2, Glycerol, 1 M Nacl, 0.5M EDTA and 1 M DTT), vortexed 30 S and rotated vigorously at 4°C for 30 mins. The pellet was centrifuged for 15 mins at maximum speed, and the supernatant was removed and transferred to a fresh, chilled tube. Assay for protein concentration for immunoblotting analysis.

Confocal Immunofluorescence Microscopy

β cells were fixed in 4% paraformaldehyde for half an hour at room temperature. Then, cells were washed three times with PBS for 5 mins at room temperature. 0.1% Triton-100 was added for permeation for 10 mins, and cells were incubated in a blocking buffer (5.0% BSA in PBS) for 1 hr at room temperature. Then we performed immunostaining using the primary antibodies SNAPIN (1:50) and insulin (1:800) incubated overnight at 4°C, followed by fluorophore-conjugated secondary antibodies. The immunolabeled cells were analyzed with a Carl Zeiss LSM5 EXITER or Leica TCS SP8 STED laser scanning confocal microscope. The green channel was imaged using a 488-nm laser line (120 mW/cm2, 2.5%). The red channel was imaged using a 559-nm laser (120 mW/cm2, 2.0%). Images were acquired in 4-s intervals (frame time 3.9 s). A pulsed 375-nm laser (10 MHz) was applied for uncaging experiments in the entire field of view for eight frames (3.2 s/frame). The dual scanner setup allowed for simultaneous laser stimulation and confocal imaging. This permitted the acquisition of cellular responses that occurred during or immediately after laser stimulation.

Cell Cycle and Flow Cytometry

Min6 cells that underwent SNAPIN overexpression or knockdown were added to 1 mL cold PBS to re-suspend cell pellet and vortexed gently and an equal volume of cold absolute ethanol (store at -20°C) was added dropwisely to cell suspension in the same 15 mL tube. Then, it was stored at – 20°C for at least 2 hrs. Before staining, cells were washed twice with cold PBS and centrifuged at 4°C, 3000g, for 5mins, and supernatant was completely removed. PI staining solution was added, and it was incubated at 37°C for 15 mins. Data were acquired on a flow cytometry. Then, we used PI to stain Min6 cells that transfected shRNA for 15 mins. Cells or nuclei were filtered through 40-mm sieves, and flow cytometry was performed on a 4-laser, LSRII (BD Biosciences). Data were analyzed with FlowJo software.

Cell Proliferation Assay

Min6 cells that underwent SNAPIN overexpression or knockdown were seeded into a 96-well plate and were incubated with the medium for 24 hrs. The cell viability was measured by MTS analysis using CellTiter 96 AQueous One Solution Cell Proliferation Assay (Promega). For the measurement of cell viability, 500μL of medium/MTS solution mix (20μL MTS/mL medium) was added per well. The plate was incubated at 37°C for 1 hr. Then, the absorbance at 490nm was measured using an automatic microplate reader. Cell viability was measured every 24 hrs for consecutive four days.

Ethynyldeoxyuridine (EdU) Analysis

Proliferating cells were assessed using a Click-iT™ EdU Proliferation Assay (Invitrogen) following the manufacturer's protocol. Briefly, Min6 cells that underwent knockdown were inoculated seeded into a 96-well plate (5000 cells/well). Then, 10 um EdU labeling media was added and cells were incubated for 24hrs. 50 μL Click-iT™ EdU fixative was added to each well for 5 mins and 50 μL 1X Click-iT™ reaction cocktail to each well for 30 mins. Then, 1.5% BSA was added to block cells for 5 mins. After washing several times, 100 μL Amplex™ UltraRed reaction mixture was added for 15 mins and followed by incubated with 10 μL Amplex™ UltraRed stop reagent. Fluorescence was measured with excitation maximum of 568 nm and emission maximum of 585 nm.

Annexin V-FITC/Propidium Iodide (PI) Staining

Apoptosis of β cells were measured by Annexin V/FITC(BD Bioscience)according to the manufacturer's protocol. Cells were harvested and resuspended in 100 μL binding buffer, followed by staining with 5 μL FITC– conjugated Annexin V and 5 μL PI in the dark for 15 mins at room temperature. Then, 00 μL binding buffer was added to resuspend cells. Cells were detected by flow cytometry (BD Biosciences). In the early stage of apoptosis, cell membranes were stained with FITC– conjugated Annexin V, whereas nuclei were not stained with PI. In the late stage of apoptosis, cells were stained with both FITC– conjugated Annexin V and PI. The results were analyzed by FlowJo vX.0.7 (FlowJo LLC).

Insulin Secretion in bb Cells

In order to test the secretory response to glucose, Min6 cells were cultured on glass coverslips for 24 hrs. After 24 hrs of plating, Min6 cells were incubated for 1 hr at 37°C in KIRH BUFFER (136 mmol/L NaCl, 4.7 mmol/L potassium chloride (KCl), 1.2 mmol/L KH2PO4, 1.2 mmol/L MgSO4, 5 mmol/L NaHCO3, 1 mmol/L CaCl2, 10 mmol/L HEPES, and 0.5% BSA, pH 7.4) supplemented with either 2.8 mmol/L or 16.7 mmol/L glucose. Insulin was detected by ELISA (wide range mouse insulin immunoassay kit, catalogue number: 32100). 5 μL of standard and sample and 100 μL detection antibody was added to each well followed by incubation at room temperature for 90 mins. After washing for several times, 100 μL of substrate solution was added to each well at room temperature for 15 mins followed by adding 100 μL of stop solution and detecting at 450 nm immediately. Cells were fixed with 4% paraformaldehyde for 20 mins, and fixed cells were permeabilized with 0.5% Triton-100 for 15 mins, treated with 0.1% Tween 20 in phosphate buffered saline for 5 mins and blocked with 5% FBS for 40 mins before incubation with the primary antibody against SNAPIN (1:50; proteintech) and insulin (1:800; Cell Signaling Technology) overnight at 4°C, followed by incubation with rhodamine-labeled anti-mouse IgG secondary antibody (1:200; Chemicon, Temecula, USA) for 1 hr at room temperature. Nuclear localization was counterstained with DAPI.

Tissues and Cells RNA Isolation

Mouse tissues were isolated from 5 days, 2, 3, 4 and 8 weeks mice. Total RNA was then extracted using TRIzol reagent (Gibco-BRL) and following the manufacturer's instructions.

Real-Time Reverse Transcriptase-Polymerase Chain Reaction

Briefly, total RNA was extracted using the TRIzol reagent (Invitrogen) and complementary DNA was generated using the PrimeScript™ reverse transcript reagent Kit (Takara, Tokyo, Japan). From 1 μg RNA aliquots, we synthesized cDNA using random hexamers or oligo (dT), and reverse transcriptase, following the manufacturer's protocol. The reactions were run for 40 cycles at 30°C for 10 mins, 42°C for 20 mins, 99°C for 5 mins, and 4°C for 5 mins using real-time PCR detection system (Bio-Rad, Hercules, USA) according to the manufacturer's instruction and verified on gel. Real-time reverse transcriptase-polymerase chain reactions (real-time RT-PCRs) were performed using the Power SYBR Green PCR Master Mix (Roche) and a 7500 Real-Time PCR Detection System (Applied Biosystems). Actin was used as an internal control. Primer sequences are listed in **Table 2**. All experiments were performed in triplicate, and the data are shown as mean ± SD.

Western Blotting

Cells were seeded at the appropriate density, and total protein of cells or tissues were using cell lysis buffer containing (50 mM Tris-HCl (pH 7.4), 150 mM NaCl, 1 mM EDTA and 1% Triton X-100)containing protease inhibitor cocktail (sigma, P2714-1BTL) on ice for 30 mins followed by centrifugation. Protein concentrations was determined with a Bicinchoninic Acid Assay Kit (Beyotime Biotechnology). Protein (20 μg/lane) was separated by 10–15% sodium dodecyl sulfate-polyacrylamide gel electrophoresis (SDS-PAGE) and transferred onto polyvinylidene fluoride membranes (Millipore, Billerica, MA). The membranes were blocked for 1.5 hrs in Tris-buffered saline and Tween 20 (TBST, pH 7.6) containing 5% non-fat milk powder at room temperature and incubated with primary

TABLE 2 | Real-time PCR primer sequences.

Gene	Forward (*5'→ 3'*)	Reverse (*5'→ 3'*)
SNAPIN	AGCTACAGAACTGTGCCGGATCAA	GCTTGGAGAACCAGGAGGGTAAA
Insulin1	AGGACCCACAAGTGGAACAA	GCTGGTAGAGGGAGCAGATG
Insulin2	GGACCCACAAGTGGAACAAC	GTGCAGCACTGATCCACAAT
CDK2	AATGCAGAGGGGTCCATCAA	GGAGTAGTACTTGCAGCCCA
Actin	TGTTACCAACTGGGACGACA	GGGGTGTTGAAGGTCTCAAA

antibodies at 4°C overnight. The membranes were then washed three times with TBST for 15 mins each and incubated with anti-rabbit secondary antibodies (1:5,000 in TBST) conjugated to HRP for 1 hr at room temperature. The blots were then developed in the dark by using an ECL detection kit (Proteintech). Band intensities were quantified by ImageJ 1.45 software (NIH, USA). Antibodies are listed in **Table 3**.

Immunoprecipitation Assay

Two days after transfection, the cells were lysed in lysis buffer (1% Triton X-100, 50 mM Tris–HCl (pH 7.4), 150 mM NaCl, 1 mM EDTA, 1% sodium deoxychlate) with protease inhibitor cocktails. Pre-washed Flag-beads were added. After immunoprecipitation, Flag-Beads were washed 4-5 times with lysis buffer (containing protease inhibitor). Flag peptides were added to elute Flag-tagged proteins. 4xSDS loading buffer was added into the supernatant after enrichment and the sample was boiled in the metal bath for 10min before being The elutes were then subjected to SDS–PAGE and Western blotting analysis.

LC–MS Analysis and Database Search

Each immunoprecipitation (IP) was carried out in triplicate. Min6 cells expressing Flag-SNAPIN or PCDH vector were grown on 15 cm plates until 90% confluent and then subjected to IP. The elutes after IP were firstly reduced in 20 mM dithiothreitol (DTT) (Sigma) at 95 °C for 5 mins, and subsequently alkylated in 50 mM iodoacetamide (IAA) (Sigma) for 30 mins in the dark at room temperature. After alkylation, the samples were transferred to a 10 kD centrifugal spin filter (Millipore) and sequentially washed with 200 mL of 8 M urea for three times and 200 mL of 50 mM ammonium bicarbonate for two times by centrifugation at 14,000 g. Next, tryptic digestion was performed by adding trypsin (Promega) at 1:50 (enzyme/substrate, m/m) in 200 mL of 50 mM ammonium bicarbonate at 37°C for 16 hrs. Peptides were recovered by transfer-ring the filter to a new collection tube and spinning at 14,000 g. To increase the yield of peptides, the filter was washed twice with 100 mL of 50 mM ammonium bicarbonate. Peptides were desalted by StageTips (34, 35).

GO and KEGG pathway analysis Gene Ontology (GO) is an ontology widely used in the field of bioinformatics for annotating large scale genes and gene products (36). KEGG is a practical database resource for genome sequencing and polymer experiment technology. It is generated by molecular- level information, especially macromolecular datasets, which can be used to predict which by pathways of a particular gene is enriched (37). It covers information resources such as diseases and pathways, GO analysis and KEGG analysis were performed by DAVID tools (https://david.ncifcrf.gov/). $P < 0.01$ was considered statistically significant.

TABLE 3 | Antibodies used in Western blotting, immunohistochemistry and immunofluorescence.

Antibody	Dilution	Host Species	Supplier
β-Actin	1:1000	Rabbit	proteintech
Snapin	1:1000	Rabbit	proteintech
Snapin	1:1000	Rabbit	Synaptic System
Insulin	1:800	mouse	Cell Signaling
Insulin	1:400	Rabbit	proteintech
Flag	1:1000	mouse	Sigma
HA	1:1000	Rabbit	Santa Cruz
CDK2	1:1000	Rabbit	proteintech
CDK4	1:1000	Rabbit	proteintech
CCND1	1:1000	Rabbit	proteintech
PARP	1:1000	Rabbit	Cell Signaling
HSP60	1:1000	Rabbit	proteintech
BLOC1S1	1:1000	Rabbit	ABclonal
HRP-anti-rabbit IgG	1:1000	Rabbit	Beyotime
CY3-anti-rabbit IgG	1:200	Rabbit	Beyotime
CY3-anti-mouse IgG	1:200	mouse	Beyotime
FITC-anti-mouse IgG	1:200	mouse	Beyotime

Statistical Analysis

Group data are displayed as means ± standard errors of the mean (SEMs). Differences between groups were calculated by Student's unpaired two-tailed t-tests or one-way analyses of variance (ANOVAs) followed by Tukey's *post hoc* tests. $P < 0.05$ was considered statistically significant.

RESULTS

SNAPIN Expression Increases With the Age of Mice and SNAPIN Is Down-Regulated in Diabetic Mice

Tissues of six mice of different ages were isolated, followed by protein extraction to detect the expression of SNAPIN (**Figures 1A, B**). We found that the expression of SNAPIN was relatively higher in liver (38), kidney (39) and pancreas (25). The expression level of SNAPIN in mouse pancreas also closely increased with the age of mice (**Figures 1C, D**).

We next investigate whether SNAPIN expression has discrepancy in its involvement with healthy and diabetic mice. Hematoxylin staining was performed to detect insulin and SNAPIN expression in wild-type and diabetic mice. Decreased β cell masses and decreased SNAPIN were observed in diabetic mice compared with WT controls. Diabetic mice had much less SNAPIN compared with WT controls (**Figure 1E**), tending to a 40% reduction. We also investigated SNAPIN expression by immunostaining, and diabetes mice had much less SNAPIN compared with WT controls (**Figures 1F, G**).

SNAPIN Is Mostly Located in the Cytoplasm, and Is Co-Located With Insulin Secretory Granules

SNAPIN was originally reported in the neurons and exclusively on the synaptic vesicle membrane (40). Later, extrarenal expression has been reported in several tissues and cell lines, including pancreatic β cells, INS1 cells, Min6 cells, brain, etc. In 3T3-L1 adipocytes, biochemical and immunofluorescence microscopy analysis showed that it locates in both diffuse cytosolic and perinuclear membrane compartments (41). We found that SNAPIN was mostly located in the cytoplasm, and we found that SNAPIN presents some diffuse cytosolic staining and is

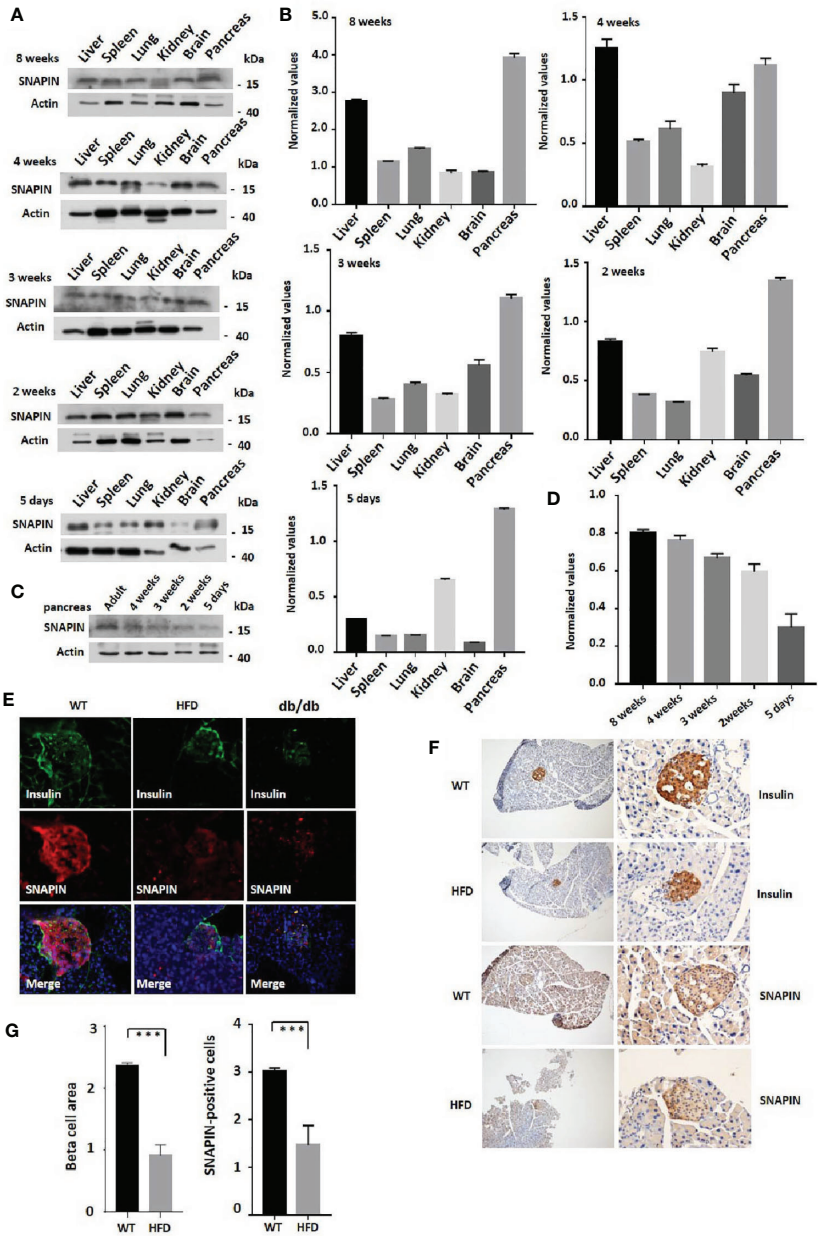

FIGURE 1 | Expression of SNAPIN in mouse tissues. **(A)** SNAPIN expression was calculated by Western blot. SNAPIN was comparable for 5 days to 8 weeks mouse. **(B)** Normalized histograms of snapin protein against actin by using imaging software. **(C)** The expression level of SNAPIN in mouse pancreas also closely increased with the age of mice. **(D)** Normalized histograms of snapin protein against actin by using imaging software. **(E)** Representative immunofluorescence images of mouse healthy and pre-diabetic pancreases using antibodies against SNAPIN and insulin. The insulin and SNAPIN of HFD mice and db/db mice were significantly lower than those of wildtype mice. **(F)** Pancreatic β cell size and SNAPIN expression were calculated from the immunohistochemistry (IHC) sections processed for insulin and SNAPIN by capturing bright field images (Leica CTR 4000 series). The β cell size of high-fat diet (HFD) mice were significantly smaller than that of wildtype mice, and SNAPIN expression of HFD mice were significantly lower than that of wildtype mice. Scale bar: 100μm (left) and 50 μm (right). Values are expressed as means ± S.E.M. P<0.001 versus control. **(G)** Statistics for β cell size and SNAPIN expression. ***P < 0.001.

clustered into punctate structures within the cell body of in rat INS1 cells and Min6 cells. Furthermore, the punctate staining pattern was similar to that seen for insulin-containing secretory granules. The two fields were then superimposed (**Figure 2A**). And fluorescence co-localization analysis showed that SNAPIN and insulin had a co-localization relationship by ImageJ (**Figure 2B**). Data analysis confirmed that there was significant co-fluorescence between the punctate insulin and SNAPIN signals, which indicates the co-localization of SNAPIN and insulin secretory granules. We also use a wildtype Min6 cell to detect

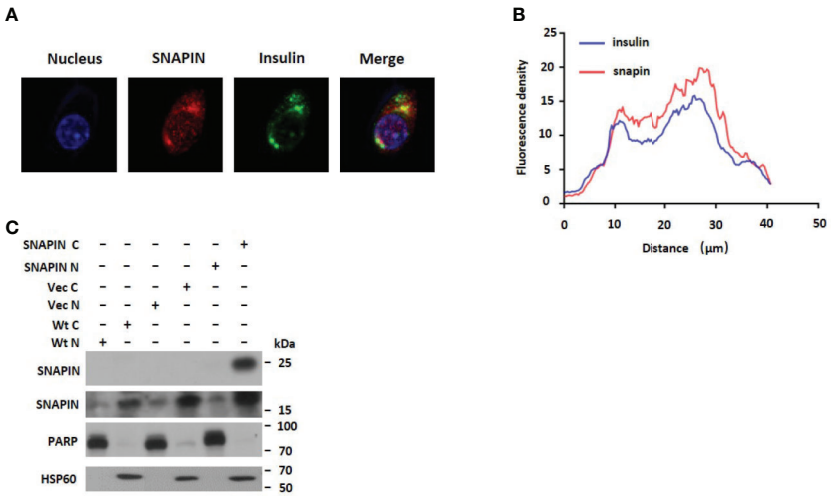

FIGURE 2 | Subcellular localization of SNAPIN. **(A)**. Immunofluorescence was performed to measure the subcellular localization of SNAPIN. SNAPIN was visualized in INS-1 and Min6 cells using anti- SNAPIN antibody in conjunction with anti-rabbit FITC, whereas insulin was visualized using anti-insulin and red-conjugated goat anti-mouse. Slides were mounted and fluorescence viewed under a laser scanning confocal microscope equipped with a 488 nm laser excitation filter for FITC. The nuclei were labeled with DAPI (blue) (4′,6-diamidino-2-phenylindole), and SNAPIN protein was labeled with the Alesa Fluor 643 (red). Scale bar, 2 mm. **(B)** The fluorescence distribution of SNAPIN and insulin was analyzed by ImageJ. **(C)** Nucleocytoplasmic separation was performed to measure the Subcellular localization of SNAPIN. PARP is the nuclear marker, and HSP60 is the cytoplasmic marker. SNAPIN is mainly located in the cytoplasm.

the subcellular localization of SNAPIN and found that nucleocytoplasmic separation showed that SNAPIN was predominantly located in cytoplasm (**Figure 2C**).

SNAPIN and Its Interacting Protein-Enriched Cell Cycle

SNAPIN is mostly located in the cytoplasm, and to elucidate the role of SNAPIN in the development and progression of diabetes, a schematic outline of the immunoprecipitation mass spectrometry procedure was used in this study. Flag- SNAPIN or empty vector was overexpressed in Min6 cells and immunoprecipitated using whole cell lysates in triplicates. Min6 cells expressing empty vector alone served as negative controls. To identify putative biological processes associated with SNAPIN interacting proteins, we performed enrichment analysis in the Gene Ontology (GO) domain "Biological Process" (**Figure 3A**) and KEGG pathway (**Figure 3B**). This analysis identified cell cycle which related to cell growth.

Immunoblot analysis of the immunoprecipitated fractions showed that tagged- SNAPIN was enriched in the pulldown (**Figure 3C**). In contrast, no SNAPIN was detected in the pulldown in the vector control. Some papers have previously demonstrated that SNAPIN associates with Bloc1s1 by immunoblot (42). As expected, Bloc1s1 was detected in the current IP-MS study (**Figure 3C**). These data demonstrate that tagged- SNAPIN can be efficiently and specifically immunoprecipitated from cell extracts.

Proteins significantly interacting with SNAPIN were classified into different protein complexes. The results of this analysis identified twenty predominant complexes:(1) Nop56p-associated pre-rRNA complex, (2) Large Drosha complex, (3) CCT complex (chaperonin containing TCP1 complex), (4) SNW1 complex, (5) PA700 complex, (6) C complex spliceosome, (7) CDC5L complex, (8) TNF-alpha/NF-Kappa B signaling complex and other known complexes: BLOC1 (biogenesis of lysosome-related organelles complex1) complex and Arp2/3 protein complex (**Figure 3D**).

Our experiments showed that SNAPIN could affect cell proliferation and cell cycle, and we analyzed the cell cycle pathway, which are closely related to cell growth (**Figure 3E**).

SNAPIN Overexpression Induces Proliferation of β Cells

SNAPIN and its interacting proteins may enrich the cell cycle pathway, which could lead to increased cellular proliferation. To directly evaluate the role of SNAPIN in β cell proliferation, we transfected Min6 cells with lentivirus for 24 hrs. MTS analysis was applied to detect the cell proliferation. We observed a significant increase in SNAPIN protein abundance in lentivirus-treated Min6 cells by Western blot analysis (**Figure 4A**). SNAPIN overexpression induced β cell proliferation (**Figure 4B**) and increased Min6 cells clone formation compared to that control group (**Figure 4C**). **Figure 4D** shows the clone statistics.

Our MS data showed an enrichment in SNAPIN and its interacting proteins that are known to regulate the cell cycle. To provide direct evidence that SNAPIN regulates the cell cycle, we transfected Min6 cells with lentivirus to quantified cellular DNA content by flow cytometry (**Figure 4E**). Compared to the control group, SNAPIN overexpression resulted in an increase in the population of cells in the S phase from 6.85% to 27.13%. We evaluated β cells for expression of CDK2, CDK4 and CCND1, which mark the S phase of the cell cycle. CDK2, CDK4 and

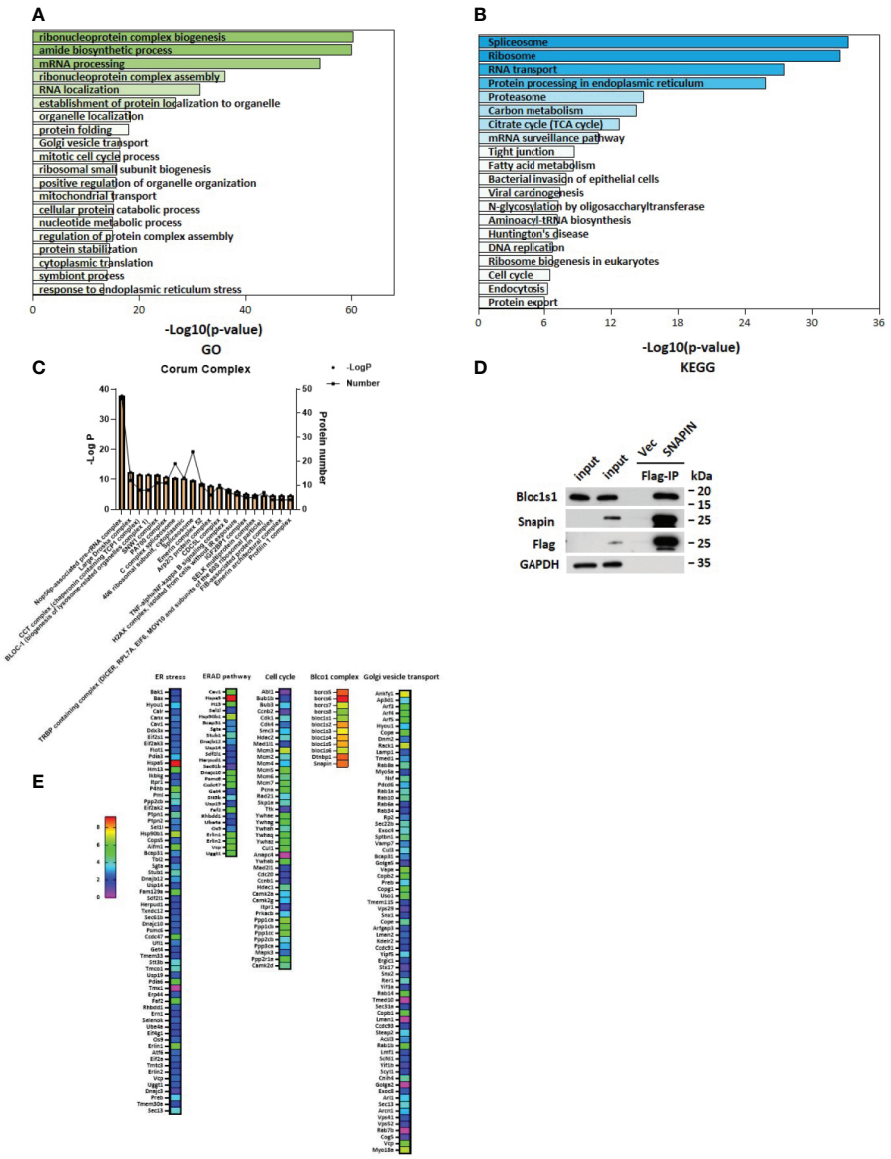

FIGURE 3 | Outputs of proteomic analysis for SNAPIN -altered proteins. Identity of the SNAPIN -binding proteins. Experimental workflow of the identification of the SNAPIN -interacting proteins. Min6 cells were transduced with SNAPIN with specific sequences containing the 3xFlag tag. The resulting cell lysate was reacted with flag beads. The bound fraction was eluted and submitted for shotgun LC–MS/MS. **(A, B)** Pathways were enriched for common genes by employing the Database for Annotation, Visualization and Integrated Discovery (DAVID) ver. 6.8, KEGG pathway and GO pathway that represent functional classes of SNAPIN interacting proteins. **(C)** Proteins significantly interacting with SNAPIN were classified into different protein complexes. **(D)** IP was performed to measure the efficiency of Flag pulldown. BLOCS1 was the positive control. **(E)** The SNAPIN - binding proteins were identified by Flag Immunoprecipitation pulldown. The heat map shows the score sequest HT, where the intensities in blue indicate the relative abundance of the protein in the sample.

CCND1 expressions were all upregulated (**Figures 4F, G**). Our results suggested that SNAPIN overexpression could promote the cell proliferation of β cells.

SNAPIN Knockdown Inhibit Proliferation of β Cells

Lentivirus shRNA to silence SNAPIN and transfected Min6 cells with lentivirus for 24 hrs. MTS analysis was applied to detect the cell variety. We observed a significant decrease in SNAPIN protein abundance in lentivirus-treated Min6 cells by Western blot analysis (**Figure 5A**). SNAPIN knockdown inhibited β cells proliferation (**Figure 5B**) and inhibited Min6 cells clone formation compared to that of the control group (**Figure 5E**). **Figure 5F** shows the clone statistics. Cell photographic also showed that SNAPIN knockdown could cause Min6 cell death (**Figure 5G**).

We also quantified cellular DNA content by flow cytometry (**Figure 5H**). Compared to control group, SNAPIN knockdown

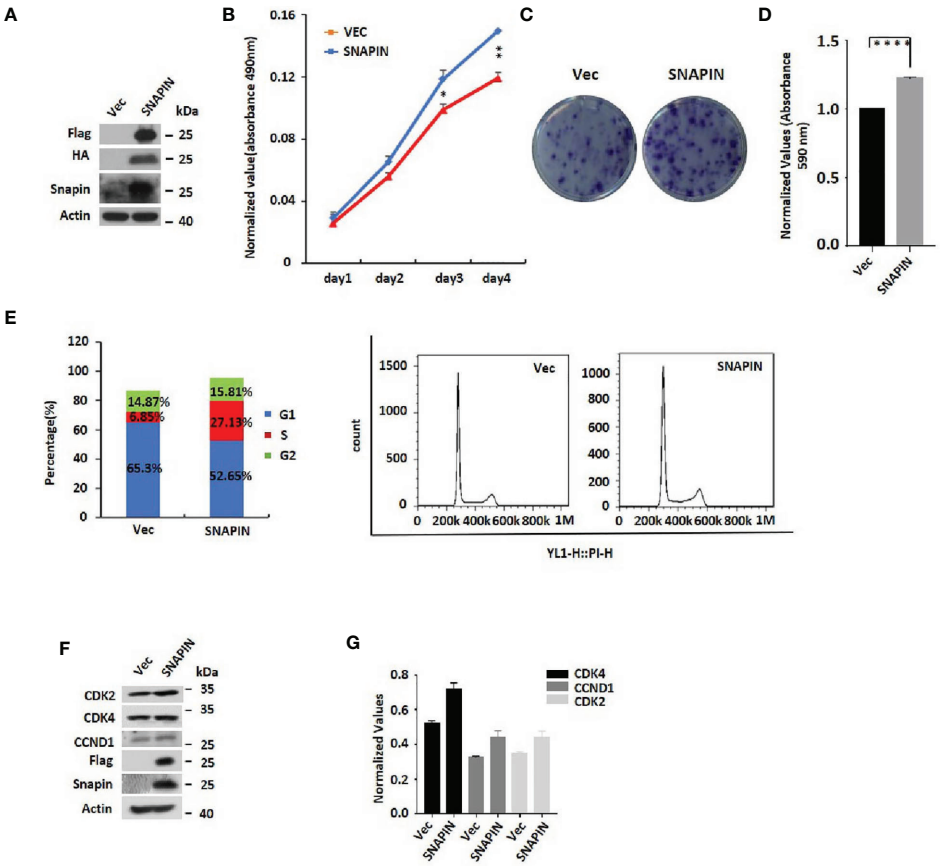

FIGURE 4 | SNAPIN overexpression induces proliferation of β cells. Min6 cells were transduced with non-specific and SNAPIN specific Sequences. **(A)** Min6 cells were treated with lentivirus. A significant increase in SNAPIN protein by Western blot analysis. **(B)** MTS analysis illustrated the proliferation of Min6 cells induced after SNAPIN overexpression. **(C, D)** Clone formation showed that SNAPIN overexpression induced the proliferation of β cells. **(E)** The cells were stained with PI staining. Adherent cells were collected, and cell cycle analysis was done by flow cytometry. SNAPIN overexpression increased the population of cells in the S phase. **(F)** The protein expression levels of CyclinD1, CDK2 and CDK4 were checked by Western blot with indicated antibodies. **(G)** Normalized histograms of snapin protein against actin by using imaging software. *P < 0.05, **P < 0.01, ****P < 0.0001.

resulted in a decrease in the population of cells in the S phase from 47% to 40% and 42.25%. We evaluated β cells for expression of CDK2, CDK4 and CCND1, which marks the G1/S phase of the cell cycle. CDK2, CDK4 and CCND1 expressions were downregulated (**Figures 5I, J**). Click-iT™ EdU Proliferation Assay measure β cells proliferation (**Figure 5C**). statistics for fluorescence intensity in 585 nm (**Figure 5D**). Our results suggested that SNAPIN knockdown could inhibit the proliferation of β cells.

SNAPIN Knockdown Induce β Cells Apoptosis

Apoptosis is a specific mode of programmed cell death (43). Inappropriate apoptosis can cause a variety of diseases, so the regulation of apoptosis has great therapeutic potential (44). As a substrate of Caspase 3, PARP cleaves during the initiation of apoptosis program (45). So Cleaved PARP is a signature protein for apoptosis. In order to study the effect of SNAPIN on apoptosis of β cells, we used shRNA to interfere with SNAPIN expression and detected cell apoptosis based on Annexin V-FITC/PI staining. The proportion of apoptotic cells in the Control group was 10.32%, and the proportion of apoptotic cells after SNAPIN interference was 50.1% (**Figures 6A, B**). This result indicated that interference with SNAPIN expression induced apoptosis of cells. we also analyzed the expression level of PARP and SNAPIN (**Figures 6C, D**).

SNAPIN Knockdown Inhibit Insulin Protein/mRNA Level

In order to evaluate the effect of SNAPIN on insulin mRNA level, we used shRNA to silence SNAPIN and transfected Min6 cells with lentivirus for 24 hrs. We observed a significant decrease in SNAPIN mRNA abundance in lentivirus treated Min6 cells by QPCR analysis (**Figure 7A**). Insulin- obtained INS1 and INS2 were inhibited after SNAPIN knockdown (**Figures 7B, C**). We also transfected Min6 cells with lentivirus to quantify insulin mRNA level.

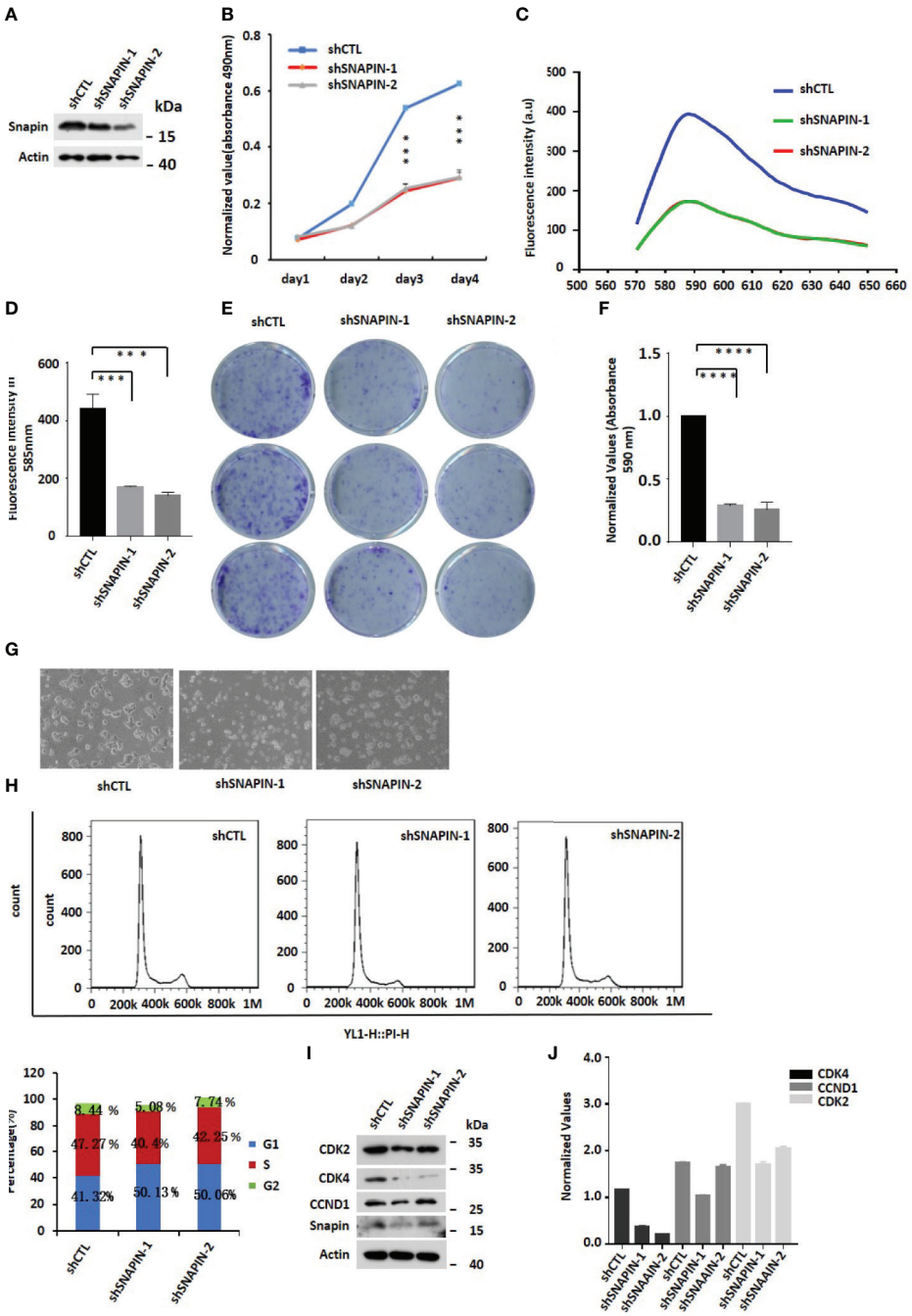

FIGURE 5 | SNAPIN knockdown inhibit proliferation of β cells. **(A)** Mouse Min6 cells were transduced with lentivirus expressing shRNA and non-specific sequences. A significant decrease in SNAPIN protein by Western blot analysis. **(B)** MTS analysis illustrated that the proliferation of Min6 cells were inhibited after SNAPIN knockdown. **(C)** Click-iT^{TM} EdU Proliferation Assay illustrated that the proliferation of Min6 cells were inhibited after SNAPIN knockdown. **(D)** Statistic for fluorescence intensity in 585nm. **(E)** Clone formation showed that SNAPIN knockdown inhibited the proliferation of β cells. **(F)** Statistic for clone formation. **(G)** Cell photography indicates Min6 cells suffer death with SNAPIN knockdown. **(H)** The cells were stained with PI staining. Adherent cells were collected, and cell cycle analysis was done by flow cytometry. SNAPIN knockdown resulted in a decrease in the population of cells in S phase. **(I)** The protein expression levels of CyclinD1, CDK2 and CDK4 were checked by Western blot with indicated antibodies. **(J)** Normalized histograms of snapin protein against actin by using imaging software. *P < 0.05, **P < 0.01, *** P< 0.001, ****P < 0.0001.

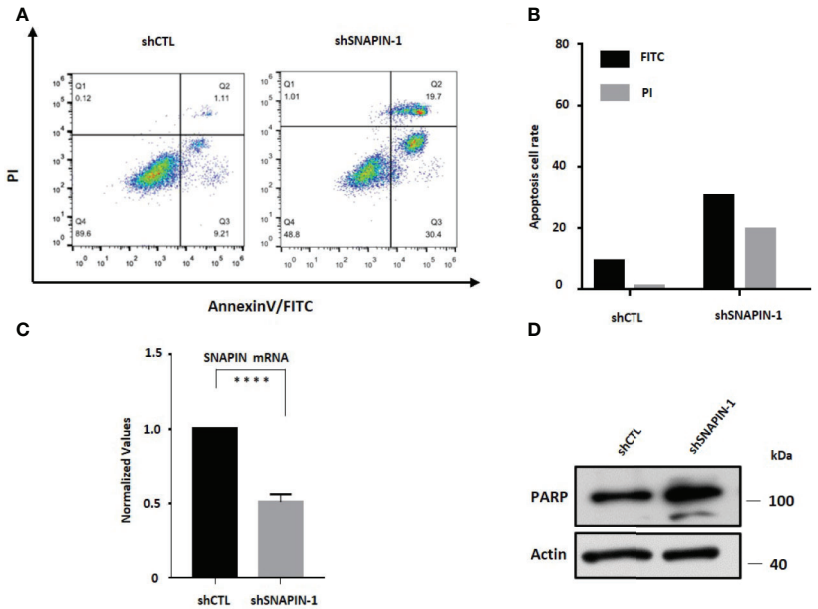

FIGURE 6 | SNAPIN knockdown induce apoptosis of β cells. **(A)** apoptosis assay indicate that the apoptosis of β cells were induced after SNAPIN knockdown. **(B)** statistic for FITC and PI of apoptotic β cells. **(C)** Mouse Min6 cells were transduced with lentivirus expressing shRNA and non-specific sequences. A significant decrease in SNAPIN expression. **(D)** SNAPIN knockdown induced PARP cleavage of apoptotic marker protein. ****P < 0.0001.

We observed an increase in SNAPIN mRNA abundance in lentivirus treated Min6 cells by QPCR analysis (**Figure 7D**), and insulin only showed a slight increase (**Figures 7E, F**).

Min6 cells were treated with two shRNA to interfere SNAPIN. Glucose-induced insulin secretion was measured by ELISA. Min6 cells were stimulated with 2.8mmol/L and 16.7mmol/L glucose solutions for 2 hr, and the supernatant was collected to detect insulin content. After SNAPIN interference, insulin expression was reduced (**Figure 7G**). Then, we treated INS1 cells with two shRNA to interfere SNAPIN and detected insulin by immunofluorescence. SNAPIN was visualized by GFP, and insulin was visualized using anti-insulin antibody in conjunction with goat anti-mouse cy3. Insulin secretion decreased when SNAPIN was knocked down (**Figure 7H**).

DISCUSSION

Diabetes mellitus is a very common metabolic disease, its acute and chronic complications have serious impacts on human health (46). Pancreatic β cells are the only cells that can produce insulin in the human body. Once the β cells are dysfunctional, the body cannot produce enough insulin to maintain the stability of blood glucose, and long-term hyperglycemia of the body will cause multiple organ dysfunction (47). The replication rate of β cells is very low, and scientists have attempted to induce the differentiation of β cells from progenitor cells or stem cells or from other islet cell lines, but the clinical progress is still very difficult. Many scientists are trying to identify small molecules or biomacromolecules that can induce β cells to self-replicate. However, there is no effective drug that can effectively induce β cells to replicate. Therefore, it is significant to find new therapeutic targets and new therapeutic methods for diabetes.

SNAPIN was originally reported to be a SNAP25-related protein that mainly interacts with SNARE complexes for vesicle transport to regulate insulin secretion (29). We compared the amino acid sequences of SNAPIN in humans, mice, and rats, and SNAPIN is highly conserved and homologous, suggesting that SNAPIN performs highly consistent biological functions in humans, mice and rats. We extracted various tissues of mice at different ages. SNAPIN was abundant in the pancreas, and its expression increases with the aging of mice, which may indicate that SNAPIN is related to the development of the pancreas. However, more experiments are needed to confirm this, we can extract the islets of mice of different gestational ages to interfere with or overexpress SNAPIN to explore the function of SNAPIN in the development of islets. SNAPIN is significantly correlated with the TMEM27 gene, which encodes a membrane protein that is cleaved and shed by pancreatic β cells, and this protein has been proposed as a biomarker for β cell quality (33). This suggests SNAPIN may also be a biomarker for β cells.

Furthermore, we used SNAPIN as bait to find SNAPIN interacting proteins and various protein complexes were enriched, including BLOC1, BORC, Arp2/3, Dynactin Complex.Snap23, Snap47 and other SNAP family members reported in the paper that interact with SNAPIN. We verify our results by using Bloc1s1 as a positive control. The proteins with high ratings were analyzed by Metascope and further enriched by BO/KEGG pathway. We enriched BLOC1/BORC,

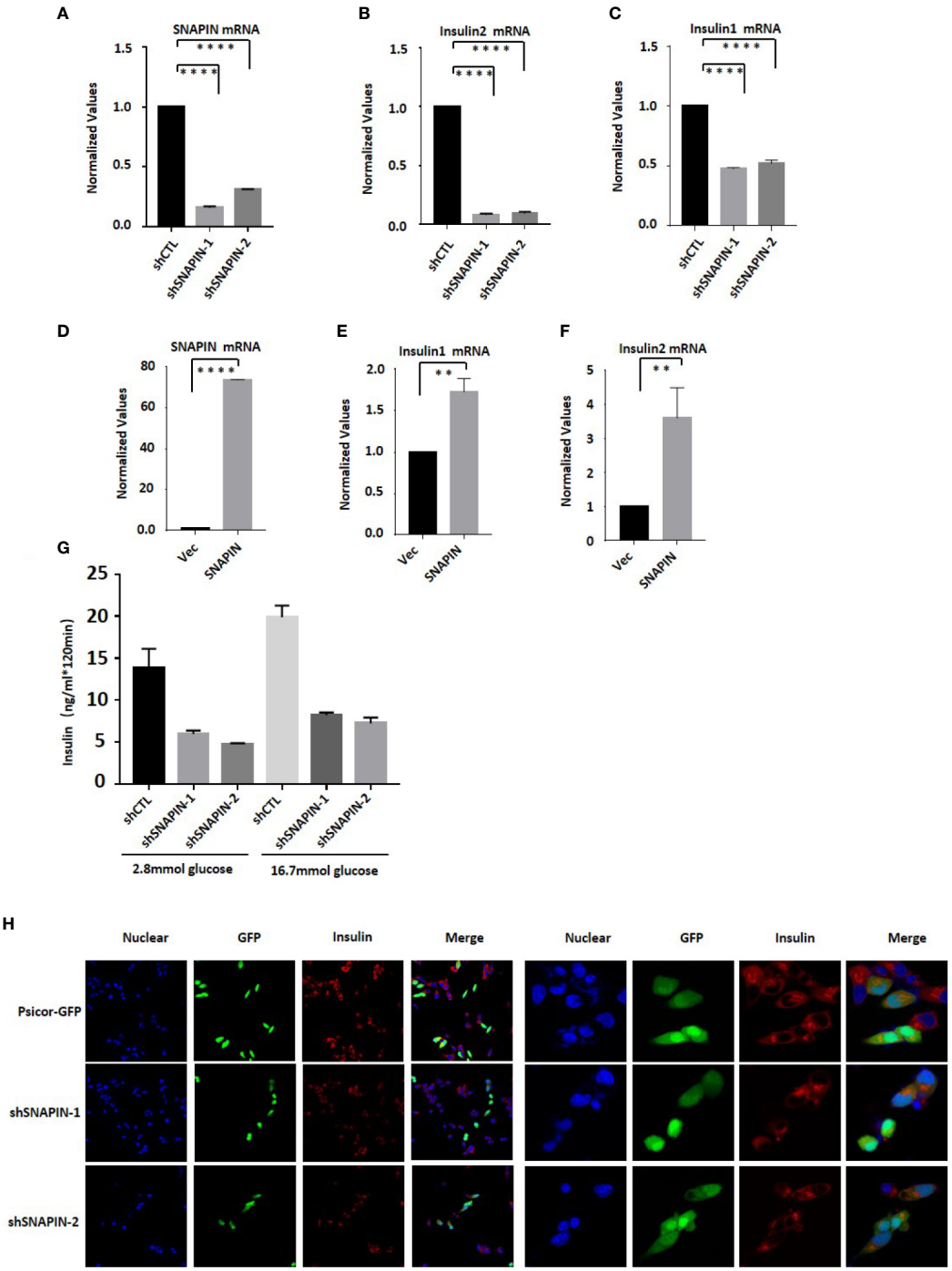

FIGURE 7 | SNAPIN affects insulin mRNA and protein levels. **(A)** SNAPIN knockdown efficiency in β cells. **(B, C)** SNAPIN knockdown inhibit Insulin mRNA expression in β cells. **(D)** SNAPIN overexpression efficiency in β cells. **(E, F)** SNAPIN overexpression increased Insulin mRNA expression in β cells. QPCR was performed to measure the mRNA expression of insulin. Data are shown as the mean ± SD, n = 3. **(G)** SNAPIN knockdown inhibits insulin protein expression in INS1 cells. Glucose-induced insulin secretion measured by ELISA. **(H)** SNAPIN knockdown inhibits insulin protein expression in Min6 cells. INS1 cells were transduced with lentivirus expressing shRNA which obtained GFP. The vector was Psicor-GFP. The insulin protein expression levels were measured by immunofluorescence. The nuclei were labeled with DAPI (blue) (4′,6-diamidino-2-phenylindole), insulin protein was labeled with the Alesa Fluor 643 (red) and shSNAPIN was labeled with the GFP (yellowish-green). **P < 0.01, ****P < 0.0001.

which is a SNAPIN family member, and cell cycle and protein processing in the endoplasmic reticulum etc, can further explore the mechanism. According to KEGG enrichment results, we detected changes in major proteins in the UPR pathway. Our experiment results show that SNAPIN affects the Min6 cell cycle and the level of cell cycle markers. We will continue to explore whether SNAPIN regulates β cell proliferation by interacting with cell cycle-related protein in follow-up work.

As the only glucose-lowering hormone in the body, insulin can also promote body growth (48). Our study shows that SNAPIN can promote insulin secretion, which is consistent with other reports (25). We found that SNAPIN promotes β cell growth, and it remains to be seen whether this pro-growth effect is due to SNAPIN or due to the increase in insulin secretion.

In conclusion, we showed that overexpression of SNAPIN is sufficient to induce β cell proliferation. We can therefore try to design agonists for the SNAPIN sequence as a new treatment for diabetes. This is a huge challenge but could provide new strategies for treating diabetes. Taking a broader perspective, SNAPIN overexpression promoting cell proliferation may open a new avenue of research in the field of tissue regeneration.

Finally, it is important to emphasize that there are many treatments available in addition to b cell proliferation. For example, many of the pathways that activate proliferation also activate survival pathways, another important therapeutic objective. Further, β cell expansion might be achieved through other approaches, notably β cell redifferentiation and trans-differentiation from a- or d-cells to β cells (49, 50). Of course, creating new β cells also requires effectively addressing autoimmunity. These are all critical, fertile and active areas of β cell therapeutic research.

DATA AVAILABILITY STATEMENT

The data presented in the study are deposited in the PRIDE repository, accession number PXD023786.

ETHICS STATEMENT

The animal study was reviewed and approved by Xiamen University Institutional Animal Care and Use Committee. Written informed consent was obtained from the owners for the participation of their animals in this study.

AUTHOR CONTRIBUTIONS

MJ designed and performed experiments, analyzed data and drafted the manuscript. ZK designed and performed experiments and analyzed data. WW, WL, and JC conceived and designed the experiments, analyzed and interpreted data, and revised the manuscript. All authors read and approved the manuscript. All authors contributed to the article and approved the submitted version.

FUNDING

This work was supported by grants from the Natural Science Foundation of China (81471081 to WW, 91953114, 81761128015, 81861130370, 31871319 to WL), the Natural Science Foundation of Fujian Province, China (2019J01010 to WW), Xiamen Research Foundation for Science and Technology Project (3502Z20194037 to WW) and Scientific Research Foundation for Advanced Talents, Xiang'an Hospital of Xiamen University (PM201809170005 to WW).

ACKNOWLEDGMENTS

The authors thank Ming Yu Li for the technical assistance db/db mice and HFD mice in this study. Psicor-GFP plasmid was a gift from Tuan Lao Wang.

REFERENCES

1. Wu X, Liang WW, Guan HY, Liu J, Liu LH, Li H, et al. Exendin-4 Promotes Pancreatic Beta-Cell Proliferation Via Inhibiting the Expression of Wnt5a. *Endocrine* (2017) 55(2):398–409. doi: 10.1007/s12020-016-1160-x
2. Chen CG, Cohrs CM, Stertmann J, Bozsak R, Speier S. Human Beta Cell Mass and Function in Diabetes: Recent Advances in Knowledge and Technologies to Understand Disease Pathogenesis. *Mol Metab* (2017) 6(9):943–57. doi: 10.1016/j.molmet.2017.06.019
3. Wang R, Munoz EE, Zhu S, McGrath BC, Cavener DR. Perk Gene Dosage Regulates Glucose Homeostasis by Modulating Pancreatic Beta-Cell Functions. *PloS One* (2014) 9(6):e99684. doi: 10.1371/journal.pone.0099684
4. Mondal P, Prasad A, Girdhar K. Interventions to Improve Beta-Cell Mass and Function. *Ann Endocrinol (Paris)* (2017) 78(5):469–77. doi: 10.1016/j.ando.2016.11.002
5. Wang P, Alvarez-Perez J-C, Felsenfeld DP. Induction of Human Pancreatic Beta Cell Replication by Inhibitors of Dual Specificity Tyrosine Regulated Kinase. *Nat Med* (2015) 21:383–8. doi: 10.1038/nm.3820
6. Cnop M, Welsh N, Jonas J-C. Mechanisms of Pancreatic-Cell Death in Type 1 and Type 2 Diabetes. *Diabetes* (2005) 54:S97–S107. doi: 10.2337/diabetes.54.suppl_2.S97
7. Kahn SE, Hull RL, Utzschneider KM. Mechanisms Linking Obesity to Insulin Resistance and Type 2 Diabetes. *Nature* (2006) 444:840–6. doi: 10.1038/nature05482
8. Rieck S, Kaestner KH. Expansion of Beta-Cell Mass in Response to Pregnancy. *Trends Endocrinol Metab* (2010) 21(3):151–8. doi: 10.1016/j.tem.2009.11.001
9. Simmons RA, Templeton L, Niu H. Intrauterine Growth Retardation in the Rat Leads to Reduced Proliferation and Increased Apoptosis of the B-Cell. *Pediatr Res* (1999) 45(4):62a–a. doi: 10.1203/00006450-199904020-00374
10. Dadon D, Tornovsky-Babaey S, Furth-Lavi J, Ben-Zvi D, Ziv O, Schyr-Ben-Haroush R. Glucose Metabolism: Key Endogenous Regulator of β-Cell Replication and Survival. *Diabetes Obes Metab* (2012) 14:101–8. doi: 10.1111/j.1463-1326.2012.01646.x
11. Stolovich-Rain M, Hija A, Grimsby J, Glaser B, Dor Y. Pancreatic Beta Cells in Very Old Mice Retain Capacity for Compensatory Proliferation. *J Biol Chem* (2012) 287(33):27407–14. doi: 10.1074/jbc.M112.350736
12. Yamamoto J, Imai J, Izumi T, Takahashi H, Kawana Y. Neuronal Signals Regulate Obesity Induced β-Cell Proliferation by FoxM1 Dependent Mechanism. *Nat Commun* (2017) 8:1930. doi: 10.1038/s41467-017-01869-7
13. Maehra R, Chena S, Snitowa M. Generation of Pluripotent Stem Cells From Patients With Type 1 Diabetes. *PNAS* (2009) 106:15768–73. doi: 10.1073/pnas.0906894106

14. Lu B, Munoz-Gomez M, Ikeda Y. The Two Major Glucokinase Isoforms Show Conserved Functionality in β-Cells Despite Different Subcellular Distribution. *Biol Chem* (2018) 399(6):565–576. doi: 10.1515/hsz-2018-0109
15. Metukuri MR, Zhang P, Basantani MK. ChREBP Mediates Glucose-Stimulated Pancreatic Beta-Cell Proliferation. *Diabetes* (2012) 61(8):2004–15. doi: 10.2337/db11-0802
16. Dai C, Hang Y, Shostak A. Age-Dependent Human Beta Cell Proliferation Induced by Glucagon-Like Peptide 1 and Calcineurin Signaling. *J Clin Invest* (2017) 127(10):3835–44. doi: 10.1172/JCI91761
17. Stewart nF, Hussain MA, García-Ocaña XXXA. Human β-Cell Proliferation and Intracellular Signaling: Part 3. *Diabetes* (2015) 64(6):1872–85. doi: 10.2337/db14-1843
18. Tiwari S, Roel C, Wills R, Casinelli G, Tanwir M, Takane KK, et al. Early and Late G1/s Cyclins and Cdks Act Complementarily to Enhance Authentic Human Beta-Cell Proliferation and Expansion. *Diabetes* (2015) 64(10):3485–98. doi: 10.2337/db14-1885
19. Nguyen-Tu MS, da Silva Xavier G, Leclerc I, Rutter GA. Transcription factor-7-like 2 (TCF7L2) Gene Acts Downstream of the Lkb1/Stk11 Kinase to Control mTOR Signaling, Beta Cell Growth, and Insulin Secretion. *J Biol Chem* (2018) 293(36):14178–89. doi: 10.1074/jbc.RA118.003613
20. Ilardi JM, Mochida S, Sheng Z-H. Snapin: A SNARE-Associated Protein Implicated in Synaptic Transmission. *Nat Neurosci* (1999) 2:119–24. doi: 10.1038/5673
21. Pu J, Schindler C, Jia R. BORC, a Multisubunit Complex That Regulates Lysosome Positioning. *Dev Cell* (2015) 33(2):176–88. doi: 10.1016/j.devcel.2015.02.011
22. Hartwig C, Monis WJ, Chen X. Neurodevelopmental Disease Mechanisms, Primary Cilia, and Endosomes Converge on the BLOC-1 and BORC Complexes. *Dev Neurobiol* (2018) 78(3):311–30. doi: 10.1002/dneu.22542
23. Zhou B, Cai Q, Xie Y, Sheng Z-H. Snapin Recruits Dynein to BDNF-TrkB Signaling Endosomes for Retrograde Axonal Transport and Is Essential for Dendrite Growth of Cortical Neurons. *Cell Rep* (2012) 2(1):42–51. doi: 10.1016/j.celrep.2012.06.010
24. Zhou B, Zhu Y-B, Lin L, Cai Q, Sheng Z-H. Snapin Deficiency is Associated With Developmental Defects of the Central Nervous System. *Biosci Rep* (2011) 31(2):151–8. doi: 10.1042/BSR20100110
25. Song WJ, Seshadri M, Ashraf U, Mdluli T, Mondal P, Keil M, et al. Snapin Mediates Incretin Action and Augments Glucose-Dependent Insulin Secretion. *Cell Metab* (2011) 13(3):308–19. doi: 10.1016/j.cmet.2011.02.002
26. Langemeyer L, Ungermann C. BORC and BLOC-1: Shared Subunits in Trafficking Complexes. *Dev Cell* (2015) 33(2):121–2. doi: 10.1016/j.devcel.2015.04.008
27. Somanath S, Partridge CJ, Marshall C. Snapin Mediates Insulin Secretory Granule Docking, But Not Trans-SNARE Complex Formation. *Biochem Biophys Res Commun* (2016) 473(2):403–7. doi: 10.1016/j.bbrc.2016.02.123
28. Yu SC, Klosterman SM, Martin AA, Gracheva EO, Richmond JE. Differential Roles for Snapin and Synaptotagmin in the Synaptic Vesicle Cycle. *PloS One* (2013) 8(2):e57842. doi: 10.1371/journal.pone.0057842
29. Gaisano HY. Recent New Insights Into the Role of SNARE and Associated Proteins in Insulin Granule Exocytosis. *Diabetes Obes Metab* (2017) 19:115–23. doi: 10.1111/dom.13001
30. Sudhof TC, Rothman JE. Membrane Fusion: Grappling With SNARE and SM Proteins. *Science* (2009) 323(5913):474–7. doi: 10.1126/science.1161748
31. Thakur P, Stevens DR, Sheng Z-H, Rettig J. Effects of PKA-mediated Phosphorylation of Snapin on Synaptic Transmission in Cultured Hippocampal Neurons. *J Neurosci* (2004) 24(29):6476–81. doi: 10.1523/JNEUROSCI.0590-04.2004
32. Fukui K, Yang Q, Cao Y, Takahashi N. The HNF-1 Target Collectrin Controls Insulin Exocytosis by SNARE Complex Formation. *Cell Metab* (2005) 2 (6):373–84. doi: 10.1016/j.cmet.2005.11.003
33. Altirriba J, Gasa R, Casas S, Ramirez-Bajo MJ, Ros S, Gutierrez-Dalmau A, et al. The Role of Transmembrane Protein 27 (TMEM27) in Islet Physiology and its Potential Use as a Beta Cell Mass Biomarker. *Diabetologia* (2010) 53 (7):1406–14. doi: 10.1007/s00125-010-1728-6
34. Gao WW, Xiao RQ, Zhang WJ, Hu YR, Peng BL, Li WJ, et al. Jmjd6 Licenses Eralpha-Dependent Enhancer and Coding Gene Activation by Modulating the Recruitment of the CARM1/MED12 Co-Activator Complex. *Mol Cell* (2018) 70(2):340–357 e8. doi: 10.1016/j.molcel.2018.03.006
35. Peng BL, Li WJ, Ding JC, He YH, Ran T, Xie BL, et al. A Hypermethylation Strategy Utilized by Enhancer-Bound CARM1 to Promote Estrogen Receptor Alpha-Dependent Transcriptional Activation and Breast Carcinogenesis. *Theranostics* (2020) 10(8):3451–73. doi: 10.7150/thno.39241
36. C. Gene Ontology. The Gene Ontology (GO) Project in 2006. *Nucleic Acids Res* (2006) 34(Database issue):D322–6. doi: 10.1093/nar/gkj021
37. Kanehisa M, Furumichi M, Tanabe M, Sato Y, Morishima K. KEGG: New Perspectives on Genomes, Pathways, Diseases and Drugs. *Nucleic Acids Res* (2017) 45(D1):D353–61. doi: 10.1093/nar/gkw1092
38. Yuan X, Shan Y, Zhao Z, Chen J, Cong Y. Interaction Between Snapin and G-CSF Receptor. *Cytokine* (2006) 33:219e225. doi: 10.1016/j.cyto.2006.01.008
39. Wang G, Ren G, Cui X, Lu Z, Ma Y, Qi Y, et al. Host Protein Snapin Interacts With Human Cytomegalovirus pUL130 and Affects Viral DNA Replication. *J Biosci* (2016) 41(2):173–82. doi: 10.1007/s12038-016-9604-2
40. Dickman DK, Tong A, Davis GW. Snapin Is Critical for Presynaptic Homeostatic Plasticity. *J Neurosci* (2012) 32(25):8716–24. doi: 10.1523/jneurosci.5465-11.2012
41. Buxton P, Zhang XM, Walsh B, Sriratana A, Schenberg I, Manickam E, et al. Identification and Characterization of Snapin as a Ubiquitously Expressed SNARE-Binding Protein That Interacts With SNAP23 in Non-Neuronal Cells. *Biochem J* (2003) 375:433–40. doi: 10.1042/Bj20030427
42. Starcevic M, Dell'Angelica EC. Identification of Snapin and Three Novel Proteins (BLOS1, BLOS2, and BLOS3/reduced Pigmentation) as Subunits of Biogenesis of Lysosome-Related Organelles Complex-1 (BLOC-1). *J Biol Chem* (2004) 279(27):28393–401. doi: 10.1074/jbc.M402513200
43. Formigli L, Papucci L, Tani A, Schiavone N, Tempestini A, Orlandini GE, et al. Aponecrosis: Morphological and Biochemical Exploration of a Syncretic Process of Cell Death Sharing Apoptosis and Necrosis. *J Cell Physiol* (2000) 182(1):41–9. doi: 10.1002/(SICI)1097-4652(200001)182:1<41::AID-JCP5>3.0.CO;2-7
44. Elmore S. Apoptosis: A Review of Programmed Cell Death. *Toxicol Pathol* (2007) 35(4):495–516. doi: 10.1080/01926230701320337
45. McIlwain DR, Berger T, Mak TW. Caspase Functions in Cell Death and Disease. *Cold Spring Harb Perspect Biol* (2013) 5(4):a008656. doi: 10.1101/cshperspect.a008656
46. Cole JB, Florez JC. Genetics of Diabetes Mellitus and Diabetes Complications. *Nat Rev Nephrol* (2020) 16(7):377–90. doi: 10.1038/s41581-020-0278-5
47. Guthrie RA, Guthrie DW. Pathophysiology of Diabetes Mellitus. *Crit Care Nurs Q* (2004) 27(2):113–25. doi: 10.1097/00002727-200404000-00003
48. Menon RK, Sperling MA. Insulin as a Growth Factor. *Endocrinol Metab Clinics North America* (1996) 25(3):633–. doi: 10.1016/S0889-8529(05)70344-3
49. Bensellam M, Jonas JC, Laybutt DR. Mechanisms of Beta-Cell Dedifferentiation in Diabetes: Recent Findings and Future Research Directions. *J Endocrinol* (2018) 236(2):R109–43. doi: 10.1530/JOE-17-0516
50. Talchai C, Xuan S, Lin HV, Sussel L, Accili D. Pancreatic Beta Cell Dedifferentiation as a Mechanism of Diabetic Beta Cell Failure. *Cell* (2012) 150(6):1223–34. doi: 10.1016/j.cell.2012.07.029

Conflict of Interest: The authors declare that the research was conducted in the absence of any commercial or financial relationships that could be construed as a potential conflict of interest.

Advantages of publishing in Frontiers

OPEN ACCESS
Articles are free to read for greatest visibility and readership

FAST PUBLICATION
Around 90 days from submission to decision

HIGH QUALITY PEER-REVIEW
Rigorous, collaborative, and constructive peer-review

TRANSPARENT PEER-REVIEW
Editors and reviewers acknowledged by name on published articles

Frontiers
Avenue du Tribunal-Fédéral 34
1005 Lausanne | Switzerland

Visit us: www.frontiersin.org
Contact us: frontiersin.org/about/contact

REPRODUCIBILITY OF RESEARCH
Support open data and methods to enhance research reproducibility

DIGITAL PUBLISHING
Articles designed for optimal readership across devices

FOLLOW US
@frontiersin

IMPACT METRICS
Advanced article metrics track visibility across digital media

EXTENSIVE PROMOTION
Marketing and promotion of impactful research

LOOP RESEARCH NETWORK
Our network increases your article's readership